# Molecular genetic aspects and characterization of the extracellular matrix of myxoid tumours of soft tissue

Molecular genetics and characterization of the extracellular matrix of myxoid tumours of soft tissue



ISBN: 978946108128

Printed by: Gildeprint, Enschede, The Netherlands

Cover art: Virchow's microscope, one of his morphological drawings of human cells and the quote he has become famous for (though originally not his!)

# Molecular genetic aspects and characterization of the extracellular matrix of myxoid tumours of soft tissue

Proefschrift

ter verkrijging van de graad van Doctor aan de Universiteit Leiden,
op gezag van de Rector Magnificus prof.mr. P.E. van der Heijden,
volgens besluit van het College van Promoties
te verdedigen op woensdag 9 februari 2011
klokke 16:15 uur

door


Stefan Martin Willems

Geboren te Brunssum
In 1979

Promotiecommissie:

| | |
|---|---|
| Promotor: | Prof. Dr. P.C.W. Hogendoorn |
| Overige leden: | Dr. H. Gelderblom |
| | Dr. L.A. McDonnell |
| | Prof. Dr. med. habil. T. Mentzel<br>(University of Freiburg, Freiburg, Germany) |
| | Prof. Dr. R. Sciot<br>(University of Leuven, Leuven, Belgium) |
| | Prof. Dr. R.A.E.M. Tollenaar |
| | Prof. Dr. B. van de Water |

The work presented in this thesis was financially supported by an AGIKO-Stipendium grant form the Netherlands Organization for Scientific Research (NWO), grant number: 920-03-403.

# Contents

*Bis vincit qui se vincit in victoria*

Publilius Syrus, Sententiae 64

Aan mijn ouders

# Chapter 1

## General Introduction

## General Introduction

### 1.1 Myxoid tumours of soft tissue

1.1.1. Classification and grading of soft tissue tumours

1.1.2. Definition of myxoid tumours of soft tissue

1.1.3. Challenges in differential diagnosis

### 1.2 Molecular genetics and cytogenetics of myxoid tumours of soft tissue

1.2.1. Activating and inactivating mutations

1.2.2. Balanced translocations

1.2.3. Gene specific amplications

1.2.4. Non-specific karyotypic aberrations

1.2.5. Hereditary syndromes involving the occurrence of mesenchymal tumours

### 1.3 Analytical tools for extracellular matrix analysis

1.3.1. Alcian Blue staining

1.3.2. Immunohistochemistry

1.3.3. Liquid-based Chromatography Mass Spectrometry

1.3.4. Imaging Mass Spectrometry

### 1.4 Defining therapeutic targets

### 1.5 Aims of the thesis

## 1.1 Myxoid tumours of soft tissue

### *1.1.1. Classification and grading of soft tissue tumours*

Uniform annotation of bone-, and soft tissue tumours is performed on the basis of the international consensus guidelines of the World Health Organization (12). Hereby, soft tissue tumours are classified according to their cell type of differentiation, e.g. adipocytic, fibroblastic, pericytic or vascular. This concept is only partial true for bone tumours which main entities are basically classified according to the dominant pattern of extracellular matrix (ECM) formation on microscopy, i.e. cartilage or osteoid. In this respect myxoid tumours of soft tissue are not a well-defined group as such in the WHO classification and rather a historically based "hybrid" concept of soft tissue tumours named after the predominant microscopy of their ECM. On the basis of their biological potential, soft tissue tumours are divided into the following four categories: (1) benign, (2) intermediate (locally aggressive), (3) intermediate (rarely metastasizing) or (4) malignant. In case of malignancy, a histological grade should be provided aiming at predicting the level of aggressiveness of the tumour (23). The world wide standard grading occurs according to the (modified) criteria of the Fédération Nationale des Centres de Lutte Contre le Cancer (25).

### *1.1.2. Definition of myxoid tumours of soft tissue*

Myxoid tumours of soft tissue are mesenchymal tumours characterized by the presence of abundant so-called "myxoid" extracellular matrix (ECM) at microscopy (24). The term "myxoid" was first used by Rudolf Virchow to describe tumours that histologically resembled the structure of the umbilical cord, referring to the substance of Wharton's jelly (figure 1) (69). Myxoid/mucoid appearance of the ECM on light microscopy can be a feature of a variety of both epithelial and mesenchymal tumours (75). In myxoid tumours of soft tissue this myxoid ECM is intrinsic to the entity though often not directional for diagnosis: this group comprises a broad spectrum of tumours with overlapping histology but different clinical behavior ranging from truly benign to frankly malignant warranting adequate recognition of the entities (24, 75).

### *1.1.3. Challenges in differential diagnosis*

The differential diagnosis of myxoid tumours of soft tissue can be very challenging especially in biopsies because of significant histological overlap between the different entities at the light microscopical level (75). As for all (soft tissue) tumours, integration of microscopy with microscopy including immunohistochemistry as well as extensive additional clinical and radiological data is essential to render the correct diagnosis. Moreover, during the recent years, many sarcomas have been shown to harbour tumour-specific genetic alterations which do not only give insight into their biology; they also provide helpful tools in differential diagnosis and treatment (table 1) (13, 23). Myxofibrosarcoma and intramuscular myxoma are relatively common soft tissue

**Figure 1:** Characteristic macroscopy and histomorphology of the myxoid ECM.

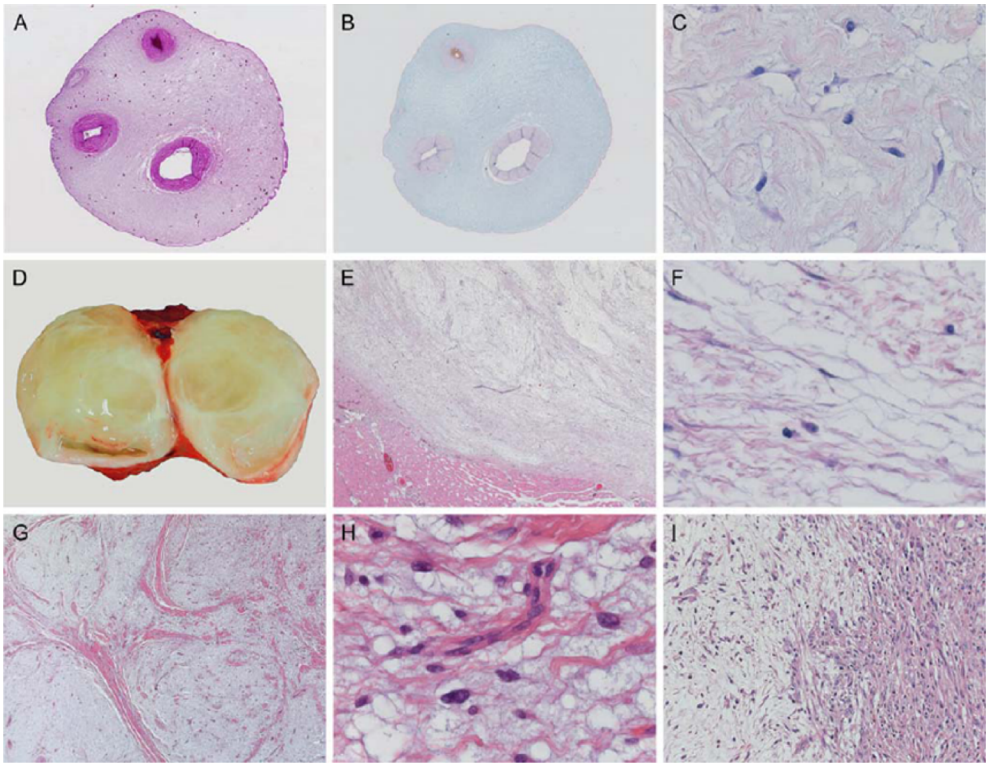


Rudolph Virchow introduced the term myxoma for those tumours morphologically resembling Wharton's jelly of the umbilical cord (a), which contains large amounts of GAGs as detected by Alcian Blue (b). High-power image of Wharton's jelly showing abundant myxoid ECM containing fibrillary collagens, interspersed between myofibroblast-like stroma cells (c). Intramuscular myxoma characteristically has a gelatinous appearance on cut surface (d) and is well circumscribed towards its peripheral tissue (e). On higher magnification, it shows the same abundant myxoid ECM as the umbilical cord (c) and no significant atypia of the sparse tumour cells (f). Histological criteria are still a hallmark of diagnosis, showing characteristic lobulated, hypocellular morphology of grade I myxofibrosarcoma at low magnification (g).Curvilinear blood vessels are quite specific for grade I myxofibrosarcoma (but are not diagnostic), whereas tumour cells show vesicular, slightly atypical nuclei compared to intramuscular myxoma (h). Another hallmark of myxofibrosarcoma is areas with abrupt transition of grade (i) which was already mentioned by Mentzel et al. (41).

tumours, usually occurring in the extremities of adult or older patients. Accurate diagnosis and grading is crucial for the decision on adjuvant therapy. According to the 2010 ESMO guidelines adjuvant radiation therapy is a standard for soft tissue tumours of high-grade deep seated tumours regardless of diameter (< or > 5 cm). Radiation therapy is added in selected cases of low-grade, superficial, >5 cm, and low-grade, deep, <5 cm soft tissue tumours. In the case of low-grade, deep, >5 cm soft tissue sarcoma, radiation therapy is recommended to be discussed in a multidisciplinary fashion. Radiation therapy is also recommendatory following marginal or R1-R2

excisions, if these cannot be rescued through re-excision (11), Compartmental resection of an intracompartmental tumour, does not require adjuvant radiation therapy. Adjuvant chemotherapy is not standard treatment in adult-type soft tissue sarcomas, although it is proposed by some as an option in high-risk patients with tumours of intermediate- or high grade, deep-seated and >5 cm) (51). Some histological types are more chemosensitive and the histotype may therefore be considered in the decision-making (11). Accurate diagnosis is thus essential warranting the need of additional diagnostical tools with high specificity, both for assessment of prognosis as well as for tailoring therapy and metastatic disease.

**Table 1:** Clinicopathological and (cyto) genetic characteristics of myxoid tumours of soft tissue

| Myxoid tumors of soft tissue | Age | Sex | Predilection site | Molecular/cytogenetic aberrations |
|---|---|---|---|---|
| Benign | | | | |
| Intramuscular myxoma (including its cellular variant) | Adults | F>M | Thigh, shoulder, buttocks, and rarely upper arm | GNAS1 mutations |
| Myxoid neurothekeoma | Young adults | F>M | Head, neck, and shoulders | Loss of 22q |
| Myxoid lipoma (myxolipoma) | Any age | F=M | Head and neck | Rearrangement of 13q and/or 16q |
| Myxoid chondroma | Adults | M>F | Hands and feet | Extra copies of chromosome 5 or 12q13–15 rearrangement |
| Myxoid neurofibroma | Any age | M=F | All over the body | NF1 mutations |
| Myxoid dermatofibroma | Young adults | F>M | Lower extremities | Unknown |
| Cardiac myxoma | Adults | F>M | Atria (predominantly left) | PRKAR1α mutations in Carney complex |
| Ossifying fibromyxoid tumor | Elderly | M>F | Extremities and trunk | Nonspecific cytogenetic aberrations |
| Cutaneous myxoid cyst | Any age | F>M | Distal and dorsal portions of fingers (and toes) | Unknown |
| Cutaneous myxoma (superficial angiomyxoma) | Adults | M>F | Trunk, lower extremities, head, and neck | PRKAR1α mutations in Carney complex |
| Myxoid nodular fasciitis | Young adults | M=F | Head, neck, and extremities | Nonspecific cytogenetic aberrations |
| Locally aggressive | | | | |
| Odontogenic myxoma | Young adults | F>M | Mandible and maxilla | PRKAR1α mutations in rare cases (not Carney complex) |
| Myxoinflammatory fibroblastic sarcoma | Adults | M=F | Feet, lower leg | t(1;10)(p22;q24) and amplification of chromosome 3 |
| Aggressive angiomyxoma | Adults | F>>M | Inguinal region | Rearrangement of 12q13-15 |
| Malignant | | | | |
| Myxofibrosarcoma | Elderly | M=F | Extremities, thigh | Nonspecific cytogenetic aberrations |
| Extraskeletal myxoid chondrosarcoma | Adults | M>F | Extremities and limb | t(9;22)(q22;q12), t(9;17)(q22;q11) or t(9;15)(q22;q21) |
| Low-grade fibromyxoid sarcoma | Young adults | M>F | Proximal extremities and trunk | t(7,16) (q33;p11) |
| Myxoid liposarcoma | Elderly | M>F | Lower extremities and thigh | t(12;16)(q13;p11) or t(12;22)(q13;q12) |
| Myxoid leiomyosarcoma of soft tissue | Adults | F>>M | Limbs, female genitalia, head, and neck | Nonspecific cytogenetic aberrations |
| Myxoid malignant peripheral nerve sheath tumor | Adults | F=M | Extremities, trunk | NF1 and TP53 mutations, P16 deletions |
| Myxoid dermatofibrosarcoma | Adults | M=F | Trunk, groin, and extremities | t(17;22)(q22;q13) |

## 1.2 Molecular genetics and cytogenetics of myxoid tumours of soft tissue

Based on molecular genetics and cytogenetics, sarcomas can be divided in two major groups: (a) sarcomas with relatively "simple" karyotypes showing specific genetic alterations (such as balanced translocations) with the formation of tumour specific fusion genes (table 2), or specific genetic mutations (often in proto-oncogenes), and (b) sarcomas with non specific gene alterations and very complex karyotypes with structural and numerical aberrations (49). Overlap exists between groups (a) and (b) with sometimes additional/secondary complex karyotypic aberrations superimposed upon initial specific driver mutations (e.g. gastrointestinal stromal tumours (GIST)) (58).

**Table 2:** Molecular genetics and cytogenetics of myxoid tumours of soft tissue

| Sarcoma | Aberration | Molecular genetic consequence |
|---|---|---|
| Atypical lipomatous tumor | Ring chromosome/giant marker | Amplification of, e.g., *MDM2*, *CDK4*, *HMGA2*, *GLI* and *SAS* |
| Myxoid/round cell liposarcoma | t(12;16)(q13;p11) | *FUS–DDIT3* |
| | t(12;22)(q13;q12) | *EWSR1–DDIT3* |
| Solitary fibrous tumor/hemangiopericytoma | der(12)(q13-15) | Unknown |
| Inflammatory myofibroblastic tumor | t(1;2)(q21;p23) | *TPM3–ALK* |
| | inv(2)(p23q35) | *ATIC–ALK* |
| | t(2;2)(p23;q13) | *RANBP2–ALK* |
| | t(2;4)(p23;q21) | *SEC31A–ALK* |
| | t(2;11)(p23;p15) | *CARS–ALK* |
| | t(2;17)(p23;q23) | *CLTC–ALK* |
| | t(2;19)(p23;p13) | *TPM4–ALK* |
| Infantile fibrosarcoma | t(12;15)(p13;q25) | *ETV6–NTRK3* |
| Myxoinflammatory fibroblastic sarcoma | t(1;10)(p22;q24) | Deregulation of *FGF8* and *NPM3* |
| | Ring chromosome | Amplification of, e.g., *VGLL3* |
| Low-grade fibromyxoid sarcoma | t(7;16)(q33-34;p11) | *FUS–CREB3L2* |
| | t(11;16)(p11;p11) | *FUS–CREB3L1* |
| Dermatofibrosarcoma protuberans | Ring chromosome, t(17;22)(q21;q13), der(22)t(17;22) | *COL1A1–PDGFB* |
| Alveolar rhabdomyosarcoma | t(1;13)(p36;q14) | *PAX7–FOXO1A* |
| | t(2;2)(p23;q36) | *PAX3–NCOA1* |
| | t(2;13)(q36;q14) | *PAX3–FOXO1A* |
| | t(X;2)(q13;q36) | *PAX3–FOXO4* |
| Angiomatoid fibrous histiocytoma | t(2;22)(q33;q12) | *EWSR1–CREB1* |
| | t(12;16)(q13;p11) | *FUS–ATF1* |
| | t(12;22)(q13;q12) | *EWSR1–ATF1* |
| Synovial sarcoma | t(X;18)(p11;q11) | *SS18–SSX1*, *SS18–SSX2* or *SS18–SSX4* |
| | t(X;20)(p11;q13) | *SS18L1–SSX1* |
| Clear cell sarcoma | t(2;22)(q33;q12) | *EWSR1–CREB1* |
| | t(12;22)(q13;q12) | *EWSR1–ATF1* |
| Desmoplastic small round cell tumor | t(11;22)(p13;q12) | *EWSR1–WT1* |
| Extraskeletal myxoid chondrosarcoma | t(3;9)(q12;q22) | *TFG–NR4A3* |
| | t(9;15)(q22;q21) | *TCF12–NR4A3* |
| | t(9;17)(q22;q11) | *TAF15–NR4A3* |
| | t(9;22)(q22;q12) | *EWSR1–NR4A3* |
| Alveolar soft part sarcoma | t(X;17)(p11;q25) | *ASPSCR1–TFE3* |

### *1.2.1. Activating and inactivating mutations*

Activating mutations in proto-oncogenes have been described in many epithelial and mesenchymal tumours (6). These mutations often act as driver mutations (22). Usually they affect directly or indirectly the de-phosphorylation (often GTPase) region of a protein involved in cell signaling (4). In a normal acting cell, phosphorylation of the

**Figure 2:** Activating mutations in *GNAS1* lead to constitutive activation of protein kinase A

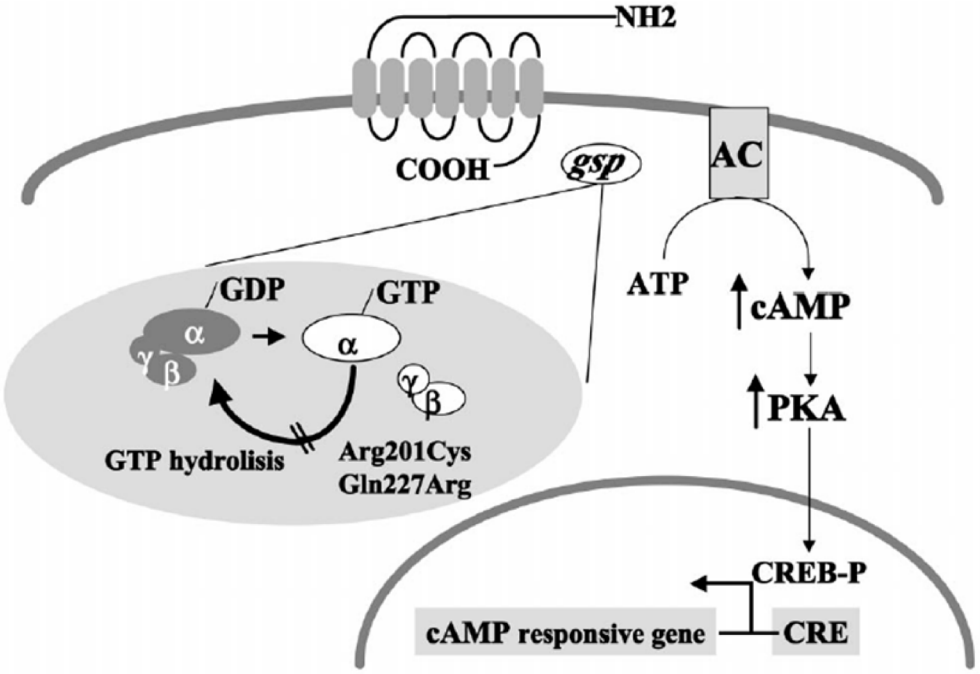


G-proteins transmiss signals from activated seven transmembrane spanning receptors to intracellular effectors, e.g. adenylate cyclase. Activation of adenylate cyclase converts ATP to cAMP which subsequently activates protein kinase A and cAMP responsive genes. In the inactive state, the G-protein is a αβγ heterotrimer with the α subunit bound to guanosine triphosphate (GTP). Binding of GTP leads to a conformational change of the α-subunit which then dissociates from the complexed βγ dimer and increased affinity for the receptor and the intracellular effector. Hydrolysis of GTP to guanosine diphosphate by the intrinsic GTPase of the G-protein leads to the re-formation of the heterotrimeric complex and subsequent ending of the activation signal. Activating mutations in codon 201 or codon 227 reduce the α subunit's GTPase activity. Hereby it prevents hydrolysis of the GTP bound to the α subunit and causes consecutive activation of adenylate cyclase and downstream cell signaling.Adapted from: Lania AG et al (36).

protein leads to the temporarily activation of cell signaling, which stops at dephosphorylation. The responsible phosphorylase which can be an intrinsic part of the protein, thereby acts as an "on-off" switch in cell signaling and transduces extracellular signals via ligand-receptor binding to a downstream target (31, 54). Activating mutations occur mostly in the binding pocket of the phosphorylase and thereby block dephosphorylation of the protein (figure 2). This results in constitutive cell signaling and continuous stimulation of pathways involved in cell growth. Activating mutations in sarcomas are exemplatory (e.g. KIT and PDGFR in GIST) and are also found in mesenchymal tumours-related syndromes (9, 18, 68). Somatic and germline mutations in GNAS1 gene have been described in fibrous dysplasia, both in isolated lesions as well patients suffering Mazabraud syndrome (mono/polyostotic fibrous dysplasia and

intramuscular myxoma) and McCune-Albright syndrome (cafe-au-lait spots, precocious puberty and fibrous dysplasia) (71). This leads to downstream activation of cFos which acts as a transcription factor (10). Activating mutations in codon 12/13 of KRAS also lead to downstream activation of c-Fos. KRAS-activating mutations have been described in both mouse and human sarcomas. Kirsch et al. showed that KRAS and TP53 mutations were sufficient to initiate high-grade sarcomas with myofibroblastic features in mice (33). P53 is a major cellular gatekeeper for cell growth and division (37). Inactivating TP53 mutations are relatively common in sarcomas with nonspecific genetic aberrations compared with sarcomas with reciprocal specific translocations (8). This was sustained by previously published data that p53 immunohistochemical staining was predominantly found in myxofibrosarcoma of grade II and III harboring non-specific cytogenetic aberrations compared to grade I tumours which have less aberrant, sometimes normal karyotypes (47, 74). Another important gene involved in cell cycle regulation is P16, Inactivation of P16 (either by promoter hypermethylation, inactivating mutations or deletions) has been extensively described in many sarcomas (43, 45, 61). Significant reduction in p16 expression has been found in the (more aggressive and therefore grade determining) round cell component of myxoid liposarcoma and is partly due to promotor hypermethylation and mutation (48). Also in myxofibrosarcoma, reduced p16 expression correlates with worse prognosis (47), suggesting that p16 might play an important role in tumourprogression in these tumours.

*1.2.2. Balanced translocations*

Balanced translocations have been described in both benign and malignant tumours, especially in hematological malignancies and sarcomas, and are increasingly recognized in epithelial tumours (5, 42, 44, 52, 67). Though the involved genes are often (but not always!) tumour specific, their fusion partners are mostly restricted to a certain group of genes. For example, EWSR1 (the Ewing sarcoma breakpoint region 1, a.k.a. EWS) is not only translocated in Ewing sarcoma (17, 59), but also in desmoplastic small round cell tumour (35), clear cell sarcoma (20) angiomatoid fibrous histiocytoma (3, 60), extraskeletal myxoid chondrosarcoma (66), and a small subset of myxoid liposarcoma (50). Interestingly, one and the same gene can be translocated in both epithelial and mesenchymal tumours, such as the Xp11.2 gene, coding for tfe3 which is translocated in both peadiatric renal cell carcinoma and alveolar soft part sarcoma (30, 72). Balanced translocations can drive tumourigenesis by different mechanisms. First, the transcribed fusion protein can act as a kinase or transcription factor and thereby activate transcription of genes and proteins involved in cell cycle, growth, angiogenesis etc (42). Hereby, they do not only play a role in tumour proliferation but sporadically also in driving tumour morphology such as FUS/DDIT3 in myxoid liposarcoma (56, 57). Secondly, balanced translocations can cause a promoter swap in which one gene involved in the translocation is placed under the transcriptional control of the promoter of an other (highly transcribed) gene. For example, in (myxoid)

dermatofibrosarcoma protuberans, the COL1A1-PDGFB fusion leads to PDGF overexpression, increased autocrine stimulation and subsequent cell proliferation (46, 64).

*1.2.3. Gene specific amplification.*
Next to non-specific randomly occurring gene amplifications, some sarcomas are characterized by gene specific amplifications, such as of CDK4 and MDM2. These amplifications are (not exclusively) present in the majority of well- and dedifferentiated liposarcoma and believed to play a role in their genesis (15, 29). Detection of these amplifications by FISH or their transcribed proteins by immunohistochemistry can be used in their differential diagnosis (29).

*1.2.4. Non-specific karyotypic aberrations*
The more frequent occurring sarcomas show non-specific numerical and structural cytogenetic changes which are the reflection of genetic instability (13). These complex karyotypic aberrations increase upon tumour progression suggesting a multistep tumour progression model and are often associated with functional and/or structural loss of genes involved in guarding the genome, such as TP53 or RB (40, 62). Superimposed, often non-specific karyotypic aberrations such as observed in myxofibrosarcoma and osteosarcoma can also be seen in translocation-driven sarcomas (16, 43, 47).

*1.2.5. Hereditary syndromes involving the occurrence of mesenchymal tumours*
During the recent years, an increased number of (Mendelian) inherited sarcoma-related syndromes has been reported. Subsequent molecular-genetic knowledge of genes predisposing to these syndromes, provide not only insight into their genetic pathways; they also serve as a solid basis for genetic counseling. Some of these relatively frequent syndromes are associated with mesenchymal and epithelial neoplasms, both benign and malignant. A not exhaustive list is summarized in table 3 and includes more general cancer syndromes such as Li Fraumeni-, and Retinoblastoma syndrome, caused by mutations in tumour suppressor genes involved in cell cycle check point regulation (such as TP53 and RB). Interestingly, hereditary syndromes including (intramuscular) myxomas involve activation of the G-protein-prkar alpha1 axis. This activation is either caused by (1) activating mutations in GNAS1 gene coding for (the alpha subunit of) the G-protein, such as in Mazabraud syndrome and McCune-Albright syndrome, or (2) activating mutations in the PRKAR gene, coding for the downstream protein kinase A receptor, such as in Carney complex. Interestingly, mutations in the GNAS1 gene are also involved in mesenchymal tumour-related syndromes without myxomas such as in Albright hereditary osteodystrophy. Interestingly, this latter syndrome is caused by inhibiting (and not activating) mutations in the GNAS1 gene (55).

**Table 3:** Molecular genetics of syndromes involving myxoid tumours of soft tissue

| Syndrome | Inhereritance | Gene locus | Gene | Sarcoma's |
|---|---|---|---|---|
| Albright hereditary osteodystrophy | AD | 20q13 | *GNAS1* | Soft tissue calcifications and osteomas |
| Beckwith-Wiedemann syndrome | Sporadic/AD | 11p15 | Multigenetic, incl. *CDKN1C* and *IGF2* | Embryonal rhabdomyosarcomas, myxomas, fibromas, hamartomas |
| Carney complex | AD | 17q23-24<br>2p16 | *PRKAR1AK*<br>unknown | Cardiac and other myxomas,<br>melanotic schwannomas |
| Li-Fraumeni syndrome | AD | 17p13<br>22q11 | *TP53*<br>*CHEK2* | Osteosarcomas, rhabdomyosarcoma<br>and other sarcomas |
| Mazabruad syndrome | Sporadic | 20q13 | *GNAS1* | Polyostotic fibrous dysplasia,<br>osteosarcomas, intramuscular myxomas |
| McCune Albright syndrome | Sporadic | 20q13 | *GNAS1* | Polyostotic fibrous dysplasia, osteosarcomas |
| Retinoblastoma | AD | 13q14 | *RB1* | Osteosarcomas and other sarcomas |

## 1.3 Analytical tools for extracellular matrix analysis

The classification of soft tissue tumours by microscopical features (i.e. on the basis of their normal cellular counterpart) corresponded wonderfully well with the increasing differential biological/molecular genetic data of these different tumour types. In this respect, the more historically originated concept of naming tumours after their (myxoid) ECM, turned out to be not so adequate. This might partially be explained by the restrictive discriminative power of examination of the ECM by microscopy alone, as the constituents which can be identified by (immuno) histochemistry are often not tumour specific (such as collagens, GAGs). Though Rudolf Virchow already mentioned that the ECM might influence the biology of (cancer) cells, study of ECM molecules was rather restricted. Indeed 150 years after the introduction of the term "myxoid" as an ubiquitous microscopical feature, knowledge of the exact constituents and possible function of this so-called myxoid ECM are still very limited. However, during the last decade, recognition of the importance of the ECM and its interactions with-tumour cells in their development and maintenance, has led to a more profound study of the ECM and its (low-abundant) molecules.

### *1.3.1. Alcian Blue staining*

Discovered in 1950, Alcian Blue (AB) is a phthalocyanine cationic dye containing copper ions and non-covalently binding negatively charged macromolecules. It was John Scott who used this staining to distinguish different glycosacominoglycans in tissue sections by varying the electrolyte concentration. By adding gradual increasing concentrations of Mg2+ which competes with AB for binding to mucopolysaccharides and glycosaminoglycans, AB selectively identifies neutral, sulphated and phosphated mucopolysaccharides (63). Kindblom et al showed that the myxoid ECM of various

(non) neoplastic lesions contained various amounts of the different GAGs (36). It has become clear during the years that myxoid changes of the extracellular matrix can be found in reactive and neoplastic (benign and malignant) lesions of both epithelial and mesenchymal origin (75). Thereby myxoid ECM is not specific for any tumour type at all (neither from mesenchymal nor epithelial origin), and nowadays AB staining of the ECM is not of much use in discriminating sarcomas anymore.

*1.3.2. Immunohistochemistry*

Immunohistochemistry is a crucial adjunct technique in routine diagnostics as well as in research. Though more expensive, the epitopes recognized by immunohistochemistry are usually much more specific than histochemical stainings (although over time this specificity always tends to be less than initially claimed, or hoped for). Immunohistochemical stainings bind to a still increasing number of epitopes identified (e.g. the cluster of differentiation) so its potential is still emerging and includes a large and broad series of validated diagnostic, predictive and prognostic markers. Proteins (i.e. their epitopes) recognized by immunohistochemical stainings can be categorized in different types: structural ECM molecules (e.g. collagens, decorin, vimentin), cell cycle related proteins (e.g. p53, cyclin D, Ki67), proteins involved in cell maturation/ differentiation (e.g. CD2, CD3, CD4, CD5, CD7, CD8), receptors (e.g. ER, PR, Her2Neu) and secretory proteins (e.g. gastrin, thyreoglobulin, ACTH, insulin). Hereby, immunohistochemistry, much more than histochemistry, links protein expression to tumour biology and bridges a gap between morphology and molecular genetics. Because of their mesenchymal origin, myxoid tumours of soft tissue nearly always express vimentin, whereas other markers are helpful for more specific classification and diagnosis, depending on the immunohistochemical expression of epitopes often reflecting the cell type of differentiation (e.g. desmin and MS actin in smooth muscle cell tumours; CD31 and CD34 in vascular tumours). In the future, protein screens of (myxoid) tumours (of soft tissue) without a priori knowledge might lead to the discovery of new biomarkers useful in their differential diagnosis.

*1.3.3. Liquid-based Chromatography Mass Spectrometry*

Besides more conventional ways of studying the proteome, there is a tendency to incorporate more high-tech procedures in the analysis of (soft tissue) tumours during the last years. With its origins in chemistry, mass spectrometry (MS) has recently entered the field of tumour biology. Recognition of the identification of many molecules (including peptides, proteins or lipids) in one single experiment makes MS a promising technique in cancer research. In contrast to (immuno) histochemistry, it uses masses (m/z values) and not charge or structure (e.g. epitope) to discriminate between molecules. Hereby, it allows the identification of many molecules (up to hundreds to thousands) without a priori knowledge of the targeted molecule. A standard mass spectrometry experiment consists mainly out of three elements: (a) creation of the ions by an ion

**Figure 3:** Simplified methodological overview of the ionisation process by LC-MS/MS

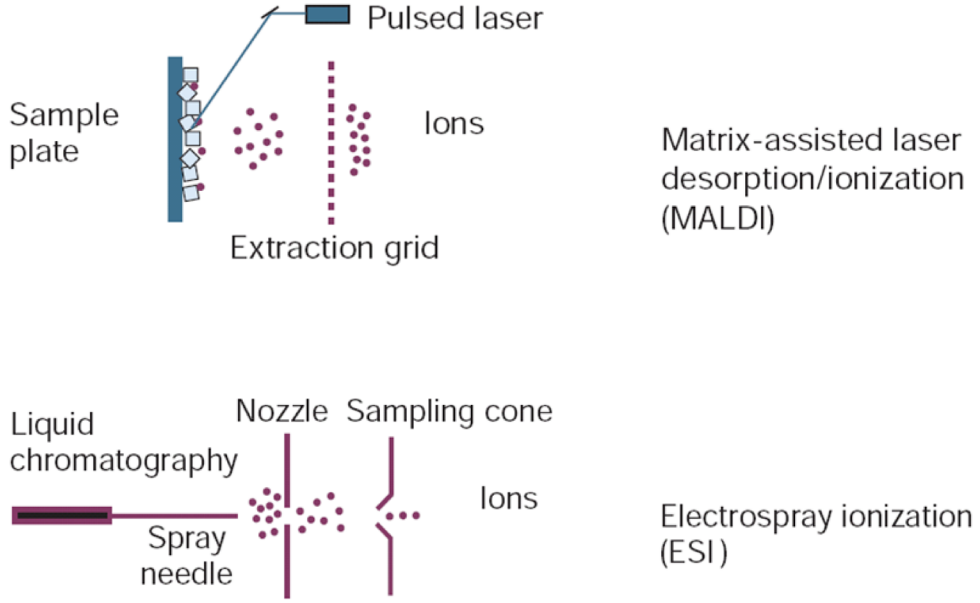


The ion sources routinely used in mass spectrometry research are matrix assisted laser desorption/ionization (MALDI) and electrospray ionization (ESI). In MALDI the sample of interest is co-crystallized with a matrix, overall organic acid.. The idendity depends on the molecules and mass range of interest (e.g. peptide/proteins, lipids). By irradiating the matrix crystals with a pulsed laser beam, the analytes are desorbed from the matrix and ionized after which they enter the mass analyzer. In ESI the liquid sample containing the analytes of interest are passed through a needle hold at high potential. The electric field between the needle and an other electrode leads to the formation of a Taylor cone at the needle orifice, from which emerges a jet of charged droplets Sequential cycles of solvent evaporation/Rayleish instability lead to the generation of very small, highly charged droplets which enter the mass spectrometer. Evaporation of the remaining solvent leads to gas-phase molecular ions ESI circumvents the need for matrix application, can be perfectly preceded by a first separation step by liquid chromatography and allows a continuous introduction of the ions into the mass spectrometer. Adapted from: Ruedi Aebersold and Matthias Mann (1).

source, (b) the mass analysis and (c) the detection of the masses. A simplified methodological overview of the ionisation process by LC-MS/MS is depicted in figure 3. Basically, two types of ion sources are used: matrix-assisted laser desorption/ionization (MALDI) and electrospray ionization (ESI) (figure 3). Different mass spectrometers are currently available, such as Time of flight (ToF), quadrupoles (such as ion trap) and Fourier Transformed (FT) techniques, such as Fourier Transformed Ion Cyclotron Resonance or Orbitrap). Each of these mass spectrometers has its own advantages and relative shortcomings so that the specific mass spectrometer of choice largely depends on the research question(s) imposed to address. A schematic overview of a routine LC-MS/MS experiment is depicted in figure 4. After data acquisition, the mass spectra are analyzed by matching the multiple peptide/protein fragments to a sequence database. Based on the amount of structural overlap of these fragments, a

**Figure 4:** Schematic overview of a routine LC-MS/MS experiment

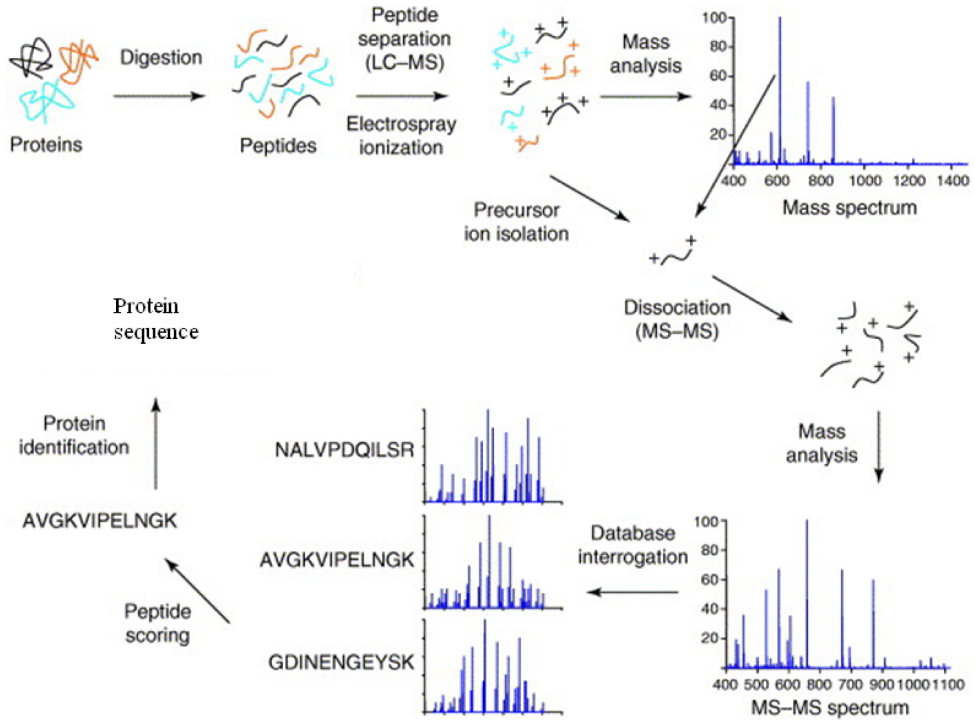


For the study of tumour tissues or cell lysates, the (often very complex) samples are analyzed with LC-MS/MS following a 1D or 2D gel electrophoresis. After isolating the spots or bands from the gel ("spot picking"), these (still complex) samples are digested using a protease (commonly trypsin). Trypsin is a serine protease, specifically cleaving the carboxyl end of lysine and arginine. The resulting tryptic peptide samples are typically separated by liquid chromatography (LC) and then ionized using electrospray ionization (ESI). After mass analysis peptides are automatically selected for tandem mass spectrometry (MS/MS). This involves the isolation of the selected peptide ion followed by its fragmentation. Peptide fragmentation follows known rules and so the peptide can be identified by comparing the experimental MS/MS spectra with a peptide (MS/MS) database. Adapted from koler et al. (34).

probability score (so-called "MASCOT" score) is calculated of the reconstructed peptide/ protein.

### *1.3.4. Imaging Mass Spectrometry*

Recently, imaging mass spectrometry was developed, a technique which combines conventional mass spectrometry (e.g. MALDI-ToF) with spatial resolution and relates the obtained spectra to their exact location in the tissue (figure 5). Imaging mass spectrometry has also entered the field of cancer research. Its particular strengths, such as the analysis of multiple molecules at the same time, in the same tissue and related this information to the spatial resolution of these molecules, without a priori

**Figure 5:** Schematic overview of a imaging MS experiment

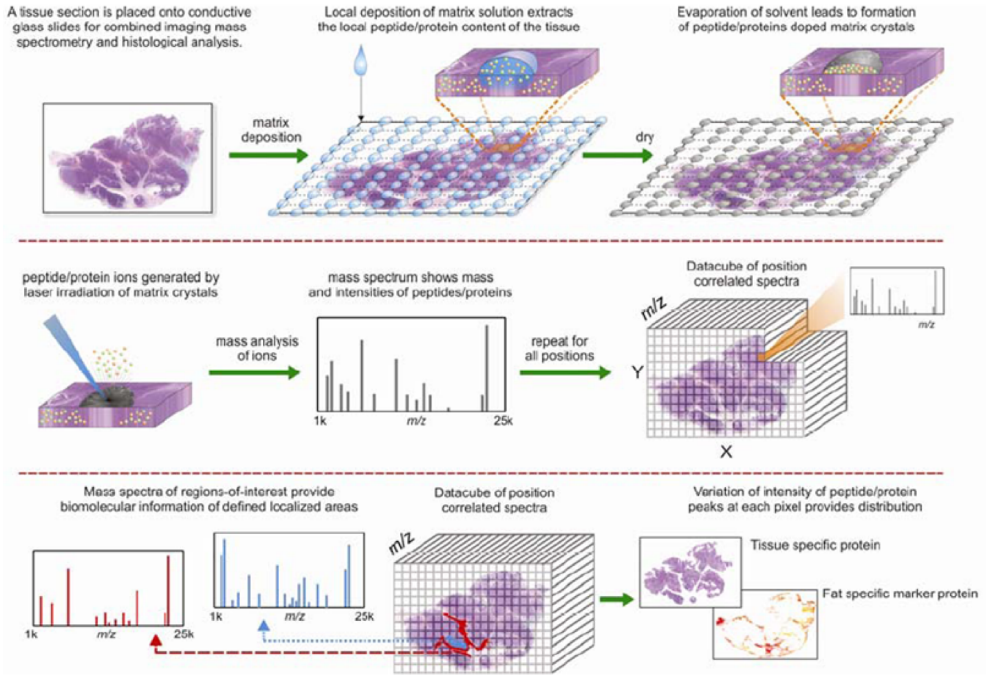


Workflow of a MALDI imaging MS experiment. A) The tissue is prepared for MALDI MS analysis by depositing a matrix solution onto the tissue. Peptides and proteins dissolved by the matrix solution become incorporated into the matrix crystals as the solvent evaporates. B) Irradiation of the matrix crytals with a UV laser leads to efficient production of gas-phase peptide and protein ions, which can then be mass analyzed in a mass spectrometer. MALDI MS analysis of an array of positions covering the tissue provides the spatial distribution of many peptides and proteins. C) The data can be analyzed to reveal the peptide and protein content of defined regions of the tissue or to reveal the distributions of specific proteins. Adapted from McDoneel LA et al (with permission)(34).

knowing them- makes it a very promising tool, at least in theory (34). A crucial step for each imaging mass spectrometry experiment, as for all mass spectrometry experiments, is the quality of the samples ("garbage in = garbage out"), the applied matrix and the matrix application itself. Depending on the range of spectra one is interested in (e.g. <1.000 Da, 3.000-20.000 Da, >20 kDa) as well as the nature of the molecules (e.g. lipids, peptides or proteins), different matrices can be applied. Matrix application can be done manually but for optimal control and reproducibility is best done in an automated fashion by computer assistance. The volume of the droplets is a delicate balance between resolution and quality of the obtained spectra: a larger droplet volume gives better extraction and thus a richer spectrum, but it decreases the resolution (and visa versa).

## 1.4 Defining therapeutic targets

The revelation of cell signaling pathways in cancer (cells) does not only provide fundamental insight into the mechanisms and biology of cancer. It has also shown to provide excellent clues for more rational-based molecular targeting of specific signaling pathways. Many cancers arise form aberrant cell signaling, which is predominantly regulated by post translational modifications, such as phosphorylation by kinases. Kinases activate proteins by phosphorylation of the amino acid residues: tyrosine, serine, or threonine. The possibilities of interfering this aberrant cell signaling by inhibitors of these kinases, opens a new era of targeted and more cancer cell specific therapy. The search for pathway discovery, including the activated kinases and their subsequent inhibitors, is especially relevant in sarcoma patients and has been underscored in the treatment of GIST. The tyrosine kinase inhibitor imatinib has quadrupled the median survival of patients with metastatic GIST. However, most patients inevitably develop resistance, which is mostly conferred by secondary mutations within the split kinase domain (exon 13 and 17) of KIT (26, 27, 70). Although mutations within the ATP-binding pocket (exon 13, exon 14) are generally sensitive to secondary generation direct KIT inhibitors such as sunitinib and nilotinib, mutations within the activation loop (exon 17) are often cross resistant to these newer generation KIT inhibitors (7, 53). In sarcoma patients, surgery and irradiation are the mainstay of curative therapy for local disease. Treatment options for patients with advanced (metastatic), or inoperable disease is rather poor (28). Conventional chemotherapy is limited and can have serious side effects, whereas kinase-inhibitors act on more specific targets and subsequently have less severe side effects (73). Downstream signalling targets, including activated kinases have been recently elucidated for well and dedifferentiated liposarcoma (29, 65), low-grade fibromyxoid sarcoma (39), extraskeletal myxoid chondrosarcoma (19), malignant peripheral nerve sheath tumours and alveolar soft part sarcoma (2).

## 1.5 Aims of the thesis

Originating from mesenchymal precursor cells, myxoid tumours of soft tissue are characterized by their loose myxoid texture of extracellular matrix. In this group, intramuscular myxoma including its cellular variant (a.k.a. cellular myxoma), myxofibrosarcoma and myxoid liposarcoma are the most common ones. Though a hallmark at microscopy, the exact composition of the myxoid ECM is not known. Interactions between tumour cells and their surrounding ECM play an important role in tumour biology. The clinical behavior of myxoid tumours of soft tissue ranges form truly benign to frankly malignant with metastatic potential. On one hand, this might suggest that the ECM of these tumours is not homogeneous and that ECM constituents

might play a role in this different tumour biology (14). On the other hand, this warrants the need of further (molecular genetic) research to define tumour-specific genetic aberrations which not only give insight in their biology, but also provide diagnostic clues for differential diagnosis and more targeted therapy. The research questions addressed in this thesis are:
(1) what is the exact constitution of the so-called myxoid extracellular matrix and does it play a potential role in the biology of these tumours, outlined in **chapters 2, 4, 5 and 6;**
(2) which molecular and cytogenetic events characterize these different myxoid tumours of soft tissue, addressed in **chapters 2, 3 and 5**;
(3) what is the role of these molecular aberrations in their tumourigenesis and do they offer clues to tumour specific targeting, studied in **chapters 3, 5 and 7**.

**References**


1. Aebersold R, Mann M: Mass spectrometry-based proteomics. Nature 422:198-207, 2003
2. Ambrosini G, Cheema HS, Seelman S, et al.: Sorafenib inhibits growth and mitogen-activated protein kinase signaling in malignant peripheral nerve sheath cells. Mol Cancer Ther 7:890-896, 2008
3. Antonescu CR, Dal Cin P, Nafa K, et al.: EWSR1-CREB1 is the predominant gene fusion in angiomatoid fibrous histiocytoma. Genes Chromosomes Cancer 46:1051-1060, 2007
4. Aoki Y, Niihori T, Narumi Y, et al.: The RAS/MAPK syndromes: novel roles of the RAS pathway in human genetic disorders. Hum Mutat 29:992-1006, 2008
5. Barr FG: Translocations, cancer and the puzzle of specificity. Nat Genet 19:121-124, 1998
6. Bignell GR, Greenman CD, Davies H, et al.: Signatures of mutation and selection in the cancer genome. Nature 463:893-898, 2010
7. Blay JY: Pharmacological management of gastrointestinal stromal tumours: an update on the role of sunitinib. Ann Oncol 21:208-215, 2010
8. Borden EC, Baker LH, Bell RS, et al.: Soft tissue sarcomas of adults: state of the translational science. Clin Cancer Res 9:1941-1956, 2003
9. Bos JL: Ras oncogenes in human cancer: a review. Cancer Res 49:4682-4689, 1989
10. Candeliere GA, Glorieux FH, Prud'homme J, et al.: Increased expression of the c-fos proto-oncogene in bone from patients with fibrous dysplasia. N Engl J Med 332:1546-1551, 1995
11. Casali PG, Blay JY: Soft tissue sarcomas: ESMO Clinical Practice Guidelines for diagnosis, treatment and follow-up. Ann Oncol 21 Suppl 5:v198-v203, 2010
12. CDM Fletcher, KK Unni, F Mertens: WHO Classification of tumours. Pathology and genetics of tumours of bone and soft tissue. Lyon, IARC Press, 2002
13. de Alava E: Molecular pathology in sarcomas. Clin Transl Oncol 9:130-144, 2007
14. de Wever O, Mareel M: Role of tissue stroma in cancer cell invasion. J Pathol 200:429-447, 2003
15. Dei Tos AP, Doglioni C, Piccinin S, et al.: Coordinated expression and amplification of the MDM2, CDK4, and HMGI-C genes in atypical lipomatous tumours. J Pathol 190:531-536, 2000
16. Dei Tos AP, Piccinin S, Doglioni C, et al.: Molecular aberrations of the G1-S checkpoint in myxoid and round cell liposarcoma. Am J Pathol 151:1531-1539, 1997
17. Delattre O, Zucman J, Plougastel B, et al.: Gene fusion with an ETS DNA-binding domain caused by chromosome translocation in human tumours. Nature 359:162-165, 1992
18. Downward J: Targeting RAS signalling pathways in cancer therapy. Nat Rev Cancer 3:11-22, 2003
19. Filion C, Motoi T, Olshen AB, et al.: The EWSR1/NR4A3 fusion protein of extraskeletal myxoid chondrosarcoma activates the PPARG nuclear receptor gene. J Pathol 217:83-93, 2009
20. Fujimura Y, Ohno T, Siddique H, et al.: The EWS-ATF-1 gene involved in malignant melanoma of soft parts with t(12;22) chromosome translocation, encodes a constitutive transcriptional activator. Oncogene 12:159-167, 1996
21. Futreal PA: Backseat drivers take the wheel. Cancer Cell 12:493-494, 2007

22. Graadt van Roggen JF: The histopathological grading of soft tissue tumours: current concepts. Current Diagnostic Pathology:1-7, 2001
23. Graadt van Roggen JF, Bovee JVMG, Morreau J, et al.: Diagnostic and prognostic implications of the unfolding molecular biology of bone and soft tissue tumours. J Clin Pathol 52:481-489, 1999
24. Graadt van Roggen JF, Hogendoorn PCW, Fletcher CDM: Myxoid tumours of soft tissue. Histopathology 35:291-312, 1999
25. Guillou L, Coindre JM, Bonichon F, et al.: Comparative study of the National Cancer Institute and French Federation of Cancer Centers Sarcoma Group grading systems in a population of 410 adult patients with soft tissue sarcoma. J Clin Oncol 15:350-362, 1997
26. Heinrich MC, Corless CL, Blanke CD, et al.: Molecular correlates of imatinib resistance in gastrointestinal stromal tumors. J Clin Oncol 24:4764-4774, 2006
27. Heinrich MC, Corless CL, Demetri GD, et al.: Kinase mutations and imatinib response in patients with metastatic gastrointestinal stromal tumor. J Clin Oncol 21:4342-4349, 2003
28. Hogendoorn PCW, Collin F, Daugaard S, et al.: Changing concepts in the pathological basis of soft tissue and bone sarcoma treatment. Eur J Cancer 40:1644-1654, 2004
29. Italiano A, Bianchini L, Gjernes E, et al.: Clinical and biological significance of CDK4 amplification in well-differentiated and dedifferentiated liposarcomas. Clin Cancer Res 15:5696-5703, 2009
30. Joyama S, Ueda T, Shimizu K, et al.: Chromosome rearrangement at 17q25 and xp11.2 in alveolar soft-part sarcoma: A case report and review of the literature. Cancer 86:1246-1250, 1999
31. Khosravi-Far R, Der CJ: The Ras signal transduction pathway. Cancer Metastasis Rev 13:67-89, 1994
32. Kindblom LG, Angervall L: Histochemical characterization of mucosubstances in bone and soft tissue-tumors. Cancer 36:985-994, 1975
33. Kirsch DG, Dinulescu DM, Miller JB, et al.: A spatially and temporally restricted mouse model of soft tissue sarcoma. Nat Med 13:992-997, 2007
34. Kolker E, Higdon R, Hogan JM: Protein identification and expression analysis using mass spectrometry. Trends Microbiol 14:229-235, 2006
35. Ladanyi M, Gerald W: Fusion of the EWS and WT1 genes in the desmoplastic small round cell tumor. Cancer Res 54:2837-2840, 1994
36. Lania AG, Mantovani G, Spada A: Mechanisms of disease: Mutations of G proteins and G-protein-coupled receptors in endocrine diseases. Nat Clin Pract Endocrinol Metab 2:681-693, 2006
37. Levine AJ: p53, the cellular gatekeeper for growth and division. Cell 88:323-331, 1997
38. McDonnell LA, Corthals GL, Willems SM, et al.: Peptide and protein imaging mass spectrometry in cancer research. J Proteomics 2010; 222 (4) :400-9.
39. Meng GZ, Zhang HY, Bu H, et al.: Low-grade fibromyxoid sarcoma versus fibromatosis: a comparative study of clinicopathological and immunohistochemical features. Diagn Cytopathol 37:96-102, 2009
40. Mentzel T: Biological continuum of benign, atypical, and malignant mesenchymal neoplasms - does it exist? J Pathol 190:523-525, 2000
41. Mentzel T, Calonje E, Wadden C, et al.: Myxofibrosarcoma. Clinicopathologic analysis of 75 cases with emphasis on the low-grade variant. Am J Surg Pathol 20:391-405, 1996
42. Mitelman F, Johansson B, Mertens F: The impact of translocations and gene fusions on cancer causation. Nat Rev Cancer 7:233-245, 2007
43. Mohseny AB, Szuhai K, Romeo S, et al.: Osteosarcoma originates from mesenchymal stem cells in consequence of aneuploidization and genomic loss of Cdkn2. J Pathol 219:294-305, 2009
44. Moller E, Stenman G, Mandahl N, et al.: POU5F1, encoding a key regulator of stem cell pluripotency, is fused to EWSR1 in hidradenoma of the skin and mucoepidermoid carcinoma of the salivary glands. J Pathol 215:78-86, 2008
45. Niini T, Lopez-Guerrero JA, Ninomiya S, et al.: Frequent deletion of CDKN2A and recurrent coamplification of KIT, PDGFRA, and KDR in fibrosarcoma of bone--an array comparative genomic hybridization study. Genes Chromosomes Cancer 49:132-143, 2010
46. O'Brien KP, Seroussi E, Dal CP, et al.: Various regions within the alpha-helical domain of the COL1A1 gene are fused to the second exon of the PDGFB gene in dermatofibrosarcomas and giant-cell fibroblastomas. Genes Chromosomes Cancer 23:187-193, 1998
47. Oda Y, Takahira T, Kawaguchi K, et al.: Altered expression of cell cycle regulators in myxofibrosarcoma, with special emphasis on their prognostic implications. Hum Pathol 34:1035-1042, 2003

48. Oda Y, Yamamoto H, Takahira T, et al.: Frequent alteration of p16(INK4a)/p14(ARF) and p53 pathways in the round cell component of myxoid/round cell liposarcoma: p53 gene alterations and reduced p14(ARF) expression both correlate with poor prognosis. J Pathol 207:410-421, 2005
49. Ordonez JL, Osuna D, Garcia-Dominguez DJ, et al.: The clinical relevance of molecular genetics in soft tissue sarcomas. Adv Anat Pathol 17:162-181, 2010
50. Panagopoulos I, Hoglund M, Mertens F, et al.: Fusion of the EWS and CHOP genes in myxoid liposarcoma. Oncogene 12:489-494, 1996
51. Pervaiz N, Colterjohn N, Farrokhyar F, et al.: A systematic meta-analysis of randomized controlled trials of adjuvant chemotherapy for localized resectable soft-tissue sarcoma. Cancer 113:573-581, 2008
52. Pierotti MA, Santoro M, Jenkins RB, et al.: Characterization of an inversion on the long arm of chromosome 10 juxtaposing D10S170 and RET and creating the oncogenic sequence RET/PTC. Proc Natl Acad Sci U S A 89:1616-1620, 1992
53. Prenen H, Cools J, Mentens N, et al.: Efficacy of the kinase inhibitor SU11248 against gastrointestinal stromal tumor mutants refractory to imatinib mesylate. Clin Cancer Res 12:2622-2627, 2006
54. Rajakulendran T, Sahmi M, Lefrancois M, et al.: A dimerization-dependent mechanism drives RAF catalytic activation. Nature 461:542-545, 2009
55. Rao VV, Schnittger S, Hansmann I: G protein Gs alpha (GNAS 1), the probable candidate gene for Albright hereditary osteodystrophy, is assigned to human chromosome 20q12-q13.2. Genomics 10:257-261, 199161.
56. Rego EM, Pandolfi PP: Reciprocal products of chromosomal translocations in human cancer pathogenesis: key players or innocent bystanders? Trends Mol Med 8:396-405, 2002
57. Riggi N, Cironi L, Provero P, et al.: Expression of the FUS-CHOP fusion protein in primary mesenchymal progenitor cells gives rise to a model of myxoid liposarcoma. Cancer Res 66:7016-7023, 2006
58. Romeo S, Debiec-Rychter M, Van Glabbeke M, et al.: Cell cycle/apoptosis molecule expression correlates with imatinib response in patients with advanced gastrointestinal stromal tumors. Clin Cancer Res 15:4191-4198, 2009
59. Romeo S, Dei Tos AP: Soft tissue tumors associated with EWSR1 translocation. Virchows Arch 456:219-234, 2010
60. Rossi S, Szuhai K, Ijszenga M, et al.: EWSR1-CREB1 and EWSR1-ATF1 fusion genes in angiomatoid fibrous histiocytoma. Clin Cancer Res 13:7322-7328, 2007
61. Schrage YM, Lam S, Jochemsen AG, et al.: Central chondrosarcoma progression is associated with pRb pathway alterations: CDK4 down-regulation and p16 overexpression inhibit cell growth in vitro. J Cell Mol Med 13:2843-2852, 2009
62. Schvartzman JM, Sotillo R, Benezra R: Mitotic chromosomal instability and cancer: mouse modelling of the human disease. Nat Rev Cancer 10:102-115, 2010
63. Scott JE, Dorling J: Differential staining of acid glycosaminoglycans (mucopolysaccharides) by alcian blue in salt solutions. Histochemie 5:221-233, 1965
64. Shimizu A, O'Brien KP, Sjoblom T, et al.: The dermatofibrosarcoma protuberans-associated collagen type I alpha1/platelet-derived growth factor (PDGF) B-chain fusion gene generates a transforming protein that is processed to functional PDGF-BB. Cancer Res 59:3719-3723, 1999
65. Snyder EL, Sandstrom DJ, Law K, et al.: c-Jun amplification and overexpression are oncogenic in liposarcoma but not always sufficient to inhibit the adipocytic differentiation programme. J Pathol 218:292-300, 2009
66. Stenman G, Andersson H, Mandahl N, et al.: Translocation t(9;22)(q22;q12) is a primary cytogenetic abnormality in extraskeletal myxoid chondrosarcoma. Int J Cancer 62:398-402, 1995
67. Tomlins SA, Rhodes DR, Perner S, et al.: Recurrent fusion of TMPRSS2 and ETS transcription factor genes in prostate cancer. Science 310:644-648, 2005
68. Vallar L, Spada A, Giannattasio G: Altered Gs and adenylate cyclase activity in human GH-secreting pituitary adenomas. Nature 330:566-568, 1987
69. Virchow RLK: in Hirschwald (ed): Die cellularpathologie in ihrer Begrundung auf physiologische und patholo gische Gewebelehre. Berlin, 1858, pp 625-626
70. Wardelmann E, Thomas N, Merkelbach-Bruse S, et al.: Acquired resistance to imatinib in gastrointestinal stro mal tumours caused by multiple KIT mutations. Lancet Oncol 6:249-251, 2005
71. Weinstein LS, Liu J, Sakamoto A, et al.: Minireview: GNAS: normal and abnormal functions. Endocrinology 145:5459-5464, 2004
72. Weterman MA, Wilbrink M, Geurts van KA: Fusion of the transcription factor TFE3 gene to a novel gene, PRCC, in t(X;1)(p11;q21)-positive papillary renal cell carcinomas. Proc Natl Acad Sci U S A 93:15294-15298, 1996

73. Widakowich C, de CG, Jr., de Azambuja E, et al.: Review: side effects of approved molecular targeted therapies in solid cancers. Oncologist 12:1443-1455, 2007
74. Willems SM, Debiec-Rychter M, Szuhai K, et al.: Local recurrence of myxofibrosarcoma is associated with increase in tumour grade and cytogenetic aberrations, suggesting a multistep tumour progression model. Mod Pathol 19:407-416, 2006
75. Willems SM, Wiweger M, Graadt van Roggen JF, et al.: Running GAGs: myxoid matrix in tumor pathology revisited : What's in it for the pathologist? Virchows Arch 456:181-192, 2010

# Chapter 2

## Running GAGs: myxoid matrix in tumor pathology revisited. What's in it for the pathologist?

Stefan M. Willems[1], Malgorzata Wiweger[1], J. Frans Graadt van Roggen[2] and Pancras C. W. Hogendoorn[1]

[1]Department of Pathology, Leiden university Medical Center, L1Q, P.O. Box 9600, 2300 RC Leiden, The Netherlands, [2]Department of Pathology, Diaconessenhuis Hospital, Leiden, The Netherlands

**Abstract**

Ever since Virchow introduced the entity myxoma, abundant myxoid extracellular matrix (ECM) has been recognized in various reactive and neoplastic lesions. Nowadays, the term "myxoid" is commonly used in daily pathological practice. But what do today's pathologists mean by it, and what does the myxoid ECM tell the pathologist? What is known about the exact composition and function of the myxoid ECM 150 years after Virchow? Here, we give an overview of the composition and constituents of the myxoid ECM as known so far and demonstrate the heterogeneity of the myxoid ECM among different tumors. We discuss the possible role of the predominant constituents of the myxoid ECM and attempt to relate them to differences in clinical behavior. Finally, we will speculate on the potential relevance of this knowledge in daily pathological practice.

## Historical perspective

In his 1858 masterpiece Cellularpathologie, Rudolph Virchow introduced the term "myxoma" to describe a soft tissue tumor, histologically resembling the structure of the umbilical cord (Figs. 1 and 2) [1]. This description of myxoma was adopted in the seventh edition of the Medical Lexicon by Robley Dunglison who remarkably added that "[myxoma] was for the first time described in 1838 by Johannes Müller as

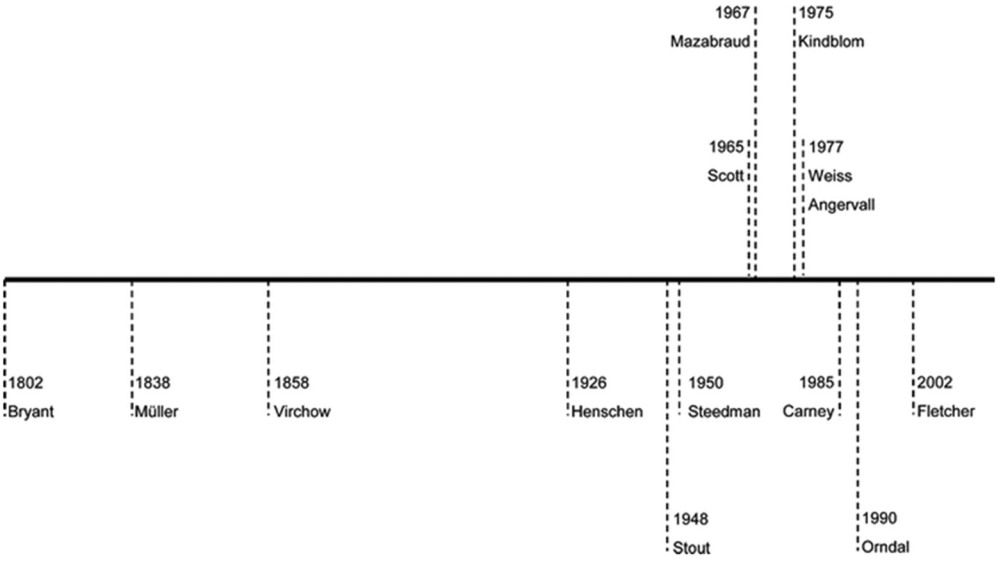


**Figure 1:** Timetable with key events in studies on myxoid tumors of soft tissue. Though Müller already mentioned tumors with a macroscopically gelatinous appearance in 1838 [3], it was in 1858 when Virchow introduced the term myxoma to describe tumors which morphologically resembled the jelly structure of the umbilical cord [1]. Ever since, the term myxosarcoma, introduced by Bryant in 1802 was reserved for the malignant counterparts [4]. Because of their morphologically overlapping features, both terms were used interchangeably, which was mentioned by Stout in 1948 as unwise, warranting for macroscopical and microscopical criteria for the reliable differential diagnosis between the two entities [5]. The relationship between myxomas and fibrous dysplasia was first described in 1926 by Henschen [90], though it was Mazabraud who proposed it as a syndrome in 1967 [91]. The association of cardiac/cutaneous myxomas, hyperpigmentation of the skin, and endocrine overactivity was only recognized in 1985 by Carney [43]. Progress in the study of the myxoid ECM was made by the invention of the alcian blue staining in 1950 by Steedman [9], and Scott who developed the CEC method to distinguish the different GAGs in 1965 [10]. Based upon this technique, Kindblom showed in 1975 that different bone and soft tissue tumors (including myxoid ones) contained different GAGs [11]. From the late 1980s, it became clear that the ECM is a key player in tumor development and tumor progression, sustained by an exponentially growing number of publications [40]. As myxoid areas were now being recognized as an intrinsic part of a subset of tumors, Weiss and Angervall simultaneously described the myxoid variant of malignant fibrous histiocytoma/myxofibrosarcoma as a distinct entity [92, 93]. Parallel to morphological classification, an increasing number of myxoid tumors showed specific molecular genetics aberrations, such as (activating) mutations and translocations. The concept of malignant progression in myxoid tumors of soft tissue (i.e., myxoid liposarcoma) due to chromosomal instability and subsequent secondary genetic events was described in 1990 by Orndal et al. [94]. Nowadays, classification of myxoid tumors of soft tissues is based upon clinicopathological and molecular/cytogenetic aberrations as published in the 2002 WHO classification [7].

Collonema" [2]. Müller used the term collonema (κολλα = glue) for "peculiar gelatinous tumours, consisting of a remarkably soft gelatiniform tissue, which trembles on being touched" [3]. Though this description is applicable to most myxoid tumors, it holds also for many nonmyxoid tumors and it is not particularly clear which tumor type Müller had in mind. Today, it has been generally accepted that it was indeed Virchow who introduced myxoma as an entity. The introduction of this new histological concept of tumors containing myxoid (μυξα = "mucus" and ειδος = "resemblance") areas soon led to the recognition of new entities, such as myxadenoma, myxochondroma, myxofibroma, and myxoneuroma [2]. The term myxosarcoma, introduced in 1802 by

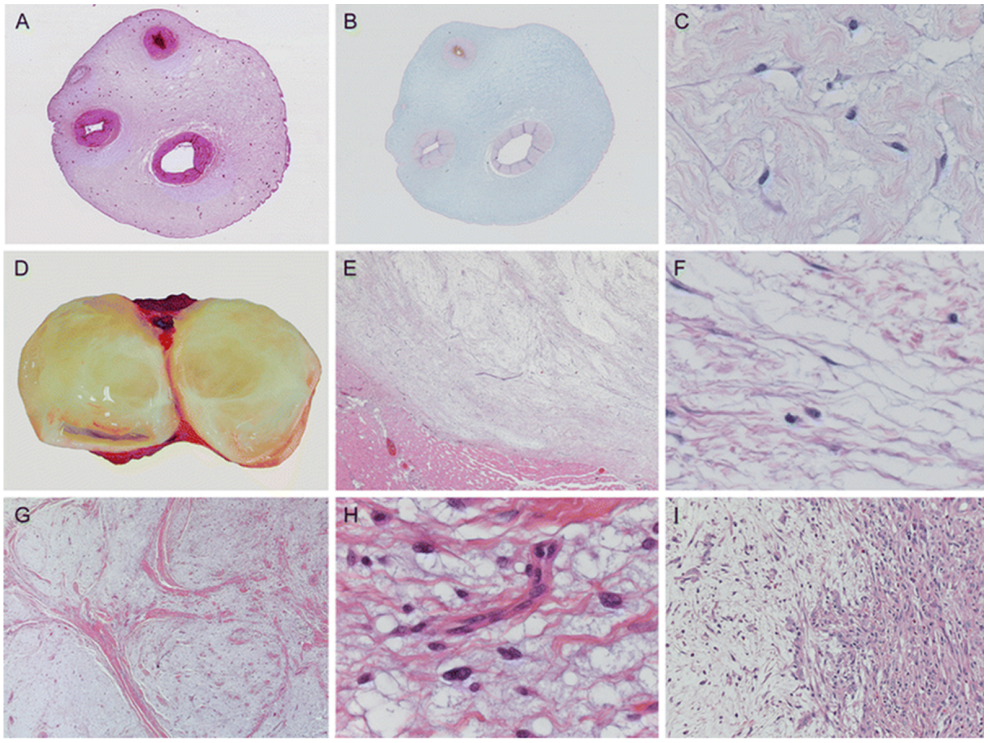


**Figure 2:** Characteristic macroscopy and histomorphology of the myxoid ECM. Rudolph Virchow introduced the term myxoma for those tumors morphologically resembling Wharton's jelly of the umbilical cord (a), which contains large amounts of GAGs as detected by alcian blue (b). High-power image of Wharton's jelly showing abundant myxoid ECM containing fibrillary collagens, interspersed between myofibroblast-like stroma cells (c). Intramuscular myxoma characteristically has a gelatinous appearance on cut surface (d) and is well circumscribed towards its peripheral tissue (e). On higher magnification, it shows the same abundant myxoid ECM as the umbilical cord (c) and no significant atypia of the sparse tumor cells (f). Histological criteria are still a hallmark of diagnosis, showing characteristic lobulated, hypocellular morphology of grade I myxofibrosarcoma at low magnification (g).Curvilinear blood vessels are often seen in grade I myxofibrosarcoma (but are not diagnostic), whereas tumor cells show vesicular, slightly atypical nuclei compared to intramuscular myxoma (h). Another hallmark of myxofibrosarcoma is areas with abrupt transition of grade (i) which was already mentioned by Mentzel et al. [95].

Bryant [4], became reserved for malignant tumors and defined as "a mucous transformation of round-celled sarcoma, malignant, and of large volume, usually attacking the omentum and the skin" [2]. Nowadays, myxoid changes/areas are recognized in both benign and malignant neoplasms (primarily classified as mesenchymal or epithelial) as well as non-neoplastic (reactive) lesions (Fig. 3).

In his first description, Virchow had already recognized the recurrent nature of some myxomatous tumors [1] and it became clear that it was difficult to predict the exact clinical behavior of these different tumors based on their myxoid morphology alone. Subsequently, the terms myxoma and myxosarcoma were used interchangeably till Arthur Stout recognized this as unwise [5] because "myxomas do not metastasize and there is no way to anticipate differences in their growth energy from their histopathology." Later studies confirmed the distinction between both entities on the basis of macroscopical and microscopical features (necrosis, nuclear atypia, and mitotic figures; Fig. 2) [6]. Today, myxoid tumors of soft tissue are classified according to the World Health Organization (WHO) formulation based on clinicopathological criteria and specific molecular/cytogenetic aberrations (Table 1) [7, 8]. So what is left of the term "myxoid" 150 years after Virchow? What do today's pathologists mean by it, and what

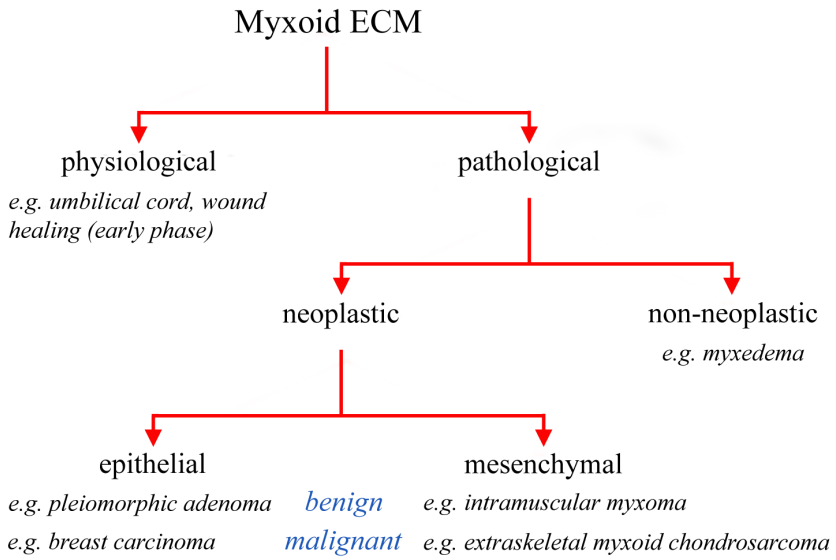


**Figure 3:** Myxoid ECM is a ubiquitously histological feature in physiological and pathological conditions. Myxoid ECM is a morphological feature in physiological and pathological conditions, such as in myxedema due to increased production of HA. Myxoid areas/changes are also commonly present in tumors (both of epithelial and mesenchymal origin). In epithelial tumors, myxoid changes are often a secondary phenomenon, whereas in mesenchymal tumors, they are more frequently an intrinsic part of the tumor entity. This group of so-called myxoid tumors of soft tissues contains an increasing number of entities (e.g., myxofibrosarcoma, formerly called myxoid variant of malignant fibrous histiocytoma), sometimes sustained by specific distinct molecular/cytogenetic aberrations (e.g., myxoid liposarcoma).

does the myxoid extracellular matrix (ECM) tell the pathologist? What is the exact composition of this myxoid ECM and does it have a function? Here, we give an overview of the composition and constituents of the myxoid ECM as known so far and demonstrate the heterogeneity of the myxoid ECM among different tumors. We discuss the possible role of the predominant constituents of the myxoid ECM and attempt to relate them to differences in clinical behavior. Finally, we will speculate on the potential relevance of this knowledge in daily pathological practice.

## Composition of the myxoid extracellular matrix

### *Glycosaminoglycans and proteoglycans*

Substantial progress in the study of the myxoid ECM was made after the introduction of alcian blue staining in 1950 [9]. John Scott was one of the pioneers who used this

**Table 1:** Myxoid tumors of soft tissue: overview of clinicopathological and genetic features

| Myxoid tumors of soft tissue | Age | Sex | Predilection site | Molecular/cytogenetic aberrations | References |
|---|---|---|---|---|---|
| **Benign** | | | | | |
| Intramuscular myxoma (including its cellular variant) | Adults | F>M | Thigh, shoulder, buttocks, and rarely upper arm | GNAS1 mutations | [34] |
| Myxoid neurothekeoma | Young adults | F>M | Head, neck, and shoulders | Loss of 22q | [8] |
| Myxoid lipoma (myxolipoma) | Any age | F=M | Head and neck | Rearrangement of 13q and/or 16q | [8] |
| Myxoid chondroma | Adults | M>F | Hands and feet | Extra copies of chromosome 5 or 12q13–15 rearrangement | [8] |
| Myxoid neurofibroma | Any age | M=F | All over the body | NF1 mutations | [8] |
| Myxoid dermatofibroma | Young adults | F>M | Lower extremities | Unknown | [42] |
| Cardiac myxoma | Adults | F>M | Atria (predominantly left) | PRKAR1α mutations in Carney complex | [43] |
| Ossifying fibromyxoid tumor | Elderly | M>F | Extremities and trunk | Nonspecific cytogenetic aberrations | [8] |
| Cutaneous myxoid cyst | Any age | F>M | Distal and dorsal portions of fingers (and toes) | Unknown | [8] |
| Cutaneous myxoma (superficial angiomyxoma) | Adults | M>F | Trunk, lower extremities, head, and neck | PRKAR1α mutations in Carney complex | [43] |
| Myxoid nodular fasciitis | Young adults | M=F | Head, neck, and extremities | Nonspecific cytogenetic aberrations | [8, 44] |
| **Locally aggressive** | | | | | |
| Odontogenic myxoma | Young adults | F>M | Mandible and maxilla | PRKAR1α mutations in rare cases (not Carney complex) | [45] |
| Myxoinflammatory fibroblastic sarcoma | Adults | M=F | Feet, lower leg | t(1;10)(p22;q24) and amplification of chromosome 3 | [46] |
| Aggressive angiomyxoma | Adults | F>>M | Inguinal region | Rearrangement of 12q13-15 | [8] |
| **Malignant** | | | | | |
| Myxofibrosarcoma | Elderly | M=F | Extremities, thigh | Nonspecific cytogenetic aberrations | [47, 48] |
| Extraskeletal myxoid chondrosarcoma | Adults | M>F | Extremities and limb | t(9;22)(q22;q12), t(9;17)(q22;q11) or t (9;15)(q22;q21) | [49] |
| Low-grade fibromyxoid sarcoma | Young adults | M>F | Proximal extremities and trunk | t(7,16) (q33;p11) | [50] |
| Myxoid liposarcoma | Elderly | M>F | Lower extremities and thigh | t(12;16)(q13;p11) or t(12;22)(q13;q12) | [51] |
| Myxoid leiomyosarcoma of soft tissue | Adults | F>>M | Limbs, female genitalia, head, and neck | Nonspecific cytogenetic aberrations | [52] |
| Myxoid malignant peripheral nerve sheath tumor | Adults | F=M | Extremities, trunk | NF1 and TP53 mutations, P16 deletions | [8, 53] |
| Myxoid dermatofibrosarcoma | Adults | M=F | Trunk, groin, and extremities | t(17;22)(q22;q13) | [54] |

histochemical stain to distinguish between the different glycosaminoglycans (GAGs) in tissue sections [10]. Kindblom et al. showed that the myxoid ECM of various (non)neoplastic tissues, i.e., Wharton's jelly and myxoid tumors of soft tissue, contained large amounts of GAGs (Figs. 1 and 2) [11]. GAGs are large macromolecules abundantly present in pericellular and extracellular matrices and consist of unbranched polysaccharide chains of disaccharides which are often sulfated. There are six different types of GAGs: hyaluronic acid (HA), keratin sulfate, chondroitin sulfate, dermatan sulfate, heparan sulfate, and heparin [12]. GAGs form proteoglycans (PGs) once covalently attached to specific core proteins. Core proteins of PGs are synthesized in the endoplasmic reticulum and post-translationally modified as they pass through the Golgi apparatus where hexuronic acid and hexosamine groups are attached. The exception is HA, which is synthesized directly under the cytoplasmic membrane by the hyaluronic acid synthetases 1, 2, and 3 [12]. The most common classification of the different PGs is based upon the properties of the core protein. The three main PG families present in the ECM are lecticans, small leucine-rich proteoglycans (SLRPs), and other ECM PG [13]. Lecticans always contain both a hyaluronan-binding domain and a C-type lectin domain. The lectican family includes: aggrecan, versican, neurocan, and brevican that can be found at different locations (Table 3) [12]. SLRPs can be found extracellularly and intracellularly and at the cell surface. They contain nine to 12 tandem repeats of leucine-rich motifs which involve their collagen-binding domains. The SLRP family includes decorin, biglycan, asporin, ECM protein 2, keratocan, proline/arginine-rich and leucine-rich repeat proteins, osteoadherin, lumican, fibromodulin, opticin, epiphycan, osteoglycin, podocan, chondroadherin, and nyctalopin [14]. ECM PGs do not show significant homology in the content of their core proteins. Perlecan, agrin, and collagen types XV and XVIII belong in this family [14]. Various GAGs and PGs have been identified in the myxoid ECM (Table 2): HA is the most common; none of them are specific for one particular lesion.

*Collagens*

One of the first papers addressing myxoma and its malignant counterpart ("myxosarcoma") mentioned the presence of fibrillary collagens as a hallmark for differential diagnosis [6]. Though this criterion did not last long, collagens (κολλα = glue; γηνε = that which produces) are a main component of the myxoid ECM. They are characterized by their regular, triple-stranded helix of so-called alpha-chains forming cord-like strands of 300 nm in length and 1.5 nm in diameter. A separate group of collagens is formed by the fibril-associated collagens with interrupted triple helices (FACIT) and includes collagen types XII and XIV. These collagens have several triple helical domains (collagen type domains [Col]) separated by nontriple helical domains (NC). All collagens contain large amounts of proline and glycine as well as hydroxyproline and hydroxylysine which are formed by post-translational modification. Based on their biochemical differences, more than 30 different types of collagens are

**Table 2:** The composition of the myxoid ECM is heterogeneous but not lesion-specific

| | Proteoglycans | Collagens (types) | Other ECM components | References |
|---|---|---|---|---|
| **Non-neoplastic myxoid lesions** | | | | |
| Follicular mucinosis | HA | | | [55] |
| Myxedema | HA | I (III) | | [56, 57] |
| Stenotic arteries | Versican, biglycan, perlecan, HA | I | TBFbeta1 | [58, 59] |
| Pseudoaneurysm | Versican | | | [60] |
| Endocardiosis | HA | | | [61] |
| Valvular degeneration of the heart | | I, III | | [62] |
| **Myxoid tumors of soft tissue** | | | | |
| Intramuscular myxoma | KS, HA, C4S, C6S | I, VI | Albumin, IgGs | [20, 34] |
| Myxofibrosarcoma | KS, HA, C4S, C6S | I, VI, XII, XIV | Thrombospondin Albumin, IgGs | [8, 20, 34] |
| Extraskeletal myxoid chondrosarcoma | C4S, C6S, HA (aggrecan) | I, III, VI (II, IV) | Albumin, IgGs | [20, 63] |
| Odontogenic myxoma | C4S, C6S, DS, KS, HS, aggrecan, versican, biglycan, decorin | | | [64] |
| Low-grade fibromyxoid sarcoma | HA | | | [65] |
| Myxoid neurothekeoma | HA | | | [66] |
| Myxoid lipoma (myxolipoma) | HA | | | [67] |
| Myxoid liposarcoma | HA | | FN | [68] |
| Myxoid chondroma | HA, KS | | | [69] |
| Myxoid neurofibroma | HA, C4S, C6S | | | [69] |
| Chondromyxoid fibroma | Aggrecan | I, III, VI | | [70] |
| Myxoid dermatofibroma | HA | | | [71] |
| Myxoid leiomyosarcoma | HA | | | [72] |
| Cardiac myxoma | C4S, C6S, (HA) | | | [73] |
| Ossifying fibromyxoid tumor | | IV (II) | | [74, 75] |
| Myxoinflammatory fibroblastic sarcoma | | | A1AT, A1ACT | [76] |
| Cutaneous myxoid cyst | HA | | | [77] |
| Aggressive angiomyxoma | HA | | | [78] |
| Cutaneous myxoma (superficial angiomyxoma) | HA | | | [79] |
| **Myxoid areas in epithelial tumors** | | | | |
| Breast carcinoma | Aggrecan, versican, HA | I, II, IV | | [80] |
| Pleiomorphic adenoma | Lumican, perlecan, aggrecan, C4S, C6S, DS, KS, HA | I, III, IV | FGF2, Tenascin, FN, ChM-I | [81–83] |
| Vulvar squamous cell carcinoma | | | CD44, TGF-beta3 | [84] |
| Mixed tumor of skin | | IV | Tenascin, FN | [85] |
| Cholangiocarcinoma | Perlecan | | | [86] |
| **Miscellaneous tumors (nonsoft tissue, nonepithelial)** | | | | |
| Myxopapillary ependymoma | HA, CS, HS | | | [87] |
| Myxoid mesothelioma | HA | | | [88] |
| Myxoid meningioma | HA, CS | | | [89] |

recognized [15]. The most common types are I, II, III, and IV, which account for 90% of all collagens in humans. Except for collagen II, which is predominantly present in cartilage, collagen types I, III, and IV as well as VI, XII, and XIV may be found in the myxoid ECM (Table 2).

*Other ECM molecules*

Other structural molecules identified in the myxoid ECM are fibronectin and tenascin C (Table 2). Fibronectin is a fibril-forming glycoprotein existing in a dimeric or

multimeric form. Each monomer contains several binding sites for fibrin, heparin, DNA, and cells. Fibronectin molecules consist of different repeats (types I, II, and III) and three different sites that can be alternatively spliced (EDA, EDB, and V). The dimeric, soluble form is produced by hepatocytes and lacks the alternative EDA and EDB variants. The multimeric form is extensively present in granulation tissue, basement membrane, and on cell surfaces and contains variable proportions of the EDA and EDB domains [16]. Until now, fibronectin has only been found in myxoid liposarcoma but might also be present in the ECM of other myxoid lesions (Table 2). Tenascin C is a highly conserved glycoprotein of the ECM consisting of 300 kDa monomers, characteristically assembled in 1,800 kDa hexamers [17, 18]. It consists of several functionally independent domains of which the number is dramatically increased by alternative splicing. The N-terminal contains the cysteine-rich assembly domain, followed by EGF-like repeats, eight constant and up to nine alternatively spliced fibronectin type III repeats and a C-terminal fibrinogen-like globular domain [18]. Till today, its presence has only been shown in myxoid areas of epithelial but not (yet) in mesenchymal tumors (Table 2).

**Functional role of the different constituents in the myxoid extracellular matrix**

*Glycosaminoglycans*

GAGs have both biophysical and biochemical functions and play important roles in physiologic and neoplastic processes (Table 3) [19]. Due to their high content of sulfate and carboxyl groups, complex patterns of sulfation and uronic acid epimerizations, GAG chains confer upon PGs the diverse capacities to function as ideal physiological barriers, reservoirs for signaling proteins, and binding partners for structural macromolecules [13]. We have shown that the myxoid ECM in soft tissue tumors is heterogeneous in composition and that the relative amount of each GAG is tumor-type- and tumor-grade-dependent [20]. Because of their negative charge, all GAGs, especially HA, are able to trap water molecules. Interestingly, HA is the common denominator in the myxoid ECM (Table 2). This suggests that HA is the major contributor to the edematous appearance of the myxoid ECM. As a result of the biophysical properties of GAGs (their high viscosity and low compressibility), they are ideal for tissue lubrication. On the other hand, their rigidity is responsible for the structural integrity of tissues facilitating diffusion of metabolites and cell migration [21]. The biochemical properties of GAGs are mediated by specific binding to other macromolecules. GAGs can bind to secreted proteases and antiproteases, growth factors, structural ECM proteins, and proteins expressed on (tumor) cells [22]. Chondroitin sulfate modulates cell fate as it appears to prevent apoptosis and is involved in cell proliferation. Since chondroitin sulfate is much more abundant in the ECM of extraskeletal myxoid chondrosarcoma compared to intramuscular myxoma and myxofibrosarcoma, it might, therefore, play a role in the more malignant behavior of

**Table 3:** GAGs and PGs: their role in physiology and pathologic processes [19]

| | Type and presence | Physiology | Pathology |
|---|---|---|---|
| C4S (CS-A) | Sulfated galactosaminoglycan; cartilage, skin and tendon | Binds $Ca^{2+}$, $Cu^{2+}$ and $Fe^{2+}$ ions; antioxidant (better then C6S and HA) | Decreased in OA, mediate adherence of plasmodium infected red blood cells |
| C6S (CS-C) | Sulfated galactosaminoglycan; cartilage, brain secretory granules | Reduces proinflammatory cytokines, MMPs, NO, and apoptosis | Laryngeal cancer, decreased in OA, increased in early atherosclerotic lesions |
| DS (CS-B) | Sulfated galactosaminoglycan; skin, blood vessels, heart, tendons, lungs | Regulation ECM integrity and cellular signaling; DS selectively activates heparin cofactor II that inactivates thrombin; carcinogenesis, wound repair, and fibrosis; DS binds water, coagulation | Dermatan sulfate accumulates abnormally in several of the mucopolysaccharidosis disorders and in myxomatous degeneration. Involved in cardiovascular disease, infection, fibrosis |
| HA | Lack sulfation and epimerization of glucuronic acid moiety to uronic acid, the only GAG synthesized in the cytoplasm at the plasma membrane and also the only GAG that is synthesized without core protein. Connective, epithelial and neural tissue. abundant in cartilage and bone | Early development, tissue organization, cell proliferation, facilitate migration and condensation of mesenchymal cells, participates in joint cavity formation, binds and immobilizes aggrecan, regulates osteoblast and osteoclast function. HA works as a scaffold for building PGs, suppresses cartilage degeneration and reduce pain perception, associated with cell adhesion and motility, suppresses prostaglandin E2 and IL-1 production, activates SRC, FAK, ERK and PKC whereas interaction with CD44 also regulates ERBB, PI3K, regu lates phosphorylation of BAD and hence promotes cell survival, contributes to cell proliferation and migration, bone turn over, involved in tissue repair in skin, binds to receptor CD44 | Used for treatment of osteoarthritis |
| HS | Sulfated glucosaminoglycan; all types of cells, highly abundant in ECM of the skeleton | Coreceptors for morphogens, sequester growth factors and cytokines to regulate cell differentiation and growth, compose ECM scaffolds that make physical separation of the niche from cellular and signaling influence of surrounding environment, involved in skeletal patterning, differentiation, growth and homeostasis, critical for hematopoietic stem cell inch, Ndst1 mutation causes brain/skull defects and lung surfactant problems resulting in perinatal lethality, Ndst2 mutant have defective granule formation in mast cells, stimulates angiogenesis, osteocastogenesis, skeletal patterning, differentiation and homeostasis, coreceptor for morphogens, sequester growth factors and cytokines to regulate cell differentiation and growth, FGF-binding, binds fibronectin | Sequesters chemokines or FGF towards migrating tumor cells, promotes metastasis, multiple osteochondromas (MO)—benign bone cartilaginous tumor caused by mutant in EXT1 or EXT2, accumulated in mucopolysaccharidoses |
| KS | Sulfated glucosaminoglycan; N-glycan KSI or O-glycan KSII. Highly abundant in cornea and cartilage. Also found in epithelial tissue, central nervous system | Maintains proper special organization of the type I collagen fibrils and promotes transparency of cornea, cellular recognition of protein ligands, cell motility | Corneal opacity and corneal dystrophy (KS lacks GleNAc sulfation), epithelial-derived carcinoma cells, alerted sulfation levels of KS was found in brain of Alzheimer patients |
| Aggrecan | O- and N-linked KSII, CS, DS, KS (HS absent), cartilage | Maintains tissue hydration, contributes to the mechanical properties of tissue, inhibits migration of neural crest cells, null mice show cartilage defects and delay in bone development | Chondrodystrophy, nanomelia, cartilage matrix deficiency (CMD), murine brachymorphism (bm), spondyloepimetaphyseal dysplasia enhanced expression in chondroblastoma, chondroma, chondrosarcoma, osteosarcoma, decreased in squamous cell carcinoma chondrodystrophy, nanomelia, |

| | Type and presence | Physiology | Pathology |
|---|---|---|---|
| | | | cartilage matrix deficiency, spondyloepimataphyseal dysplasia |
| Biglycan | CS, DS (HS absent), bone, cartilage, skin, connective tissue | Activates cell division, organization of collage fibers, increased in vascular injury, upregulates p27 and downregulates cyclin A and proliferating cell nuclear antigen, maintaining proper number of mature osteoblasts and survival of bone marrow stromal cells, organization of collagen fibers, regulator of cell cycle, binds TGF-beta | Overexpressed in pancreatic cancer and hyperplasic thymus osteoporosis |
| Decorin | CS, DS (HS absent), connective tissue, cornea | Inhibits collagen fiber formation by interaction with col I, col II, and col VI, inhibits cell division, adhesion, increased in vascular injury, downregulates Erbb2 and MAP kinases, upregulates p21 CDK inhibitor leading to inhibition of cell proliferation and specific induction of apoptosis in transformed cells. maintaining proper number of mature osteoblasts and maintaining survival of bone marrow stromal cells, bind nonfibril collagens XII and XIV, regulates cell proliferation, binds TGF-beta, mediates EGF signaling by binding to EGFR | Antiproliferative properties in tumor growth, overexpressed in colorectal carcinoma, colon adenocarcinoma, melanoma, osteosarcoma, basal cell carcinoma, inhibits migration of MG-63 osteosarcoma cells, reduced decorin levels were found in lung adenocarcinoma, squamous carcinoma, breast carcinoma, hepatocellular carcinoma and ovarian tumors, may regulate tumor angiogenesis, overexpression is often associated with shift from DS to CS, osteoporosis |
| Lumican | KS, cornea | Upregulates p27 and downregulates cyclin A and proliferating cell nuclear antigen, regulates collagen fibril organization and circumferential growth, corneal transparency, and epithelial cell migration and tissue repair | Upregulated in pancreatic, colorectal and breast cancers, stroma of salivary pleiotropic adenoma, reduced expression is correlated with progression of breast carcinoma |
| Perlecan | HS, CS, cartilage, limb bud mesenchyme, articular cartilage, bone marrow stroma, all basal membranes, vasculature | Growth factor signaling, collagen fibrillogenesis, structural stability, vasculogenesis, endorepellin, antiangiogenic factor, chondrocyte proliferation and differentiation, collagen I and II fibrillogenesis, vasculogenesis, mediator of Shh signaling, Wnt signaling, TGF-beta signaling in the skeleton, regulates FGF2 signaling | Schwartz–Jampel syndrome, dyssegmental dysplasia Silverman–Handmaker type (DDSH), perlecan-null embryo chondroplasia, prostate tumor metastasis |
| Versican | C6S>C4S>DS (HS, KS absent), connective tissue, aorta, brain; fibroblasts. important for vascular biology | Lipid retention, modification and accumulation, hydration of ECM, cell proliferation, migration, embryo development, binds HA, CD44, and chemokines | Promotes tumor growth and spread, expressed in the stroma of nearly all human cancers (prostate, breast, lung, ovarian cancers and odontogenic tumors, melanoma, brain tumors, pharyngeal squamous cell carcinoma, keratinocyte tumors, atherosclerosis) |

this tumor [20]. Large multidomain ECM molecules such as collagen types I, III, V, and XIV and fibronectin contain at least one GAG binding site. This allows them to bind to heparan and chondroitin sulfates on cells or in the ECM, contributing to proper ECM formation.

*Proteoglycans*

PGs exhibit a wide variety of functions due to their structural diversity (Table 3). As PGs avidly bind proteins, they are involved in all cellular processes concerning cell-matrix, cell-cell, and ligand-receptor interactions. PGs are known to have affinity for a variety of ligands, including growth factors, cell adhesion molecules, ECM

components, enzymes, and enzyme inhibitors [22]. Lecticans bind other ECM proteins with its C-type lectin motif, facilitating the formation of networks permissive for cell growth [23]. For example, aggrecan and versican associate tightly with both HA, thereby maintaining tissue hydration. Due to the EGF-like repeats, lecticans are directly involved in growth control. Versican stimulates the proliferation of fibroblasts and is highly expressed by fast-growing cells and present in myxoid areas of both reactive and neoplastic (mesenchymal and epithelial) lesions (Table 2) [24].

*Small leucine-rich proteoglycans*

SLRPs are structurally and functionally related ECM molecules and abundantly expressed in connective tissues. Decorin and biglycan bind to collagen and influence collagen fibrillogenesis and ECM assembly in various ways: (a) due to its curved shape, decorin is able to bind to collagen types I, II, VI, and XIV linking them together and to fibronectin [25], (b) by decorating collagen fibers, decorin protects them from degradation by collagenases [25, 26], and (c) by its attached GAG chain, decorin is capable of modulating the activity of TGF-beta, which plays a central role in fibrogenesis [13, 25, 27]. Biglycan- and decorin-deficient mice show irregular and defective collagen fibrils, fragile skin, and a phenotype that closely resembles that of patients with Ehlers-Danlos syndrome [28]. In wound healing, there is a spatial temporal regulation of the expression of the different SLRPs (decorin, lumican, fibromodulin, and biglycan) tightly controlling the transformation of the myxoid ECM of granulation tissue towards fibrotic scar formation [29]. Myxoid areas in pleomorphic adenoma of the salivary gland and odontogenic myxoma lack expression of biglycan, lumican, and decorin, whereas these SLRPs are diffusely present in the fibrotic parts of the ECM of these tumors (Table 2). This suggests that the absence of SLRPs might contribute to impaired ECM formation resulting in a mere myxoid morphology.

*Collagens*

As form follows function [30], different collagens have different properties. In the initial phase of wound healing, collagen type I is quickly produced by fibroblasts and replaced by collagen type III in the later stage of scar formation [29]. The FACIT collagen types XII and XIV do not form collagen fibrils themselves but associate with fibrillary collagens, such as collagen type I, decorin, and GAGs, linking them together [31-33]. Collagen type XIV interacts with dermatan sulfate sequences on the single chondroitin sulfate/dermatan sulfate chain attached to decorin, thereby providing a link between the fibril-forming and the fibril-associated collagens [32]. Collagen type XIV is expressed significantly higher in grade I myxofibrosarcoma than in intramuscular myxoma (including its cellular variant) [34]. On one hand, this might have implications for ECM assembly and tumor development, thereby playing a potential role in the different biology and clinical behavior of these different entities; on the other hand, the effect of cell-ECM interaction in these tumors might work the other way around, as

collagen XIV induces differentiation of fibroblastic cells [35]. Higher expression of collagen XIV in myxofibrosarcoma is associated with a more mature morphology of the tumor cells compared to intramuscular myxoma [5].

*Other ECM molecules*

Fibronectin plays a role in various biological processes, such as wound healing, host defense, regulation of ECM assembly, adhesion, and proliferation [36]. It is also a key molecule in cell-ECM signaling, and aberrant activation of fibronectin-ECM signaling has been described in many tumors [37]. Likewise, tenascin C is an ECM glycoprotein of which the spatial and temporal expression is tightly regulated during fetal development [38]. It has been shown that the tenascin C-encoding gene is upregulated in several pathologic conditions, such as wound healing, inflammation, and malignancies [38]. Elevated tenascin C expression has been found in epithelial and mesenchymal tumors, both in tumor and stromal cells, and is associated with unfavorable disease outcome (Table 2) [18]. Tenascin C attaches to cells via integrins, though the effect of this interaction on cellular signaling and tumor development is largely unknown [39].

## Putative relevance for routine pathology practice

In routine general practice, one encounters a group of tumors, mesenchymal as well as epithelial, which may show variable degrees of myxoid appearance of their ECM. Myxoid tumors of soft tissue, the focus of this paper, encompass a heterogeneous group of lesions characterized by a marked abundance of extracellular mucoid/myxoid matrix (Table 1). This group of tumors exhibits a broad range of biological behavior varying from those which are entirely benign via locally aggressive (but nonmetastasizing) behavior to those which are frankly malignant; hence, accurate histopathological diagnosis is essential for appropriate clinical management. Till today, there have been no convincing data which demonstrate that the composition of the myxoid matrix significantly differ between tumors (both of mesenchymal and/or epithelial origin) and reactive lesions. From a biochemical point of view, the term "myxoid" is best considered a wastebasket of many different proteins and other (macro)molecules which might all have a different function (Tables 2 and 3). While determination of the different GAGs in myxoid tumors is interesting from a research point of view, Scott's critical electrolyte concentration (CEC) method is no longer a routinely used technique by pathologists. Most myxoid tumors of soft tissue tumors contain HA (Table 2), and consequently, its detection is no longer regarded as discriminatory in differential diagnoses. Outside the academic setting (where recourse to sophisticated biochemical and molecular genetics techniques is generally not possible), when confronted with challenging myxoid lesions, the diagnostic process relies primarily on careful and discriminatory histopathological evaluation in order to reach a correct diagnosis. Routine histological criteria (e.g., tumor demarcation, growth and vascular

pattern, and nuclear atypia) remain the hallmarks of diagnosis. (Immuno-)histochemistry may be useful as a adjunct in the setting of certain differential diagnostic considerations, but is often not discriminatory and, therefore, not diagnostically useful [8]. Molecular cytogenetics is of increasing importance for diagnosis in difficult cases, as the genetic makeup of an increasing number of myxoid tumors of soft tissue is being elucidated (Table 1). Next to genetic causes (such as driver mutations, translocations, or gene amplifications), environmental factors have been shown to play an important role in tumorigenesis of both epithelial and mesenchymal tumors [40]. Virchow already mentioned the possible relationship between the histological appearance of the myxoid ECM of tumors and their differences in biological behavior [1]. It is very tempting to believe that GAGs and PGs play an important role in the biology of myxoid lesions rather than just being a byproduct of (myo)fibroblastic differentiation. Intramuscular myxoma expresses significantly less decorin and collagen VI and XIV (both protein and mRNA level) than grade I myxofibrosarcoma [34]. Next to decorin, liquid chromatography-mass spectrometry revealed other SLRPs (i.e., lumican, prolargin 4, biglycan) present in tumor lysates of grade I myxofibrosarcoma but not of intramuscular myxoma [34]. This suggest that ECM formation in intramuscular myxoma is impaired compared to grade I myxofibrosarcoma. Increased ECM rigidity activates integrins and subsequently leads to stimulation of the rho/Rock pathway and cell migration and invasion [41]. In this respect, the morphological similarity between the process of wound healing and myxoid changes/areas in (non)neoplastic lesions is rather striking. In the early phase, granulation tissue shows a loose, edematous/myxoid ECM rich in GAGs. In the subsequent phase, there is structural organization of the ECM with deposition of collagens produced by myofibroblasts which locally (de)differentiate from fibroblast/smooth muscle cells or are derived from the bone marrow. The term "myxoid" might not only be synonymous with (aberrant turnover and) the presence of GAGs, but also reflects the absence of proper ECM assembly or incomplete ECM formation. This might well explain that a myxoid morphology of the ECM is not specific at all and can be seen in reactive/non-neoplastic processes as well as in benign and malignant tumors (Fig. 3). As already extensively discussed in this paper, the ECM is dependent on the interplay of various macromolecules (polysaccharides and proteins) which determine its texture and consistency. It is becoming increasingly clear that, within this group of lesions, various tumor types may show differences in the biological composition of their myxoid matrix, as determined by differences in the relative proportions of the constituent macromolecules and the presence or absence of specific stromal constituents. Clearly, this is an important and highly relevant area for further research in order to identify tumor-specific markers and to consequently develop economically viable and user-friendly detection methods to facilitate the diagnostic process and ensure increasingly accurate histopathologic diagnosis.

## Acknowledgements

Stefan M. Willems was financially supported by a grant from The Netherlands Organization for Health Research and Development (project no. 920-03-403).

**References**

1. Virchow R. Die cellularpathologie in ihrer Begrundung auf physiologische und pathologische Gewebelehre. Berlin: Hirschwald; 1858.
2. Dunglison R. Medical lexicon. A dictionary of medical science. Philadelphia: Blanchard and Lea; 1865.
3. Muller J. Uber den feineren bau und die formen der krankhaften geschwulste. Berlin: Haberling; 1838.
4. Bryant T. Tumors and tumor formation. New York: Churchill; 1802.
5. Stout AP. Myxoma, the tumor of primitive mesenchyme. Ann Surg. 1948;127:706-719.
6. Sponsel KH, McDonald JR, Ghormley RK. Myxoma and myxosarcoma of the soft tissues of the extremities. J Bone Joint Surg Am. 1952;34(A):820-826.
7. Fletcher CDM, Unni KK, Mertens F. WHO classification of tumours. Pathology and genetics of tumours of soft tissue and bone. Lyon: IARC; 2002.
8. Graadt van Roggen JF, Hogendoorn PCW, Fletcher CDM. Myxoid tumours of soft tissue. Histopathology. 1999;35:291-312.
9. Steedman HF. Alcian Blue 8 GS: a new stain for mucin. Q J Microsc Sci. 1950;3:477-479.
10. Scott JE, Dorling J. Differential staining of acid glycosaminoglycans (mucopolysaccharides) by alcian blue in salt solutions. Histochemie. 1965;5:221-233.
11. Kindblom LG, Angervall L. Histochemical characterization of mucosubstances in bone and soft tissue-tumors. Cancer. 1975;36:985-994.
12. Gandhi NS, Mancera RL. The structure of glycosaminoglycans and their interactions with proteins. Chem Biol Drug Des. 2008;72:455-482.
13. Kresse H, Schonherr E. Proteoglycans of the extracellular matrix and growth control. J Cell Physiol. 2001;189:266-274.
14. Schaefer L, Iozzo RV. Biological functions of the small leucine-rich proteoglycans: from genetics to signal transduction. J Biol Chem. 2008;283:21305-21309.
15. Kadler KE, Hill A, Canty-Laird EG. Collagen fibrillogenesis: fibronectin, integrins, and minor collagens as organizers and nucleators. Curr Opin Cell Biol. 2008;20:495-501.
16. White ES, Baralle FE, Muro AF. New insights into form and function of fibronectin splice variants. J Pathol. 2008;216:1-14.
17. Bosman FT, Stamenkovic I. Functional structure and composition of the extracellular matrix. J Pathol. 2003;200:423-428.
18. Orend G, Chiquet-Ehrismann R. Tenascin-C induced signaling in cancer. Cancer Lett. 2006;244:143-163.
19. Lamoureux F, Baud'huin M, Duplomb L, et al. Proteoglycans: key partners in bone cell biology. BioEssays. 2007;29:758-771.
20. Willems SM, Schrage YM, Baelde JJ, et al. Myxoid tumours of soft tissue: the so-called myxoid extracellular matrix is heterogeneous in composition. Histopathology. 2008;52:465-474.
21. Almond A. Hyaluronan. Cell Mol Life Sci. 2007;64:1591-1596.
22. Rodgers KD, San Antonio JD, Jacenko O. Heparan sulfate proteoglycans: a GAGgle of skeletal-hematopoietic regulators. Dev Dyn. 2008;237:2622-2642.
23. Evanko SP, Angello JC, Wight TN. Formation of hyaluronan- and versican-rich pericellular matrix is required for proliferation and migration of vascular smooth muscle cells. Arterioscler Thromb Vasc Biol. 1999;19:1004-1013.
24. Zimmermann DR, Dours-Zimmermann MT, Schubert M, et al. Versican is expressed in the proliferating zone in the epidermis and in association with the elastic network of the dermis. J Cell Biol. 1994;124:817-825.
25. McEwan PA, Scott PG, Bishop PN, et al. Structural correlations in the family of small leucine-rich repeat proteins and proteoglycans. J Struct Biol. 2006;155:294-305.
26. Geng Y, McQuillan D, Roughley PJ. SLRP interaction can protect collagen fibrils from cleavage by collagenases. Matrix Biol. 2006;25:484-491.
27. Ferdous Z, Wei VM, Iozzo R, et al. Decorin-transforming growth factor- interaction regulates matrix organization and mechanical characteristics of three-dimensional collagen matrices. J Biol Chem. 2007;282:35887-35898.

28. Danielson KG, Baribault H, Holmes DF, et al. Targeted disruption of decorin leads to abnormal collagen fibril morphology and skin fragility. J Cell Biol. 1997;136:729-743.
29. Martinez DA, Vailas AC, Vanderby R, et al. Temporal extracellular matrix adaptations in ligament during wound healing and hindlimb unloading. Am J Physiol Regul Integr Comp Physiol. 2007;293:R1552-R1560.
30. Sullivan LH. The tall office building artistically considered. Lippincott's Magazine. 1896;57:403-409.
31. Ehnis T, Dieterich W, Bauer M, et al. Localization of a binding site for the proteoglycan decorin on collagen XIV (undulin). J Biol Chem. 1997;272:20414-20419.
32. Ehnis T, Dieterich W, Bauer M, et al. A chondroitin/dermatan sulfate form of CD44 is a receptor for collagen XIV (undulin). Exp Cell Res. 1996;229:388-397.
33. Canty EG, Kadler KE. Procollagen trafficking, processing and fibrillogenesis. J Cell Sci. 2005;118:1341-1353.
34. Willems SM, Mohseny AB, Balog C, et al. Cellular/intramuscular myxoma and grade I myxofibrosarcoma are characterized by distinct genetic alterations and specific composition of their extracellular matrix. J Cell Mol Med. 2009;7:1291-1301.
35. Ruehl M, Erben U, Schuppan D, et al. The elongated first fibronectin type III domain of collagen XIV is an inducer of quiescence and differentiation in fibroblasts and preadipocytes. J Biol Chem. 2005;280:38537-38543.
36. Vakonakis I, Campbell ID. Extracellular matrix: from atomic resolution to ultrastructure. Curr Opin Cell Biol. 2007;19:578-583.
37. Larsen M, Artym VV, Green JA, et al. The matrix reorganized: extracellular matrix remodeling and integrin signaling. Curr Opin Cell Biol. 2006;18:463-471.
38. Harty M, Neff AW, King MW, et al. Regeneration or scarring: an immunologic perspective. Dev Dyn. 2003;226:268-279.
39. Jones FS, Jones PL. The tenascin family of ECM glycoproteins: structure, function, and regulation during embryonic development and tissue remodeling. Dev Dyn. 2000;218:235-259.
40. Wever O, Mareel M. Role of tissue stroma in cancer cell invasion. J Pathol. 2003;200:429-447.
41. Berrier AL, Yamada KM. Cell-matrix adhesion. J Cell Physiol. 2007;213:565-573.
42. Fletcher CDM. Benign fibrous histiocytoma of subcutaneous and deep soft tissue: a clinicopathologic analysis of 21 cases. Am J Surg Pathol. 1990;14:801-809.
43. Carney JA, Gordon H, Carpenter PC, et al. The complex of myxomas, spotty pigmentation, and endocrine overactivity. Medicine (Baltimore). 1985;64:270-283.
44. Meng GZ, Zhang HY, Zhang Z, et al. Myofibroblastic sarcoma vs nodular fasciitis: a comparative study of chromosomal imbalances. Am J Clin Pathol. 2009;131:701-709.
45. Perdigao PF, Stergiopoulos SG, Marco L, et al. Molecular and immunohistochemical investigation of protein kinase a regulatory subunit type 1A (PRKAR1A) in odontogenic myxomas. Genes Chromosomes Cancer. 2005;44:204-211.
46. Hallor KH, Sciot R, Staaf J, et al. Two genetic pathways, t(1;10) and amplification of 3p11-12, in myxoinflammatory fibroblastic sarcoma, haemosiderotic fibrolipomatous tumour, and morphologically similar lesions. J Pathol. 2009;217:716-727.
47. Calonje E, Mentzel T, Fletcher CDM. Cellular benign fibrous histiocytoma. Clinicopathologic analysis of 74 cases of a distinctive variant of cutaneous fibrous histiocytoma with frequent recurrence. Am J Surg Pathol. 1994;18:668-676.
48. Willems SM, Debiec-Rychter M, Szuhai K, et al. Local recurrence of myxofibrosarcoma is associated with increase in tumour grade and cytogenetic aberrations, suggesting a multistep tumour progression model. Mod Pathol. 2006;19:407-416.
49. Enzinger FM, Shiraki M. Extraskeletal myxoid chondrosarcoma. An analysis of 34 cases. Hum Pathol. 1972;3:421-435.
50. Evans HL. Low-grade fibromyxoid sarcoma. A report of 12 cases. Am J Surg Pathol. 1993;17:595-600.
51. Turc-Carel C, Limon J, Dal CP, et al. Cytogenetic studies of adipose tissue tumors. II. Recurrent reciprocal translocation t(12;16)(q13;p11) in myxoid liposarcomas. Cancer Genet Cytogenet. 1986;23:291-299.
52. Rubin BP, Fletcher CDM. Myxoid leiomyosarcoma of soft tissue, an underrecognized variant. Am J Surg Pathol. 2000;24:927-936.
53. Brems H, Beert E, Ravel RT, et al. Mechanisms in the pathogenesis of malignant tumours in neurofibromatosis type 1. Lancet Oncol. 2009;10:508-515.
54. Pedeutour F, Simon MP, Minoletti F, et al. Translocation, t(17;22)(q22;q13), in dermatofibrosarcoma protuberans: a new tumor-associated chromosome rearrangement. Cytogenet Cell Genet. 1996;72:171-174.
55. Kaya G, Augsburger E, Chavaz P, et al. CD44 and hyaluronate expression in follicular mucinosis. J Cutan Pathol. 2006;33:227-230.

56. Alves MF, Filgueira AL, Lorena DE, et al. Type I and type III collagens in cutaneous mucinosis. Am J Dermatopathol. 1998;20:41-47.
57. Lengyel J, Vertes B. Hyaluronic acid studies of local myxedema and of the stroma of skin cancer. Dermatologica. 1956;113:219-225.
58. Chung IM, Gold HK, Schwartz SM, et al. Enhanced extracellular matrix accumulation in restenosis of coronary arteries after stent deployment. J Am Coll Cardiol. 2002;40:2072-2081.
59. Wight TN. Versican: a versatile extracellular matrix proteoglycan in cell biology. Curr Opin Cell Biol. 2002;14:617-623.
60. Burke AP, Jarvelainen H, Kolodgie FD, et al. Superficial pseudoaneurysms: clinicopathologic aspects and involvement of extracellular matrix proteoglycans. Mod Pathol. 2004;17:482-488.
61. Black A, French AT, Dukes-McEwan J, et al. Ultrastructural morphologic evaluation of the phenotype of valvular interstitial cells in dogs with myxomatous degeneration of the mitral valve. Am J Vet Res. 2005;66:1408-1414.
62. Nasuti JF, Zhang PJ, Feldman MD, et al. Fibrillin and other matrix proteins in mitral valve prolapse syndrome. Ann Thorac Surg. 2004;77:532-536.
63. Aigner T, Oliveira AM, Nascimento AG. Extraskeletal myxoid chondrosarcomas do not show a chondrocytic phenotype. Mod Pathol. 2004;17:214-221.
64. Zhao M, Lu Y, Takata T, Mock D, Nikia H, et al. Immunohistochemical and histochemical characterization of the mucosubstances of odontogenic myxoma: histogenesis and differential diagnosis. Pathol Res Pract. 1999;195:391-397.
65. Zamecnik M, Michal M. Low-grade fibromyxoid sarcoma: a report of eight cases with histologic, immunohistochemical, and ultrastructural study. Ann Diagn Pathol. 2000;4:207-217.
66. Gallager RL, Helwig EB. Neurothekeoma-a benign cutaneous tumor of neural origin. Am J Clin Pathol. 1980;74:759-764.
67. Hajdu SI. Pathology of soft tissue Tumors. Philadelphia: Lea and Febiger; 1979.
68. Fukuda T, Tsuneyoshi M. Adhesion proteins, cellular morphology and fibrous components around the cell/extracellular-matrix interface in myxoid liposarcomas. J Cancer Res Clin Oncol. 2000;126:320-324.
69. Mackenzie DH. The myxoid tumors of somatic soft tissues. Am J Surg Pathol. 1981;5:443-458.
70. Soder S, Inwards C, Muller S, et al. Cell biology and matrix biochemistry of chondromyxoid fibroma. Am J Clin Pathol. 2001;116:271-277.
71. Calikoglu E, Chavaz P, Saurat JH, et al. Decreased CD44 expression and stromal hyaluronate accumulation in myxoid dermatofibroma. Dermatology. 2003;207:104-106.
72. Yasui W, Oda N, Ito H, et al. Myxoid leiomyosarcoma of the stomach: a case report. Jpn J Clin Oncol. 1991;21:447-452.
73. Lam RM, Hawkins ET, Roszka J. Cardiac myxoma: histochemical and ultrastructural localization of glycosaminoglycans and proteoglycans. Ultrastruct Pathol. 1984;6:69-81.
74. Folpe AL, Weiss SW. Ossifying fibromyxoid tumor of soft parts: a clinicopathologic study of 70 cases with emphasis on atypical and malignant variants. Am J Surg Pathol. 2003;27:421-431.
75. Yang P, Hirose T, Hasegawa T, et al. Ossifying fibromyxoid tumor of soft parts: a morphological and immunohistochemical study. Pathol Int. 1994;44:448-453.
76. Hassanein AM, Atkinson SP, Al-Quran SZ, et al. Acral myxoinflammatory fibroblastic sarcomas: are they all low-grade neoplasms? J Cutan Pathol. 2008;35:186-191.
77. Johnson WC, Graham JH, Helwig EB. Cutaneous myxoid cyst. A clinicopathological and histochemical study. JAMA. 1965;191:15-20.
78. Begin LR, Clement PB, Kirk ME, et al. Aggressive angiomyxoma of pelvic soft parts: a clinicopathologic study of nine cases. Hum Pathol. 1985;16:621-628.
79. Calikoglu E, Augsburger E, Masouye I, et al. Hyaluronate accumulation and decreased CD44 expression in perifollicular solitary cutaneous myxoma. Dermatology. 2002;205:122-126.
80. Kusafuka K, Muramatsu K, Kasami M, et al. Cartilaginous features in matrix-producing carcinoma of the breast: four cases report with histochemical and immunohistochemical analysis of matrix molecules. Mod Pathol. 2008;21:1282-1292.
81. Kusafuka K, Ishiwata T, Sugisaki Y, et al. Lumican expression is associated with the formation of mesenchyme-like elements in salivary pleomorphic adenomas. J Pathol. 2004;203:953-960.
82. Nara Y, Takeuchi J, Yoshida K, et al. Immunohistochemical characterisation of extracellular matrix components of salivary gland tumours. Br J Cancer. 1991;64:307-314.

83. Kusafuka K, Hiraki Y, Shukunami C, et al. Cartilage-specific matrix protein chondromodulin-I is associated with chondroid formation in salivary pleomorphic adenomas: immunohistochemical analysis. Am J Pathol. 2001;158:1465-1472.
84. Ambros RA, Kallakury BV, Malfetano JH, et al. Cytokine, cell adhesion receptor, and tumor suppressor gene expression in vulvar squamous carcinoma: correlation with prominent fibromyxoid stromal response. Int J Gynecol Pathol. 1996;15:320-325.
85. Franchi A, Dini M, Paglierani M, et al. Immunolocalization of extracellular matrix components in mixed tumors of the skin. Am J Dermatopathol. 1995;17:36-41.
86. Sabit H, Tsuneyama K, Shimonishi T, et al. Enhanced expression of basement-membrane-type heparan sulfate proteoglycan in tumor fibro-myxoid stroma of intrahepatic cholangiocarcinoma. Pathol Int. 2001;51:248-256.
87. Giordana MT, Bertolotto A, Mauro A, et al. Glycosaminoglycans in human cerebral tumors. Part II. Histochemical findings and correlations. Acta Neuropathol. 1982;57:299-305.
88. Shia J, Qin J, Erlandson RA, et al. Malignant mesothelioma with a pronounced myxoid stroma: a clinical and pathological evaluation of 19 cases. Virchows Arch. 2005;447:828-834.
89. Harrison JD, Rose PE. Myxoid meningioma: histochemistry and electron microscopy. Acta Neuropathol. 1985;68:80-82.
90. Henschen F. Fall von ostitis Fibrosa mit multiplen Tumoren in deer umgebenden Muskulatur. Verh Dtsch Ges Pathol. 1926;21:93-97.
91. Mazabraud A, Semat P, Roze R. A propos de l'association de fibromyxomes des tissus mous à la dysplasie fibreuse des os. Presse Med. 1967;75:2223-2228.
92. Weiss SW, Enzinger FM. Myxoid variant of malignant fibrous histiocytoma. Cancer. 1977;39:1672-1685.
93. Angervall L, Kindblom LG, Merck C. Myxofibrosarcoma. A study of 30 cases. Acta Pathol Microbiol Scand A. 1977;85A:127-140.
94. Orndal C, Mandahl N, Rydholm A, et al. Chromosomal evolution and tumor progression in a myxoid liposarcoma. Acta Orthop Scand. 1990;61:99-105.
95. Mentzel T, Calonje E, Wadden C, et al. Myxofibrosarcoma. Clinicopathologic analysis of 75 cases with emphasis on the low-grade variant. Am J Surg Pathol. 1996;20:391-405.

# Chapter 3

## Local recurrence of myxofibrosarcoma is associated with increase in tumour grade and cytogenetic aberrations, suggesting a multistep tumour progression model

Stefan M Willems[1], Maria Debiec-Rychter[2], Károly Szuhai[3], Pancras C W Hogendoorn[1] and Raphäel Sciot[4]

[1]Department of Pathology, Leiden University Medical Center, Leiden, The Netherlands, [2]Departmentof Human Genetics, University Hospitals, Catholic University of Leuven, Leuven, Belgium, [3]Department of Molecular Cell Biology, Leiden University Medical Center, Leiden, The Netherlands, [4]Department of Morphology and Molecular Pathology, University Hospitals, Catholic University of Leuven, Leuven, Belgium

**Abstract**

Myxofibrosarcoma is one of the most frequent soft tissue tumours in elderly patients, mostly arising in the extremities. Grade I lesions are only locally aggressive whereas grade II and grade III lesions have metastatic potential. The differential diagnosis contains several other (benign) myxoid soft tissue tumours. A number of sarcomas are characterised by specific cytogenetic aberrations, giving not only insight in their biological pathways; they also serve as molecular markers in difficult diagnoses. Cytogenetic data on myxofibrosarcoma are scarce with only few isolated cases described in the literature. No specific chromosomal aberrations have been detected so far. Moreover, molecular pathways in tumorigenesis and progression of myxofibrosarcoma are barely understood. We studied the clinicopathologic data and karyotypes of 32 myxofibrosarcomas using conventional banding and multicolour COmbined Binary RAtio labelling fluorescence in situ hybridisation technique. We included eight grade I, eight grade II and 16 grade III lesions. In all, 22 were primary tumours, nine were local recurrences and one a lymph node metastasis. The myxofibrosarcomas showed equal sex distribution, were mostly located at the extremities with two thirds deep-seated and had an average age of occurrence of 66 years. We found normal karyotypes in eight cases and clonal beside nonclonal aberrations in 22 cases. Complex cytogenetic anomalies were found in all grades. However, no tumour-specific chromosomal abnormalities could be withdrawn. Local recurrences showed increase in grade compared to their primary lesions. Interestingly, these recurrences showed more complex cytogenetic aberrations. Increase in grade seems to parallel increase in cytogenetic aberrations and malignant potential. Since the chromosomal aberrations found were not tumour type specific, they seem to be rather the result of secondary events in tumour progression and tumour genetic instability. Based on these findings, we suggest that tumorigenesis of myxofibrosarcoma is mainly a multistep genetic process, probably ruled by genetic instability caused by targeted checkpoint genes.

Myxofibrosarcoma, formerly also known as the myxoid variant of malignant fibrous histiocytoma, is one of the most frequent sarcomas in elderly patients with the majority arising in the extremities, clinically most often presenting as a slowly increasing mass [1, 2, 3]. Histologically, myxofibrosarcomas show a wide range from hypocellular grade I tumours with oval to spindle form cells in a myxoid stroma, to hypercellular grade III lesions of solid sheets with pleomorphic nuclei [4]. According to the French Fédération Nationale des Centres de Lutte Contre le Cancer (FNCLCC) grading system, three histological grades are recognised, that is, grade I, II and III [5]. Metastatic potential is closely related to tumour grade, with a preference for lung, bone and lymph nodes. Importantly, increasing grade is seen in subsequent recurrences [4]. Cytogenetic data on myxofibrosarcoma are scarce with 30 isolated cases described in the literature. Most often, karyotypes are very complex, including ring chromosomes, deletions, translocations and double minutes. Here, we present the clinicopathologic data and karyotypes of 32 cases of myxofibrosarcoma and discuss our findings in the light of tumour grade and clinical behaviour.

## Materials and methods

*Patient Data*

Thirty-two cases of myxofibrosarcoma were identified on which cytogenetic data were available and collected retrospectively from the files of the Pathology Departments of the University Hospitals of Leuven and Leiden University Medical Center. Patient and tumour characteristics were described in Table 1. In each case, 4 m-thick sections of formalin-fixed, paraffin-embedded material were stained with haematoxylin and eosin (H&E). Slides were revised and classified according to the 2002 World Health Organization (WHO) criteria and histological grading was performed according to the FCNLCC [2, 5].

*Cytogenetic Data*

Chromosomes were obtained using short-term cultures and harvesting procedures as described previously [6]. Briefly, nonfixed tissue fragments were disaggregated mechanically and enzymatically and then cultured on chamber slides in DMEM-F12 medium (Gibco, Invitrogen, Breda, The Netherlands), supplemented with 10% fetal bovine serum and 0,5% penicillin-streptomycin (Irvine Scientific, Santa Anna, CA, USA) for 4-9 days. For cases 1-17 and 19-29 the protocol was as follows. At 17 h before harvest, cells were exposed to Colcemid (0.005 g/ml; Gibco, Invitrogen, Breda, The Netherlands). After hypotonic treatment (0.8% sodium citrate for 25 min), the preparations were fixed three times with methanol-glacial acetic acid (3:1). Cytogenetic analysis was performed on GTG-banded chromosomes and the karyotypes were classified according to the International System for Human Cytogenetic Nomenclature [7].

**Table 1:** Patient and tumour characteristics

| Case | P/R/M [a] | Sex [b] | Age | Site | Grade |
|---|---|---|---|---|---|
| 1 | P | M | 61 | In left musculus gracilis | I |
| 2 | P | M | 46 | In left musculus deltoideus | I |
| 3 | P | F | 55 | In left vastus lateralis | I |
| 4 | P | M | 81 | Right upper arm (superficial) | I |
| 5 | P | F | 64 | In right musculus quadriceps | I |
| 6 | P | F | 64 | In right musculus quadriceps | I |
| 7 | P | M | 60 | Left thigh (superficial) | I |
| 8 | P | F | 49 | In left musculus gluteus | I |
| 9 | P | F | 79 | Forearm (superficial) | II |
| 10 | P | M | 55 | In musculus biceps femoris | II |
| 11 | P | M | 69 | Right lower leg (intramuscular) | II |
| 12 | R | M | 81 | Right upper arm (superficial) | II |
| 13 | P | M | 69 | In right thoracic muscle | II |
| 14 | R | F | 63 | Left thigh (superficial) | II |
| 15 | R | F | 63 | Left thigh (superficial) | II |
| 16 | P | F | 68 | Right elbow (superficial) | II |
| 17 | P | M | 77 | Right thigh (superficial) | III |
| 18 | P | F | 70 | Pretibial (superficial) | III |
| 19 | R | M | 61 | In left musculus gracilis | III |
| 20 | P | M | 65 | Right lower leg | III |
| 21 | R | M | 43 | In right musculus deltoideus | III |
| 22 | P | M | 43 | In right musculus deltoideus | III |
| 23 | R | F | 89 | Left elbow (intramuscular) | III |
| 24 | R | F | 89 | Left elbow (intramuscular) | III |
| 25 | P | F | 76 | In musculus sartorius | III |
| 26 | P | M | 66 | Left thigh (invading the fascia) | III |
| 27 | R | F | 71 | Whole arm (invading the bone) | III |
| 28 | P | M | 68 | Left thigh (intramuscular) | III |
| 29 | M | M | 69 | Right axillary lymph node | III |
| 30 | P | F | 45 | Right upper arm (superficial) | III |
| 31 | R | F | 64 | Left lower leg (superficial) | III |
| 32 | P | M | 71 | Left lower arm (intramuscular) | III |

[a] P=primary lesion; R=local recurrence; M=metastasis.
[b] M=male; F=female.

*Multicolor Fluorescence In Situ Hybridisation*

For cases 18, 30-32, cells were harvested, after which a 48-color fluorescence in situ hybridisation (FISH) staining was carried out, staining every chromosome-arm in a different colour combination, after which digital imaging and analysis was performed as previously described [8, 9, 10]. Hybridisations with individual libraries labeled with single fluorochromes were used to confirm the detected rearrangements. Breakpoints were assigned by using inverted DAPI counterstained images of the chromosomes.

## Results

*Patient Data*

The study of myxofibrosarcoma included eight grade I, eight grade II and 16 grade III cases. The morphological spectrum ranging from low- to high-grade morphology is depicted in Figure 1. Patient and tumour characteristics are depicted in Table 1, showing equal sex distribution between males and females with an average age of occurrence of 66 years. In all, 22 cases were primary lesions; nine of these lesions recurred locally and one was a lymph node metastasis. Of the six cases recurring as grade III lesions, the primary lesions were either grade III (four cases), grade II (one case) or grade I (one case). All three grade II recurrences were all primarily grade I. The metastasis was a grade III lesion. Except for this lymph node metastasis and one lesion occurring in the thoracic muscles (case 13), all lesions occurred at the extremities (upper ones: 12; lower: 19). In all, 19 were deeply/intramuscular seated (case 13 included), 11 superficially with one not specified regarding the depth of the lesion (case 20).

*Cytogenetics*

The cytogenetics findings are listed in Table 2 showing normal to very complex karyotypes. None of them were published in previous publications including these entities by the authors.11 Eight normal karyotypes were found among these 32 myxofibrosarcoma. Clonal, besides nonclonal, aberrations were found in 22 cases. These aberrations were present in all grades. Complex cytogenetic anomalies were not restricted to grade III, but also seen in grade II and grade I cases. There was no difference in affected chromosomes depending on grade. Although some chromosomes were more involved than others (Figure 2), there were no consistent chromosomal abnormalities. In general, grade III lesions showed more complex karyotypes than lower grades. Remarkably, recurrences (indicated by asterisk) showed more complex karyotypes than both their grade II and grade III primary lesions. Furthermore, we found the presence of a ring chromosome, possibly originating from chromosome 3 (case 7).

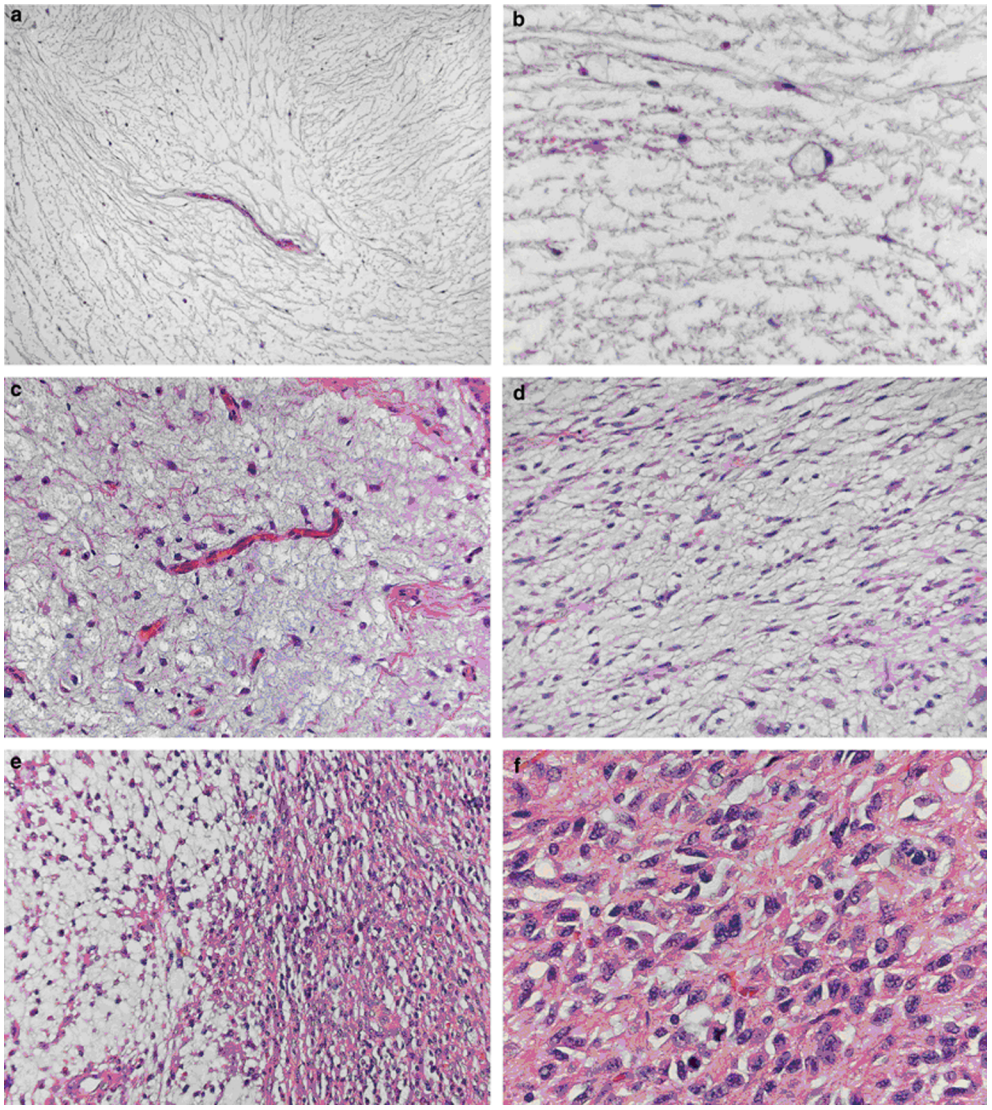


**Figure 1:** Light micrographs displaying the morphological spectrum of myxofibrosarcoma. (**a**–**c**) Grade I myxofibrosarcoma showing a hypocellular lesion with typical elongated curvilinear blood vessels in a myxoid background with (pseudo)lipoblasts and slight nuclear atypia. (**d**) Grade II myxofibrosarcoma showing a more cellular lesions with increased nucleair atypia. (**e**, **f**) Grade III myxofibrosarcoma consisting out of solid sheets of spindled, atypical cells and multinucleated giant cells with abundant eosinophillic cytoplasm. In the same tumour, there is often a remarkable but characteristic sharp transition between hypo-and hypercellular areas.

**Table 2:** Cytogenetic analysis of the 32 myxofibrosarcoma

| *Case* | *Grade* | *Karyotype* |
|---|---|---|
| 1 | I | 82–142,COMPLEX,+1–2M |
| 2 | I | 46,XY; 45,XY,-22/46,XY,t(1;10)(q22;p11) |
| 3 | I | 46,XX; 45,XX,-21/92,XXXX/92,XXXX |
| 4 | I | 46,XY; 43,Y,-X,-19,-20/45,X,-Y/46,XY,+dmin/47,XY,+X/46,XY,del(4)(Q22)/90,XXY,-Y,-12/91,XXYY,add(1)(P36), del(2)(Q31),-10,add(14)(P11),-16,-16,+M ×2 |
| 5 | I | 46,XX |
| 6 | I | 46,XX |
| 7 | I | 46,XY,del(1)(p21–p31?),r(3)(q),del(5)(q),-13,del(15)(q13–26.3?) |
| 8 | I | 46, XX [25} with random nonclonal aberrations |
| 9 | II | 44–47,XX,NCA; 46,XX |
| 10 | II | 46,XY; 47,XY,+M; 44,XY,-7,-21 |
| 11 | II | 82–82〈N〉,very complex with clonal aberrations |
| 12 | II | 70–77〈N〉,complex clonal aberrations |
| 13 | II | 46,XY; 45,X,-Y/45,XY,-20/46,XY,t(2;7)(q37;q22)/46,XY,t(2;12)(q23;q12); 61–63〈3〉, complex and numerous chromosomal aberrations |
| 14 | II | 72–85〈N〉 ,X,X,+1,add(1)(Q42),del(1)(Q32),2,del(2)(P23),add(3)(Q24),del(3)(P23P25),del(4)(Q22),del(5)(P13),+7,+8,DEL(8)(Q22)X2,+9, add(9)(P24),add(10)(Q22),add(11)(P13),add(12)(P13),del(12)(P11),-13,add(13)(Q32),add(13)(Q31),14,add(14)(P13),add(16)(P13),del(16)(P11), add(17)(Q25),+19,add(19)(Q13)X2,add(19)(P13),add(22)(P11),+9–14M(inc18); 46,XX |
| 15 | II | 46,XX;45,XX,-21/46,XX,inv(12)(p11q21) |
| 16 | II | 46,XX |
| 17 | III | 46,XY |
| 18 | III | 56–64〈3N〉, complex with clonal and nonclonal aberrations; 106–123〈6N〉,IDEMX2; 46,XX |
| 19 | III | Polyploid,complex,+1–2M |
| 20 | III | 46 XY,-X,t(X;17)(p;p),del(3)(3p),der3(3pter →3q□□8q →8q□□9q →9qter),der8(8pter →8q□□3q → 3qter),der9(9pter →9q□□8q →8qter),t(11;16)(q;q) |
| 21 | III | 46,XY; 48,XY,+7,+11 |
| 22 | III | 46,XY |
| 23 | III | 46,XY; 44,XX,-8,-17/45,X,-X/41,XX,-5,-8,-15,-22,-22/46,XX, t(4;9)(q31;q34)/82, multiple and complex clonal aberrations |
| 24 | III | 46,XX, nonclonal aberrations; 80〈4N〉, nonclonal aberrations; 46,XX |
| 25 | III | 58–109, complex clonal structural aberrations; 68–84, complex structural aberrations |
| 26 | III | Very abnormal karyotype with many clonal markers, for example, 1p-, 6q+, 7q+, 8q+, 10q+, and extra copynumbers of CHR.1q, 6, 7, 8 61–66,XXX,INC; 46,XY |
| 27 | III | 46,XX; 2 ×-18,1 ×Xq- |
| 28 | III | 46,XY |
| 29 | III | 46,XY |
| 30 | III | 46,XX |
| 31 | III | 45,XX,T(13;14)(Q10;Q10); near-triploid, few abnormal chromosomes, DMIN |
| 32 | III | Highly complex with clonal and non clonal structural aberrations, 61–74XXY〈3N〉del(1)1qter → q10:),der(1)del(1)(p?)del(1)(q?),der(2)t(2;18)(p?;q?),der(2),der(3)del(3)(p?)del(3)q?), del(3)(3pter → q1.3–2?),der(4)(4pter →4p1□□17q10 →17qter),der(6)(del(6)(p?)del(6)(q?),i(7)(q10),der(7)(7pter → 7p1□□18q10 →18qter), der(9)(4pter →4p1□□9q10 →9qter),-9,der(10)del(10)(p?)del(10)(q??),-10,+12,der(13)13pter →13q2–3□□hs□□13q3? →13qter), der(13)(9q12 →9q2?□□9q2?□□ →9p1?□□ 13q10 →13qter),-13,der(14)(22qter →22q?□□14p10 →14qter),add(14)(q3),der(16)(16pter → 16p1□□18q10 →18qter),der(16)del(16)(p?), der(17)del(17)(p?)del(17)(q?),-17,der(18)(17qter → q10□□18q10 →18qter),der(19)del(19)(p11)(19p1019q13□□4p1? →4pter),-21,-22, 2–3 min.ish(der17)/idem 2×〈6N〉[cp17] |

## Discussion

Myxofibrosarcoma is one of the most frequent sarcomas in elderly patients, mainly located on the extremities [2]. Histologically, they compromise a continuous range from hypocellular tumours, consisting of small spindle cells widely spaced among the myxoid matrix, to more cellular variants with pleomorphic nuclei and pseudolipoblasts [1, 2, 3, 4]. A consistent morphologic feature is the presence of curvilinear blood vessels. Enzinger and Weiss [3] classified the high-grade variant of these tumours as the myxoid variant of malignant fibrous histiocytoma, besides the storiform-pleomorphic, giant cell type and inflammatory subtypes. Angervall and Kindblom [1], almost simultaneously, first used the term myxofibrosarcoma, as they recognised this tumour as a distinct entity. Nowadays, the recognition as a distinct, separate entity is generally accepted and included in the 2002 WHO classification of tumours [2]. According to previous studies, grade II and III tumours are true malignant tumours since they have metastastic potential. This is in contrast to grade I lesions, which are only locally aggressive [4]. However, since local recurrence goes together with increase in grade, grade I myxofibrosarcoma may finally gain metastatic potential, warranting close surveillance.

The differential diagnoses of myxofibrosarcoma include other myxoid tumours often hard to distinguish from each other, since differences are often very subtle [12]. However, the distinction between all these myxoid subtypes is truly important from a clinical point of view, both for required therapy as for follow-up. Therefore, the existence of a specific (cyto) genetic aberration could serve as a welcome diagnostic marker and a helpful tool to distinguish these subtypes. However, cytogenetic data on myxofibrosarcoma are scarce, with only a few isolated cases described in literature showing complex, but nonspecific cytogenetic aberrations (Table 3). These include the presence of ring chromosomes, deletions and translocations. No specific chromosomal rearrangement has been identified so far.

Here, we investigated the clinicopathologic and cytogenetic data of 32 myxofibrosarcoma in order to find tumour and/or grade specific cytogenetic aberrations. Patient and tumour characteristics were in accordance to previous studies (Table 1) [1, 2, 3]. Although some authors suggested that deep-seated lesions were of higher grade, a large study of grade I myxofibrosarcoma could not confirm this, which is in accordance to our findings [4, 25, 26]. Interestingly, the grade I tumours progressing to grade II were located superficially which shows that progression to recurrence is not exclusive for deep-seated lesions. Normal karyotypes were seen in eight cases (five grade III, two grade II and one grade I lesion). Aberrations occurred in all chromosomes; no consistent tumour-specific cytogenetic rearrangement was identified. Those cases with cytogenetic abnormalities were not restricted to a certain grade with grade I, II and III lesions showing a wide range from normal till very complex, polyploid karyotypes (Figures 2, 4). Grade III tumours had, overall, more complex karyotypes than grade I

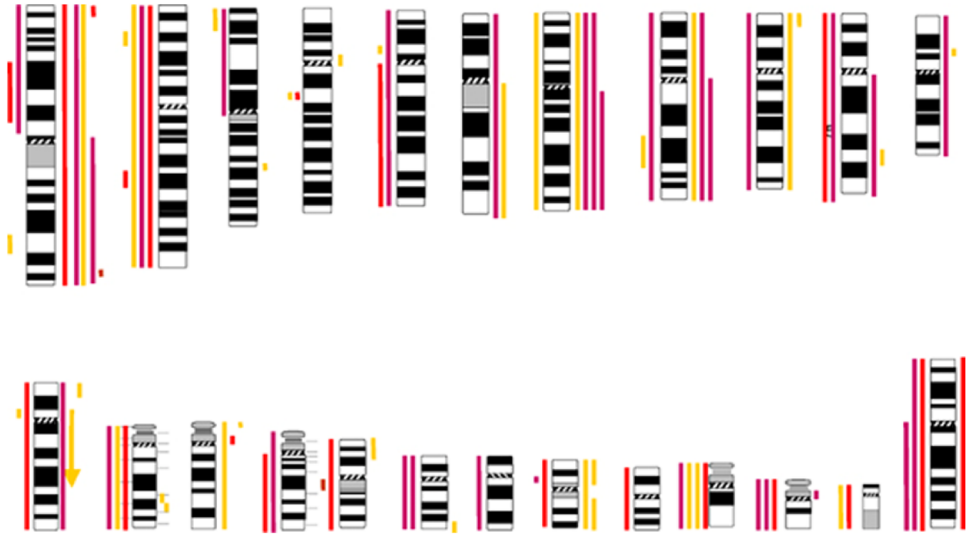

**Figure 2:** Karyotypic aberrations in 32 myxofibrosarcomas. *Red=Grade I, Orange=Grade II, Purple=Grade III*. Ideogram showing the distribution of the numerical and structural aberrations of 32 myxofibrosarcoma. Aberrations were found in all grades, including all chromosomes. No tumour or grade specific cytogenetic aberration could be withdrawn. Gains are shown on the right side of each chromosome diagram, losses on the left. Arrows indicate inversions.

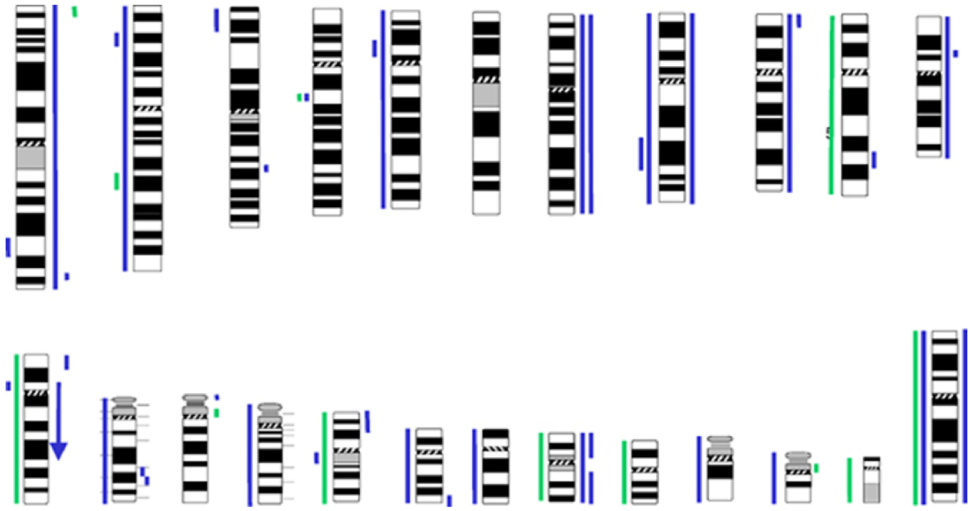

**Figure 3:** Karyotypic aberrations in nine myxofibrosarcomas comparing primary lesions to their recurrences. *Green: Primary tumour, Blue: Recurrence*. Ideogram showing the distribution of the numerical and structural aberrations of primary tumours compared to their local recurrences. Recurrences show more complex cytogenetic aberrations than the primary tumours. Gains are shown on the right side of each chromosome diagram, losses on the left. Arrows indicate inversions. In general, there is gain of cytogenetic aberrations with recurrence though no specific pattern is observed for this phenomenon.

**Table 3:** Karyotypes of the 30 Myxofibrosarcoma described in literature

| Refs | Karyotype | |
|---|---|---|
| Clawson *et al* [13] | ● | 46,XX,t(2;15)(p23;q21),del(7)(q?11q?22) |
| Johansson *et al* [14] | ● | 116–118,XXX,-Y,-Y,-1,-1,del(1)(q42),t(2;3)(p13;q11),-3,-5,-6,-6,dic(7;11)(q21;p13)×2,-8,-9,-9,add(12)(p13),add(12)(q24),der(12)t(1;12)(p13;p11),add(13)(p11)×2,add(14)(q2?4),-15,-15,add(16)(q22–24),?der(17)t(17;18)(p12;q12)×2,-18,add(19)(p13),add(22)(p11)×2,inc |
| Mandahl *et al* [15] | ● | 44–46,X,-Y,add(19)(p13),inc/74–82,idem×2 |
| | ● | 76–80,XX,-X,+add(7)(q36)×2,+der(7)del(7)(p13),add(7)(q32),+der(9)hsr(9)(p24)add(9)(p24)×2,+add(11)(p11)×2,der(12)t(1;12)(q23;p13)×2, add(17)(p11)×2,+der(19)add(19)(p13)add(19)(q13)×2,+6–12mar,inc/37–41,X,-X,inc |
| | ● | 59–65,X,-X,-X,del(1)(p13)×2,+del(1)(q11)×2,-2,del(2)(p12)×2,del(3)(p12),del(3)(q11),-4,add(4)(q25),der(4)add(4)del(4)(p11),-5,-6,der(7)add(7)(q?)del(7)(p?),-8,-9,-10,del(11)(p11),-12,add(12)(p?),-13,add(15)(q?),-17,-18,add(19)(p13),add(20)(q13),+3–8mar |
| | ● | 46,XX,inv(3)(p25q13)/46,XX,del(1)(p12),der(3)del(3)(p25)ins(3;14)(q21;q32q23)t(3;3)(q29;p25) |
| | | t(1;3)(p12;p26),del(14)(q23)/44–45,X,-X,add(3)(p25),der(3)add(3)(p25)add(3)(q13),+7,+7,add(9)(p24),add(9)(q34),-10,-12,-13,+add(14)(p11), +18,-19,+add(20)(q13),-21,-21,-22,-22,+1–2r,+1–3mar |
| | ● | 65–69,X,-X,-X,+del(1)(q11),+del(1)(q12),del(2)(q31),+del(3)(p12),add(4)(p16),add(4)(p11),+6,+der(7),inv(7)add(7)(q36),+inv(7)(p15q11),del(8)(q?),del(9)(q11),add(11)(q25),del(11)(p11),+der(11)add(11),del(11)(p15),add(13)(q?),+14,+14,+15,add(16)(q23),del(17)(p11),+18,+19,+21,add(22)(q13),+3–7mar |
| Meis-Kindblom *et al* [16] | ● | 44–46,XX,-16 |
| Meloni-Ehrig *et al* [17] | ● | 47,XX,+r(20)(q?)/48,idem,+r |
| Mertens *et al* [11] | ● | 55–60,XXY,+Y,-1,-2,-3,-4,add(4)(p16),add(5)(p15),der(5)t(4;5)(q12;p11–13),-6,+7,-9,-10,del(10)(q24),-13,der(14)t(9;14)(q13;p11),-16,-17,-18,-19,-21,-22,+mar,2–30dmin |
| | ● | 43–44,XY,-2,-5,add(7)(q32),add(8)(p11),-9,add(13)(p11),i(14)(q10),-17,-18,-20,inc/81–84,idem×2,add(12)(p11)×2 |
| | ● | 80–85,XXXX,del(1)(q12),add(6)(q15),add(11)(p15),add(12)(q22),add(18)(p11),inc41,XX,del(1),add(6),add(11),add(12),inc |
| | ● | 66–73,XXX,add(1)(p32),der(1)add(1)(p36)del(1)(q12),der(3)add(3)(p13)add(3)(q27),der(3)del(3)(p11) |
| | | add(3)(q27),add(6)(p24),del(7)(p12),del(7)(q32),add(8)(p11)×2,der(9)del(9)(p21)add(9)(q34)×2,del(10)(p11),der(11)t(11;15)(p11;q12),add(12)(p11),add(14)(q32),add(16)(q12),add(19)(p12),der(20) |
| | | t(8;20)(q13;q13),der(20)t(17;20)(q21;q13),add(21)(q22),add(22)(p12),inc |
| | ● | 76–81,XX,-Y,add(2)(q37),del(4)(p15),del(11)(p11),der(11;16)(q10;q10),del(12)(p12),add(19)(p13),inc |
| | ● | 37–44,XY,del(1)(p11),add(5)(p15),del(5)(p14),der(10;12)(q10;q10),der(15)t(11;15)(q13;p11),add(19)(p11),inc/67–69,idem×2 |
| | ● | 37–40,X,-X,-1,add(1)(q21),-2,der(2)t(1;2)(q21;p2?5),add(3)(q13),-4,-5,add(6)(q15),add(6)(q27),-8,add(8)(p11),add(10)(p11), add(10)(p15),-11,i(11)(q10),-13,add(13)(q34),-14,-14,add(15)(p11),add(19)(p11),add(19)(q13),-22,+r,inc/74–78,idem×2 |
| | ● | 66–78,XY,-X,del(1)(q11),del(1)(q21),add(2)(q37), del(5)(p13),add(12)(p11),inc |

| ***Refs*** | ***Karyotype*** | |
|---|---|---|
| Mertens *et al* [18] | ● | 46,XX,del(2)(q23q31),der(3)del(3)(p21)add(3)(q23),del(4)(q31),t(6;14)(p11;q11),der(7)t(3;7)(q23;q22) |
| | | ins(7;?)(q22;?),der(13)t(4;13)(q31;q32),+der(?),t(?;21)(?;q11)/46,XX,der(1)t(1;6)(p34;p25)add(1)(q12),add(3)(q12),der(6)t(1;6)(p34;p25),der(20),t(1;20)(q25;p13)/46,XX,add(9)(q34),del(13)(q12q21), add(21)(q22)/46,t(X;16)(p22;q13),t(X;17)(p11;q23)/43–47,X,-X,+r,inc/47,X,-X,der(1)t(1;10)(p12;q11),der(1)del(1)(p32)dup(1)(p32p11),-4,+7,add(10)(q11),der(17)t(4;17)(q21;q23),+2mar |
| Nilsson *et al* [19] | ● | 42,XY,dic(1;?)(p11;?),-2,der(3)t(3;??)(p12;q21),-9,-10,add(12)(p11),add(13)(p11),add(14)(q32),?der(16)add(16)(p11)del(16)(q22),add(17)(p11),add(21)(p11),-22,-22 |
| | ● | 39–48,-X,-Y,del(6)(q15),-10,add(11)(p15),+r(12) ×1–2,inc,40–48,X,-Y,del(6),-9,-10,-?11,-15,+der(?)r(?;12) ×2,inc |
| | ● | 49–50,X,-X,+1,+der(1;14)(p10;q10),der(1)add(1)(p22)add(1)(q32) ×2,+5,add(5)(p15) ×2,+12,?del(16)(q22),?dup(17)(q21q25),-18,+19,+22,+mar |
| | ● | 32–35,X,-X,-1,del(2)(p11),-3,der(7;15)(q10;q10),-8,add(9)(p11),-10,-11,del(11)(p11),-13,add(14)(p11),add(16)(q13),-17,-18,-19,-20,-21,-22, inc/62–68,idem ×2,add(13)(p13) |
| Simons *et al* [20] | ● | 85–87,X?,del(1)(q42),add(2)(q11),add(3)(q12) ×2,?add(6)(q15),del(7)(q13),del(11)(p13),?del(11)(q23),?del(12)(p11),add(15)(q22),add(17)(q25), add(19)(q13) ×1–3,inc |
| | ● | 68–75,XX,add(X)(p22),del(1)(p13),del(1)(p33),der(1)t(1;5)(q21;q13) ×2,del(2)(p14),-3,-3,del(3)(q21),-4,-4, add(4)(p15),-5,-5,del(6)(q21),+7,-9,add(9)(p22),del(9)(p13),-10,-10,add(11)(q23),del(17)(p13),add(19)(q13) ×2,+del(20)(q13),add(22)(p13),+4–11mar |
| Szymanska *et al* [21] | ● | 58–71,XX?,+4mar,20–23dmin,inc |
| | ● | 46,XX,add(1)(q21) or add(1)(q32),t(1;10)(p22;q22),tas(5;5)(q35;q35),tas(10;?)(q26;?),+14,tas(18;?)(q23;?)/46,XX,add(21)(p11) |
| Orndal *et al* [22] | ● | 46–51,X,-Y,-22,+2–7r/45–50,idem,-18 |
| Orndal *et al* [23] | ● | 81–88,-X,-X,-X,del(1)(p21),del(1)(q11),der(1),add(1)(p36)del(1)(q12),add(2)(q11),del(3)(p11) ×2,del(6)(q15),add(14)(p13),add(17)(p11–12), add(19)(p13),add(20)(q13) ×2,inc82–110,-X,-X,-X,-X,add(1)(q21),del(1)(q11),del(1)(q21),add(2)(q11),add(3)(q29),del(3)(p11),del(6)(q15), add(7)(p22),add(12)(p11),add(14)(p13),add(17)(p11–12),add(20)(q13) ×2,inc65–90,-X,-X,-X,del(1)(q11),der(1)add(1)(p36)del(1)(q12), add(2)(q11),del(3)(p11) ×2,del(6)(q15),del(7)(q31),add(11)(q23),add(14)(p13),add(15)(p13),add(16)(p13),add(17)(p11–12),add(18)(p11), add(19)(p13),add(20)(q13) ×2,inc73–101,-X,-X,-X,add(1)(q21),del(1)(q21),add(2)(q11),add(3)(q29),del(3)(p11),del(6)(q15),add(7)(p22), add(14)(p13),add(15)(p13),add(16)(p13),add(19)(p13),add(20)(q13) ×2,inc |
| Orndal *et al* [24] | ● | 54–61,-X,-X,der(1)del(1)(q11)add(1)(p36),der(1),del(1)(p13)add(1)(q42),del(3)(q11),der(19) |
| | | add(19)(p13)add(19)(q13),inc,99–115,-X,-X,-X,-X,del(1)(q12) ×2,add(3)(q27) ×2,add(6)(q15),inc |
| | ● | 61–67,XX,-X,add(1)(p36),add(2)(q21),del(2)(q32),add(3)(q11),add(4)(p16),der(4)add(4)(p16) |
| | | add(4)(q?),add(5)(q35),del(6)(q11),del(7)(q31),der(7)add(7)(p22),add(7)(q32),add(8)(q24),?del(10)(p12),der(11),add(11)(p15)add(11)(q22), der(11)t(11;11)(p15;q11) |
| | | ins(11;?)(p15;?),der(12)t(5;12)(q13;q13),dic(16;18)(q13;q23),add(17)(p11),?add(17)(p13), add(19)(q13),der(20)t(1;20)(q44;p13)del(1)(q12),?i(22)(q10),inc |

and grade II lesions. This suggests that these complex karyotypic abnormalities occur rather randomly as secondary events. We showed that local recurrences occurred in all grades, with increase in grade upon recurrence, which is in accordance to the literature [2, 27]. We hypothesised that in the same lesion, increase in grade goes together with increase in cytogenetic aberrations. Therefore, we compared the karyotypes of primary lesions to these of the corresponding local recurrences. Recurrences showed increase in grade and more complex aberrations than the primary tumours (Figure 3). These complex aberrations suggest additional chromosomal events, corresponding with an increase in histological grade and, subsequently, increase in malignant potential.
Besides nonclonal and clonal aberrations, we found the presence of a ring chromosome in one case of low-grade myxofibrosarcoma. The presence of ring chromosomes has also have been described in one case of myxofibrosarcoma possibly originating from 20q [17]. Ring chromosomes have been described in many tumours, both benign as well as malignant, including dedifferentiated liposarcoma, a differential diagnosis of grade III myxofibrosarcoma [11, 28]. However, this is certainly not a consistent feature and its molecular and biological significance has not been revealed yet. Previous reports described several translocations in myxofibrosarcoma. Although all of them were different and nonspecific, some of these involve interesting regions. For example, Clawson et al [13] described a case of grade I myxofibrosarcoma with translocation t(2;15)(p23;q21.2). The band 2p23 is a site of *ALK* gene, expressed in normal tissue and rearrangements have been described in anaplastic large cell lymphomas, and inflammatory myofibroblastic tumours [29, 30]. Translocations involving 2p23 have been found in a case of synovial sarcoma as t(2;15)(p23;q26) and also in one case of

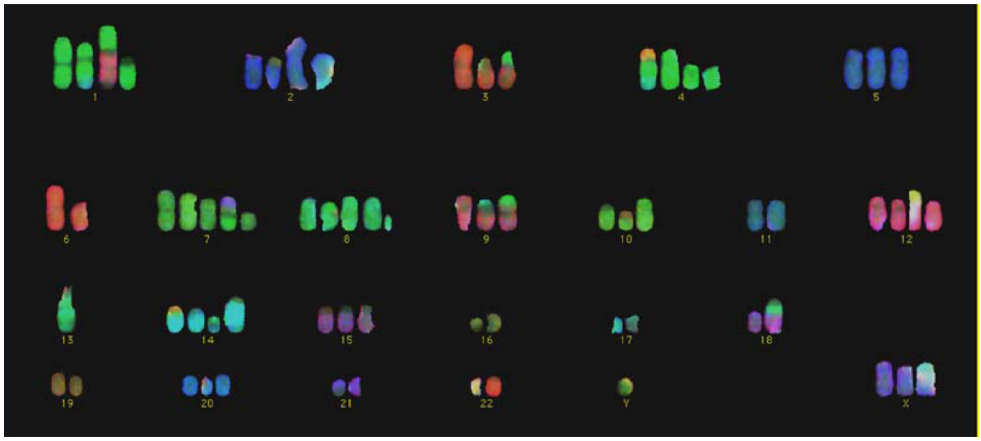


**Figure 4:** COBRA-FISH in a case of a high-grade myxofibrosarcoma. Example of highly complex cytogenetic aberrations in a case of high-grade myxofibrosarcoma (case 32). For karyotypic aberrations see Table 2.

'malignant fibrous histiocytomas not otherwise specified' as t(2;5)(p23;q13) [31, 32]. Frequent loss of 9p21 (p16) has been reported in malignant fibrous histiocytomas including also some cases of myxofibrosarcoma [20, 33, 34]. We could not confirm these aberrations in our study. Some studies showed add2(q37) in myxofibrosarcoma and in several types of leukaemia [11]. Interestingly, the COL6A1 gene is localised to 2q37, coding for collagen VI alpha-3 polypeptide. At least three other extra cellular matrix genes are also located on 2q: 2 collagen genes, COL3A1 and COL5A2 and the fibronectin gene [35]. As described above, myxofibrosarcoma contains areas of abundant extracellular matrix although only little is known about its constitution. Ultrastructural studies showed that the majority of cells in myxoid areas of myxofibrosarcoma showed secretory activity with dilated rough endoplasmatic reticulum. Although further study is needed, alterations in genes coding for matrix proteins might lead to increased or impaired matrix production. Interestingly, a myxofibrosarcoma-like appearance appears to be quite frequent in pleomorphic liposarcoma, thereby including it in the differential diagnosis [36]. In the light of this differential diagnosis, the cases reported here were carefully characterised, explicitly excluding contaminations with pleomorphic liposarcoma karyotypes in this series of myxofibrosarcoma. Finally, a recent study using comparative genomic hybridisation (CGH) showed very similar chromosome imbalances between myxoid malignant fibrous histiocytoma and pleomorphic liposarcoma, suggesting partially common genetics and biology [37]. This study showed gain of 5p and loss of 4q in myxofibrosarcoma of higher grade compared to tumours of lower grade. Whether these and other myxoid soft tissue tumours, in parallel to their morphologic resemblance, also share genetic overlap is a very interesting hypothesis, which, however, still needs to be confirmed.

**Acknowledgements**

We thank M Yszenga for performing the COBRA-FISH experiments. This project was financially supported by a Grant (RUL 2001-2526) from the Dutch Cancer Foundation. This text presents research results of the Belgian program on Interuniversity Poles of Attraction initiated by the Belgian Sate, Prime Minister's Office, Science Policy Programming. Its authors assume the scientific responsibility. The authors would like to acknowledge the COST support through the COST ACTION B19 'Molecular cytogenetics of solid tumors' in carrying out this work.

**References**


1. Angervall L, Kindblom LG, Merck C. Myxofibrosarcoma. A study of 30 cases. Acta Pathol Microbiol Scand [A] 1977;85A:127-140.
2. Mentzel T, Van den Berg E, Molenaar WM. Myxofibrosarcoma. In: Fletcher CDM, Unni KK, Mertens F (eds). World Health Organization classification of tumours. pathology and genetics. Tumours of soft tissue and bone, 2002 edn. IARC press: Lyon, 2004, pp 102-103.
3. Weiss SW, Enzinger FM. Myxoid vaiant of malignant fibrous histiocytoma. Cancer 1977;39:1672-1685.
4. Mentzel T, Calonje E, Wadden C, et al. Myxofibrosarcoma. Clinicopathologic analysis of 75 cases with emphasis on the low-grade variant. Am J Surg Pathol 1996;20:391-405.
5. Trojani M, Contesso G, Coindre JM, et al. Soft-tissue sarcomas of adults; study of pathological prognostic variables and definition of a histopathological grading system. Int J Cancer 1984;33:37-42.
6. Limon J, Dal Cin P, Sandberg AA. Application of long-term collagenase disaggregation for the cytogenetic analysis of human solid tumors. Cancer Genet Cytogenet 1986;23:305-313.
7. ISCN. An international system for human cytogenetic nomenclature. S.Karger: Basel, 1995.
8. Szuhai K, Knijnenburg J, Ijszenga M, et al. Multicolor fluorescence in situ hybridization analysis of a synovial sarcoma of the larynx with a t(X;18)(p11.2;q11.2) and trisomies 2 and 8. Cancer Genet Cytogenet 2004;153:48-52.
9. Tanke HJ, Wiegant J, Van Gijlswijk RPM, et al. New strategy for multi-colour fluorescence in situ hybrydisation: COBRA: COmbined Binary RAtio labelling. Eur J Hum Genet 1999;7:2-11.
10. Wiegant J, Bezrookove V, Rosenberg C, et al. Differentially painting human chromosome arms with combined binary ratio-labeling fluorescence in situ hybridization. Genome Res 2000;10:861-865.
11. Mertens F, Fletcher CD, Dal Cin P, et al. Cytogenetic analysis of 46 pleomorphic soft tissue sarcomas and correlation with morphologic and clinical features: a report of the CHAMP Study Group. Chromosomes and MorPhology. Genes Chromosomes Cancer 1998;22:16-25.
12. Graadt van Roggen JF, Hogendoorn PCW, Fletcher CDM. Myxoid tumours of soft tissue. Histopathology 1999;35:291-312.
13. Clawson K, Donner LR, Dobin SM. Translocation (2;15)(p23;q21.2) and interstitial deletion of 7q in a case of low-grade myxofibrosarcoma. Cancer Genet Cytogenet 2001;127:140-142.
14. Johansson M, Karauzum SB, Dietrich C, et al. Karyotypic abnormalities in adenocarcinomas of the lung. Int J Oncol 1994;5:17-26.
15. Mandahl N, Heim S, Willén H, et al. Characteristic karyotypic anomalies identify subtypes of malignant fibrous histiocytoma. Genes Chromosomes Cancer 1989;1:9-14. |
16. Meis-Kindblom JM, Sjogren H, Kindblom LG, et al. Cytogenetic and molecular analyses of liposarcoma and its soft tissue simulators: recognition of new variants of differential diagnosis. Virchows Arch 2001;439:141-151.
17. Meloni-Ehrig AM, Chen Z, Guan XY, et al. Identification of a ring chromosome in a myxoid malignant fibrous histiocytoma with chromosome microdissection and fluorescence in situ hybridization. Cancer Ge net Cytogenet 1999;109:81-85.
18. Mertens F, Larramendy M, Gustavsson A, et al. Radiation-associated sarcomas are characterized by com plex karyotypes with frequent rearrangements of chromosome arm 3p. Cancer Genet Cytogenet 2000;116:89-96.
19. Nilsson M, Meza-Zepeda LA, Mertens F, et al. Amplification of chromosome 1 sequences in lipomatous tumors and other sarcomas. Int J Cancer 2004;109:363-369.
20. Simons A, Schepens M, Jeuken J, et al. Frequent loss of 9p21 (p16(INK4A)) and other genomic imbalances in human malignant fibrous histiocytoma. Cancer Genet Cytogenet 2000;118:89-98.
21. Szymanska J, Tarkkanen M, Wiklund T, et al. A cytogenetic study of malignant fibrous histiocytoma. Cancer Genet Cytogenet 1995;85:91-96.
22. Orndal C, Mandahl N, Rydholm A, et al. Supernumerary ring chromosomes in 5 bone and soft-tissue tu mors of low or borderline malignancy. Cancer Genet Cytogenet 1992;60:170-175.
23. Orndal C, Mandahl N, Willen H, et al. Cytogenetic evolution in primary tumors, local recurrences, and pulmonary metastases of 2 soft-tissue sarcomas. Clin Exp Metast 1993;11:401-408.
24. Orndal C, Rydholm A, Willen H, et al. Cytogenetic intratumor heterogeneity in soft-tissue tumors. Cancer Genet Cytogenet 1994;78:127-137.

25. Huang HY, Lal P, Qin J, et al. Low-grade myxofibrosarcoma: a clinicopathologic analysis of 49 cases treated at a single institution with simultaneous assessment of the efficacy of 3-tier and 4-tier grading systems. Hum Pathol 2004;35:612-621.
26. Merck C, Angervall L, Kindblom LG, et al. Myxofibrosarcoma. A malignant soft tissue tumor of fibroblastic-histiocytic origin. A clinicopathologic and prognostic study of 110 cases using multivariate analysis. Acta Pathol Microbiol Immunol Scand Suppl 1983;282:1-40.
27. Ferguson PC, Deshmukh N, Abudu A, et al. Change in histological grade in locally recurrent soft tissue sarcomas. Eur J Cancer 2004;40:2237-2242.
28. Dei Tos AP, Doglioni C, Piccinin S, et al. Coordinated expression and amplification of the MDM2, CDK4, and HMGI-C genes in atypical lipomatous tumours. J Pathol 2000;190:531-536.
29. Lawrence B, Perez-Atayde A, Hibbard MK, et al. TPM3-ALK and TPM4-ALK oncogenes in inflammatory myofibroblastic tumors. Am J Pathol 2000;157:377-384.
30. Mitelman F, Mertens F, Johansson B. A breakpoint map of recurrent chromosomal rearrangements in human neoplasia. Nat Genet 1997;15(Spec No):417-474.
31. Mandahl N, Heim S, Arheden K, et al. Multiple karyotypic rearrangements, including t(X;18)(p11;q11), in a fibrosarcoma. Cancer Genet Cytogenet 1988;30:323-327.
32. Mandahl N, Heim S, Arheden K, et al. Separate karyotypic features in a local recurrence and a metastasis of a fibrosarcoma. Cancer Genet Cytogenet 1989;37:139-140.
33. Weng WH, Ahlen J, Lui WO, et al. Gain of 17q in malignant fibrous histiocytoma is associated with a longer disease-free survival and a low risk of developing distant metastasis. Br J Cancer 2003;89:720-726.
34. Martignetti JA, Gelb BD, Pierce H, et al. Malignant fibrous histiocytoma: inherited and sporadic forms have loss of heterozygosity at chromosome bands 9p21-22-evidence for a common genetic defect. Genes Chromosomes Cancer 2000;27:191-195.
35. Weil D, Mattei MG, Passage E, et al. Cloning and chromosomal localization of human genes encoding the three chains of type VI collagen. Am J Hum Genet 1988;42:435-445.
36. Hornick JL, Bosenberg MW, Mentzel T, et al. Pleomorphic liposarcoma: clinicopathologic analysis of 57 cases. Am J Surg Pathol 2004;28:1257-1267.
37. Idbaih A, Coindre JM, Derre J, et al. Myxoid malignant fibrous histiocytoma and pleomorphic liposarcoma share very similar genomic imbalances. Lab Invest 2005;85:176-181.

# Chapter 4

## Myxoid tumours of soft tissue: the so-called myxoid extracellular matrix is heterogeneous in composition

S.M. Willems, Y.M. Schrage, J.J. Baelde, I.H. Briaire-de Bruijn, A. Mohseny, R. Sciot[1], J.V.M.G. Bovée, P.C.W. Hogendoorn

Department of Pathology, Leiden University Medical Center, Leiden, The Netherlands, and [1]Department of Morphology and Molecular Pathology, University Hospitals, Catholic University of Leuven, Leuven, Belgium

**Abstract**

Myxoid tumours of soft tissue are characterized by their so-called 'myxoid' extracellular matrix. The aim was to investigate the composition and possible function of this matrix which is poorly understood. Using Alcian Blue staining with and without pretreatment with hyaluronidase and application of the critical electrolyte concentration method followed by densitometry, the glycosaminoglycan composition of three different myxoid tumours was studied. The composition of glycosaminoglycans varied with tumour type and grade, despite their general characterization as myxoid tumours. Intramuscular myxoma contained similar amounts of the various glycosaminoglycans as grade I myxofibrosarcoma; grade III myxofibrosarcoma contained less hyaluronic acid and more heparan sulphate, whereas extraskeletal myxoid chondrosarcoma contained predominantly chondroitin-4 and -6 sulphates. Western blot identified albumin as a major protein in tumour lysates, and its presence in the extracellular matrix and cytoplasm of the majority of tumours was demonstrated by immunohistochemistry; production of albumin by the tumour cells was confirmed by quantitative polymerase chain reaction. The extracellular matrix of myxoid tumours of soft tissue has a heterogeneous composition consisting of, amongst others, glycosaminoglycans and albumin, which appear to play an active role in their morphogenesis.

## Introduction

Myxoid tumours of soft tissue are a heterogeneous group of tumours characterized histologically by their abundant mucoid/myxoid extracellular matrix (ECM)(1). The main clinicopathological entities in this group are intramuscular myxoma, myxofibrosarcoma and extraskeletal myxoid chondrosarcoma and encompass a broad spectrum of clinical behaviour, ranging from benign to truly malignant. Although these tumours share a typical ECM, the exact constitution and possible functions of this myxoid ECM remains poorly understood. Over recent decades, biochemical studies have emphasized that glycosaminoglycans (GAGs) are important constituents of the ECM (2) The main GAGs in the ECM of these tumours are hyaluronic acid, heparan sulphate, chondroitin sulphate and keratan sulphate. Due to the negative charge of the above-mentioned GAGs, their high viscosity and low compressibility, these molecules provide structure to the ECM and facilitate the extracellular transport of molecules. Kindblom and Angervall have demonstrated that the GAGs in the ECM of myxoid tumours of soft tissue differ from those in the ECM of bone tumours (2). The nature of, and variation in GAGs among myxoid tumours of soft tissue has not as yet been studied in any great detail. GAGs are important for signal transduction, sequestration of growth factors, receptor-ligand recognition during development and interactions between tumour cells. Together with their surrounding ECM, they play an important role in tumour progression and invasion (3). We investigated whether the composition of ECM shows significant variation between myxoid tumours of soft tissue and might be related to differences in their clinical behaviour. In addition, the aim was to elucidate how these GAGs, together with other proteins, might play a role in the morphogenesis of this characteristic myxoid morphology.

## Materials and methods

*Clinicopathological data and procedures*

Nine intramuscular myxomas and seven grade I and eight grade III myxofibrosarcomas were collected retrospectively from the files of the Pathology Departments of Leiden and Leuven University Medical Centre. Twelve extraskeletal myxoid chondrosarcomas were retrospectively collected from the files of the Institute of Pathology, University of Bern, Switzerland and kindly provided by Dr P. Mainil-Varlet. Patient and tumour characteristics are described in Table 1. Slides were re-evaluated histologically by two experienced soft tissue pathologists (R.S., P.C.W.H.), classified according to the 2002 World Health Organization criteria and histologically graded according to the French Fédération Nationale des Centres de Lutte Contre le Cancer (FNCLCC) when applicable (4-6). All tissue samples were handled in a coded fashion, according to Dutch national ethical guidelines (Code for proper secondary use of human tissue, Dutch Federation of Medical Scientific Societies).

**Table 1:** Clinicopathological data of included patients with myxoid tumours

| Case | P/R/M* | Age (years) | Gender† | Location | Site | Diagnosis | Grade‡ |
|---|---|---|---|---|---|---|---|
| 1 | P | 51 | F | Proximal leg muscles | Left | Intramuscular myxoma | NA |
| 2 | P | 56 | F | m. psoas | Right | Intramuscular myxoma | NA |
| 3 | P | 59 | M | Proximal leg muscles | Right | Intramuscular myxoma | NA |
| 4 | P | 66 | M | Proximal leg muscles | Left | Intramuscular myxoma | NA |
| 5 | P | 33 | M | Knee | Right | Intramuscular myxoma | NA |
| 6 | P | 40 | F | Proximal arm muscle | Right | Intramuscular myxoma | NA |
| 7 | P | 61 | F | m. vastus lateralis | Left | Intramuscular myxoma | NA |
| 8 | P | 62 | M | Proximal leg muscles | Right | Intramuscular myxoma | NA |
| 9 | P | 55 | F | m. triceps medialis | Right | Intramuscular myxoma | NA |
| 10 | M | 58 | M | Vertebral Th V | NA | Extraskeletal myxoid chondrosarcoma | NA |
| 11 | P | 54 | M | Groin | Left | Extraskeletal myxoid chondrosarcoma | NA |
| 12 | P | 32 | M | Neck | NA | Extraskeletal myxoid chondrosarcoma | NA |
| 13 | P | 48 | M | Proximal leg | Left | Extraskeletal myxoid chondrosarcoma | NA |
| 14 | P | 67 | F | Thigh | Right | Extraskeletal myxoid chondrosarcoma | NA |
| 15 | P | 76 | F | Talus | Right | Extraskeletal myxoid chondrosarcoma | NA |
| 16 | P | 76 | F | m. femoris | Right | Extraskeletal myxoid chondrosarcoma | NA |
| 17 | P | 22 | F | Foot | Right | Extraskeletal myxoid chondrosarcoma | NA |
| 18 | P | 50 | F | Proximal leg | Left | Extraskeletal myxoid chondrosarcoma | NA |
| 19 | P | 77 | M | Proximal leg | Right | Extraskeletal myxoid chondrosarcoma | NA |
| 20 | P | 50 | F | Proximal leg | Left | Extraskeletal myxoid chondrosarcoma | NA |
| 21 | P | 66 | M | Thorax | Right | Extraskeletal myxoid chondrosarcoma | NA |
| 22 | P | 78 | M | Proximal leg | Left | Myxofibrosarcoma | I |
| 23 | P | 53 | M | Flank | Left | Myxofibrosarcoma | I |
| 24 | P | 62 | M | Proximal leg | Left | Myxofibrosarcoma | I |
| 25 | P | 47 | M | m. deltoideus | Left | Myxofibrosarcoma | I |
| 26 | P | 56 | F | m. vastus lateralis | Left | Myxofibrosarcoma | I |
| 27 | P | 82 | M | Proximal leg | Right | Myxofibrosarcoma | I |
| 28 | P | 52 | M | Lung | NA | Myxofibrosarcoma | I |
| 29 | P | 65 | F | m. vastus lateralis | Right | Myxofibrosarcoma | I |
| 30 | P | 36 | M | Hamstring muscles | Right | Myxofibrosarcoma | III |
| 31 | P | 73 | M | Distal arm | Left | Myxofibrosarcoma | III |
| 32 | P | 57 | M | m. gluteus | Right | Myxofibrosarcoma | III |
| 33 | P | 46 | F | m. gluteus | Left | Myxofibrosarcoma | III |
| 34 | P | 46 | M | Distal leg | Right | Myxofibrosarcoma | III |
| 35 | P | 91 | M | Distal leg | Left | Myxofibrosarcoma | III |
| 36 | P | 64 | F | Hamstring muscles | Right | Myxofibrosarcoma | III |

*P, primary; R, recurrence; M, metastasis; †F, female; M, male; ‡Histological grading was performed according to the FNCLCC. Accordingly, intramuscular myxoma and extraskeletal myxoid chondrosarcoma were not graded (NA).

*Determination of glycosaminoglycan composition*

For hyaluronidase digestion, slides were incubated for 18 h at 37°C with bovine testes hyaluronidase (Sigma-Aldrich, Zwijndrecht, the Netherlands) and dissolved in a 0.2 M sodium acetate buffer (pH 5.6). For Alcian blue staining following critical electrolyte concentration, paraffin slides were incubated for 18 h in 0.1% Alcian Blue 8GX solution (Sigma-Aldrich) dissolved in 0.2 M sodium acetate buffer (pH 5.6) together with magnesium chloride in variable concentrations (0, 0.3, 0.6 and 1.2 M). With this technique, each biochemically determined GAG possesses its own specific critical electrolyte concentration (Table 2). Chondrosarcoma served as an external positive control. Densitometry was performed with a Leica DM-RXA microscope (Leica, Chicago, IL, USA) with an HQ tetrarhodamine isothiocyanate red filter connected to a digital camera. For computerized analysis of the absorption the program ColourProc 2003c was used. Average absorption was calculated after measuring six separate fields, using a threshold set at 2600 and 3800 to distinguish the nuclei from ECM absorption.

*Protein analysis of tumour lysates*

To identify other major ECM proteins, we analysed tumour lysates of three intramuscular myxomas (cases 2, 7 and 8), three extraskeletal myxoid chondrosarcomas (cases 14, 15 and 16), three grade I, and three grade III myxofibrosarcomas (cases 24, 25, 26 and 32, 33 and 36. respectively). Forty slides of 20 μm were cut from each tumour. After adding 2 ml of Aurum serum protein binding buffer (Bio-Rad, Hercules, CA, USA), samples were mixed for 15 s using a homogenizer (Ultra-Turrax T8; Rose Scientific, Edmonton, Canada). Reduced samples were separated by sodium dodecyl sulphate polyacrylamide gel electrophoresis (SDS-PAGE) on 10% gel and stained with Coomassie Brilliant Blue (Merck, Amsterdam, the Netherlands). Tumour tissue lysates were separated by SDS-PAGE on 10% gel and transferred to polyvinylidene fluoride membrane filters. Transferred membranes were blocked with phosphate-buffered saline (PBS)-Tween (0.05%) for IgG staining and skimmed milk in PBS-Tween for albumin staining. Polyvinylidene fluoride filters were washed and incubated for 30 min with polyclonal α-rabbit albumin and polyclonal α-rabbit IgG antibodies (both 1:20 000; DakoCytomation, Glostrup, Denmark) in PBS-Tween. After incubating the filters, enhanced chemiluminescence (Amersham, Diegem, Belgium) was used as a detection method. To evaluate the relative contribution of albumin and IgG to the total protein content of the ECM, samples were depleted of albumin and IgG using the Aurum Serum Protein kit (Bio-Rad). Protein concentrations were measured with a detergent

**Table 2:** Identification of GAGs by applying differences in CEC

| GAG | CEC (molarity of magnesium chloride) |
|---|---|
| Hyaluronic acid | 0.0 |
| Chondroitin-4 and -6 sulphate | 0.3 |
| Heparan | 0.6 |
| Keratan sulphate | 1.2 |

compatible protein assay (Bio-Rad). Relative amounts of albumin and IgG were calculated as the differences in protein concentrations before and after depletion.

*Tissue microarray construction*

To validate the specificity of albumin staining in myxoid soft tissue tumours, a soft tissue tumour microarray was constructed. Seventy-nine soft tissue tumours (28 different entities) with well-documented clinicopathological data and follow-up were selected from the files of the Pathology Department of Leiden University Medical Centre. The slides were reviewed by an experienced pathologist (P.C.W.H.), classified according to the 2002 World Health Organization criteria (7) and histologically graded according to the FNCLCC (5, 6). Representative tumour areas were selected and four tissue cores from each specimen were obtained using a manual tissue arrayer (Beecher Instruments, Silver Springs, MD, USA). The punches with a diameter of 0.6 mm were arrayed on a recipient paraffin block, using standard procedures (8, 9).

*Immunohistochemistry and criteria for scoring*

Sections (4 μm thick) were mounted on 3-aminopropylethoxysilane (Sigma, St Louis, MO, USA) and glutaraldehyde-coated slides and dried overnight at 37°C. Immunohistochemistry was performed as previously described with rabbit polyclonal anti-albumin antibody (1:20 000; DakoCytomation), using antigen retrieval (citrate 10 min, microwave)(10). Normal liver was used as a positive control. ECM and cytoplasm of slides and punches were scored by three different observers (S.M.W., J.V.M.G.B. and P.C.W.H.) separately. ECM of whole sections and punches were scored as either positive (+) or negative (-). Cytoplasmic expression of whole sections was scored as previously described (11). Cytoplasmic expression of tissue microarray punches was scored as either positive (>10% of cells positive) or negative (<10% of cells positive).

*Real-time polymerase chain reaction for albumin*

RNA was isolated from formalin-fixed paraffin-embedded material as described previously (12). Real-time polymerase chain reaction (PCR) was performed as described previously (13). The following primers were used: forward, 5'-AGA GGT TTA AAT TCA TCG AAC ACT TTG-3' and reverse, 5'-CGT GCT GCT GCT GCT GAG ACT TG-3'. After real-time PCR, the products were purified using Qiagen QIAquick PCR Purification Kit (Qiagen, GmbH, Hilden, Germany) prior to sequencing. For sequence confirmation of the products the ABI PRISM® Big Dye Terminators v. 2.0 Cycle Sequencing Kit was used (Applied Biosystems, Foster City, CA, USA). Samples were run on an ABI 3700 Genetic Analyser (Applied Biosystems). TATA box binding protein (TBP) was used as a housekeeping gene to check for the quality of the mRNA using the following primers: forward, 5'-CAC GAA CCA CGG CAC TGA T-3'and reverse, 5'-TTT TCT TGC TGC CAG TCT GGA C-3'.

*RNA in situ hybridization*

A 450-bp product coding for albumin RNA probe was generated using the following primers: forward, 5'-CTT TCA AAG CAT GGG CAG TAG C-3' and reverse, 5'-GCA GCG GCA CAG CAC TTC-3' on DNA from liver Hep-G2 cells. This fragment was cloned into a pGEM easy (t) vector (Promega, Madison, WI, USA). After transfection in Escherichia coli HB101, plasmids were isolated using the QIAfilter Maxi KITS protocol (Qiagen GmbH).14 RNA in situ hybridization was performed as previously described (14).

*Confocal microscopy for albumin-Golgi double staining*

One each of extraskeletal myxoid chondrosarcoma, intramuscular myxoma and grade I myxofibrosarcoma with cytoplasmic albumin expression were selected. For immunofluorescence double staining polyclonal rabbit albumin (1:20 000; DakoCytomation) and polyclonal rabbit 58 Golgi protein antibodies (1:100; Abcam Ltd, Cambridge, UK) were used both with antigen retrieval (citrate, 10 min microwave). Immunoreactivity was detected using Alexa Fluor 488, or 647 secondary antibodies (Molecular Probes, Invitrogen, Breda, the Netherlands). Scanning was done as previously described, using a Laser Scanning Microscope (LSM) 510 confocal fluorescence microscope (Zeiss, Jena, Germany)(15).

*Statistical analysis*

Differences in intensity of immunoreactivity following critical electrolyte concentration were calculated with the one-way ANOVA test and post hoc comparisons. Differences in the outcome of the hyaluronidase experiment were calculated with a two-tailed t-test. To calculate differences in protein concentration, a two-tailed Student's t-test was used.

## Results

*Clinicopathological data*

Patient and tumour characteristics are depicted in Table 1. Intramuscular myxoma occurred in the extremities only, showed equal sex distribution and a median age of occurrence of 54 years. All myxofibrosarcomas, regardless of grade, occurred in the extremities, except for case 28 (lung). They showed a male predominance and a median age of occurrence at 62 (grade I) and 59 years (grade III) of age. Extraskeletal myxoid chondrosarcomas occurred predominantly in the extremities and occasionally in the thoracic and neck region. The median age of occurrence was 56 years. All tumours, except for case 10 (vertebral metastasis), were primary lesions, not treated by any form of preoperative radiotherapy or chemotherapy. Examples of the histology are shown in Figure 1.

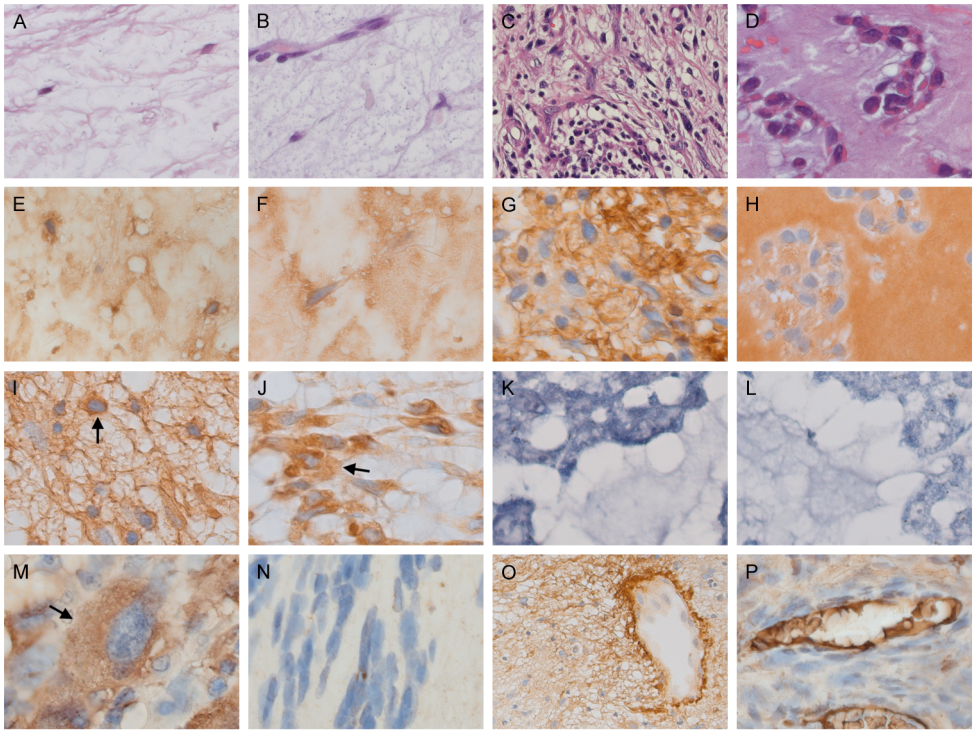


**Figure 1:** Characteristic morphology, immunohistochemistry and in situ hybridization for albumin in myxoid tumours of soft tissue. Intramuscular myxoma shows a hypocellular lesion with myxoid background and sparsely distributed tumour cells without atypia (A). Grade I myxofibrosarcoma is usually more cellular than intramuscular myxoma, shows more nuclear atypia and is hypervascular with typical curvilinear vessels (B). Grade III myxofibrosarcoma shows increased cellularity, more nuclear atypia and more collagenous extracellular matrix (ECM) than grade I myxofibrosarcoma (C). Extracellular myxoid chondrosarcoma has a rather chondro-myxoid ECM with tumour cells forming strands and cords (D). E-H, Immunohistochemistry for albumin shows diffuse reactivity of the ECM in intramuscular myxoma (E), grade I and grade III myxofibrosarcoma (F and G, respectively) and extraskeletal myxoid chondrosarcoma (H). Interestingly, tumour cells show cytoplasmic reactivity for albumin, as in this case of grade I myxofibrosarcoma (I) and extraskeletal myxoid chondrosarcoma (J). RNA in situ hybridization with antisense probes for albumin show diffuse cytoplasmic reactivity of tumour cells in the case of extraskeletal myxoid chondrosarcoma (K), whereas the sense probes are negative (L). Immunohistochemistry of the tissue microarray for albumin shows cytoplasmic expression in desmoid-type fibromatosis (M), whereas schwannoma is completely negative (N). Interestingly, grade III myxofibrosarcoma and solitary fibrous tumour show perivascular accentuation (O and P).

*Determination of glycosaminoglycans*

The ECM of intramuscular myxoma, extraskeletal myxoid chondrosarcoma, grade I and grade III myxofibrosarcoma showed a statistically significant decrease in absorption after treatment with hyaluronidase (results not shown). The decline in absorption did not differ significantly between tumours and was almost equal between intramuscular myxoma and grade I myxofibrosarcoma. Applying the method of critical electrolyte concentration, the ECM of intramuscular myxoma, extraskeletal myxoid

chondrosarcoma, grade I and grade III myxofibrosarcoma showed heterogeneity in the various GAGs present in the ECM within this group of tumours (Figure 2).

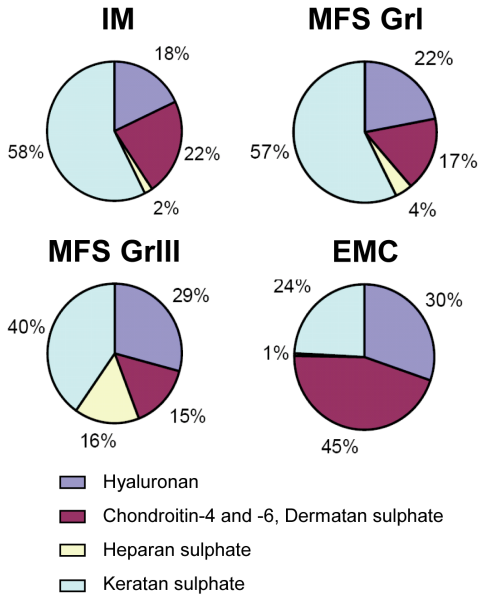


**Figure 2:** Extracellular matrix of myxoid soft tissue tumours contain different amounts of glycosaminoglycans (GAGs). Pie charts showing relative amounts of GAGs. Intramuscular myxoma (IM) contains the same amounts of various GAGs as grade I myxofibrosarcoma (MFS Gr I). Grade III myxofibrosarcoma (MFS Gr III) contains less hyaluronic acid and more heparan sulphate. Extra-skeletal myxoid chondrosarcoma (MCS) contains chondroitin-4 and -6 sulphates.

*Protein analysis of tumour lysates*

Coomassie brilliant blue staining of undepleted tumour lysates showed clear, dominant bands at 66, 75 and 200 kDa (Figure 3). Western blot analysis confirmed that the 66-kDa band corresponded to albumin and the 200-kDa band to IgG (results not shown). Contribution of albumin and IgG to the total ECM protein content is depicted in Figure 3. The results of the immunohistochemistry for albumin on sections and tissue microarray are shown in Figure 1.

*Immunohistochemistry for albumin*

Results of the immunohistochemistry with antibodies directed against albumin are shown in Figure 1. All tumours showed diffuse reactivity for albumin in the ECM and cytoplasm. Interestingly, perivascular staining for albumin was present in the majority of cases. Neither extracellular nor cytoplasmic reactivity for albumin were tumour-type specific, and both were also present in the majority of the non-myxoid tumours in the tissue microarray, although schwannoma and synovial chondromatosis were completely negative.

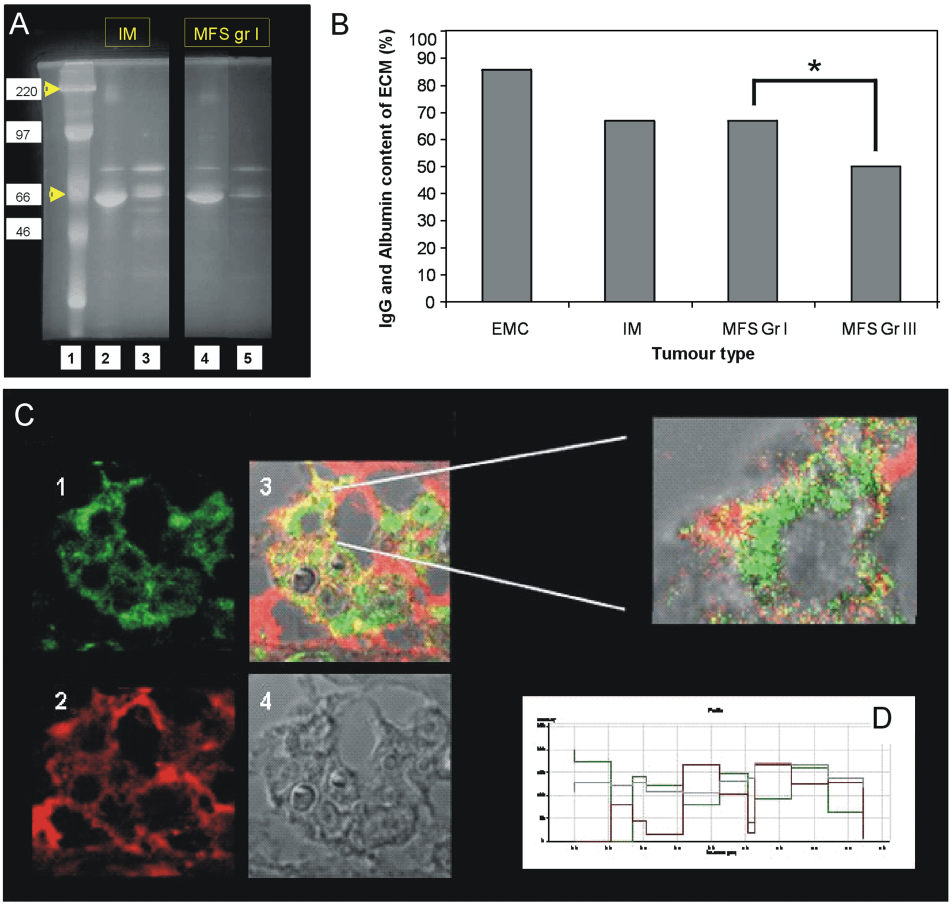


**Figure 3:** Albumin is a major extracellular matrix (ECM) protein of myxoid tumours of soft tissue and is produced by the tumour cells. A, Intramuscular myxoma (IM) and grade I myxofibrosarcoma (MFS), showing an intense band at 66 kDa and a smaller band at 200 kDa (A, lanes 2 and 4). Western blot analysis confirmed that these bands correspond to albumin (66 kDa) and IgG (200 kDa, not shown). There is a marked decrease in intensity of both 66-kDa and 200-kDa bands after depletion for albumin and IgG (A, lanes 3 and 5).B, Histogram showing that albumin is a major protein in the ECM of extraskeletal myxoid chondrosarcoma (EMC), IM and grade I and III MFS (Gr I and Gr III). Note that there is a significant decrease in albumin content in the ECM of myxofibrosarcoma with increased grade (*P = 0.004). C and D, Tumour cells of myxoid soft tissue tumours produce albumin, as in this case of extraskeletal myxoid chondrosarcoma. Two-colour immunofluorescence staining of 58K Golgi protein (green) and albumin (red) in extraskeletal myxoid chondrosarcoma. Note the overlap of the green and the red signal in the cytoplasm of the cells, indicative of co-localization (1, Golgi-immunofluorescence staining; 2, albumin-immunofluorescence staining; 3, Golgi-albumin immunofluorescence double staining; 4, Nomarski). Colocalization is shown as an intensity profile for one cell (C).

*RNA in situ hybridization, real-time PCR and sequencing*
Real-time PCR showed mRNA expression for albumin by the tumour cells in all cases, except for case 33. This was not due to the quality of the cDNA, as there was normal TBP expression. Sequencing of the samples confirmed that the reaction product was albumin. In situ hybridization with probes against albumin showed mRNA in the cytoplasm of the tumour cells, but not in the endothelial, perivascular cells or lymphocytic infiltrate (Figure 1).

*Confocal microscopy for albumin-Golgi double staining*
Colocalization of immunoreactivity for Golgi and albumin was found in the cytoplasm of tumour cells, as depicted in Figure 3.

**Discussion**

The term 'myxoid' was first used by Rudolf Virchow in 1871 to describe tumours that shared morphological features with the jelly-like structure of the umbilical cord (16). Nowadays, more than 60 reactive and neoplastic entities have been described as being predominantly myxoid or containing myxoid areas.1 Although GAGs undoubtedly contribute at least to some extent to the myxoid nature of the ECM, the exact composition and function of this so-called myxoid ECM are unknown. Interactions between tumour cells and their ECM are important in tumour progression and tumour invasion (17). Interestingly, we found that the distribution of the different GAGs in the ECM of intramuscular myxoma was identical to that of grade I myxofibrosarcoma. This corresponds to the comparable morphology of these tumours (Figure 1), but not to their clinical behaviour, as the former is truly benign (18) and the latter shows an increase in histological grade (19) and cytogenetic aberrations (20) on recurrence, probably responsible for the increase in metastatic potential. We have shown that for myxofibrosarcoma there is a significant increase in the amount of heparan sulphate with an increase in grade. Heparan sulphate facilitates metastasis by sequestering chemokines and/or growth factors, establishing a haptotactic gradient that drives tumour cells to specific stimuli. Furthermore, heparan sulphates are thought to aid in protection and localization of proteases and hinder the interactions between tumour cells and other adhesion molecules (21) The core protein of heparan sulphate interacts as a co-receptor with growth factors. This might explain how an increase in heparan sulphate in the ECM of myxofibrosarcoma is related to tumour progression. We have shown that the ECM of extracellular myxoid chondrosarcoma contains significantly more chondroitin-4 and -6 sulphates than intramuscular myxoma and myxofibrosarcoma. In this respect, our results correspond to previous cDNA microarray studies of extraskeletal myxoid chondrosarcoma showing overexpression of chondroitin sulphate proteoglycan 2 (versican)(22). Chondroitin sulphate interacts with several different ECM molecules and plays a crucial role in ECM assembly. Perhaps the best known

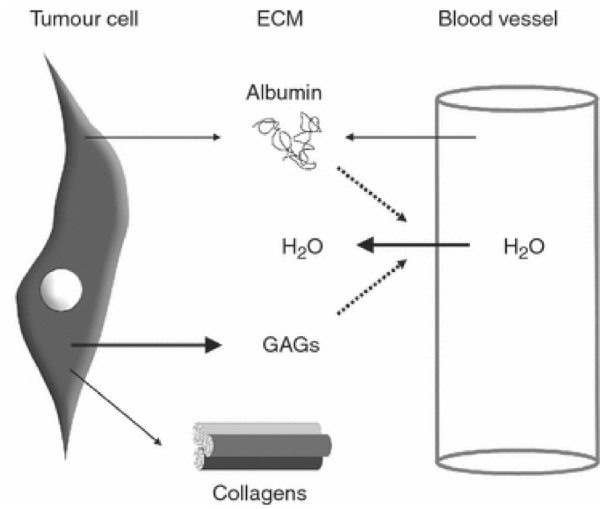


**Figure 4:** Proposed model for the role of glycosaminoglycans (GAGs) and albumin in extracellular matrix (ECM) formation in myxoid tumours of soft tissue. Interplay between GAGs and albumin in ECM formation and morphogenesis of myxoid tumours of soft tissue. Tumour cells produce GAGs and albumin, which attract water from adjacent blood vessels (interrupted arrows), which in turn is subsequently trapped in the interstitial space by GAGs.

interaction is between the amino-terminal domain of chondroitin sulphate and hyaluronic acid, which we have shown to be the second most abundant GAG in these tumours.23 Both GAGs are therefore crucial for ECM assembly and stability in extraskeletal myxoid chondrosarcoma. Chondroitin sulphate is involved in cell proliferation and migration, and appears to prevent apoptosis. Its abundant presence in the ECM of extraskeletal myxoid chondrosarcoma might play a role in the malignant behaviour of these tumours (Figure 2), although the exact underlying mechanisms are not yet fully understood.We have demonstrated that albumin is a major protein in the myxoid ECM, which we have confirmed by immunohistochemistry in a larger series (Figures 1 and 3). Albumin is the most abundant plasma protein, is important for transporting fatty acids, thyroid hormones and steroid hormones and is produced mainly by the liver. As a result of leakage of tumour vessels, at least part of the albumin in the ECM might be blood-borne, which is supported by the finding of other plasma proteins in the ECM. Interestingly, tumour cells of intramuscular myxoma, myxofibrosarcoma and extraskeletal myxoid chondrosarcoma also showed cytoplasmic staining for albumin, suggesting that it might be produced by the tumour cells. However, this pattern of immunoreactivity is not specific for myxoid tumours of soft tissue, since it is also found in many other tumours, including those without a myxoid morphology. Thus, the presence of albumin in itself cannot explain the myxoid ECM. Nevertheless, we hypothesize that albumin plays an important role in the morphogenesis of the ECM of myxoid tumours of soft tissue. Tumour cells produce collagens, GAGs and albumin,

as illustrated in Figure 4. Albumin and GAGs attract water from adjacent blood vessels by osmosis. This extracellular water percolates the tissue, delivering nutrients and oxygen and carrying away metabolites. Albumin is freely mobile in the ECM. Therefore, its presence does not depend heavily on production by (tumour) cells, but relies on stereometric and charge exclusion by trapped (macro)molecules such as collagens and hyaluronic acid (24) Following an increase in histological grade, the ECM of myxofibrosarcoma shows an increase in collagen, but no significant difference in hyaluronic acid (Figure 3). Thus, exclusion of albumin from the ECM in myxofibrosarcoma appears to be primarily regulated by collagen, but not by hyaluronic acid. This corresponds to our findings showing an inverse correlation between collagen and albumin (and IgG) content upon increase in histological grade. Morphologically, this is reflected in the transition from the more jelly-like ECM of grade I myxofibrosarcoma to the more collagenous ECM in grade III myxofibrosarcoma (Figure 1). Based on these results, we propose a model illustrating the interplay between albumin, GAGs and collagens in ECM formation as depicted in Figure 4. Albumin mRNA has been detected in several tissues such as the gastrointestinal tract, kidney, striated muscle, pancreas, placenta, spleen and uterus (http://cgap.nci.nih.gov). This suggests that albumin has important functions other than merely serving as a plasma protein. Perivascular albumin is essential for the integrity of the endothelial-ECM barrier (25). Interestingly, we observed that albumin present in the ECM has a perivascular accentuation (Figure 1). As the percentage of myxoid ECM inversely correlates with the vessel density in myxofibrosarcoma (19) albumin might act as an important transport molecule for diffusion of metabolic substrates in these tumours. This corresponds to our finding that the ECM of grade I myxofibrosarcoma (and intramuscular myxoma) contains significantly more albumin (and IgG) than grade III myxofibrosarcoma (Figure 3).

**Acknowledgements**

We thank Heidi van Paassen for preparing the tissue microarray and Dr Ir. J. Vrolijk for developing the software for image analysis (Molecular Cell Biology, Leiden University, Leiden). The Hep-G2 cells were a kind gift from Dr Menno Hoekstra (Leiden/Amsterdam Centre for Drug Research, Gorlaeus Laboratories, Leiden University, Leiden). Paraffin blocks from extraskeletal myxoid chondrosarcomas were kindly provided by Dr P. Mainil-Varlet (Institute of Pathology, University of Bern, Bern, Switzerland). We are grateful to Dr J. F. Graadt van Roggen for grammatical and textual corrections. This project was financially supported by a grant from The Netherlands Organization for Health Research and Development (project no. 920-03-403).

**References**


1. Graadt van Roggen JF, Hogendoorn PCW, Fletcher CDM. Myxoid tumours of soft tissue. Histopathology 1999; 35; 291-312.
2. Kindblom LG, Angervall L. Histochemical characterization of mucosubstances in bone and soft tissue-tumors. Cancer 1975; 36; 985-994.
3. Knudson CB, Knudson W. Cartilage proteoglycans. Semin. Cell Dev. Biol. 2001; 12; 69-78.
4. Mentzel T, Van den Berg E, Molenaar WM. Myxofibrosarcoma. In Fletcher CDM, Unni KK, Mertens F eds. World Health Organization classification of tumours. Pathology and genetics. Tumours of soft tissue and bone, 2002 edn. Lyon: IARC Press, 2004; 102-103.
5. Trojani M, Contesso G, Coindre JM et al. Soft-tissue sarcomas of adults; study of pathological prognostic variables and definition of a histopathological grading system. Int. J. Cancer 1984; 33; 37-42.
6. Coindre JM. Grading of soft tissue sarcomas: review and update. Arch. Pathol. Lab. Med. 2006; 130; 1448-1453.
7. Fletcher CDM, Unni KK, Mertens F. WHO classification of tumours. Pathology and genetics of tumours of soft tissue and bone. Lyon: IARC Press, 2002.
8. Kononen J, Bubendorf L, Kallioniemi A et al. Tissue microarrays for high-throughput molecular profiling of tumor specimens. Nat. Med. 1998; 4; 844-847.
9. Goethals L, Perneel C, Debucquoy A et al. A new approach to the validation of tissue microarrays. J. Pathol. 2006; 208; 607-614.
10. Bovée JVMG, Van den Broek LJCM, Cleton-Jansen AM, Hogendoorn PCW. Up-regulation of PTHrP and Bcl-2 expression characterizes the progression of osteochondroma towards peripheral chondrosarcoma and is a late event in central chondrosarcoma. Lab. Invest. 2000; 80; 1925-1933.
11. Romeo S, Bovée JVMG, Jadnanansing NAA, Taminiau AHM, Hogendoorn PCW. Expression of cartilage growth plate signalling molecules in chondroblastoma. J. Pathol. 2004; 202; 113-120.
12. Specht K, Richter T, Muller U, Walch A, Werner M, Hofler H. Quantitative gene expression analysis in microdissected archival formalin-fixed and paraffin-embedded tumor tissue. Am. J. Pathol. 2001; 158; 419-429.
13. Romeo S, Eyden B, Prins FA, Briaire-de Bruijn IH, Taminiau AH, Hogendoorn PC. TGF-beta1 drives partial myofibroblastic differentiation in chondromyxoid fibroma of bone. J. Pathol. 2006; 208; 26-34.
14. De Boer WI, Sont JK, van Schadewijk A, Stolk J, van Krieken JH, Hiemstra PS. Monocyte chemoattractant protein 1, interleukin 8, and chronic airways inflammation in COPD. J. Pathol. 2000; 190; 619-626.
15. Annels NE, Da Costa CE, Prins FA, Willemze A, Hogendoorn PCW, Egeler RM. Aberrant chemokine receptor expression and chemokine production by Langerhans cells underlies the pathogenesis of Langerhans cell histiocytosis. J. Exp. Med. 2003; 197; 1385-1390.
16. Virchow RLK. Cellular pathology as based upon physiological and pathological histology. Philidelphia: Lippincott, 1863; 625-626.
17. de Wever O, Mareel M. Role of tissue stroma in cancer cell invasion. J. Pathol. 2003; 200; 429-447.
18. Nielsen G, Stenman G. Intramuscular myxoma. In Fletcher CDM, Unni KK, Mertens F eds. Pathology and genetic. Tumours of soft tissue and bone. Lyon: IARC Press, 2002; 186-187.
19. Mentzel T, Calonje E, Wadden C et al. Myxofibrosarcoma. Clinicopathologic analysis of 75 cases with emphasis on the low-grade variant Am. J. Surg. Pathol. 1996; 20; 391-405.
20. Willems SM, Debiec-Rychter M, Szuhai K, Hogendoorn PC, Sciot R. Local recurrence of myxofibrosarcoma is associated with increase in tumour grade and cytogenetic aberrations, suggesting a multistep tumour progression model. Mod. Pathol. 2006; 19; 407-416.
21. Sanderson RD, Yang Y, Suva LJ, Kelly T. Heparan sulfate proteoglycans and heparanase - partners in osteolytic tumor growth and metastasis. Matrix Biol. 2004; 23; 341-352.
22. Subramanian S, West RB, Marinelli RJ et al. The gene expression profile of extraskeletal myxoid chondrosarcoma. J. Pathol. 2005; 206; 433-444.
23. Wight TN. Versican: a versatile extracellular matrix proteoglycan in cell biology. Curr. Opin. Cell Biol. 2002; 14; 617-623.
24. Comper WD, Laurent TC. Physiological function of connective tissue polysaccharides. Physiol. Rev. 1978; 58; 255-315.
25. Venkatachalam MA, Karnovsky MJ. Extravascular protein in the kidney. An ultrastructural study of its relation to renal peritubular capillary permeability using protein tracers. Lab. Invest. 1972; 27; 435-444.

# Chapter 5

## Cellular/intramuscular myxoma and grade I myxofibrosarcoma are characterized by distinct genetic alterations and specific composition of their extracellular matrix

Stefan M. Willems[1], Alex B. Mohseny[1], Crina Balog[2], Raj Sewrajsing[1], Inge H. Briaire-de Bruijn[1], Jeroen Knijnenburg[3], Anne-Marie Cleton-Jansen1, Raf Sciot[4], Christopher D. M. Fletcher[5], André M. Deelder[2], Karoly Szuhai[3], Paul J. Hensbergen[2], Pancras C. W. Hogendoorn[1]

[1]Department of Pathology, Leiden University Medical Center, Leiden, the Netherlands, [2]Department of Parasitology, Biomolecular Mass Spectrometry Unit, Leiden University Medical Center, Leiden, the Netherlands, [3]Department of Molecular Cell Biology, Leiden University Medical Center, Leiden, the Netherlands [4]Department of Morphology and Molecular Pathology, University Hospitals, Leuven, Belgium, [5]Department of Pathology, Brigham and Women's Hospital, Harvard University, Boston, MA, USA

**Abstract**

Cellular myxoma and grade I myxofibrosarcoma are mesenchymal tumours that are characterized by their abundant myxoid extracellular matrix (ECM). Despite their histological overlap, they differ clinically. Diagnosis is therefore difficult though important. We investigated their (cyto) genetics and ECM. *GNAS1*-activating mutations have been described in intramuscular myxoma, and lead to down-stream activation of cFos. *KRAS* and *TP53* mutations are commonly involved in sarcomagenesis whereby *KRAS* subsequently activates cFos. A well documented series of intramuscular myxoma (three typical cases and seven cases of the more challenging cellular variant) and grade I myxofibrosarcoma (n 10) cases were karyotyped, analyzed for *GNAS1*, *KRAS* and *TP53* mutations and downstream activation of cFos mRNA and protein expression. ECM was studied by liquid chromatography mass spectrometry and expression of proteins identified was validated by immunohistochemistry and qPCR. Grade I myxofibrosarcoma showed variable, non-specific cytogenetic aberrations in 83,5% of cases (n 6) whereas karyotypes of intramuscular myxoma were all normal (n 7). *GNAS1*-activat-ing mutations were exclusively found in 50% of intramuscular myxoma. Both tumour types showed over-expression of cFos mRNA and protein. No mutations in *KRAS* codon 12/13 or in TP53 were detected. Liquid chromatography mass spectrometry revealed structural proteins (collagen types I, VI, XII, XIV and decorin) in grade I myxofibrosarcoma lacking in intramuscular myxoma. This was confirmed by immunohistochemistry and qPCR. Intramuscular/cellular myxoma and grade I myxofibrosarcoma show different molecular genetic aberrations and different composition of their ECM that probably contribute to their diverse clinical behaviour. *GNAS1* mutation analysis can be helpful to distinguish intramuscular myxoma from grade I myxofibrosarcoma in selected cases.

## Introduction

Myxoid tumours of soft tissue comprise a heterogeneous group of mesenchymal tumours characterized by abundant extracellular matrix (ECM). In this group, intramuscular myxoma and myxofibrosarcoma are most frequent, usually occurring in the extremities and at older age [1]. Histologically, intramuscular myxoma, and in particular its cellular variant (i.e. cellular myxoma), and grade I myxofibrosarcoma show considerable overlapping fea-tures [2]. Clinically, they differ as intramuscular myxoma shows no recurrence except for the cellular variant and never metastasizes. This is in contrast to myxofibrosarcoma that has a tendency to recur and, importantly, shows increase in tumour grade upon recurrence, thereby gaining metastatic potential [3]. Thus, the differential diagnosis between these two entities is important though can be challenging especially when presenting as an intramuscular tumour. Myxofibrosarcoma is usually characterized by complex, non-specific karyotypic aberrations. (Cyto) genetic data on intramuscular myxoma are sparse with only two cases described in the literature showing normal karyotypes [4, 5]. Recently, activating mutations in codon 201 of the *GNAS1* gene have been described in intramuscular myxoma [6]. This gene encodes, among others, for the alpha-sub-unit of the heterotrimeric G-protein. This protein is involved in cell signalling and leads to the transcription of the protein cFos and subsequently activation of the cell cycle. Activating *GNAS1* mutations and the subsequent activation of cFos are involved in the pathogenesis of fibrous dysplasia, which is a benign bone tumour associated with intramuscular myxoma in Mazabraud syndrome [7]. Activating mutations in codon 12/13 of *KRAS* also lead to downstream activation of cFos. *KRAS*-activating mutations have been described in both mouse and human sarcomas. Kirsch et al. showed that *KRAS* and *TP53* mutations were sufficient to initiate high-grade sarcomas with myofibroblastic features in mice [8]. *TP53* mutations are relatively common in sarcomas with nonspecific genetic aberrations compared with sarcomas with reciprocal specific translocations [9]. Previous studies showed immunohistochemical p53 expression in 33% of myxofibrosarcoma, mainly occurring in grade II and grade III tumours [10]. We studied the genetic make-up of these tumours at levels of karyotype, *GNAS1*, *TP53* and *KRAS* mutations and down-stream expression of cFos in order to find a potential tool for differential diagnosis and to get more insight into the biology of these tumours. The constitution and function of their so-called myxoid ECM are poorly understood. Previously, we demonstrated that intramuscular myxoma and grade I myxofibrosarcoma showed no significant differences in the glycosaminoglycans present in their ECM [11]. To study the differences in ECM organization and association with clinical behaviour, we screened ECM lysates of intra-muscular myxoma and grade I myxofibrosarcoma in a broad liquid chromatography mass spectrometry (LC-MS)-based survey.

## Materials and methods

*Patient data*
The study included 10 intramuscular myxoma cases and 10 grade I myxofibrosarcoma cases that were collected retrospectively from the files of the Pathology Departments of the University Hospitals of Leuven and Leiden University Medical Center. In each case, 4-mm-thick sections of formalinfixed, paraffin-embedded material were stained with haematoxylin and eosin (H&E). The histological diagnoses were revised (CDMF, PCWH, RS) and classified according to the 2002 WHO criteria. In case of myxofibrosarcoma, histological grading was performed according to the FNCLCC [12, 13]. Patient and tumour characteristics are shown in Table 1. Characteristic morphology of intramuscular myxoma, cellular myxoma and grade I myxofibrosarcoma is depicted in Fig. 1.

*Karyotyping*
Cells were harvested and 48-colour fluorescence in situ hybridization (FISH) staining was carried out, which stains every chromosome arm in a different colour combination. This was followed by digital imaging and analysis as previously described [5, 14]. Hybridizations with individual libraries labelled with single fluorochromes were used to confirm the detected re-arrangements. Break-points were assigned by using inverted DAPI counterstained images of the chromosomes.

*GNAS1 direct sequencing*
*GNAS1* mutation analysis was performed for codon 201 (exon 8) and codon 227 (exon 9) using oligonucleotide primers extended with an M13-forward or reverse sequence (see supplementary Table 1). Tumour tissue was isolated from formalin-fixed, paraffin-embedded material (FFPE) by microdissection to enrich for tumour cells and avoid 'contamination' of non-neoplastic cells, that is, lymphocytes, endothelial cells/pericytes or muscular tissue at the periphery of the tumour. Genomic DNA was isolated from 10 consecutive 10-mm sections using a Chelex extraction method, as described earlier [15]. Polymerase chain reaction (PCR) was carried out to amplify the *GNAS1* gene with the primers for exon 8 and exon 9, as previously reported [16]. PCR products were visualized and sequenced as previously described [17, 18].

*GNAS1 multiplex ligation-dependent probe amplification (MLPA)*
To detect mutations that are missed by direct sequencing due to contamination with normal cells, we set up *GNAS1* MLPA for the mutations already detected by direct sequencing. MLPA was performed using the following oligonucleotide probes attached to M13-tail, depicted in supplementary Table 3. For the R201C mutant, probes with additional stuffer sequence were added: forward: 5-CAGAC-3 and reverse 5-GATGTGCT-3. MLPA was performed as previously described [19]. In short, adjacently

**Table 1:** Patient and tumour characteristics

| Case | Diagnosis | P/R/M | Age | Gender | Site | Follow-up |
|---|---|---|---|---|---|---|
| 1 | IM | P | 55 | F | Left vastus lateralis muscle | NSR at 37 months |
| 2 | IM | P | 32 | M | Retroperitoneal right | NSR at 94 months |
| 3 | IM | P | 48 | F | Adductor muscles right leg | NSR at 34 months |
| 4 | IM* | P | 73 | F | Subcutaneous tight upper arm | NSR at 17 months |
| 5 | IM* | P | 59 | F | Right lateral upper leg | NSR at 31 months |
| 6 | IM* | P | 53 | F | Right psoas muscle | NSR at 62 months |
| 7 | IM* | P | 53 | F | Right hamstring muscle | NSR at 69 months |
| 8 | IM* | P | 59 | F | Left vastus lateralis muscle | NSR at 39 months |
| 9 | IM* | P | 61 | M | Right upper leg | NSR at 41 months |
| 10 | IM* | P | 62 | M | Left vastus medialis muscle | NSR at 68 months |
| 11 | MFS | P | 55 | M | Right vastus lateralis muscle | NSR at 66 months |
| 12 | MFS | P | 74 | M | Left lower arm | LR at 14 months |
| 13 | MFS | P | 71 | M | Left lower arm | LR at 36 months |
| 14 | MFS | P | 63 | F | Right hamstring muscles | NSR at 41 months |
| 15 | MFS | R | 84 | M | Subcutaneous left lower arm | LR at 12 months |
| 16 | MFS | P | 87 | M | Right upper arm | NSR at 18 months |
| 17 | MFS | P | 49 | F | Left gluteus muscle | LR at 2 months |
| 18 | MFS | P | 81 | M | Right upper arm | NSR at 60 months |
| 18 | MFS | P | 61 | M | Right gracilis muscle | LR at 42 months |
| 20 | MFS | P | 39 | F | Subcutaneous occiput | NSR at 25 months |

*These were all cellular myxomas.
Abbreviations: IM, intramuscular myxoma; MFS, myxofibrosarcoma; P, primary lesion; R, local recurrence; M, metastasis, NSR, no sign of recurrence; LR, local recurrence. Intramuscular myxoma showed a female predominance and myxofibrosarcoma a slight male predominance. The median age of occurrence was 56 years for intramuscular myxoma and 66 years for myxofibrosarcoma. All cases were primaries except for case 15, which was a local recurrence. Except for case 2 and 20, all lesions occurred at the extremities. Out of the intramuscular myxomas, eight were truly intramuscular, whereas single cases were identified at other sites (case 2 and 4). None of the lesions were situated near articular surfaces. Clinical, radiological and histological follow-up (17–94 months) showed no local recurrence for intramuscular myxoma but did in half of the cases of myxofibrosarcoma. No patients had any clinical evidence for endocrinopathy or café-au-lait spots. One patient (case 1) suffered monostotic fibrous dysplasia of the distal femoral bone, diagnosed by conventional radiological examination and MRI, and was therefore suspected for Mazabraud or a partial form of McCune–Albright syndrome.

annealing oligonucleotide probes were hybridized and ligated. After ligation, the common ends of the probes served as a template for PCR amplification using the primer pairs that are depicted in supplementary Table 3, with one of each pair fluorescently labelled. Products were separated on the ABI 3700 genetic analyser (Applied Biosystems, Foster City, CA) and analyzed.

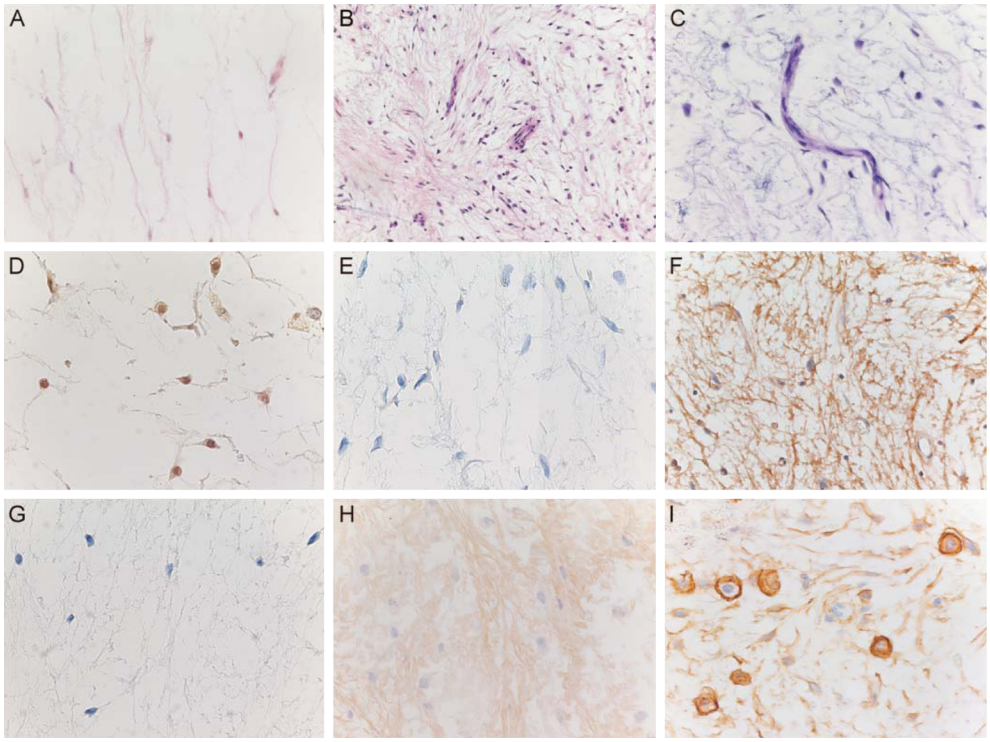


**Figure 1:** Overlapping histology of intramuscular myxoma, cellular myxoma and grade myxofibrosarcoma and their immunohistochemical expression for cFos, decorin, collagen I, collagen VI and CD44. (**A**) Low-power view of intramuscular myxoma showing a hypocellular and hypovascular tumour. Its cellular variant is both more cellular and more vascular (**B**) but lacks the cytonuclear atypia and characteristic curvilinear vascular pattern of grade I myxofibrosarcoma (**C**). Low-power view of intramuscular myxoma (**D**) showing moderate cytoplasmic and nuclear expression for cFos in the majority (75%) of tumour cells. (**E**) Low-power view of intramuscular myxoma was completely negative for decorin, whereas grade I myxofibrosarcoma showed diffuse fibrillary staining for decorin in the ECM (**F**). Lack of collagen I expression in the ECM of intramuscular myxoma (**G**) and moderate stain-ing for collagen VI in the ECM of grade I myxofibrosarcoma (**H**). A majority of tumour cells of grade I myxofibrosarcoma showed strong membranous staining for CD44 in the majority of tumour cells (**I**).

*KRAS mutation analysis*

*KRAS* mutation analysis was performed on microdissected FFPE tumour tissue using two primer sets in a nested PCR which specifically amplifies a 114 bp fragment of *KRAS* exon 2, including codons 12 and 13 (supplementary Table 1). All primer sequences and amplification protocols have been previously described [20]. PCR products were purified with the QIAquick PCR Purification Kit (Qiagen, Germantown, MD) and sequenced with the fluorescent Big-Dyes Terminators Sequencing Kit (Applied Biosystems).

**Table 2** Cytogenetic findings and GNAS1, KRAS and TP53 mutation analysis in intramuscular myxoma and grade I myxofibrosarcoma

| Case | Diagnosis | Karyotype | Mutation analysis | | | |
|---|---|---|---|---|---|---|
| | | | GNAS 1 | | KRAS | TP53[a] |
| | | | exon 8 | exon 9 | exon 2 | |
| 1 | IM | NA | R201S | wt | wt | wt |
| 2 | IM | 46, XY | wt | wt | wt | wt |
| 3 | IM | 46, XX | wt | wt | wt | wt |
| 4 | IM[i] | 46, XX | wt | wt | wt | wt |
| 5 | IM | NA | R201H | wt | wt | wt |
| 6 | IM | NA | wt | wt | wt | wt |
| 7 | IM | 46, XY | wt | wt | wt | wt |
| 8 | IM | 46, XY | R201C | wt | wt | wt |
| 9 | IM | 46, XY | R201C | wt | wt | wt |
| 10 | IM | 46, XY | R201H | wt | wt | wt |
| 11 | MFS | NA | wt | wt | wt | wt |
| 12 | MFS | NA 45, XX,-21/92,XXXX/92,XXXX[b] | wt | wt | wt | wt |
| 13 | MFS | 46, XY balanced translocation t(9,12) | wt | wt | wt | wt |
| 14 | MFS | NA | wt | wt | wt | wt |
| 15 | MFS | 46, XY | wt | wt | wt | wt |
| 16 | MFS | NA | wt | wt | wt | wt |
| 17 | MFS | 43,Y,-X,-19,-20/45,X,-Y/46,XY,+dmin/47,XY,+X/46,XY, del(4)(q22)/90,XXY,-Y,12/91,XXYY,add(l )(p36),del(2)(q31 ),-10,add(14)(p11),-16,-16+Mx2[b] | wt | wt | wt | wt |
| 18 | MFS | 82-l42,COMPLEX,1l-2M[b] | wt | wt | wt | wt |
| 19 | MFS | NA | wt | wt | wt | wt |
| 20 | MFS | 46,XY,del(l)(p2l-p3l?),r(3)(q),del(5)(q),-l3,del(l5)(ql3-26.3?)[b] | wt | wt | wt | wt |

[a]TP53 analysis was performed for exons 4a, 4b, 5c, 6, 7 and 8.
[b]Karyotypes were previously published [5].
Abbreviation: NA, not available.

*TP53 mutation analysis*

*TP53* hotspot mutation analysis was performed on microdissected FFPE tumour tissue using primer sets for exons 4a, 4b, 5c, 6, 7 and 8 in a nested PCR (supplementary Table 2). Samples were used in high-resolution melting curve analysis as previously described [46]. PCR products were purified with the QIAquick PCR Purification Kit (Qiagen) and sequenced with the fluorescent Big-Dyes Terminators Sequencing Kit (Applied Biosystems).

*SDS-PAGE, in-gel tryptic digestion and mass spectrometry*

Tumour lysates of intramuscular myxoma and grade I myxofibrosarcoma were prepared and depleted of albumin and IgG as previously described [11]. From each sample, 150 g was separated by SDS-PAGE and stained with Colloidal Coomassie (Invitrogen,

**Table 3:** Proteins identified in MFS and IM

| IPI number | Protein name | Protein score | Matched queries | Seq. coverage (%) | Identified in IM |
|---|---|---|---|---|---|
| IPI00745872 | Serum albumin | 5315 | 231 | 40 | + |
| IPI00072917 | COL6A3 α 3 type VI collagen isoform 3 | 4263 | 201 | 24 | + |
| IPI00022463 | Serotransferrin | 4066 | 205 | 49 | + |
| IPI00553177 | α-1-anti-trypsin | 3593 | 164 | 40 | + |
| IPI 00845263 | Fibronectin 1 | 2443 | 123 | 21 | + |
| IPI00007960 | Periostin | 1230 | 62 | 37 | – |
| IPI00291136 | COL6A1 collagen α-1(VI) | 953 | 43 | 12 | + |
| IPI00465248 | ENO1 isoform α-enolase of α-enolase | 905 | 37 | 29 | + |
| IPI00020986 | LUM lumican precursor | 827 | 52 | 33 | + |
| IPI 00418471 | VIM vimentin | 803 | 42 | 31 | + |
| IPI00465028 | Triosephosphate isomerase | 645 | 26 | 47 | – |
| IPI 00021440 | Actin | 547 | 35 | 32 | + |
| IPI00329801 | Annexin A5 | 543 | 44 | 47 | + |
| IPI 00656111 | PRG4 | 436 | 30 | 12 | – |
| IPI 00020987 | Prolargin | 374 | 23 | 20 | – |
| IPI00022429 | ORM1 α-1-acid glycoprotein 1 precursor | 374 | 27 | 34 | + |
| IPI00418169 | Annexin A2 | 352 | 24 | 40 | + |
| IPI00302944 | COL12A1 isoform 4 of collagen α-1(XII) | 348 | 17 | 5 | – |
| IPI00304840 | COL6A2 isoform 2C2 of collagen α-2(VI) | 334 | 19 | 7 | + |
| IPI 00291262 | CLU clusterin precursor | 304 | 13 | 20 | – |
| IPI 00021841 | APOA1 apolipoprotein A-I precursor | 271 | 7 | 21 | – |
| IPI00176193 | COL14A1 isoform 1 of collagen α-1(XIV) | 264 | 12 | 9 | – |
| IPI 00793199 | Annexin IV | 257 | 10 | 30 | – |
| IPI 00013808 | α-actinin-4 | 212 | 6 | 5 | + |
| IPI 00012119 | Decorin | 194 | 23 | 25 | – |
| IPI 00010790 | Big lye an | 192 | 7 | 11 | – |
| IPI 00166729 | α-2-glycoprotein 1 | 192 | 6 | 12 | + |
| IPI 00026314 | Gelsolin | 186 | 7 | 9 | + |

Extracellular protein extracts from MFS and IM were depleted for albumin and IgG, separated by SDS-PAGE, in-gel digested with trypsin and analyzed by LC-MS. Shown are the top 30 proteins identified in MFS. Proteins that were also identified in IM are indicated with a sign. Many forms of keratins and IgGs were also identified within the initial top 30 protein list, but for the sake of clarity, they have been removed.

Leek, The Netherlands). The complete lanes from both intramuscular myxoma and grade I myxofibrosarcoma were cut into approximately 30 protein bands, and these samples were subsequently reduced, alkylated and in-gel digested using trypsin as described previously [21]. Peptides were subsequently collected using two rounds of extraction with 20 l of 0.1% trifluoroacetic acid and were stored at -20-C prior to analysis by mass spectrometry. Samples were injected onto a nano-LC system (Ultimate, Dionex, Amsterdam, the Netherlands) equipped with a peptide trap column (Pepmap 100, 0.3 i.d. 1 mm) and an analytical column (Pepmap 100, 0.075 i.d. 150 mm, Dionex). The mobile phases consisted of (A) 0.04% formic acid/0.4% acetonitrile and (B) 0.04%

formic acid/90% acetonitrile. A 45-min. linear gradient from 0% to 60% B was applied at a flow rate of 0.2 ml/min. The outlet of the LC system was coupled to an HCT Ultra ion-trap mass spectrometer (Bruker Daltonics, Bremen, Germany) using a nano-electrospray ionization source. The spray voltage was set at 1.2 kV, and the temperature of the heated capillary was set to 165-C. Eluting peptides were analyzed in the data-dependent MS/MS mode over a 400-1600 m/z range. The five most abundant fragments in each MS spectrum were selected for MS/MS analysis by collision induced dissociation. Mass spectra were evaluated using the DataAnalysis 3.1 software package (Bruker Daltonics) and exported as a Mascot Generic File (MGF). MGF files were merged using the OMSSA Browser version 2.1.0. and searched against the human International Protein Index (IPI) database using the Mascot search algorithm (version 2.2, Matrixscience, London, UK), allowing mass tolerances of 0.5 Da for MS (# 13 C 1) and 0.75 Da for MS/MS. One missed cleavage site was allowed for tryptic peptides. Carbamidomethylcysteine was taken as a fixed modification and oxidation of methionine as a variable modification.

*qPCR for mRNA expression*

Following microdissection, RNA isolation and purification, qPCR was performed for c-Fos, decorin, collagen I alpha 1, collagen VI alpha 1, collagen XII alpha 1 and collagen XIV alpha 1, as described previously [11, 22, 23]. Primers (including those of the housekeeping genes) and controls are summarized in supplementary Table 1. A reference control panel, including a variety of neoplastic and non-neoplastic tissue was used as described previously [24]. After qPCR, the products were purified using QIAquick PCR Purification Kit (Qiagen). For sequence confirmation of the products, we used the Big Dyes Terminators Sequencing Kit (Applied Biosystems).

*Immunohistochemistry*

Immunohistochemistry was performed for c-Fos, decorin, collagen I-A1, collagen VI-A1 and CD44. Sections (4-m-thick) were mounted on 3-aminopropylethoxysilane (Sigma, St. Louis, MO) and glutaraldehyde-coated slides and dried overnight at 37-C. Immunohistochemistry was per-formed as previously described, using the antibodies, conditions and controls described in supplementary Table 4 [11, 25]. For c-Fos and CD44, only nuclear and membranous staining were assessed, respectively, and scored as previously described [26]. For decorin, collagen I-A1 and collagen VI-A1, the ECM of whole sections were assessed. Scores of 0 (absent) and 1 (weak) were considered negative; scores of 2 (moderate) and 3 (strong) were considered positive.

*Statistical analysis*

Wilcoxon-Mann-Whitney test was used to calculate the differences for both the immunohistochemical and qPCR results.

## Results

*Karyotyping*
Karyotypes were available for seven intramuscular myxomas (five cases were of the cellular variant) and six grade I myxofibrosarcomas. The karyotypes of the intramuscular myxomas (both typical and cellular cases) were all normal. Out of the grade I myxofibrosarcoma cases, only one case showed a normal karyotype, whereas five out of six cases showed variable, non-specific cyto-genetic aberrations (Table 2).

*GNAS1, KRAS and TP53 mutation analysis*
By direct sequencing, we found codon 201 activating *GNAS1* mutations in 50% of intramuscular myxoma cases (including its cellular variant), but none in grade I myxofibrosarcoma cases. All *GNAS1* mutations occurred in exon 8 with the base pair substitutions as shown in Table 2. *GNAS*1 MLPA confirmed the mutations detected by direct sequencing. In theory, MLPA should be able to detect mutant alleles in a background of wild-type alleles. Here, we show that this technique picks up mutations if only 10% of the alleles is mutated, which is superior to direct sequencing (requiring at least 25% mutated alleles). *GNAS1* MLPA could not detect additional mutations. We did not observe any mutations in codon 12 or 13 of the *KRAS* gene in neither the intramuscular myxoma nor the grade I myxofibrosarcoma cases. Hotspot mutation analysis for *TP53* showed wild-type sequences in all samples (Table 2).

*LC-MS*
The top 30 proteins identified in a proteomic screen of tumour lysates of grade I myxofibrosarcoma and intramuscular myxoma are shown in Table 3. Even after depletion, albumin was still the most prominent protein, and also other 'classical' serum proteins were among the most significant hits. We found five collagens (VI-A1, 2 and 3, XII-A1, XIV-A1) and five proteoglycans (lumican, PRG4, prolargin, decorin

**Table 4:** Log2-transformed relative expression data in qPCR

| Genes | IM (median ± S.D.) | Grade I MFS (median ± S.D.) | IM vs grade I MFS (*P*-value) |
|---|---|---|---|
| *FOS* | 4.06 ± 0.87 | 4.61 ± 0.89 | 0.105 |
| *DCN* | –6.92 ± 1 | 2.81 ± 0.79 | 0.001 |
| *COL1A1* | 1.95 ± 1.84 | 6.71 ± 1.71 | 0.003 |
| *COL6A1* | 0.14 ± 0.22 | 2.37 ± 0.47 | 0.023 |
| *COL12A1* | –0.85 ± 1.11 | –0.22 ± 1.28 | 0.09 |
| *COL14A1* | –0.29 ± 0.49 | 1.49 ± 0.59 | 0.001 |

Abbreviations: FOS, FBJ murine osteosarcoma viral oncogene homolog; DCN, decorin; COL1A1, collagen, type I, α1; COL6A1, collagen VI, α1; COL12A1, collagen, type XII, α1; COL14A1, collagen, type XIV, α1.

and biglycan) among the top 30 proteins in MFS. Only the collagen VI isoforms and lumican were identified in IM. Besides collagen VI isoforms and lumican, the other four collagens and four proteoglycans were not shown to be present in IM using mass spectrometry. qPCR for mRNA expression Results of relative mRNA expression are shown in Table 4 and boxplots in Fig. 2. qPCR showed that cFos RNA was over-expressed in all tumours compared with control tissue, but not significantly differently expressed between intramuscular myxoma and grade I myxofibrosarcoma. No significant differences were seen between typical intramuscular myxoma and cellular myxoma. Grade I myxofibrosarcoma showed significant expression of decorin mRNA, whereas decorin mRNA was barely detectable in intramuscular myxoma. Grade I myxofibrosarcoma clearly showed significant over-expression of mRNA expression for collagens I-A1, VI-A1 and XIV-A1 compared with intramuscular myxoma (including cellular myxoma).

*Immunohistochemistry*

The majority of intramuscular myxomas and grade I myxofibrosarcomas showed diffuse cytoplasmic and nuclear staining for cFos (Table 5). Both cytoplasmic and nuclear staining for c-Fos have been obtained in FFPE materials from other tumours [27]. However, the biological role of cytoplasmic cFos expression is not fully understood. And because c-Fos is a transcription factor that is active in the nucleus, we assessed only nuclear staining in scoring. Intramuscular myxoma and grade I myxofibrosarcoma did not show significantly different cFos expression (P 0.648; Table 5). Decorin, collagen I-A1 and collagen VI-A1 were only present in the ECM. Strong positive staining for decorin was detected in all grade I myxofibrosarcomas but not in intramuscular myxoma, including its cellular variant (P 0.0000). Collagen I-A1 expression was found to be equally present in the ECM of grade I myxofibrosarcoma and intramuscular

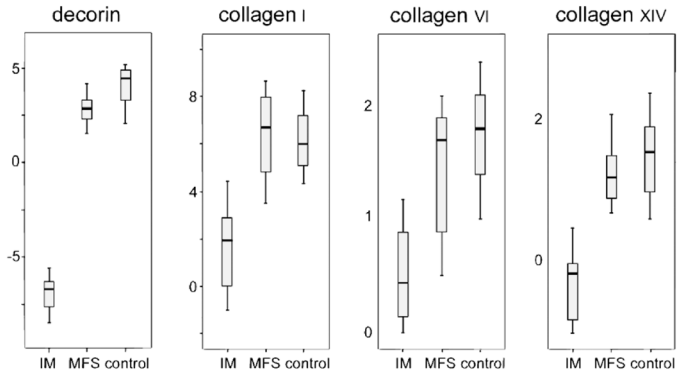


**Figure 2:** Box-plots showing qPCR results of structural ECM proteins. Abbreviations: IM, intramuscular myxoma; MFS, grade I myxofibrosarcoma. Intramuscular myxoma showed significantly lower mRNA expression for decorin (P 0.000), collagen I-A1 (P 0.003), collagen VIA1 (P 0.023) and collagen XIV-A1 (P 0.001).

myxoma (P 1.000). Collagen VI-A1 expression was present in 40% of the ECM of intramuscular myxoma and all grade I myxofibrosarcoma (P 0.004). Illustrations of collagen I-A1 and VI-A1 protein expression are shown in Fig. 1. Both grade I myxofibrosarcoma and intramuscular myxoma showed membranous and cytoplasmic staining for CD44 in the majority of cases, the latter most probably due to its production in the rough endoplasmic reticulum. As we were interested in the role of CD44 as a cell surface receptor for ECM molecules, only membranous staining was assessed in statistical analysis. Tumour cells of intramuscular myxoma and grade I myxofibrosarcoma showed no significantly different expression for CD44 (P 0.0542; Table 5). Illustrations are shown in Fig. 1.

## Discussion

The cellular variant of intramuscular myxoma, also known as cellular myxoma, is the morphological intermediate between intramuscular myxoma and grade I myxofibrosarcoma. Compared with typical intramuscular myxoma, cellular myxoma is hypercellular, usually more vascular and shows increase in collagenous stroma. However, it lacks clear cytonuclear atypia and classical curvilinear blood vessels [2]. The risk of recurrence is rather low, which is sustained by the present data showing local recurrence in 50% of grade I myxofibrosarcoma but not in intramuscular myxoma. This includes the cases of the cellular variant, even after long-term follow-up, which is in accordance with the literature [2, 28]. It should be noted that not all cellular myxomas are truly intramuscular (see Table 1), which was already demonstrated by Van Roggen et al. [2]. In a previous study, we showed that myxofibrosarcoma is characterized by complex, non-specific cytogenetic aberrations probably reflecting genomic instability [5]. Chromosomal instability is often an early event in tumourigenesis, and there is a significant correlation between chromosomal instability phenotype and poor biological behaviour [29]. This is sustained by our data showing karyotypic aberrations only in myxofibrosarcoma but not in intramuscular myxoma. *TP53* is an important mitotic check-point regulator, and p53 deficiency plays an important role in chromosomal instability and ploidy control [29]. Mutations in *TP53* resulting in dysfunctional p53

**Table 5:** Results for immunohistochemical staining in intramuscular myxoma and grade I myxofibrosarcoma

| | c-fos | | dcn | | col1a1 | | col6a1 | | cd44 | |
|---|---|---|---|---|---|---|---|---|---|---|
| | pos* | pos# | pos* | pos# | pos* | pos# | pos* | pos# | pos* | pos# |
| IM | 6/10 | 60 | 0/0 | 0 | 7/10 | 70 | 4/10 | 40 | 8/10 | 80 |
| Grade I MFS | 7/10 | 70 | 10/10 | 100 | 7/10 | 70 | 10/10 | 100 | 9/10 | 90 |

Abbreviations: IM, intramuscular myxoma; MFS, myxofibrosarcoma; dcn, decorin; pos*, number of positive tumours/total number of tumours that could be evaluated; pos#, percentage of cases that were positive.

occur mostly (93%) in exons 4-8, which are therefore called hotspot mutations [30]. We did not detect any *TP53* hotspot mutations in intramuscular myxoma or in grade I myxofibrosarcoma. This means that *TP53* mutations might not be involved in the tumourigenesis of either tumour. Otherwise, it might support the notion that structural loss of p53 is not always the cause of aneuploidy and that loss of p53 might represent a late event in tumourigenesis of myxofibrosarcoma, whereas aneu-ploidy occurs early [31]. This was sustained by previous data that p53 immunohistochemical staining was predominantly found in myxofibrosarcoma of grade II and III [10]. Cytogenetic data on intramuscular myxoma are sparse in the literature, with only two isolated cases described showing normal karyotypes [4, 32]. The present study confirms in a larger series that intramuscular myxoma has a normal karyotype. Cytogenetics might therefore be helpful in the differential diagnosis but are not always easily available in routine laboratories. Okamoto et al. showed *GNAS1*-activating mutations in a small series of intramuscular myxoma [6]. We showed that *GNAS1* codon 201 mutations were present in 50% of intramuscular myxoma and not in grade I myxofibrosarcoma. All mutations were heterozygous. Direct sequencing of codon 201 *GNAS1* mutations is therefore a highly specific, not very sensitive but easy to perform method to distinguish intramuscular myxoma from grade I myxofibrosarcoma. Interestingly, here we report for the first time the R201S mutation in intramuscular myxoma. We could not detect any mutation in codon 227 (exon 9) of the *GNAS1* gene, previously detected in fibrous dysplasia [33]. The *GNAS1* gene encodes for the alpha sub-unit of the G-protein. Somatic-activating mutations in codon 201 and 227 of the *GNAS1* gene have been described in fibrous dysplasia and the related Mazabraud and McCune Albright syndromes, leading to increased levels of cAMP and activation of protein kinase A and the MAPK pathway [7, 33-35]. This leads to increased transcription of the cFos protein, which is involved in growth and the inhibition of apoptosis [36]. We showed both RNA and protein over-expression for cFos in each of the tumour samples of intramuscular myxoma and grade I myxofibrosarcoma, suggesting that the MAPK signalling pathway is activated in these tumours. We did not detect *GNAS1*-activating mutations in myxofibrosarcoma nor did we detect codon 201 or 227 activating mutations in the other 50% of the intramuscular myxoma cases. As both are hypocellular tumours, we hypothesized that wild-type DNA of blood vessels and lymphocytes might interfere with the detection of this heterozygous mutation. Neither enrichment for mutated DNA by microdissection nor the use of more sensitive method to detect the mutations (MLPA) with a detection threshold of only 10% could increase the number of mutations found. Therefore, we believe that activation of the MAPK pathway in the tumours with no detectable mutations is caused by a different mechanism than *GNAS1*-activating mutations, possibly downstream of the G-protein. In vivo studies on mice showed that *KRAS*-activating mutations play an important role in sarcomagenesis [8]. In general, about 30% of solid tumours show activating mutations in codon 12 and 13 of the *KRAS* gene causing activation of the MAPK pathway and increased transcription of c-

Fos [37, 38]. Moreover, KRAS mutations have been associated with chromosomal instability suggesting a potential role of KRAS in the tumourigenesis of grade I myxofibrosarcoma [39]. However, we could not detect any activating mutations in codon 12 and 13 of the *KRAS* gene in intramuscular myxoma nor grade I myxofibrosarcoma. Intramuscular myxoma (including its cellular variant) and grade I myxofibrosarcoma are both characterized by their abundant so-called myxoid ECM. We have shown recently that glycosaminoglycans (e.g. hyaluronic acid) are major polysaccharides in the myxoid ECM of intramuscular myxoma and myxofibrosarcoma [11]. Based on the present, more detailed LC-MS-based survey, we showed that decorin, collagen VI-A1 and XIV-A1 were significantly overexpressed in the ECM of grade I myxofibrosarcoma compared with that of intramuscular myxoma. Decorin is a small leucine-rich proteoglycan (SLRP) in the ECM that 'decorates' collagens by interaction with their 'd' and 'e' bands. Decorin links these collagens (especially collagens I, VI and XIV) and plays an important role in fibrillogenesis and ECM formation. Decreased and impaired expression of decorin leads to abnormal ECM formation as in Ehlers-Danlos syndrome [40, 41]. Next to decorin, LC-MS revealed other SLRPs (i.e. lumican, PRG4, prolargin, biglycan) present in tumour lysates of grade I myxofibrosarcoma but not of intramuscular myxoma. Collagens XII and XIV are fibril-associated collagens with triple helices (FACIT) and modify the interactions between collagen I fibrils and the surrounding ECM [42]. Increased ECM rigidity activates integrins to promote focal adhesion families, leading to stimulation of the rho/Rock pathway and increased cell contractility, cell migration and invasion [43]. Intramuscular myxoma was found to express significantly less decorin and collagen VI and XIV (both protein and mRNA level) than grade I myxofibrosarcoma, suggesting that ECM formation in intramuscular myxoma is impaired compared with grade I myxofibrosarcoma. Validation of these immunohistochemical results in an independent series of both entities would be interesting though is hampered by the availability of well-characterized frozen material. Cell surface receptors facilitate the assembly and retention of the ECM and link changes in the ECM to activation of signal transduction pathways [44]. CD44 glycoprotein is a well-characterized cell adhesion molecule that is ubiquitously expressed on tumour cells of intramuscular myxoma and grade I myxofibrosarcoma. Its principal ligand is hyaluronic acid which was, however, not expressed significantly differently in intramuscular myxoma compared with grade I myxofibrosarcoma [11]. CD44 is also an important cell surface receptor for collagen I and XIV, suggesting that ECM-cell signalling via CD44 might play a role in these myxoid tumours of soft tissue [45]. Although grade I myxofibrosarcoma showed significantly higher mRNA expression for collagen I and XIV, this was not obvious at the protein level for collagen I. Whether differences in (the assembly of) the ECM of myxoid tumours of soft tissue effectively affect cell signalling and subsequent tumour growth and progression is still unknown. The evidence in our studies to support this theory is indirect and our results cannot exclude that the content and organization of

the myxoid ECM might be just an epiphenomenon, driven by the initiating genetic event(s) or by the precise lineage or subtype of the cell that is transformed. Based on our results, we suggest that molecular and cytogenetic aberrations as well as proper ECM organization might explain the different biology of these tumours.

## Acknowledgements

We acknowledge Judith V.M.G. Bovée for critical comments and discussion, Marjo van Puijenbroek for performing the *KRAS* mutation analysis, Ronald van Eijk for help with *TP53* mutation analysis and Marije IJszenga for performing the COBRA-FISH experiments. Rabbit polyclonal anti-decorin antibody was kindly provided by Annemiek van der Wal (Department of Pathology, Leiden University Medical Center, Leiden, the Netherlands). This project was financially supported by a grant from The Netherlands Organization for Health Research and Development (project number 920-03-403).

**References:**

1. Graadt van Roggen JF, Hogendoorn PCW, Fletcher CDM. Myxoid tumours of soft tis-sue. Histopathology. 1999; 35: 291-12.
2 Graadt van Roggen JF, McMenamin ME, Fletcher CDM. Cellular myxoma: a clinico-pathologic study of 38 cases confirming indolent clinical behavior. Mod Pathol. 2001; 39: 287-97.
3. Mentzel T, Calonje E, Wadden C, et al. Myxofibrosarcoma. Clinicopathologic analysis of 75 cases with emphasis on the low-grade variant. Am J Surg Pathol. 1996; 20: 391-05.
4. Meis-Kindblom JM, Sjogren H, Kindblom LG, et al. Cytogenetic and molecular genetic analyses of liposarcoma and its soft tissue simulators: recognition of new vari-ants and differential diagnosis. Virchows Arch. 2001; 439: 141-51.
5. Willems SM, Debiec-Rychter M, Szuhai K, et al. Local recurrence of myxofibrosar-coma is associated with increase in tumour grade and cytogenetic aberrations, suggesting a multistep tumour progres-sion model. Mod Pathol. 2006; 19: 407-16.
6. Okamoto S, Hisaoka M, Ushijima M, et al. Activating Gs(alpha) mutation in intramuscular myxomas with and without fibrous dysplasia of bone. Virchows Arch. 2000; 437: 133-37.
7. Candeliere GA, Glorieux FH, Prud'homme J, St.-Arnaud R. Increased expression of the c-fos proto-oncogene in bone from patients with fibrous dysplasia. N Engl J Med. 1995; 332: 1546-51.
8. Kirsch DG, Dinulescu DM, Miller JB, et al. A spatially and temporally restricted mouse model of soft tissue sarcoma. Nat Med. 2007; 13: 992-97.
9. Borden EC, Baker LH, Bell RS, et al. Soft tissue sarcomas of adults: state of the translational science. Clin Cancer Res. 2003; 9: 1941-56.
10. Oda Y, Takahira T, Kawaguchi K, et al. Altered expression of cell cycle regulators in myxofibrosarcoma, with special emphasis on their prognostic implications. Hum Pathol. 2003; 34: 1035-42.
11. Willems SM, Schrage YM, Baelde JJ, et al. Myxoid soft tissue tumours have a heterogeneous composition of their extra-cellular matrix. Histopathology. 2008; 52: 465-74.
12. Mentzel T, Van den Berg E, Molenaar WM. Myxofibrosarcoma. World Health Organization classification of tumours: pathology and genetics. In: Fletcher CDM, Unni KK, and Mertens FL, editors. Tumours of soft tissue and bone. Lyon: IARC Press, 2004. pp. 102-03.
13. Trojani M, Contesso G, Coindre JM, et al. Soft-tissue sarcomas of adults; study of pathological prognostic variables and defi-nition of a histopathological grading sys-tem. Int J Cancer. 1984; 33: 37-42.
14. Szuhai K, Tanke H. COBRA: combined binary ratio labeling of nucleic-acid probes for multi-color fluorescence in situ hybridization karyotyping. Nat. Protoc. 2006; 1: 264-75.

15. De Leeuw WJ, Dierssen J, Vasen HF, et al. Prediction of a mismatch repair gene defect by microsatellite instability and immunohistochemical analysis in endome-trial tumours from HNPCC patients. J Pathol. 2000; 192: 328-35.
16. Candeliere GA, Roughley PJ, Glorieux FH. Polymerase chain reaction-based technique for the selective enrichment and analysis of mosaic arg201 mutations in G alpha s from patients with fibrous dysplasia of bone. Bone. 1997; 21: 201-06.
17. Bovée JVMG, Devilee P, Cornelisse CJ, et al. Identification of an EWS-pseudo-gene using translocation detection by RT-PCR in Ewing's sarcoma. Biochem Biophys Res Commun. 1995; 213: 1051-60.
18. Rozeman LB, Hameetman L, Cleton-Jansen AM, et al. Absence of IHH and retention of PTHrP signalling in enchondromas
and central chondrosarcomas. J Pathol. 2005; 205: 476-82.
19. White SJ, Vink GR, Kriek M, et al. Twocolor multiplex ligation-dependent probe amplification: detecting genomic rearrangements in hereditary multiple exostoses. Hum Mutat. 2004; 24: 86-92.
20. Brink M, de Goeij AF, Weijenberg MP, et al. K-ras oncogene mutations in sporadic colorectal cancer in The Netherlands Cohort Study. Carcinogenesis. 2003; 24: 703-10.
21. Steen H, Pandey A, Andersen JS, Mann M. Analysis of tyrosine phosphorylation sites in signaling molecules by a phosphotyrosine-specific immonium ion scanning method. Sci STKE. 2002; 2002: L16.
22. Romeo S, Eyden B, Prins FA, et al. TGF-beta1 drives partial myofibroblastic dif-ferentiation in chondromyxoid fibroma of bone. J Pathol. 2006; 208: 26-34.
23. Vandesompele J, De Preter K, Pattyn F, et al. Accurate normalization of real-time quantitative RT-PCR data by geometric averaging of multiple internal control genes. Genome Biol. 2002; 3: research0034.1-.11.
24. Rozeman LB, Hameetman L, van Wezel T, et al. cDNA expression profiling of central chondrosarcomas: Ollier disease resembles solitary tumors and alteration in genes coding for energy metabolism with increasing grade. J Pathol. 2005; 207: 61-71.
25. Koop K, Bakker RC, Eikmans M, et al. Differentiation between chronic rejection and chronic cyclosporine toxicity by analysis of renal cortical mRNA. Kidney Int. 2004; 66: 2038-46.
26. Bovée JVMG, Van den Broek LJCM, et al. Up-regulation of PTHrP and Bcl-2 expres-sion characterizes the progression of osteochondroma towards peripheral chon-drosarcoma and is a late event in central chondrosarcoma. Lab Invest. 2000; 80: 1925-33.
27. Hoyland J, Sharpe PT. Upregulation of c-fos protooncogene expression in pagetic osteoclasts. J Bone Miner Res. 1994; 9: 1191-4.
28. Nielsen GP, O'Connell JX, Rosenberg AE. Intramuscular myxoma: a clinicopathologic study of 51 cases with emphasis on hypercellular and hypervascular variants. Am J Surg Pathol. 1998; 22: 1222-7.
29. Tomasini R, Mak TW, Melino G. The impact of p53 and p73 on aneuploidyaneuploidy and cancer. Trends Cell Biol. 2008; 18: 244-52.
30. Hernandez-Boussard T, Rodriguez-Tome P, Montesano R, Hainaut P. IARC p53 mutation database: a relational database to ompile and analyze p53 mutations in human tumors and cell lines. International Agency for Research on Cancer. Hum Mutat. 1999; 14: 1-8.
31. Lengauer C, Kinzler KW, Vogelstein B. Genetic instabilities in human cancers. Nature. 1998; 396: 643-9.
32. Lopez-Ben R, Pitt MJ, Jaffe KA, Siegal GP. Osteosarcoma in a patient with McCune- Albright syndrome and Mazabraud's syndrome. Skeletal Radiol. 1999; 28: 522-6.
33. Weinstein LS, Liu J, Sakamoto A, et al. Minireview: GNAS: normal and abnormal functions. Endocrinology. 2004; 145: 5459-64.
34. Vallar L, Spada A, Giannattasio G. Altered Gs and adenylate cyclase activity in human GH-secreting pituitary adenomas. Nature. 1987; 330: 566-8.
35. Weinstein LS, Shenker A, Gejman PV, et al. Activating mutations of the stimula-tory G protein in the McCune-Albright syn-drome. N Engl J Med. 1991; 325: 1688-95.
36. Wada T, Penninger JM. Mitogen-activated protein kinases in apoptosis regulation. Oncogene. 2004; 23: 2838-49.
37. Dhillon AS, Hagan S, Rath O, Kolch W. MAP kinase signalling pathways in cancer. Oncogene. 2007; 26: 3279-90.
38. Kranenburg O. The KRAS oncogene: past, present, and future. Biochim Biophys Acta. 2005; 1756: 81-2.
39. Castagnola P, Giaretti W. Mutant KRAS, chromosomal instability and prognosis in colorectal cancer. Biochim Biophys Acta. 2005; 1756: 115-25.
40. Ferdous Z, Wei VM, Iozzo R, et al. Decorin-transforming growth factor- interaction regulates matrix organization and mechanical characteristics of threedimensional collagen matrices. J Biol Chem. 2007; 282: 35887-98.
41. Ruhland C, Schonherr E, Robenek H, et al. The glycosaminoglycan chain of decorin plays an important role in collagen fibril formation at the early stages of fibrillogenesis. FEBS J. 2007; 274: 4246-55.

42. Canty EG, Kadler KE. Procollagen traffick-ing, processing and fibrillogenesis. J Cell Sci. 2005; 118: 1341-53.
43. Berrier AL, Yamada KM. Cell-matrix adhesion. J Cell Physiol. 2007; 213: 565-73.
44. Toole BP. Hyaluronan: from extracellular glue to pericellular cue. Nat Rev Cancer. 2004; 4: 528-39.
45. Ehnis T, Dieterich W, Bauer M, et al. A chondroitin/dermatan sulfate form of CD44 is a receptor for collagen XIV (undulin). Exp Cell Res. 1996; 229: 388-97.
46. Romeo S, Debiec-Rychter M, Van Glabbecke M, et al. Cell cycle/apoptosis molecule expression correlates with imatinib response in patients with advanced gastrointestinal stromal tumors. Clin Cancer Res. 2009; 15: 4191-8.

# Chapter 6

## Imaging mass spectrometry of myxoid sarcomas identifies proteins and lipids specific to tumour type and grade, and reveals biochemical intratumour heterogeneity

Stefan M. Willems[1]*, Alexandra van Remoortere[2]*, René van Zeijl[2], André M. Deelder[2], Liam A. McDonnell[2]**, Pancras C.W. Hogendoorn[1]**
* and ** contributed equally to manuscript

[1]Department of Pathology and [2]Biomolecular Mass Spectrometry Unit, Department of Parasitology, Leiden University Medical Center, Leiden, the Netherlands

**Abstract**

Myxofibrosarcoma and myxoid liposarcomas are relatively common soft tissue tumours that are characterized by their so-called myxoid extracellular matrix and have to some extent overlap in histology. The exact composition and potential role of their myxoid extracellular matrix are insufficiently understood. To gain more insight into the biomolecular content of these tumours we have studied 40 well-documented myxofibrosarcoma and myxoid liposarcoma cases using imaging mass spectrometry. This technique provides a multiplex biomolecular imaging analysis of the tissue, spanning multiple molecular domains and without a priori knowledge of the tissue's biomolecular content. We have developed experimental protocols for analyzing the peptide, protein and lipid content of myxofibrosarcoma and myxoid liposarcomas, and have detected proteins and lipids that are tumour-type and tumour-grade specific. In particular lipid changes observed in myxoid liposarcomas could be related to pathways known to be affected during tumour progression. Unsupervised clustering of the biomolecular signatures was able to classify myxofibrosarcoma and myxoid liposarcomas according to tumour type and tumour grade. Closer examination of histologically similar regions in the tissues revealed intratumour heterogeneity, which was a consistent feature in each of the myxofibrosarcoma studied. In intermediate grade myxofibrosarcoma it was found that single tissue sections could contain regions with biomolecular profiles similar to high-grade and low-grade tumours, and that these regions were associated with the tumour's nodular structure, thus supporting a concept of tumour progression through clonal selection.

## Introduction

Myxoid tumours of soft tissue are a heterogeneous group of mesenchymal origin and characterized by their so-called myxoid extracellular matrix (ECM)[1,2]. In this group, myxofibrosarcoma and myxoid liposarcoma are relatively common, mostly occurring in the extremities. Although their histology overlaps to some extent, these tumours have different clinical behaviour[3]. Recently, we demonstrated that the composition of the myxoid ECM is tumour type and tumour grade dependent by conventional histochemical techniques as well as by mass spectrometry-based proteomics[3,4]. We illustrated that these differences in ECM composition paralleled the different biological and clinical behaviour of these tumours[4]. Myxofibrosarcoma is characterized by non-specific cytogenetic aberrations that increase with grade, suggesting a multistep tumour progression model due to acquired genetic instability[5]. Low-grade myxofibrosarcoma is microscopically characterized by a multinodular growth pattern[6]. Most human malignancies originate from a single cell but display intratumour heterogeneity by the time of diagnosis. This heterogeneity might be due to metabolic and epigenetic differences in the tumour though strong evidence showed that intratumour heterogeneity also arises from genetically distinct clones within the tumour[7-13]. This suggests that these tumours progress through multiple nodules, one of which becomes more dominant and will progress towards high-grade myxofibrosarcoma, as has been shown in other neoplasms[14-16]. How this clonal selection is reflected at the level of protein expression is still unclear. Furthermore, methods for the combined analysis of phenotypic and protein diversity at microscopical level in-situ in tissue sections are also lacking. In contrast to myxofibrosarcoma, myxoid liposarcoma is characterized by its predominant tumour specific translocation t(12;16) (q13;p11) involving the FUS and DDIT3 genes, whose transcribed fusion protein acts as a transcription factor[17-20]. This transcription factor plays a pivotal role in its tumourigenesis by regulating the expression of genes involved in cell proliferation[20-22]. It also controls the transcription of C/EBP which affects the expression of peroxisome proliferator-activated receptor gamma, a key player in adipocytic differentiation[19,23,24]. This links the FUS/DDIT3 fusion protein to its histological phenotype. To get more insight into (changes in) the expression of peptides, proteins and lipids during tumour progression we studied a well documented series of myxoid liposarcoma and myxofibrosarcoma tissues using MALDI imaging mass spectrometry. This rapidly developing technique uses spatially resolved proteomic and metabolomic methods to simultaneously trace the distributions of hundreds of peptides, proteins, or metabolites in a tissue section[25]. The technique uses the masses of the biomolecules to distinguish between different species and thus does not require any form of labelling. The biomolecular profiles can be used to obtain biomolecular signatures associated with specific histological features, to distinguish different regions within a tissue or to differentiate and classify tissues and is beginning to have in impact in cancer research[26-31]. In the present study we

investigated the ECM of myxofibrosarcoma and myxoid liposarcoma by using MALDI imaging mass spectrometry to analyze the peptide, protein and lipid content of low- and high-grade myxofibrosarcoma and low- and high-grade myxoid liposarcoma. This allowed a detailed examination of the myxoid ECM of these tumours, especially in relation to their grade specific phenotype and indicated that the technique may also reveal the intertumoural and intratumoural biomolecular heterogeneity of histologically contiguous tumours.

## Material and Methods

*Tissue/clinicopathological data*
Slides were re-evaluated histologically and classified according to the 2002 World Health Organization criteria[32,33]. Myxofibrosarcoma cases were histologically graded according to the French Fédération Nationale des Centres de Lutte Contre le Cancer[34]. Myxoid liposarcoma cases were graded on the basis of percentage of their round cell component[32,33]. All tissue samples were handled in a coded fashion, according to Dutch national ethical guidelines (Code for proper secondary use of human tissue, Dutch Federation of Medical Scientific Societies).

*Sample preparation*
Tumour tissue samples obtained form surgical resection specimens were snap frozen in liquid isopentane and then stored at -80 °C until sectioning. 5 µm thick tissue sections were cut at -20 °C using a cryomicrotome and stained with hematoxylin & eosin (H&E) to check diagnosis and viability of the tissue. For the MALDI imaging mass spectrometry experiments 12 µm thick tissue sections were cut at -20 °C and thaw mounted onto conductive glass slides (Delta Technologies, Stillwater, USA). The tissues were then slowly brought to room temperature in a desiccator and prepared for MALDI analysis of the tissue's peptides, proteins, or lipids.

Protein and peptide imaging: The tissues were washed in ice-cold 70% ethanol (2x30 seconds), dried under a stream of nitrogen and a uniform coating of the MALDI matrix deposited onto the tissue using an ImagePrep device (Bruker, Bremen, Germany) and a 20 mg/ml solution of sinapinic acid in 6:4 AcN:0.5% TFA(aq.).

Peptide and protein profiling: The tissues were washed in ice-cold 70% ethanol (2x30 seconds), dried under a stream of nitrogen and 1 l droplets of the sinapinic acid matrix solution deposited onto the tissue.Lipid imaging: A uniform coating of 2,5-dihydroxybenzoic acid was added using an ImagePrep device and a 10 mg/ml solution in 7:3 MeOH:H2O.
Immediately prior to loading the sample in the mass spectrometer, a 1200 dpi scan was recorded using a flatbed scanner.

*Mass Spectrometry*

Peptides and proteins

All peptide and protein mass spectrometry experiments were performed on an Autoflex III mass spectrometer (Bruker Daltonics, Bremen, Germany) and were acquired in fully automated mode using the Flex software suite (FlexControl 3.0, FlexImaging 2.1, FlexAnalysis 3.0, Bruker). Imaging mass spectrometry experiments were performed using 100 µm pixel size, 600 laser shots per pixel (50 laser shots per position of a random walk within each pixel). During definition of the imaging mass spectrometry experiment the dataset is manually aligned with an optical image of the tissue, and were then subsequently aligned with an optical image of the H&E stained tissue (tissue stained after the imaging mass spectrometry experiment[35]. Profiling mass spectrometry experiments were performed by accumulating the signals from 1200 laser shots (50 laser shots per position of a random walk within each matrix spot).

Lipids

Lipid imaging mass spectrometry experiments were performed using an UltrafleXtreme mass spectrometer (Bruker Daltonics, Bremen, Germany) and were acquired in fully automated mode using the Flex software suite (FlexControl 3.3, FlexImaging 2.1, FlexAnalysis 3.3) and used 100 ?m pixel size with 500 laser shots per pixel (100 laser shots per position of a random walk within each pixel). Lipid peak assignments were made by first comparing each peak's accurate mass measurement with the LIPID MAPS database (http://lipidmaps.org, mass accuracy  0.005 Da) and then confirming the assignments by MS/MS of selected peaks.

*Data Analysis*

Each pixel's spectrum was first processed using a smoothing and baseline subtraction routine using FlexAnalysis. A Gaussian smoothing algorithm was used for mass spectral smoothing (proteins: width 2 m/z and 4 cycles; lipids: width 0.05 m/z and 3 cycles) and a ConvexHullV3 algorithm was used for baseline subtraction. Each pixel's or each profile's mass spectrum was then normalized to its total ion count. These mass spectral processing steps have been previously shown to result in superior quantitative capabilities[36,37]. Statistical analysis was performed using ClinProtTools 2.2 and the results visualized in FlexImaging 2.1 (Bruker Daltonics, Bremen, Germany). An automated peak selection algorithm then reduced the dimensionality of the dataset to the 300 most intense peptide and protein peaks.

Unsupervised analysis:Principal component analysis was performed using mean-centring and auto-scaling. Hierarchical clustering was performed by first reducing non-correlated signals in the data by applying a principal component analysis data reduction step[38]. All data that constituted 90% of the variance was retained, the 10% omitted from the analysis was found to contain mostly uncorrelated signals. Hierarchical

clustering was performed using the Euclidian distance between each pixel's mass spectrum and an average linkage. All results of hierarchical clustering or principal component analysis were then presented as false colour images on the tissue sections to examine the spatial variation of the pixels found to have correlated mass spectra, and to compare these results with each tissue's histology.
Supervised analysis: all tissues were first annotated based on a histological analysis of the H&E stained tissues. Mass spectra from multiple patients with low grade MFS, defined as class 1, and spectra from multiple patients with high grade MFS, defined as class 2, were used to build a support vector machine classification algorithm, which was then used to reveal the regions with a low/high grade biomolecular signature in intermediate grade MFS.
To compare and contrast intratumour heterogeneity across multiple patient samples six localized regions within one intermediate grade MFS were selected, based on a histological analysis of the tissue, and used to create a support vector machine model. This SVM classifier was then applied to additional patient samples of intermediate grade MFS, the results presented as false colour images and compared with each tissue's histology.

**Results**

*Clinicopathological data*
Clinicopathological data are summarized in table 1. Myxofibrosarcomas and myxoid liposarcomas both showed a slight male predominance. The median age of occurrence was 67,9 years for myxofibrosarcomas (low-grade: 66,4 and 69,4 for high-grade) and 44,9 for myxoid liposarcomas (low-grade: 42,2 and high-grade: 47,6). All tumours occurred in the extremities, except for one low-grade myxofibrosarcoma (case 10: occiput) and 1 high-grade myxoid liposarcoma (case 37: pelvic region). Most cases were primary tumours including a higher number of (non-related) local recurrences and metastasis in both groups of high-grade tumours. All myxofibrosarcomas exhibited increased numerical and structural non-specific cytogenetic aberrations upon increase in grade[4,5]. All myxoid liposarcomas contained the tumour specific t(12;16) translocation as confirmed by FISH and/or RT-PCR (data not shown).

*Tissue profiling*
Aged tissue samples or tissues that have been in contact with Tissue-Tek optimal cutting temperature polymer can lead to poor MALDI mass spectrometry results[39]. A quality-control experiment was first performed to ensure that tissues included in the subsequent imaging mass spectrometry analysis generated rich peptide and protein profiles. Immediately after mass spectrometry analysis the matrix was removed and the tumours H&E stained[35]. Each tissue was then examined to make sure the tissues did not contain necrotic areas. Tissue sections from ten low-grade myxofibrosarcoma, ten

**Table 1:** Clinicopathological data of included myxoid soft tissue tumours

| *Sample* | *Tumour type* | *Grade* | *P/R/M* | *Age* | *Gender* | *Site* |
|---|---|---|---|---|---|---|
| 1 | MFS | low grade | P | 55 | M | right vastus lateralis |
| 2* | MFS | low grade | P | 74 | M | left lower arm (intramuscular) |
| 3* | MFS | low grade | P | 71 | M | left lower arm (intramuscular) |
| 4 | MFS | low grade | P | 63 | F | right hamstring muscles |
| 5* | MFS | low grade | R | 84 | M | subcutaneous left lower arm |
| 6 | MFS | low grade | P | 87 | M | right upper arm |
| 7* | MFS | low grade | P | 49 | F | left gluteus muscle |
| 8 | MFS | low grade | P | 81 | M | right upper arm |
| 9* | MFS | low grade | P | 61 | M | right gracilis muscle |
| 10 | MFS | low grade | P | 39 | F | subcutaneous occiput |
| 11* | MFS | high grade | P | 70 | F | pretibial superficial |
| 12* | MFS | high grade | R | 61 | M | in left musculus gracilis |
| 13 | MFS | high grade | P | 65 | M | right lower leg |
| 14 | MFS | high grade | R | 43 | M | in right musculus deltoideus |
| 15* | MFS | high grade | R | 89 | F | left elbow (intramuscular) |
| 16 | MFS | high grade | R | 57 | F | right elbow (intramuscular) |
| 17 | MFS | high grade | P | 76 | F | in musculus sartorius |
| 18* | MFS | high grade | P | 66 | M | left thigh (invading the fascia) |
| 19 | MFS | high grade | R | 64 | F | left lower leg (superficial) |
| 20* | MFS | high grade | P | 71 | M | left lower arm (intramuscular) |
| 21 | MLS | low grade | P | 33 | M | popliteal fossa left |
| 22* | MLS | low grade | P | 54 | F | adductor compartment left femur |
| 23* | MLS | low grade | P | 46 | M | upper leg left, subfacial |
| 24 | MLS | low grade | P | 29 | M | upper leg right, subcutaneous |
| 25* | MLS | low grade | P | 62 | M | right solear muscle |
| 26 | MLS | low grade | R | 39 | M | right quadriceps muscles |
| 27 | MLS | low grade | R | 42 | F | intra-abdominal |
| 28* | MLS | low grade | P | 41 | M | left gastrocnemius muscle |
| 29* | MLS | low grade | P | 43 | F | right hamstring muscles |
| 30 | MLS | low grade | P | 33 | F | left hamstring muscles |
| 31 | MLS | high grade | P | 52 | M | left quadricps muscles |
| 32* | MLS | high grade | R | 45 | M | left hamstring muscles |
| 33 | MLS | high grade | P | 34 | F | right vastus lateralis muscle |
| 34 | MLS | high grade | M | 52 | M | left abdominal muscles |
| 35* | MLS | high grade | P | 57 | F | left adductor muscles upper leg |
| 36* | MLS | high grade | P | 45 | F | right gluteal muscle |
| 37 | MLS | high grade | P | 60 | F | pelvis |
| 38* | MLS | high grade | P | 50 | M | left hamstring muscles |
| 39 | MLS | high grade | M | 39 | M | right popliteal fossa |
| 40* | MLS | high grade | R | 42 | F | right vastus medialis/semitendinosis muscles |

Abbreviations: MFS: myxofibrosarcoma; MLS: myxoid liposarcomas: P: primary tumour; R: local recurrence; M: metastasis: M: male; F: female.
Cases with asterisk (*) were included in imaging mass spectrometry experiments.

high-grade myxofibrosarcoma, ten low grade-myxoid liposarcoma, and ten high-grade myxoid liposarcoma patients were analyzed using MALDI-ToF protein profiling. Tissues free of necrosis, which did not exhibit Tissue-Tek contamination and which generated rich peptide and protein profiles were retained. Five tissues from each tumour group were then randomly selected for MALDI imaging mass spectrometry.

*Unsupervised clustering distinguishes myxofibrosarcoma and myxoid liposarcoma according to tumour type and tumour grade*

For the profiling experiments approximately 2000 spectra were recorded from each tissue. Random selections of 200 spectra from each tissue were then imported into the statistical analysis software ClinProtTools. Figure 1 shows examples of mass spectra obtained from the different individual tissue sections, and clearly demonstrates that low-grade myxofibrosarcoma, high-grade myxofibrosarcoma, low-grade myxoid liposarcoma and high-grade myxoid liposarcoma generate different peptide and protein profiles, and that each tumour's profile is highly reproducible. An automated feature recognition system was then used to reduce these spectra to the 300 most abundant peaks (each peak corresponds to the mass of a peptide or protein), and principal component analysis performed. This is a multivariate analysis technique frequently used to distinguish underlying trends in highly complex datasets[30]. The results are a series of principal components which describe the largest variance (spread) in the dataset (principal component 1), the next largest variance (principal component 2), and so on. The first three principal components of the myxoid tumour profiling data reveal four specific groupings which differentiate between high-grade myxofibrosarcoma, low-grade myxofibrosarcoma, high-grade myxoid liposarcoma and low-grade myxoid liposarcomas (figure 1). Principal components 1 and 2, which describe the largest variance in the data, discriminate between low-grade myxofibrosarcoma, low-grade myxoid liposarcomas and the high-grade tumours. High-grade myxofibrosarcoma and high-grade myxoid liposarcoma showed considerable overlap in principle component 1 and principal component 2 but were clearly separated in principal component 3. Principal component analysis also provides the contribution of each protein to each principal component and thus revealed which protein peaks discriminate between the different myxoid tumours and grades. This included peaks consistent with proteins previously shown to discriminate between high-grade and low-grade soft-tissue sarcomas including calgizzarin, calcyclin, calgranulin, histone H2A, histone H2B, histone H3 and histone H4 [40].

*MALDI imaging mass spectrometry of peptide and proteins in myxoid soft tissue tumours*

Tissues sections from the five selected patient samples of high-grade myxofibrosarcoma, low-grade myxofibrosarcoma, high-grade myxoid liposarcoma and low-grade myxoid liposarcoma were prepared for peptide and protein MALDI imaging mass spectrometry and analyzed with a pixel size of 100  m using an Autoflex III MALDI-ToF. Each tissue generated rich datasets describing the distributions of a large number of peptide and protein ions, and included several proteins that were upregulated in specific tumour types and grades. Figure 2 shows examples of tumour specific proteins detected by imaging mass spectrometry and also includes a table listing the masses of multiple tumour and grade specific protein peaks, several of which are consistent with identified

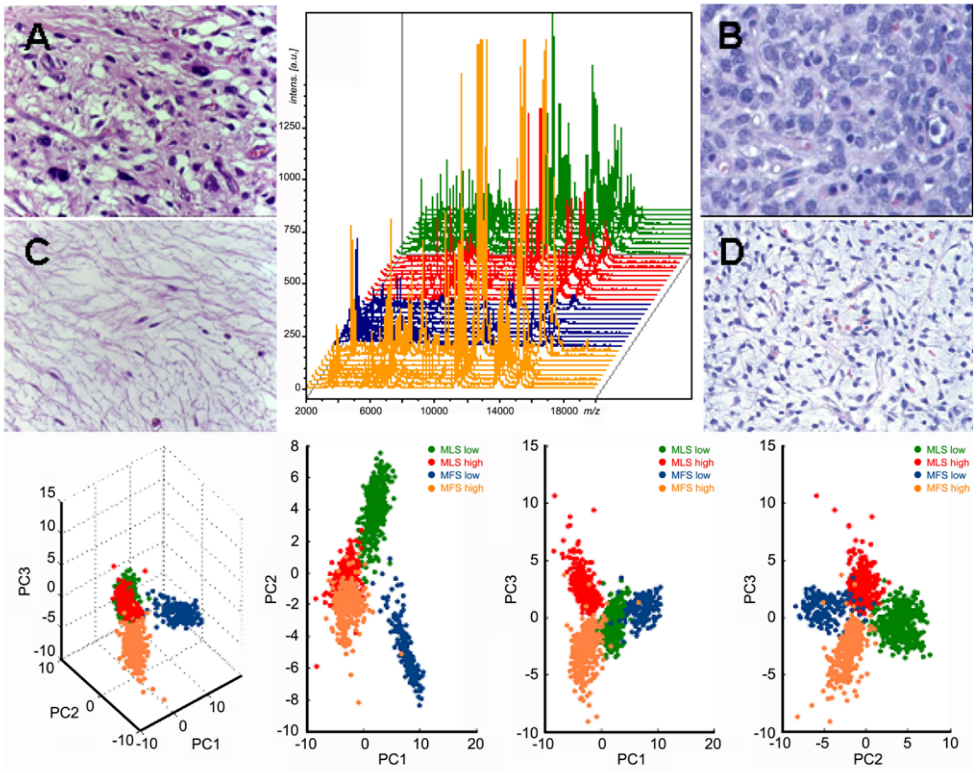


**Figure 1:** Initial screening of spectra obtained form the tissues of 10 high-grade and 10 low-grade myxofibrosarcoma (A and C) and 10 high-grade and 10 low-grade myxoid liposarcomas (B and D) was used to select tissues that generate rich high quality peptide/protein spectra (E). F: 3D plotting graph of principal component analysis of these samples separate low-grade tumours in principal component 1 (PC1) and principal component 2 (PC2) and high-grade tumours in principal component 3 (PC3). Corresponding 2D plots of the same analysis were visualized in figure panels G-I. Orange: high-grade myxofibrosarcoma; red: high-grade myxoid liposarcoma; blue: low-grade myxofibrosarcoma; green: low-grade myxoid liposarcoma.

proteins previously revealed found to discriminate between high-grade and low-grade soft-tissue sarcomas (calcylin, m/z 10090; Histone H2A, m/z 14007)[40].

*Lipid profiling of myxoid liposarcoma separates low-grade from high-grade tumours*

MALDI imaging mass spectrometry of myxoid liposarcoma revealed differential lipid profiles according to tumour grade that could be used to classify the tissues and that are consistent with the known molecular pathology of the tumour. A comparison of the lipid signatures obtained from low- and high-grade liposarcomas is shown in figure 3. Low- and high-grade tumours each contain specifically expressed lipids and whose images clearly reveal their localization to one grade. These lipids were then identified using MS/MS and the lipidmaps database. Phospholipids, particularly phosphocholines, were detected in both low and high-grade tumours but were detected at higher levels in

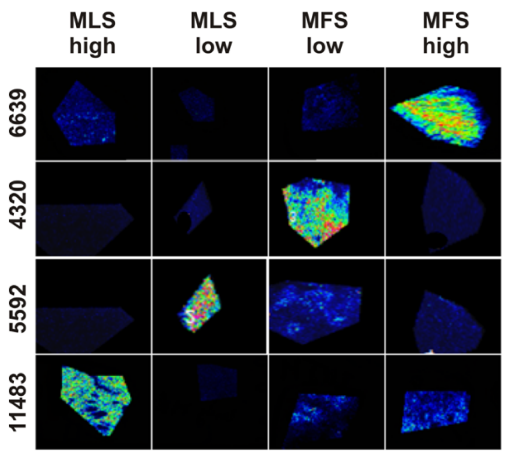


| Tumor upregulated/specific peptide and protein peaks | | | |
|---|---|---|---|
| MLS high | MLS low | MFS low | MFS high |
| 4634 | 4320 | 3440 | 10100 |
| 6179 | | 3710 | 11483 |
| 6639 | | 4138 | 14017 |
| 9272 | | 5592 | 15554 |

**Figure 2:** Discriminating power of imaging mass spectrometry illustrated by tumour and grade specific m/z values. The images illustrate the distribution of intensities of tumour type and grade specific m/z values (left panel). Table shows tumour-and grade specific m/z values. Abbreviations: MFS: myxofibrosarcoma; MLS: myxoid liposarcomas: low: low-grade; high: high-grade.

the high-grade tumours. Low-grade myxoid liposarcoma contained additional peaks due to triacylglycerols.

*Myxofibrosarcoma shows intratumour heterogeneity*

MALDI imaging mass spectrometry enables the variation of biomolecular content within single tissues to be examined and compared with its histology. Macroscopically and microscopically, myxofibrosarcoma is characterized by a multinodular growth pattern[6]. Close examination of low- and intermediate-grade myxofibrosarcoma datasets revealed that different locations within the same tumour generated different peptide/protein spectra and that these differences appear to be related to the nodular structure of the tissue.

Mass spectra from the peptide and protein datasets of high grade, low grade and intermediate grade myxofibrosarcoma samples were analyzed using a hierarchical clustering algorithm. Figure 4A shows that a significant number of the spectra (329) from the intermediate-grade tumour clustered with the high grade myxofibrosarcoma patient samples, and the remaining spectra (706) clustered with the low grade myxofibrosarcoma patient samples. In both instances the intermediate-grade spectra were separated from the high-/low- grade spectra at the next level of hierarchical tree, indicating that the intermediate spectra were high-/low-grade-like but were also quite distinct from the real high-/low-grade tumours.

To investigate this intratumour heterogeneity further the mass spectra from multiple high grade myxofibrosarcoma patient samples and multiple low grade myxofibrosarcoma patient samples were used to build a support vector machine

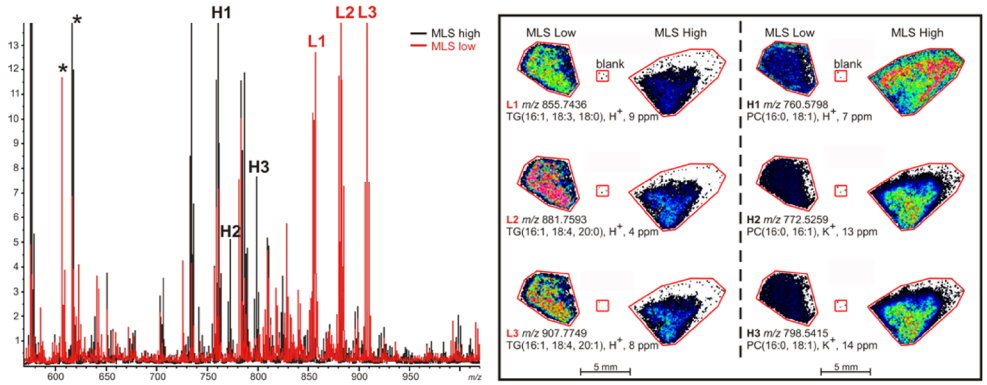


**Figure 3:** Lipid imaging mass spectrometry of high- and low-grade myxoid liposarcoma reveals differential lipid profiles and the spatial distributions show the localization of specific lipids in one tumour grade. The lipids were identified using tandem mass spectrometry. The experimental mass, the assignment and the mass accuracy of the assignments are provided alongside the image. * matrix clusters.

classification algorithm. Application of this high-grade/low-grade classifier to intermediate grade myxofibrosarcoma samples revealed that different regions of the intermediate grade tissue samples generated biomolecular MS signatures consistent with high-grade or low-grade tumours, and which resembled the characteristic multinodular morphology of myxofibrosarcoma tumours (figure 4B).

Figures 4A and 4B indicate that the intermediate grade myxofibrosarcoma tissue possessed nodules with high-grade- and low-grade-like character, but did not address if the nodules can be further subdivided on the basis of their biochemical signatures nor if the same intratumour heterogeneity is present in multiple tissues. To address these questions six different regions-of-interest were selected in a tissue sample (indicated in figure 4C left panel), based on a histological analysis of the tissue, and a new support vector machine classification model generated. This model was then applied to multiple intermediate grade myxofibrosarcoma patient samples. The results of this analysis demonstrate that many intermediate grade tissues exhibit significant biochemical intratumour heterogeneity, figure 4C. Within the two areas highlighted at low-grade-like and high-grade-like in figure 4B, figure 4C indicates that both areas consist of multiple nodules with different protein signatures.

## Discussion

Myxofibrosarcoma and myxoid liposarcoma are, as their names imply, characterized by their abundant so-called myxoid ECM. To study the molecular composition of the ECM of these tumours in relation to tumour progression, we performed imaging mass spectrometry in a well-documented series representing their low-grade and high-grade

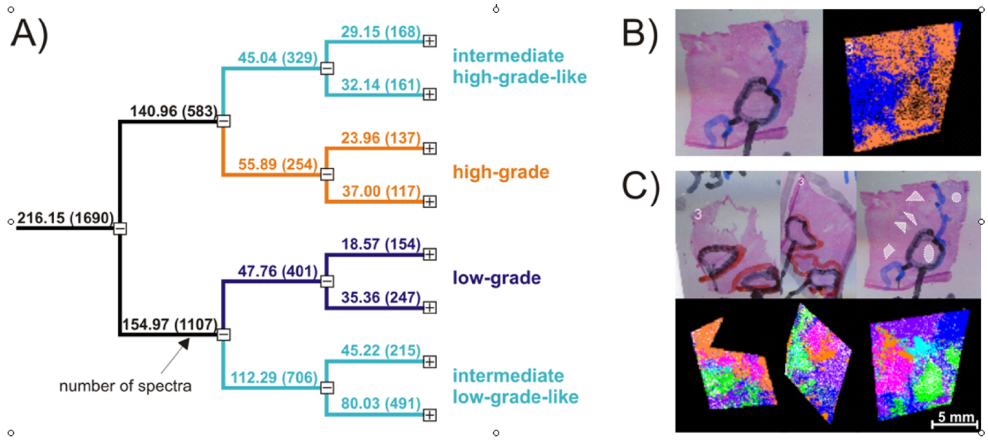


**Figure 4:** A) Hierarchical clustering analysis of mass spectra from low-(dark blue), intermediate-(light blue) and high-grade (orange) myxofibrosarcoma reveals differential clustering of the intermediate grade spectra into low-grade-like and high-grade-like spectra. B) Application of classification algorithm to an intermediate-grade myxofibrosarcoma tissue, which was developed to distinguish between high-grade and low-grade myxofibrosarcoma tissues using five patient samples of each class, indicates the nodular structure of the low-grade-like and high-grade-like regions of the tissue. C) Six localized regions were selected on the basis of a histological examination of an H&E stained tissue section (indicated) and a classification algorithm developed to distinguish between the different regions. Application of the classification algorithm to multiple intermediate-grade myxofibrosarcoma tissues reveals a nodular like structure in each tissue.

variants. The imaging mass spectrometry experiments were performed using matrix assisted laser desorption/ionization (MALDI), an ionization technique that enables highly sensitive mass analysis of biomolecules[41]. MALDI imaging mass spectrometry combines the advantages of biomolecular mass spectrometry, unbiased and simultaneous analysis of multiple biomolecules (peptides, proteins and lipids), with an analysis of their spatial distribution[25,42-44]. Principle component analysis of total m/z spectra showed that myxofibrosarcoma and myxoid liposarcoma clustered separately according to tumour type and tumour grade (figure 1). Based on the principle component analysis and corresponding loading plots, m/z values that contributed most to the separation of each group could be identified. From principal component 1 and principal component 2 it is clear that high-grade myxofibrosarcoma and high grade myxoid liposarcoma show considerable overlap. Low-grade myxofibrosarcoma and low-grade myxoid liposarcoma clustered most separately. In other words, most variance is seen between the two different groups of low-grade tumours compared to the two different groups of high-grade tumours. This means that although both low-grade tumours show some degree of histological overlap (i.e. their abundant myxoid ECM), the biochemical composition of their ECM differed significantly. Imaging mass spectrometry identified tumour type and tumour grade specific peptides, proteins and lipids in the tissue section (figures 2 and 3).

Myxofibrosarcoma is characterized by multinodular growth[6]. These nodules, especially in low-grade tumours, can be histologically identical. The results reported here, and intimated previously[31,38,45], indicate that imaging mass spectrometry may be used to study intratumour biomolecular heterogeneity of primary human tumours, directly on tissue slides. Despite their histological resemblance imaging mass spectrometry revealed that intratumour heterogeneity was a consistent feature in each of the myxofibrosarcomas studied, and revealed that different nodules exhibited high-grade-/low-grade-like biomolecular signatures (figure 4). Intratumour heterogeneity has been described in many neoplasms, as well in soft tissue sarcomas[13,46]. Orndal et al. have already shown intratumoural cytogenetic variability by identifying karyotypically different though cytogenetically related clones in different parts of the same tumour. Hence, cytogenetic heterogeneity and clonal evolution seem to be common in soft tissue sarcoma and have been detected most often in malignant fibrous histiocytoma and leiomyosarcoma[47]. Similar intratumour heterogeneity was detected in a number of patient tissues. From a conceptual point of view, this might suggest that one of the nodules in low-grade myxofibrosarcoma becomes more dominant over time and turns into a dominant tumour nodule with a more histologically homogeneous growth pattern, though as other possibilities cannot be ruled out as only part of the tumour in selected cases was studied. Indeed, an attractive alternative hypothesis is a multifocal clonal evolution in myxofibrosarcoma and has already been shown in other neoplasms [48,49].

Lipid analysis of myxoid liposarcomas by imaging mass spectrometry revealed differences between low- and high-grade tumours (figure 3). The spectra from high-grade tumours revealed higher levels of phosphocholines. Phosphocholines are commonly detected by MALDI [48] and are thought to derive from (cell) membranes. The higher levels of these lipids in high grade tumours is consistent with the higher cellularity of higher grade tumours[50] (figure 3). These results are consistent with previous studies of Singer and coworkers which already demonstrated increased phosphocholines in high-grade myxoid liposarcoma using high resolution ex vivo NMR spectroscopy. These studies already demonstrated a correlation of lipid content and composition with the histology and grade in liposarcoma and how NMR-derived parameters can be used to classify liposarcoma subtypes [51,52]. These findings were underscored by our study using a different method (i.e. imaging mass spectrometry) in a different group of myxoid liposarcoma patient samples. Moreover, relative phosphocholine contents detected with high-resolution NMR spectroscopy predicted histological response of myxoid liposarcoma after treatment with troglitazone (a PPARγ agonist) [53]. Identification of lipids by imaging mass spectroscopy showed a predominant expression of PPARγ induced fatty acids in low-grade tumours such as triacylglycerols. PPARγ plays a key role in fatty acid synthesis[54]. Active PPARγ signalling promotes adipocytic differentiation in pre-adipocyts and is active in myxoid liposarcoma cells[24,55]. Our data suggest decreased PPARγ regulated fatty acid

synthesis in myxoid liposarcoma upon increase in grade, histologically reflected in a diminished adipocytic phenotype, and consistent with recent work that established that PPARγ inactivation by the FUS/DDIT3 liposarcoma specific fusion protein is required for liposarcoma development[56].
Activation of PPARγ signalling also stimulated cell cycle withdrawal and PPARγ agonists have been shown to be promising in cancer treatment[57]. This is an attractive drug target as treatment options for myxoid liposarcoma patients with advanced disease are poor. However, phase II trials with rosiglitazone (a PPARγ agonist) in myxoid liposarcoma patients with advanced disease showed no effect on tumour size[58].

In conclusion, we have demonstrated that imaging mass spectrometry can distinguish between different types and different grades of myxoid tumours based solely on their biomolecular signatures, and can be used to identify proteins lipids specific to each type. Close examination of the data revealed previously unreported biomolecular changes consistent with the known tumour biology of myxofibrosarcoma and myxoid liposarcoma. Substantial intratumour heterogeneity was detected in the biomolecular profiles of myxofibrosarcoma tissues, consistent across multiple patient samples, that is consistent with the clonal selection model of myxofibrosarcoma tumour development. For myxoid liposarcoma tumour development is associated with inactivation of PPARγ by the FUS/DDIT3 fusion protein; PPARγ plays a crucial role in adipocytic differentiation and so led to the observed reduction in triacylglycerols with increasing tumour grade.

**Acknowledgements**

This work was funded by the ZonMw Horizon program,' project number 935-19-026 (L.McD) and a ZonMW Agiko Stipendium grant, project number 920-03-403 (S.W.).

**Author contributions:**

SW, AR and RZ carried out experiments. AR and LMD analyzed data. LMD, AD and PH designed experiments. SW, AR, LMD and PH wrote manuscript. All authors approved manuscript prior to submission.

**Reference List**


1. Graadt van Roggen JF, Hogendoorn PCW, Fletcher CDM. Myxoid tumours of soft tissue. Histopathology 1999;35:291-312.
2. Willems SM, Wiweger M, Graadt van Roggen JF, et al. Running GAGs: myxoid matrix in tumor pathology revisited : What's in it for the pathologist? Virchows Arch 2010;456:181-192.
3. Willems SM, Schrage YM, Baelde JJ, et al. Myxoid tumours of soft tissue: the so-called myxoid extracellular matrix is heterogeneous in composition. Histopathology 2008;52:465-474.
4. Willems SM, Mohseny AB, Balog C, et al. Cellular/intramuscular myxoma and grade I myxofibrosarcoma are characterized by distinct genetic alterations and specific composition of their extracellular matrix. J Cell Mol Med 2009;13:1291-1301.
5. Willems SM, Debiec-Rychter M, Szuhai K, et al. Local recurrence of myxofibrosarcoma is associated with increase in tumour grade and cytogenetic aberrations, suggesting a multistep tumour progression model. Mod Pathol 2006;19:407-416.
6. Mentzel T, Calonje E, Wadden C, et al. Myxofibrosarcoma. Clinicopathologic analysis of 75 cases with emphasis on the low-grade variant. Am J Surg Pathol 1996;20:391-405.
7. Campbell LL, Polyak K. Breast tumor heterogeneity: cancer stem cells or clonal evolution? Cell Cycle 2007;6:2332-2338.
8. Gonzalez-Garcia I, Sole RV, Costa J. Metapopulation dynamics and spatial heterogeneity in cancer. Proc Natl Acad Sci U S A 2002;99:13085-13089.
9. Konishi N, Hiasa Y, Matsuda H, et al. Intratumor cellular heterogeneity and alterations in ras oncogene and p53 tumor suppressor gene in human prostate carcinoma. Am J Pathol 1995;147:1112-1122.
10. Maley CC, Galipeau PC, Finley JC, et al. Genetic clonal diversity predicts progression to esophageal adenocarcinoma. Nat Genet 2006;38:468-473.
11. Marusyk A, Polyak K. Tumor heterogeneity: causes and consequences. Biochim Biophys Acta 2010;1805:105-117.
12. Merlo LM, Pepper JW, Reid BJ, et al. Cancer as an evolutionary and ecological process. Nat Rev Cancer 2006;6:924-935.
13. Park SY, Gonen M, Kim HJ, et al. Cellular and genetic diversity in the progression of in situ human breast carcinomas to an invasive phenotype. J Clin Invest 2010;120:636-644.
14. Beerman H, Smit VT, Kluin PM, et al. Flow cytometric analysis of DNA stemline heterogeneity in primary and metastatic breast cancer. Cytometry 1991;12:147-154.
15. Bonsing BA, Corver WE, Fleuren GJ, et al. Allelotype analysis of flow-sorted breast cancer cells demonstrates genetically related diploid and aneuploid subpopulations in primary tumors and lymph node metastases. Genes Chromosomes Cancer 2000;28:173-183.
16. Mentzel T. Biological continuum of benign, atypical, and malignant mesenchymal neoplasms - does it exist? J Pathol 2000;190:523-525.
17. Crozat A, Aman P, Mandahl N, et al. Fusion of CHOP to a novel RNA-binding protein in human myxoid liposarcoma. Nature 1993;363:640-644.
18. Engstrom K, Willen H, Kabjorn-Gustafsson C, et al. The myxoid/round cell liposarcoma fusion oncogene FUS-DDIT3 and the normal DDIT3 induce a liposarcoma phenotype in transfected human fibrosarcoma cells. Am J Pathol 2006;168:1642-1653.
19. Goransson M, Elias E, Stahlberg A, et al. Myxoid liposarcoma FUS-DDIT3 fusion oncogene induces C/EBP beta-mediated interleukin 6 expression. Int J Cancer 2005;115:556-560.
20. Riggi N, Cironi L, Provero P, et al. Expression of the FUS-CHOP fusion protein in primary mesenchymal progenitor cells gives rise to a model of myxoid liposarcoma. Cancer Res 2006;66:7016-7023.
21. Uranishi H, Tetsuka T, Yamashita M, et al. Involvement of the pro-oncoprotein TLS (translocated in liposarcoma) in nuclear factor-kappa B p65-mediated transcription as a coactivator. J Biol Chem 2001;276:13395-13401.
22. Zinszner H, Albalat R, Ron D. A novel effector domain from the RNA-binding protein TLS or EWS is required for oncogenic transformation by CHOP. Genes Dev 1994;8:2513-2526.
23. Perez-Mancera PA, Bermejo-Rodriguez C, Sanchez-Martin M, et al. FUS-DDIT3 prevents the development of adipocytic precursors in liposarcoma by repressing PPARgamma and C/EBPalpha and activating eIF4E. PLoS One 2008;3:e2569.
24. Tontonoz P, Spiegelman BM. Fat and beyond: the diverse biology of PPARgamma. Annu Rev Biochem 2008;77:289-312.
25. McDonnell LA, Heeren RM. Imaging mass spectrometry. Mass Spectrom Rev 2007;26:606-643.

26. Cazares LH, Troyer D, Mendrinos S, et al. Imaging mass spectrometry of a specific fragment of mitogen-activated protein kinase/extracellular signal-regulated kinase kinase kinase 2 discriminates cancer from uninvolved prostate tissue. Clin Cancer Res 2009;15:5541-5551.
27. Djidja MC, Claude E, Snel MF, et al. Novel molecular tumour classification using MALDI-mass spectrometry imaging of tissue micro-array. Anal Bioanal Chem 2010;397:587-601.
28. Groseclose MR, Massion PP, Chaurand P, et al. High-throughput proteomic analysis of formalin-fixed paraffin-embedded tissue microarrays using MALDI imaging mass spectrometry. Proteomics 2008;8:3715-3724.
29. Kang S, Shim HS, Lee JS, et al. Molecular Proteomics Imaging of Tumour Interfaces by Mass Spectrometry. J Proteome Res 2010;
30. McDonnell LA, Corthals GL, Willems SM, et al. Peptide and protein imaging mass spectrometry in cancer re search. J Proteomics 2010;
31. Oppenheimer SR, Mi D, Sanders ME, et al. Molecular analysis of tumor margins by MALDI mass spectrometry in renal carcinoma. J Proteome Res 2010;9:2182-2190.
32. Antonescu C, Ladanyi M. Myxoid liposarcoma. In World Health Organization classification of tumours. pathology and genetics. Tumours of soft tissue and bone., (2002 edn), Fletcher C.D.M., Unni KK, Mertens F (eds). IARC press: Lyon, 2004; 40-43
33. Mentzel T, Van den Berg E, Molenaar WM. Myxofibrosarcoma. In World Health Organization classification of tumours. pathology and genetics. Tumours of soft tissue and bone., (2002 edn), Fletcher C.D.M., Unni KK, Mertens F (eds). IARC press: Lyon, 2004; 102-103
34. Guillou L, Coindre JM, Bonichon F, et al. Comparative study of the National Cancer Institute and French Federation of Cancer Centers Sarcoma Group grading systems in a population of 410 adult patients with soft tissue sarcoma. J Clin Oncol 1997;15:350-362.
35. Schwamborn K, Krieg RC, Reska M, et al. Identifying prostate carcinoma by MALDI-Imaging. Int J Mol Med 2007;20:155-159.
36. McDonnell LA, van Remoortere A, van Zeijl RJ, et al. Mass spectrometry image correlation: quantifying colocalization. J Proteome Res 2008;7:3619-3627.
37. Norris JL, Cornett DS, Mobley JA, et al. Processing MALDI Mass Spectra to Improve Mass Spectral Direct Tissue Analysis. Int J Mass Spectrom 2007;260:212-221.
38. Deininger SO, Ebert MP, Futterer A, et al. MALDI imaging combined with hierarchical clustering as a new tool for the interpretation of complex human cancers. J Proteome Res 2008;7:5230-5236.
39. Schwartz SA, Reyzer ML, Caprioli RM. Direct tissue analysis using matrix-assisted laser desorption/ionization mass spectrometry: practical aspects of sample preparation. J Mass Spectrom 2003;38:699-708.
40. Caldwell RL, Holt GE, Caprioli RM. Tissue profiling by mass spectrometry distinguishes clinical grades of soft tissue tumours. Cancer Genomics Proteom 2005;2:333-346.
41. Karas M, Bachmann D, Bahr U, et al. Matrix-assisted ultraviolet laser desorption of non-volatile compunds. Int J Mass Spectrom Ion Proc 1987;53-68.
42. Chaurand P, Sanders ME, Jensen RA, et al. Proteomics in diagnostic pathology: profiling and imaging proteins directly in tissue sections. Am J Pathol 2004;165:1057-1068.
43. Cornett DS, Reyzer ML, Chaurand P, et al. MALDI imaging mass spectrometry: molecular snapshots of biochemical systems. Nat Methods 2007;4:828-833.
44. Seeley EH, Caprioli RM. Molecular imaging of proteins in tissues by mass spectrometry. Proc Natl Acad Sci U S A 2008;105:18126-18131.
45. Caldwell RL, Gonzalez A, Oppenheimer SR, et al. Molecular assessment of the tumor protein microenviroment using imaging mass spectrometry. Cancer Genomics Proteom 2006;3:279-288.
46. Francis P, Fernebro J, Eden P, et al. Intratumor versus intertumor heterogeneity in gene expression profiles of soft-tissue sarcomas. Genes Chromosomes Cancer 2005;43:302-308.
47. Orndal C, Rydholm A, Willen H, et al. Cytogenetic intratumor heterogeneity in soft tissue tumors. Cancer Genet Cytogenet 1994;78:127-137.
48. Prat E, Del RJ, Camps J, et al. Genomic imbalances in urothelial cancer: intratumor heterogeneity versus multifocality. Diagn Mol Pathol 2008;17:134-140.
49. Jovanovic L, Delahunt B, McIver B, et al. Most multifocal papillary thyroid carcinomas acquire genetic and morphotype diversity through subclonal evolution following the intra-glandular spread of the initial neoplastic clone. J Pathol 2008;215:145-154.
50. Guillou L, Aurias A. Soft tissue sarcomas with complex genomic profiles. Virchows Arch 2010;456:201-217.
51. Singer S, Millis K, Souza K, et al. Correlation of lipid content and composition with liposarcoma histology and grade. Ann Surg Oncol 1997;4:557-563.

52. Millis K, Weybright P, Campbell N, et al. Classification of human liposarcoma and lipoma using ex vivo proton NMR spectroscopy. Magn Reson Med 1999;41:257-267.
53. Chen JH, Enloe BM, Weybright P, et al. Biochemical correlates of thiazolidinedione-induced adipocyte differentiation by high-resolution magic angle spinning NMR spectroscopy. Magn Reson Med 2002;48:602-610.
54. Bensinger SJ, Tontonoz P. Integration of metabolism and inflammation by lipid-activated nuclear receptors. Nature 2008;454:470-477.
55. Willems SM, Schrage YM, Briaire-de Bruijn IH, et al. Kinome profiling of myxoid liposarcoma reveals NF-kB-pathway activity and casein kinase II inhibition as a potential treatment option. Mol Cancer 2010;
56. Perez-Mancera PA, Vicente-Duenas C, Gonzalez-Herrero I, et al. Fat-specific FUS-DDIT3-transgenic mice establish PPARgamma inactivation is required to liposarcoma development. Carcinogenesis 2007;28:2069-2073.
57. Grommes C, Landreth GE, Heneka MT. Antineoplastic effects of peroxisome proliferator-activated receptor gamma agonists. Lancet Oncol 2004;5:419-429.
58. Debrock G, Vanhentenrijk V, Sciot R, et al. A phase II trial with rosiglitazone in liposarcoma patients. Br J Cancer 2003;89:1409-1412.

# Chapter 7

## Kinome profiling of myxoid liposarcoma reveals NF-kappaB-pathway kinase activity and Casein Kinase II inhibition as a potential treatment option

Stefan M. Willems[1], Yvonne M. Schrage[1], Inge H. Briaire-de Bruijn[1], Karoly Szuhai[2], Pancras C. W. Hogendoorn[1], Judith V. M. G. Boveé[1]

[1]Department of Pathology and [2]Department of Molecular Cell Biology, Leiden University Medical Center, L1Q, P.O. Box 9600, 2300 RC Leiden, The Netherlands

## Abstract

Myxoid liposarcoma is a relatively common malignant soft tissue tumor, characterized by a (12;16) translocation resulting in a FUS-DDIT3 fusion gene playing a pivotal role in its tumorigenesis. Treatment options in patients with inoperable or metastatic myxoid liposarcoma are relatively poor though being developed and new hope is growing. Using kinome profiling and subsequent pathway analysis in two cell lines and four primary cultures of myxoid liposarcomas, all of which demonstrated a FUS-DDIT3 fusion gene including one new fusion type, we aimed at identifying new molecular targets for systemic treatment. Protein phosphorylation by activated kinases was verified by Western Blot and cell viability was measured before and after treatment of the myxoid liposarcoma cells with kinase inhibitors. We found kinases associated with the atypical nuclear factor-kappaB and Src pathways to be the most active in myxoid liposarcoma. Inhibition of Src by the small molecule tyrosine kinase inhibitor dasatinib showed only a mild effect on cell viability of myxoid liposarcoma cells. In contrast, inhibition of the nuclear factor-kappaB pathway, which is regulated by the FUS-DDIT3 fusion product, in myxoid liposarcoma cells using casein kinase 2 inhibitor 4,5,6,7-tetrabromobenzotriazole (TBB) showed a significant decrease in cell viability, decreased phosphorylation of nuclear factor-kappaB pathway proteins, and caspase 3 mediated apoptosis. Combination of dasatinib and TBB showed an enhanced effect. Kinases associated with activation of the atypical nuclear factor-kappaB and the Src pathways are the most active in myxoid liposarcoma in vitro and inhibition of nuclear factor-kappaB pathway activation by inhibiting casein kinase 2 using TBB, of which the effect is enhanced by Src inhibition using dasatinib, offers new potential therapeutic strategies for myxoid liposarcoma patients with advanced disease.

## Background

Myxoid liposarcoma accounts for 40% of all liposarcomas and occurs most commonly in the extremities [1]. In about 95% of cases, myxoid liposarcoma is cytogenetically characterized by t(12;16)(q13;p11), creating a chimerical FUS/DDIT3 gene which has been thought to play a pivotal role in its tumourigenesis [2-4]. The cornerstone of curative treatment for myxoid liposarcoma is surgery with an overall 10 years survival of 80%. Prognosis is mainly determined by the percentage of round cell component of the tumor. Myxoid liposarcoma with more than 5% round cell component are defined as high-grade and prone to metastasis[5]. Treatment options for patients with inoperable or metastatic disease are relatively poor, though trials with new drugs reveal good perspectives for the future[6, 7]. Therefore, clinical trials to test and validate new treatment options for liposarcoma subtypes (such as myxoid liposarcoma) are necessary[6]. Nowadays, (neo) adjuvant chemotherapy of liposarcoma patients is limited with only ifosfamide and anthracyclins showing 20-40% response rates in untreated patients[8]. Trabectedin (Yondelis, ET 743) is a novel chemotherapeutic agent derived from the marine tunicate Ecteinascidia turbinate. By binding to the DNA minor groove, ET-743 forms covalent adducts with the N2-position of guanine through its carbinolamine moiety. As a result, the minor groove bends toward the major groove. The cytotoxic activity of ET-743 is largely based on its interaction with nucleoside excision repair machinery, as well as through the induction of double strand breaks[9-11]. Phase I and II studies showed promising results in myxoid liposarcoma patients with advanced disease though recent studies reported an increasing number of side effects[12, 13]. During the last years, tumor specific targeted therapy has shown to be effective in many cancers, including sarcomas. Especially kinase inhibitors are an emerging class of small molecule inhibitors that target unique kinase conformational forms and binding sites[14]. Notable advantages are higher specificity and generally more manageable and reversible side effects [15]. This necessitates the study of separate soft tissue tumour entities[7]. In the present study, we explored the activated pathways in myxoid liposarcoma cells using kinome profiling to find new treatment possibilities. Kinases phosphorylate tyrosine, threonine or serine residues on proteins, thereby serving as a switch to (in) activate pathways involved in cell cycle, cell survival and differentiation. Moreover, kinases are promising targets for anti-cancer therapy as they do not require new protein synthesis, therefore act rapidly and are also promising in slow-cycling tumors [16, 17]. Data on activated pathways in myxoid liposarcoma are sparse[18, 19]. By using a kinase substrate specific protein array chip combining 1024 different kinase substrates, we identified kinases associated with Src and NF-kappaB pathways to be active in myxoid liposarcoma. NF-kappaB is an inducible cellular transcription factor that regulates a variety of cellular genes, including those involved in immune regulation, inflammation, cell survival and cell proliferation. Hereby, active NF-kappaB plays a pivotal role in tumorigenesis and increased expression of

the phosphorylated NF-kappaB protein is found in many tumors[20, 21]. We showed that in myxoid liposarcoma cells, inhibition of kinases associated with the NF-kappaB pathway (by TBB) resulted in decreased viability and that this effect was enhanced by Src-inhibitor dasatinib. These results show that targeting NF-kappaB pathway might be a potential treatment option in myxoid liposarcoma patients with advanced disease.

## Results

*Molecular and cytogenetic analysis*

FISH of the primary myxoid liposaromas showed the tumor specific t(12;16) in three out of four cases (table 1).

All four primary cultures showed the FUS/DDIT3 fusion transcripts[22]. Case

**Table 1:** clinicopathological and genetic data of myxoid liposarcoma samples

| | Sample ID | Type | Gender | Age | P/R/M | Location | FUS/DDIT3 transcript size | FUS/DDIT3 transcript type | (COBRA) FISH |
|---|---|---|---|---|---|---|---|---|---|
| 1 | L1187 | primary culture | F | 20 | P | left hamstrings | 1033 bp | X | t(12;16) |
| 2 | L1357 | primary culture | M | 50 | P | left hamstrings | 654 bp | I | t(12;16) |
| 3 | L1434 | primary culture | F | 43 | P | right hamstrings | 654 bp | I | t(12;16) |
| 4 | L2187 | primary culture | F | 42 | P | subcutaneously | 378 bp | II | N/A |
| 5 | 402-91 | cell line | M | unknown | unknown | unknown | unknown | N/A | t(12;16) |
| 6 | 1765-92 | cell line | unknown | unknown | unknown | unknown | unknown | N/A | t(12;16) |

Primary cultures of samples L1187, L1357, L1434 and L2187 were obtained from fresh tumors. Tumors L1187 and L1357 were high grade (>5% round cell component), whereas L1434 and L2187 were low-grade (<5 % round cell component). These differences in grade however were not reflected in growth rate of the primary cultures (doubling times of primary cultures were all ~ 4 days; doubling times of cell lines ~ 2 days).

L1187 showed a 1033 bp long fusion transcript involving exon 11 of the FUS and exon 2 of the DDIT3 gene, which has not been reported previously (figure 1). This chimera includes the RNA-binding domain (exon 8-11) of the FUS gene as in fusion type 8, which is absent in the other fusion types. This new FUS/DDIT3 fusion type was deposited in GenBank (GenBank accession number GU933437). COBRA-FISH of both myxoid liposarcoma cell lines showed the myxoid liposarcoma specific t(12;16) translocation. The precise karyotype of 402-91 was: 46, X, der(Y)t(Y;19)(q11;p11), t(1;7)(p12;p12), der(8)t(8;21)(p11;p11)[7], der(8)t(8;9)(p11;p11)[7], del(8)(p11)[4], del(10)(p11), t(12;16)(q13;p11), del(18)(p11), -19,+20, -21[7][cp20], several additional, non-clonal rearrangements involving chromosomes 4, 5, 6 and 8 with various partner chromosomes.

The precise karyotype of 1765-92 was 90-99, XX, der(1)inv(1)(p32q31)t(1;10)(p33;p12), der(1)inv(1)(p32q31)t(1;10) (p33;p12), -1,del(2)(p11), -3, +5, der(6)t(4;6)(4q,6q), der(6)t(6;10)(p;q), +der(6)t(6;10) (p;q), der(8)t(3;8), i(8)(q10), +i(8)(q10), +9, der(10)t(1;10)(1p32,p12), der(10)t(1;10) (1p32,p12), -10, +11, t(12;16)(q13;p11), t(12;16)(q13;p11), -13,der(13)t(6;13)(q;q), +14, +15, +18, +20, +20 [cp20].

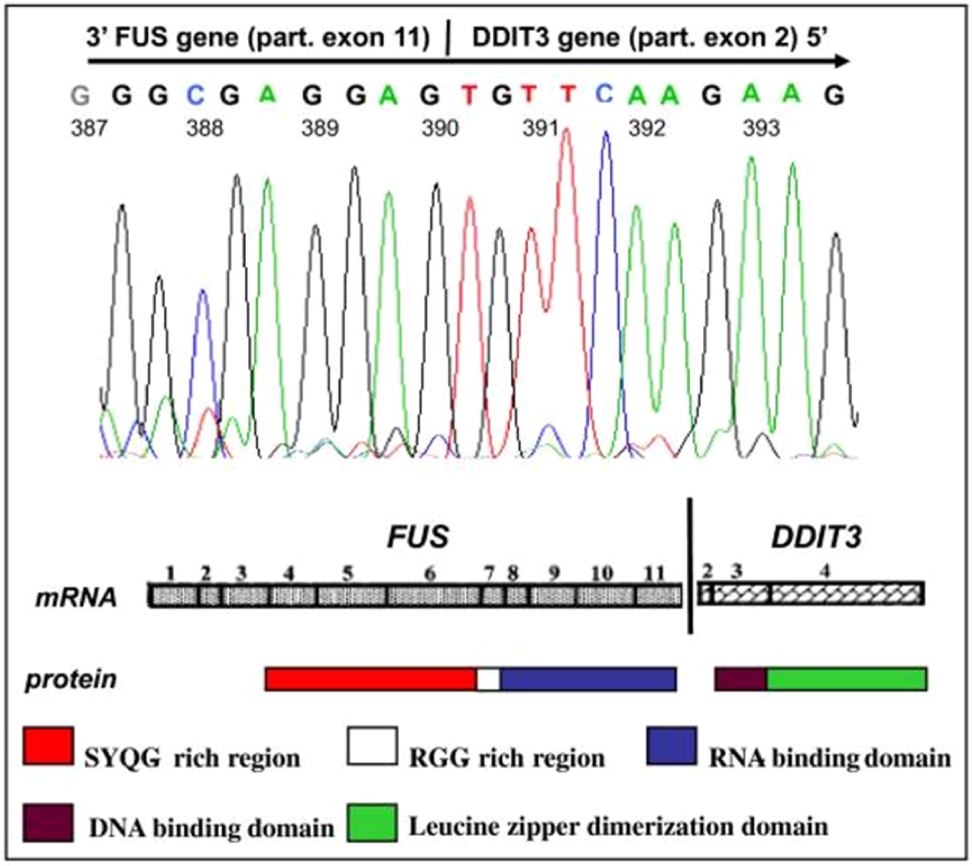


**Figure 1:** Exon 11 of the FUS gene is fused to exon 2 of the DDIT3 gene. The corresponding chimeric protein retains the RNA binding domain of the FUS protein.

*Identification of active kinases and pathways*

A list of phosphorylated targets and their corresponding active kinases was created by kinome profiling of two cell lines and four primary cultures of myxoid liposarcoma. Average spot intensity and target frequency of the top 100 phosphorylated substrates revealed the most activated kinases in myxoid liposarcoma (table 2). Both in myxoid liposarcoma cell lines as well as in primary cultures, casein kinase 2, alpha 1 (ck2a1), lymphocyte-specific protein tyrosine kinase (lck), fyn oncogene related to SRC (fyn), Gardner-Rasheed feline sarcoma viral (v-fgr) oncogene homolog (fgr), v-yes-1 Yamaguchi sarcoma viral oncogene homolog (yes), calcium/calmodulin-dependent protein kinase II beta (camk2b) and protein kinase, cAMP-dependent, catalytic, alpha (prkaca) were most activated (table 2). There were no clear differences between the cell lines and the primary cultures. The specificity of the list of substrates for myxoid liposarcomas was verified by comparing the intensity of the signals with those for

**Table 2:** Top 100 activated kinases and targeted drugs in myxoid liposarcoma cell lines and primary cultures.

| | Intensity | Kinase | Number of hits | Description | Drugs |
|---|---|---|---|---|---|
| 1 | 7965,340 | CK2 | 9 | Casein kinase 2, alpha 1 | 4,5,6,7-tetrabromobenzotriazole |
| 2 | 5932,666 | LCK | 3 | Lymphocyte-specific protein tyrosine kinase | dasatinib |
| 3 | 5932,666 | FYN | 2 | FYN oncogene related to SRC, FGR, YES | dasatinib |
| 4 | 4716,473 | CAMK2B | 5 | Calcium/calmodulin-dependent protein kinase II beta | |
| 5 | 3998,331 | PRKACA | 8 | Protein kinase, cAMP-dependent, catalytic, alpha | |
| 6 | 3922,920 | MAPK1 | 4 | Mitogen-activated protein kinase 1 [ | |
| 7 | 3922,920 | KIT | 1 | V-kit Hardy-Zuckerman 4 feline sarcoma viral oncogene homolog | dasatinib, sunitinib ao |
| 8 | 3402,973 | CSNK1A1 | 1 | Casein kinase 1, alpha 1 | |
| 9 | 3402,973 | CIB | 2 | Calcium and integrin binding family | |
| 10 | 3317,951 | GSK3 | 2 | Glycogen synthase kinase 3 | |
| 11 | 3144,082 | LYN | 1 | V-yes-1 Yamaguchi sarcoma viral related oncogene homolog | |
| 12 | 3144,082 | BTK | 1 | Bruton agammaglobulinemia tyrosine kinase | |
| 13 | 3114,907 | PKC | 19 | Protein kinase C | |
| 14 | 3057,647 | AKT1 | 3 | V-akt murine thymoma viral oncogene homolog 1 | enzastaurin |
| 15 | 3033,443 | PKM2 | 1 | Pyruvate kinase, muscle | |
| 16 | 2928,117 | CAMK1 | 1 | Calcium/calmodulin-dependent protein kinase I | |
| 17 | 2893,922 | CHEK1 | 1 | CHK1 checkpoint homolog | |
| 18 | 2893,922 | CHEK2 | 2 | CHK2 checkpoint homolog | |
| 19 | 2893,922 | PLK3 | 2 | Polo-like kinase 3 | |
| 20 | 2890,210 | TTN | 1 | Titin | |
| 21 | 2712,053 | ABL | 2 | Abelson murine leukemia viral (v-abl) oncogene homolog | imatinib, temozolomide |
| 22 | 2596,825 | INSR | 1 | Insulin receptor | lispro,aspart, glargine |
| 23 | 2596,825 | EGFR | 2 | Epidermal growth factor receptor | cetuximab,canertinib ao |
| 24 | 2596,825 | MET | 1 | Met proto-oncogene | |
| 25 | 2483,173 | SRC | 6 | V-src sarcoma (Schmidt-Ruppin A-2) viral oncogene homolog | |
| 26 | 2443,714 | RPS6 | 4 | Ribosomal protein S6 | |
| 27 | 2382,003 | CK | 1 | Choline kinase | |
| 28 | 2314,823 | MAP2K3 | 1 | Mitogen-activated protein kinase kinase 3 | |
| 29 | 2294,228 | GRK1 | 2 | G protein-coupled receptor kinase 1 | |
| 31 | 2216,637 | JAK1 | 1 | Janus kinase 1 | |
| 32 | 2214,443 | MAPKAPK2 | 1 | Mitogen-activated protein kinase-activated protein kinase 2 | |
| 33 | 2179,345 | ALK | 1 | Anaplastic lymphoma receptor tyrosine kinase | |
| 34 | 2052,700 | ATM | 2 | Ataxia telangiectasia mutated | |
| 35 | 2040,371 | PKN1 | 2 | Protein kinase N1 | |
| 36 | 1913,813 | PDGFRB | 1 | Platelet-derived growth factor receptor, beta polypeptide | dasatinib,sunitib ao |
| 37 | 1870,956 | CDK2 | 1 | Cyclin-dependent kinase 2 | BMS-387032, flavopiridol |
| 38 | 1849,628 | CCRK | 1 | Cell cycle related kinase | |
| 39 | 1806,824 | CDC2 | 1 | Cell division cycle 2, G1 to S and G2 to M | flavopiridol |

Top list of kinases was based on the intensity of incorporated radioactively labeled phosphorus, corresponding with kinase activity. The number of hits corresponds to the number of substrates to be phosphorylated by a specific kinase, not necessarily associated with kinase activity as substrates were not equally covered by the different kinases.

normal MSCs which served as a normal control for this tumor type, using Limma (additional file 1). Specificity of the activated kinases in this type of cancer (i.e. myxoid liposarcoma) was additionally verified by comparison with the same analysis in four colorectal carcinoma cell lines and thirteen chondrosarcoma cell lines and cultures using Limma, which revealed a different list of substrates and kinases[16]. Pathway analysis based on the most active kinases (table 3) identified kinases associated with NF-kappaB pathway (ck2a1, fgr, inhibitor of kappa light polypeptide gene enhancer in B-cells, kinase (ikk), protein kinase RNA-activated (pkr), v-akt murine thymoma viral oncogene homolog (akt), NF-kappa-beta-inducing kinase (nik), mitogen-activated protein kinase kinase kinase 3 (mekk3) and focal adhesion kinase 1 (fak1) to be most activated. Also kinases associated with Src-pathway (lck, fyn) were highly active. In addition, retinoic acid receptor pathway (RAR) and peroxisome proliferator-activated receptor (PPAR) activation pathway were found. The top 5 of activated pathways was identical in cell lines and primary cultures. Results of the analysis leaving out all cell cycle related kinases (27% of all kinases detectable), which might be artificially upregulated due to cell culturing, and results of analysis after starvation of the cell lines are shown in table 3.

**Additional file 1:** Top 100 of activated kinases in MSCs obtained by kinome analysis.

| | Intensity | Kinase | Number of hits |
|---|---|---|---|
| 1 | 186992,3 | MAPK8 | 2 |
| 2 | 186992,3 | MAPK | 4 |
| 3 | 110682,2 | RET | 5 |
| 4 | 101178,8 | EIF2AK2 | 1 |
| 5 | 94551,1 | EGFR | 5 |
| 6 | 85436,2 | EPHB1 | 2 |
| 7 | 82852,7 | MARK1 | 1 |
| 8 | 81393,4 | SRC | 2 |
| 9 | 80335,4 | PKGIalpha | 3 |
| 10 | 79229,2 | ZAP70 | 1 |
| 11 | 78905,1 | FRAP1 | 2 |
| 12 | 78329,8 | ABL1 | 1 |
| 13 | 78168,9 | ERBB2 | 2 |
| 14 | 77714,7 | MAPK3 | 1 |
| 15 | 74233,4 | PKCdelta | 1 |
| 16 | 74121,0 | CAMK2B | 1 |
| 17 | 74121,0 | PKC | 9 |
| 18 | 71671,0 | CAMK4 | 2 |
| 19 | 69217,6 | AKT1 | 1 |
| 20 | 68871,6 | AKT2 | 4 |
| 21 | 66976,4 | PKA | 1 |
| 22 | 66976,4 | PRKG1 | 5 |
| 23 | 66868,2 | CHEK2 | 2 |
| 24 | 66276,6 | MET | 2 |
| 25 | 64716,5 | BCR | 8 |
| 26 | 63267,5 | HIPK2 | 1 |
| 27 | 63080,7 | PTK2 | 1 |
| 28 | 61562,8 | GRB2 | 1 |
| 29 | 61531,8 | GRK1 | 2 |
| 30 | 61472,3 | SYK | 1 |
| 31 | 61410,3 | CDK5 | 1 |
| 32 | 60241,0 | PTPN11 | 1 |
| 33 | 59255,2 | FYN | 2 |
| 34 | 59092,8 | FGFR2 | 1 |
| 35 | 58359,4 | CDC2 | 1 |
| 36 | 56754,2 | ATR | 1 |
| 37 | 56747,8 | LCK | 2 |
| 38 | 55736,2 | CDK2 | 1 |
| 39 | 55631,0 | SGK1 | 1 |
| 40 | 55529,5 | PRKAB1 | 1 |
| 41 | 55501,3 | BTK | 1 |
| 42 | 55391,4 | MAPK14 | 1 |
| 43 | 55391,4 | MAPK9 | 1 |
| 44 | 54605,9 | NEK9 | 1 |
| 45 | 54523,6 | KIT | 1 |
| 46 | 53125,4 | PKD1 | 1 |
| 47 | 53097,9 | MAP4K1 | 1 |
| 48 | 52753,3 | PKCepsilon | 1 |
| 49 | 51971,9 | BCR/ABL | 1 |
| 50 | 51677,6 | DNAPK | 1 |
| 51 | 50594,8 | LYN | 1 |
| 52 | 50264,4 | INSR | 1 |
| 53 | 50175,2 | CSK | 1 |
| 54 | 49874,6 | GSK3 | 1 |

Table shows list of kinases found to be activated in mesenchymal stem cells, in decreasing order. The intensity correlates with the radioactivity of $^{33}P$ incorporated in the substrates by their active kinases. The number of hits are the number of substrates related to the respective kinase.

**Table 3:** Top lists of activated kinases and pathways in different conditions.

| | top five activated kinases | top activated signalling pathway |
|---|---|---|
| normal medium condition (including all kinases in the analysis) | ck2a1 | NF-kappaB |
| | lck | Src |
| | fyn | RAR |
| | fgr | PPAR |
| | yes | |
| normal medium condition (leaving out cell cycle related kinases in the analysis) | ck2a1 | NF-kappaB |
| | lck | Src |
| | fyn | RAR |
| | camk2b | PPAR |
| | prkcd | |
| starved medium condition | mapk14 | NF-kappaB |
| | ck2a1 | RAR |
| | akt1 | p53 |
| | | G1/S transition of the cell |
| | egfr | cycle |
| | erbb2 | oxidative stress response |

Whereas activated kinases differed between cells grown in normal medium (RMPI supplemented with 10% inactivated calf serum), top five of activated signaling pathways were identical. Results were identical for cell lines and primary cultures. Cell lines cultured in starved medium conditions revealed a different top list of both kinases and activated signaling pathways. However, in all three different conditions, NF-kappaB was the most activated signaling pathway identified.
prkcd: protein kinase C, delta; mapk14: mitogen-activated protein kinase 14; egfr: epidermal growth factor receptor; erbb2: v-erb-b2 erythroblastic leukemia viral oncogene homolog 2

*Verification of kinome profiling*

Western blotting showed that all myxoid liposarcoma samples (both cell lines and primary cultures) expressed comparable amounts of total Src and NF-kappaB p65. Phosphorylation of Src (Y419) was present in all samples (figure 2) confirming activation of Src pathway. Likewise, western blotting showed the presence of ck2a1 and phosphorylated NF-kappaB p65 (S468) in all samples, confirming the results of the IPA analysis that kinases associated with NF-kappaB pathway are active in myxoid liposarcoma cells.

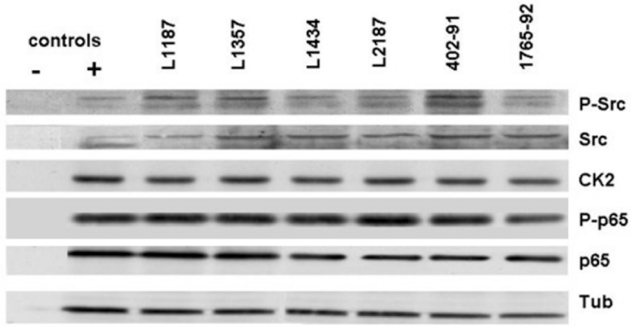


**Figure 2:** Immunoblotting was used for verification of the results obtained by Pepchip analysis. Band heights were all corresponding to the manufacturer's datasheets (P-Src: 2 bands between 56-61 kDa, Src: 60 kDa, Casein Kinase 2: 42 kDa, P-p65: 65 kDa and p65: 65 kDa). Both cell lines and primary cultures showed phosphorylation of Src and slight variation in amounts of total Src. Casein Kinase 2 and p65 protein were present in all samples in comparable amounts, as is phosphorylated p65, indicating active NF-kappaB signaling.

*In vitro targeting of kinases associated with Src and NF-kappaB pathways by dasatinib and TBB*

WST-1 analysis of GIST882 showed a profound decrease in cell viability of up to ~ 80% relative to the DMSO control at even low dosages of Src-inhibitor dasatinib (figure 3). The decrease in cell viability of myxoid liposarcoma cells treated with dasatinib was rather mild as WST-1 analysis of all four cell cultures and 1 out of 2 cell lines showed a maximum decrease in cell viability of 40% at higher doses (figure 3). Cell line 1765-92 did not respond to dasatinib. In contrast, myxoid liposarcoma cells showed a decline of more than 50% in viability after treatment with casein kinase 2-inhibitor TBB in two out of four cultures and in both cell lines. This effect was also observed in Jurkat cells as described (positive control)[23]. There was no relation between the response rate and type of fusion gene. For combination experiments, the two cell lines (402-91 and 1765-92) and the two most sensitive myxoid liposarcoma primary cultures (L1357 and L2187) were treated with both dasatinib and TBB.

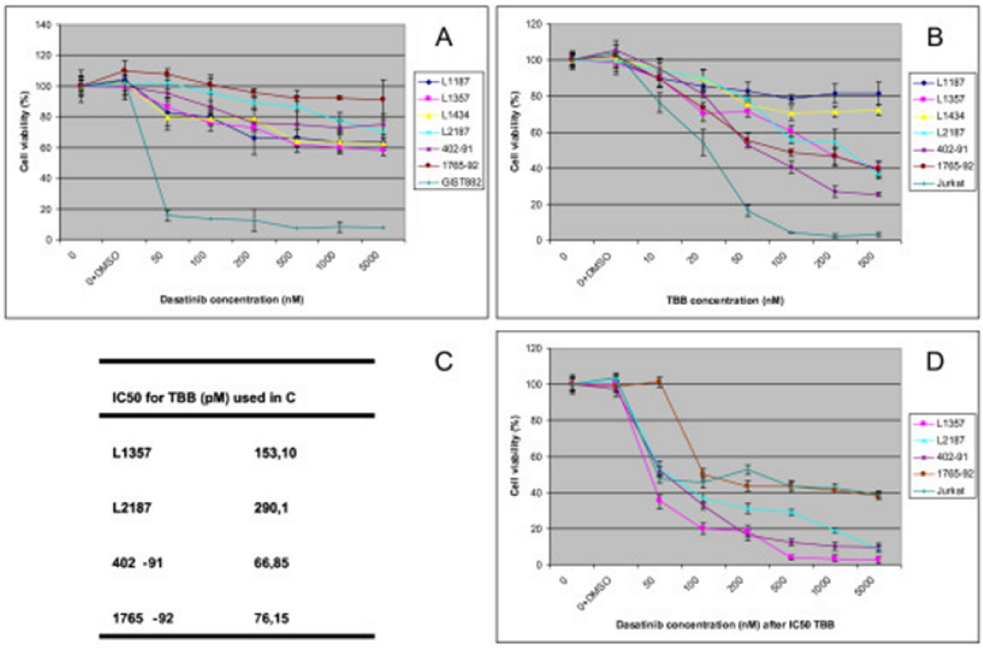


**Figure 3:** Effect of dasatinib and TBB treatment on cell viability of myxoid liposarcoma cells." 3A) Treatment of myxoid liposarcoma cell cultures with dasatinib leads to maximum 20% decrease in viability at the concentrations higher than 200 nM, though this effect is limited as compared to GIST882. 3B) Treatment with TBB shows a 20% decrease at lower concentrations (20 μM) and a maximum decrease of 75% at 200 M (cell line 402-92) in the majority of cases. Cell viability with IC50s as depicted in 3C. 3D) Combined treatment with TBB (at IC50 concentration) and dasatinib (concentrations as in 3A).Jurkat cells where susceptible to TBB, but not to dasatinib. Interestingly, the effect of dasatinib when preceded by TBB was significantly more pronounced than dasatinib in monodrug treatment which means that dasatinib and TBB have an enhanced effect. Graphs show data from four representative experiments. Error bars indicate the standard error of the mean.

Combined administration of both drugs led to a dramatic decrease in cell viability and showed an enhanced effect (figure 3D), for instance: L1357 cells show 80% viability at maximum dasatinib dose (5000 nM), whereas viability was only 5% at lower concentration of dasatinib (500 nM) at IC 50 for TBB (figure 3D).

*Dasatinib inhibits phosphorylation of Src but does not cause apoptosis*

To investigate the effect of dasatinib on Src signalling, a good responsive (60 % cell viability at 500 nM; figure 3A) myxoid liposarcoma cell culture (L1357) was treated with 50, 200 and 500 nM of dasatinib for 6 hours. Whereas levels of total Src did not visibly decrease upon dasatinib treatment, a decrease in phosphorylated Src (p-Src) (Y419) was found (figure 4). At a dose of 200 nM dasatinib p-Src staining the lower band faded and at 500 nM both bands disappeared. Interestingly, a similar decrease in p-Src was also observed at 200 nM dasatinib when post-treated with TBB. There was no effect of dasatinib treatment on total NF-kappaB p65 or phosphorylated NF-kappaB p65 and there was no caspase-3 mediated apoptosis, since the level of caspase-3 did not increase upon dasatinib treatment (figure 4).

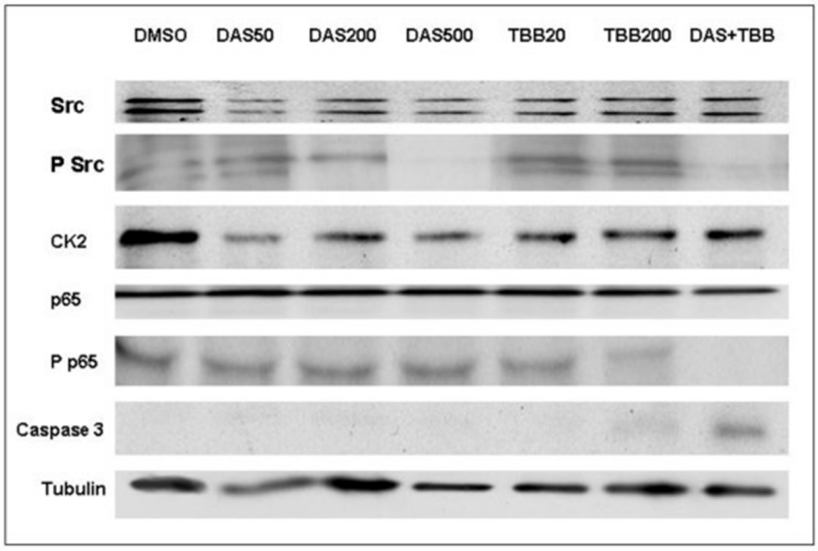


**Figure 4:** Effect of dasatinib and TBB treatment on phosphorylation of Src and NF-kappaB related proteins. Experiments were run in duplicate and showed similar results in two cell lines (402-91 and 1765-92) and primary cultures (L1357 and L2187). Treatment of L1357 with dasatinib did not affect total levels of Src, but gradually decreased P-Src levels at 200 nM to almost absence at 500 nM. There was no effect of dasatinib on total p65 and phosphorylated-p65 levels. Treatment of L1357 with TBB did not affect total levels of p65, but gradually decreased P-p65 levels at 200 ìM. TBB treatment had no effect on the levels of total Src and phosphorylated Src. Interestingly, TBB and dasatinib showed enhancement to decrease levels of phosphorylated Src and p65. Strikingly, there was a gradual increase in caspase-3 levels upon treatment with TBB, which was enhanced by combination with dasatinib, suggesting caspase-3 mediated apoptosis underlying the observed decrease in cell viability. Abbreviations: DAS50 = dastinib 50 nM, etc. DAS and TBB = 200 ìM dasatinib and IC50 concentration for TBB.

*TBB inhibits NF-kappaB p65-phosphorylation resulting in caspase-3 mediated apoptosis*

To investigate the effect of TBB on kinases associated with NF-kappaB signalling, L1357 was treated with increasing doses for 6 hours. Whereas levels of total NF-kappaB p65 did not decrease upon treatment, a decrease in phosphorylated p65 (p-p65) was found (figure 4).

At a dose of 20 μM TBB p-p65 staining slightly started to fade and obviously decreased at 200 μM TBB. Casein Kinase 2 levels of TBB treated samples were lower than the DMSO control, but remained unchanged compared to samples treated with various concentrations TBB or dasatinib, suggesting that TBB does not alter the overall expression of casein Kinase 2, which is in accordance with the literature[24]. TBB treatment had no effect on the levels of total Src and phosphorylated Src. Strikingly, the effect of TBB was increased by pretreatment with dasatinib (figure 4), which was also visible in the viability assay (figure 3D). Moreover, there was a gradual increase in caspase-3 levels upon treatment with TBB, suggesting caspase-3 mediated apoptosis.

**Discussion**

Treatment options for myxoid liposarcoma patients with advanced disease are poor. Recently, the chemotherapeutic drug Trabectedin showed promising results in phase I and II trials in advanced disease though adverse effects have also been reported[13, 25]. Small molecule targeting, especially with kinase inhibitors, has shown to be effective and more specific in many tumors with less severe side effects than conventional chemotherapeutic agents. To identify new potential treatment options for myxoid liposarcoma patients with advanced disease, we explored the kinome of myxoid liposarcoma cells in vitro and performed subsequent pathway analysis. We previously established the reliability of kinome profiling using Pepchip in untreated versus imatinib treated GIST882 cell line which correctly identified the pathways known to be involved in GIST[16]. Moreover, we previously demonstrated the reliability of our analysis which is based on averaging results of a number of samples to get an impression of the most activated kinases in a series of tumors[16]. By additionally performing the Pep-chip experiments in the myxoid liposarcomas cell lines after serum starvation as well as by excluding cell cycle related kinases from the analysis we determined that the detected kinases in the present analysis are indeed tumor specific and not related to the high proliferation rate of the myxoid liposarcoma cell lines. Moreover, by comparing with previously analyzed series of colorectal cancer and chondrosarcoma, as well as by comparing with mesenchymal stem cells we could confirm that the list of kinases was specific for myxoid liposarcomas. We could demonstrate activation of the peroxisome proliferator-activated receptor gamma pathway, which could be expected since it has been shown to play a pivotal role in adipocytic differentiation and is regulated by the FUS-DDIT3 fusion product[26-28](Figure 5). The DDIT3 gene encodes a DNA-damage inducible member of the C/EBP family of transcription factors and inhibits

adipocytic conversion of preadipocytes[29, 30]. Transfection of primary mesenchymal progenitor and human fibrosarcoma cells with the FUS/DDIT3 fusion protein induces a myxoid liposarcoma phenotype[31, 32]. Treatment of myxoid liposarcoma cells in vitro and in vivo with peroxisome proliferator-activated receptors gamma agonists induced terminal differentiation[33], although phase II studies with the peroxisome proliferator-activated receptors gamma agonist Rosiglitasone did not show the anti-tumor effect in advanced myxoid liposarcoma patients[34]. Until today, nine different types of FUS/DDIT3 fusion genes have been described, involving predominantly the central and C-terminal parts of the FUS-gene and nearly always the whole DDIT3 gene[22]. We describe here for the first time a new fusion type (Figure 1) including the RNA binding domain of the FUS gene, which is not found in the other fusion types except for type 8. Whether this new rare fusion gene will be translated to a protein or will have any promoting effect on tumor development is not clear and is hard to study due to the rarity of these variants. We found no differences between the type of FUS/DDIT3 fusion gene and kinases activated. Till now, the molecular variability of fusion types has not shown to have any effect on transforming capacities, adipogenesis nor prognosis in myxoid liposarcoma[5, 35]. We showed that kinases associated with NF-kappaB pathway were highly active in myxoid liposarcoma. In the atypical (IKK independent) NF-kappaB pathway, phosphorylation of inhibitors of NF-kappaB (IkB), and subsequent activation of NF-kappaB (p65) is controlled by casein kinase 2 and tyrosine kinase-dependent pathways (figure 5)[36, 37]. We did not measure NF-kappaB pathway activation by analysis of downstream products or electrophoretic mobility shift assays. Göransson et al. has recently shown that NF-kappaB is a major factor controlling IL8 transcription in FUS-DDIT3 expressing cells. This could be explained by direct binding of FUS/DDIT3 to the C/EBP-NF-kappaB composite site of the immediate promoter region of IL8. Moreover, FUS/DDIT3-GFP expressing cell lines showed upregulation of the NF-kappaB controlled genes LCN2 and MMP1 whereas DDIT3 had little effect. These findings were also quantitatively confirmed by RT-PCR[17]. Active (phosphorylated) p65 was present in cell lysates of myxoid liposarcoma cell cultures and cell lines. We did not explicitly show that the phosphorylated p65 protein was located in the nucleus/nuclear fraction. Phosphorylation of p65 could be counteracted by TBB, an inhibitor of the casein kinase 2 and resulted in decreased cell viability as shown in figure 3 and 4. This suggests that NF-kappaB signaling is active in myxoid liposarcoma and that its activation is, at least in part, regulated via the atypical pathway. This is an important finding which suggests that NF-kappaB pathway inhibition might be beneficial in myxoid liposarcoma patients with advanced disease. The exact driving force behind NF-kappaB activation in myxoid liposarcoma is unclear. Gene expression studies revealed that p50 was significantly upregulated in FUS/DDIT3 transfected fibroblastic cell lines[38]. This suggests that NF-kappaB (p50) transcription in myxoid liposarcoma might be regulated by the FUS/DDIT3 fusion gene. After translocation to the nucleus, transcriptional activation of NF-kappaB requires multi-

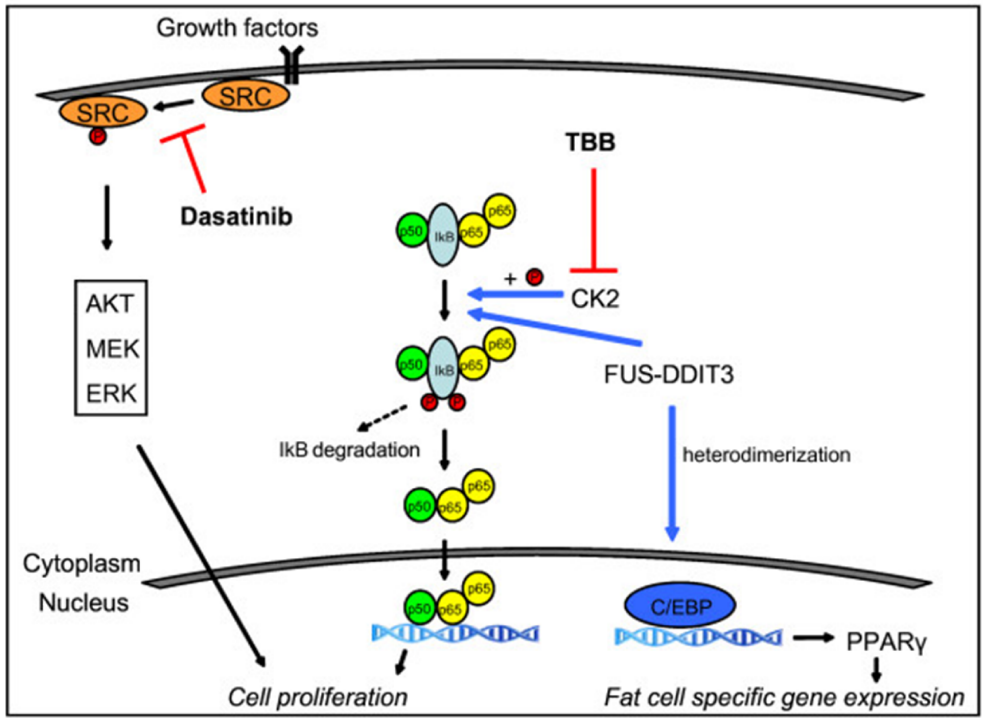


**Figure 5:** In myxoid liposarcoma, the FUS/DDIT3 protein has been shown to upregulate the expression of CCAAT/enhancer binding protein (C/EBP) which leads to the transcription of peroxisome proliferator-activated receptors gamma and other genes involved in adipocytic differentiation. We showed that in myxoid liposarcoma, the atypical NFkappaB pathway is active. Hereby casein kinase 2 phosphorylates the nuclear factor of kappa light polypeptide gene enhancer in B-cells inhibitor (IkB), which releases from the NF-kappaB p50/p65 complex and gets degraded. The NF-kappaB p50/p65 complex then shuttles into the nucleus were it promotes the transcription of genes involved in cell proliferation. Recent studies showed that the FUS/DDIT3 protein facilitates DNA binding of the NF-kappaB p50/p65 complex in a non-direct manner, probably by interfering with IkB. Also Src pathway is activated in myxoid liposarcoma, which leads through different signaling pathways (AKT, MEK, ERK) to tumor growth and cell survival. This pathway can be inhibited *in vitro* by Src-inhibitor dasatinib.

ple co-activating proteins[39]. The C-terminus of FUS co-activates p65 and plays a pivotal role in NF-kappaB mediated transcription though this C-terminus is lost in the FUS/DDIT3 fusion protein. Recent studies showed that the FUS/DDIT3 fusion protein facilitates NF-kappaB binding to its target genes, probably in an indirect manner[19, 39-41]. The FUS-DDIT3 fusion protein deregulates NF-kappaB controlled genes by interaction with nuclear factor of kappa light polypeptide gene enhancer in B-cells inhibitor zeta (NFKBIZ)[19]. This synergistic role between a fusion protein and activation of NF-kappaB signaling might also be important in other translocation based sarcomas and has already been shown in Bcr-Abl mediated leukemias[42].

In all myxoid liposarcoma samples we showed overexpression of casein kinase 2, which has been shown in many other neoplasms[43]. We showed inhibition of casein kinase 2 and subsequent decreased levels of active p65 to be associated with decreased

viability and increase in caspase 3 protein expression in myxoid liposarcoma cells. Caspase 3 is released by cleavage of its inactive precursor procaspase 3, and mediates apoptosis[44, 45]. Decreased cell viability with increased levels of the effector caspase 3 therefore suggests caspase 3 mediated apoptosis. Recently, phase I trials have been started to test the effect of casein kinase 2 inhibitors in vivo which seems to be promising[46]. In addition to kinases associated with NF-kappaB, Fyn, Lck and Yes were most active as indicated by specific sequences on the chip. They are members of the Src family of kinases. Src plays an important role in embryonic development, cell growth and cell survival and activating mutations in Src have been reported in colorectal carcinoma[47, 48]. Src signaling can lead to downstream activation of ERK/MAPK and PI3K/AKT signaling. Activation of both pathways in myxoid liposarcoma is associated with more aggressive behavior[49]. The Src pathway can be inhibited by the small molecule tyrosine kinase inhibitor dasatinib limiting cell growth in various cancers in vitro, thereby having promising therapeutic potential[16, 50, 51]. Immunoblotting confirmed the expression of Src and phosphorylation of Src at Y419 in myxoid liposarcoma cell cultures and cell lines. Dasatinib treatment showed a reduction in phosphorylated (active) Src and a decrease in cell viability. However, this latter effect was only very mild with maximum decrease in viability of only 40% maximally, and no IC50 levels could be calculated. This might be explained by Src pathway activation occurring upstream, close to its receptor (figure 5) and that the effect of the inhibition of Src phosphorylation might be (partly) circumvented by cross-talk activation downstream. Our data suggest that the active Src pathway is not crucial for myxoid liposarcoma survival and that monotherapy with dasatinib is no suitable option for treatment, although the additional effect of dasatinib in vivo through inhibition of angiogenesis is not encountered here. Combinations of different drugs (including dasatinib) have been shown to act synergistically in many tumors and combination drug therapy is commonly used in cancer treatment[50]. Recently, a synergistic effect of dasatinib when combined with other drugs (i.e. oxaliplatin) has been described in colorectal carcinoma[50]. Since we showed NF-kappaB and Src to be the two most active pathways we studied the effect of combination of dasatinib and TBB and we found a enhanced effect on cell viability of myxoid liposarcoma cells in vitro. To be more specific: L1357 cells show 80% viability at maximum dasatinib dose (5000 nM), whereas viability was only 5% at lower concentration of dasatinib (500 nM) at IC50 for TBB (figure 3). However, it was not possible to calculate if this enhancement was also a true synergistic effect as IC50 values for dasatinib could not be calculated (figure 3)[52]. IC50 values for TBB (but not for dasatinib) could be calculated for most primary cultures and cell lines, but not for L1187 and L1434. Though cell line 1765-92 responded well to TBB treatment, no enhancement could be observed upon addition of dasatinib, which might be related to a relative resistance of 1765-92 cells to

dasatinib as also visible from figure 3A. Future experiments, for instance studying the changes at the kinome level upon dasatinib treatment may reveal (1) why dasatinib is not effective as a monotherapy but is effective in combination with TBB, and (2) what might be the exact underlying mechanism why 1765-92 myxoid liposarcoma cells showed resistance for dasatinib treatment and thereby the absence of enhancement in combination treatment as was observed for the other cell line and primary cultures.

**Conclusion**

In conclusion our results indicate that the NF-kappaB and Src pathway include the most active kinases in myxoid liposarcoma, and inhibition of casein kinase 2 and thereby interference with kinases associated with the NF-kappaB pathway decreases cell viability in vitro, the effect of which can be enhanced by inhibiting src- signalling using dasatinib.

**Methods**

*Reagents*

Dasatinib (Sprycel, BMS- 354825) was obtained from Bristol-Myers Squibb (New York, USA) and TBB from Calbiochem (San Diego, CA). Both drugs were dissolved in Dimethylsulfoxide (DMSO).

*Cell cultures and cell lines*

The two myxoid liposarcoma cell lines 402-91 and 1765-92, and gastro-intestinal stroma cell tumor cell line (GIST882) were kindly provided by Prof. Dr. P. Aman (Lundberg Laboratory for Cancer Research, Department of Pathology, Göteborg University, Goteburg, Sweden) and Prof. Dr. J. Fletcher (Brigham and Women's Hospital, Boston, USA) respectively[53, 54]. Jurkat and HeLa cell lines (American Type Culture Collection, Rockville, MD) were used as positive controls for Western blotting. Myxoid liposarcoma cell lines, primary cultures of four myxoid liposarcomas (L1187, L1357, L1434 and L2187) and two cell cultures of normal bone marrow derived mesenchymal stem cells (L2361 and L2370) were cultured in RPMI 1640 (Gibco, Invitrogen Life-Technologies, Scotland, UK), supplemented with 10% heat-inactivated fetal calf serum (Gibco). Cells were grown in a humidified incubator at 37ºC with 5% CO2. In addition, two samples (402-19 and L1357) were analyzed after also culturing in starved RPMI 1640, containing 0,5% fetal calf serum.

*RT-PCR and karyotyping*

Diagnosis of the primary tumors from which the cultures were obtained was performed on histology. Primary tumors were analyzed for their tumor specific translocation with double-fusion fluorescence in situ hybridization (FISH) and cell lines were karyotyped with Combined Binary Ratio Labeling (COBRA) as previously described [55-57]. In primary cultures, tumor cells were genotyped for the presence of the fusion gene by

RT-PCR. Total RNA was isolated using TRIzol (Invitrogen, Breda, The Netherlands). Complementary DNA was synthesized from 1 μg of total RNA using oligo dT primers and Superscript II MMLV reverse transcriptase (Life Technologies, Carlsbad, CA). Reverse-transcription polymerase chain reaction (RT-PCR), sample purification and DNA sequence analysis were performed as described previously [58]. The following primers were used: FUS-forward, CAG AGC TCC CAA TCG TCT TAC GG and DDIT3-reverse, GAG AAA GGC AAT GAC TCA GCT GCC.

*Kinome array analysis*

Kinase substrate peptide arrays (Pepchip Kinomics, Pepscan Presto, Lelystad, the Netherlands) containing 1024 different kinase substrates spotted in triplicate together with 16 negative, and 16 positive controls were used and successfully used in prior studies [16, 59]. The distribution of the target sequences in terms of kinase recognition is described in detail on the website (http://www.pepscanpresto.com/index.php?id=30). Cells were harvested during their exponential growth phase and lysated as previously described. Concentration of the protein lysates was measured using the DC Protein Assay (Biorad, Hercules, CA, USA). Analysis was performed as described earlier, including the two serum-starved samples[16]. Autoradiographic signals were sensed by phosphoimage screen and scanned by Typhoon 9400 phosphoimager (GE Healthcare, Piscataway, NJ). At least 1x106 hits were collected.

*Data analysis*

The scanned images were analyzed and quantified using ImageQuant software (Molecular Dynamics, Sunnyvale, CA). For further data mining R-packages Affyio and Limma were used (http://www.bioconductor.org). Quality of the triplicates and distribution of the data was assessed and quartile normalization (Affyio) was performed as previously described[16]. Median intensities of the triplicates were calculated and the top 100 spots were imported for core analysis in Ingenuity Pathway Analysis (IPA, Ingenuity Systems, http://www.ingenuity.com). IPA is a literature based program that calculates the probability of involvement of identifiers, in this case combinations of kinases, in 74 different pathways. Data of the myxoid liposarcoma cell lines and cultures were averaged to find the common denominators that are active in all cultures[16]. To ensure that artificially induced kinase activity due to cell culturing interfered with tumor specific kinase activity, the same analysis was run excluding cell cycle related kinases as well as after starvation. Specificity of activated kinases and activated pathways in myxoid liposarcoma was verified by comparison the same analysis of four colorectal carcinoma cell lines and thirteen chondrosarcoma cell lines and cultures using Limma[16].

*Immunoblotting*
Western blotting was performed as previously described[58]. Rabbit polyclonal antibody to phosphorylated Src (Y419) was obtained from R&D Systems (1/2000; Minneapolis, MN USA). Monoclonal antibody to total Src and alpha-tubulin were obtained from Upstate Biotechnology (clone GD11, 1/2000, Lake Placid, NY, USA) and Sigma Aldrich (St. Louise, MO, USA), respectively. Rabbit polyclonal antibodies against casein kinase 2alpha; NF-kappaB p65, phospho- NF-kappaB p65 (S468) and caspase 3 were obtained from Cell Signaling Technology (Beverly, MA). HeLa cell lines, untreated and treated with TNFalpha (20 ng/ml) were used as a positive control for casein kinase 2alpha and NF-kappaB p65/phospho- NF-kappaB p65, respectively, according to the manufacturer's protocol.

*In vitro viability assays*
Measurement of metabolic activity by a WST-1 colorimetric assay (Roche Diagnostics GmbH, Penzberg, Germany) was used as a read-out system for cell viability in response to kinase inhibitors. Dasatinib was used to inhibit Src-pathway; TBB was used to inhibit casein kinase 2, which is an important kinase in atypical NF-kappaB signalling. After harvesting, 2000 cells/well of every cell line and primary culture were seeded into 96-well flat-bottom plates. After 24 hours, increasing concentrations of the drugs (50, 100, 200, 500, 1000 and 5000 nM for dasatinib and 10, 20, 50, 100, 200 and 500 μM for TBB respectively) were added or 0,1% DMSO as vehicle control, each condition in quadruplicate. Ten percent serum supplementation was used for all experiments. After 3 days of treatment, absorbance was measured on a Victor Multilabel Counter 1420-042 (Perkin Elmer, Groningen, The Netherlands) at 450 nm, and was corrected for background and averaged. GIST882 and Jurkat cell lines were used as positive controls for dasatinib and TBB experiments, respectively[16]. In combination experiments, 2000 cells were plated overnight followed by treatment with dasatinib which was added 30 minutes after TBB administration. In these experiments, increasing concentrations of dasatinib at IC50 concentrations of TBB were used.

**Competing interests**
The authors declare no conflict of interest

**Authors' contributions**

SMW carried out kinome studies, immunoblotting, in vitro studies and DNA sequencing and drafted the manuscript.
YMS participated in design of the kinome assay, immunoblotting and statistical analysis.
IHB participated in kinome studies and immunoblotting.
KS carried out the karyotyping, analysis of DNA sequences and participated in design of cell culturing.

PCWH participated in design and coordination and helped to draft the manuscript.
JVMGB designed and supervised the study and helped to draft the manuscript.
All authors read and approved the final manuscript.

**Acknowledgements**
The authors are grateful to Prof. Dr. Pierre Aman (Lundberg Laboratory for Cancer Research (LLCR), Department of Pathology, Sahlgrenska Academy at University of Gothenburg, Gothenburg, Sweden) for providing myxoid liposarcoma cell lines 402-91 and 1765-92, Prof. Dr. J. Fletcher (Brigham and Women's Hospital, Boston, USA) for providing the GIST882 cell line, Prof. Dr. Bob van de Water and Ine Tijdens (both from the Division of Toxicology, Leiden Amsterdam Center for Drug Research (LACDR), Leiden University, Leiden, The Netherlands) for expert technical support with the read out of the Pepchips. We are grateful to Jolieke van Oosterwijk for help with the WST experiments and Dr. Christianne Reijnders for culturing the mesenchymal stem cells. Brandt Meylis is acknowledged for expert technical assistance. This work was supported by a grant from the Netherlands Organisation for Scientific Research [920-03-403].

**References**

1. Antonescu C, Ladanyi M: Myxoid liposarcoma. In World Health Organization classification of tumours. pathology and genetics. Tumours of soft tissue and bone. 2002 edition. Edited by Fletcher C.D.M., Unni KK, Mertens F. Lyon: IARC press; 2004:40-43.
2. Willems SM, Wiweger M, Graadt van Roggen JF, Hogendoorn PCW: Running GAGs: myxoid matrix in tumor pathology revisited : What's in it for the pathologist? Virchows Arch 2010, 456:181-192.
3. Turc-Carel C, Limon J, Dal Cin P, Rao U, Karakousis C, Sandberg AA: Cytogenetic studies of adipose tissue tumors. II. Recurrent reciprocal translocation t(12;16)(q13;p11) in myxoid liposarcomas. Cancer Genet Cytogenet 1986, 23:291-299.
4. Panagopoulos I, Hoglund M, Mertens F, Mandahl N, Mitelman F, Aman P: Fusion of the EWS and CHOP genes in myxoid liposarcoma. Oncogene 1996, 12:489-494.
5. Antonescu CR, Tschernyavsky SJ, Decuseara R, Leung DH, Woodruff JM, Brennan MF, Bridge JA, Neff JR, Goldblum JR, Ladanyi M: Prognostic impact of P53 status, TLS-CHOP fusion transcript structure, and histological grade in myxoid liposarcoma: a molecular and clinicopathologic study of 82 cases. Clin Cancer Res 2001, 7:3977-3987.
6. Grosso F, Jones RL, Demetri GD, Judson IR, Blay JY, Le CA, Sanfilippo R, Casieri P, Collini P, Dileo P, Spreafico C, Stacchiotti S, Tamborini E, Tercero JC, Jimeno J, D'Incalci M, Gronchi A, Fletcher JA, Pilotti S, Casali PG: Efficacy of trabectedin (ecteinascidin-743) in advanced pretreated myxoid liposarcomas: a retrospective study. Lancet Oncol 2007, 8:595-602.
7. Grosso F, Sanfilippo R, Virdis E, Piovesan C, Collini P, Dileo P, Morosi C, Tercero JC, Jimeno J, D'Incalci M, Gronchi A, Pilotti S, Casali PG: Trabectedin in myxoid liposarcomas (MLS): a long-term analysis of a single-institution series. Ann Oncol 2009, 20:1439-1444.
8. Dalal KM, Antonescu CR, Singer S: Diagnosis and management of lipomatous tumors. J Surg Oncol 2008, 97:298-313.
9. Soares DG, Escargueil AE, Poindessous V, Sarasin A, de Gramont A, Bonatto D, Henriques JA, Larsen AK: Replication and homologous recombination repair regulate DNA double-strand break formation by the antitumor alkylator ecteinascidin 743. Proc Natl Acad Sci U S A 2007, 104:13062-13067.
10. Pommier Y, Kohlhagen G, Bailly C, Waring M, Mazumder A, Kohn KW: DNA sequence- and structure-selective alkylation of guanine N2 in the DNA minor groove by ecteinascidin 743, a potent antitumor compound from the Caribbean tunicate Ecteinascidia turbinata. Biochemistry 1996, 35:13303-13309.

11. Zewail-Foote M, Hurley LH: Ecteinascidin 743: a minor groove alkylator that bends DNA toward the major groove. J Med Chem 1999, 42:2493-2497.
12. Theman TA, Hartzell TL, Sinha I, Polson K, Morgan J, Demetri GD, Orgill DP, George S: Recognition of a new chemotherapeutic vesicant: trabectedin (ecteinascidin-743) extravasation with skin and soft tissue damage. J Clin Oncol 2009, 27:e198-e200.
13. Demetri GD, Chawla SP, von Mehren M, Ritch P, Baker LH, Blay JY, Hande KR, Keohan ML, Samuels BL, Schuetze S, Lebedinsky C, Elsayed YA, Izquierdo MA, Gomez J, Park YC, Le Cesne A: Efficacy and safety of trabectedin in patients with advanced or metastatic liposarcoma or leiomyosarcoma after failure of prior anthracyclines and ifosfamide: results of a randomized phase II study of two different schedules. J Clin Oncol 2009, 27:4188-4196.
14. Tuveson DA, Fletcher JA: Signal transduction pathways in sarcoma as targets for therapeutic intervention. Curr Opin Oncol 2001, 13:249-255.
15. Widakowich C, de CG, Jr., de Azambuja E, Dinh P, Awada A: Review: side effects of approved molecular targeted therapies in solid cancers. Oncologist 2007, 12:1443-1455.
16. Schrage YM, Briaire-de Bruijn IH, de Miranda NF, van Oosterwijk J, Taminiau AHM, van Wezel T, Hogendoorn PCW, Bovee JVMG: Kinome profiling of chondrosarcoma reveals SRC-pathway activity and dasatinib as option for treatment. Cancer Res 2009, 69:6216-6222.
17. Goransson M, Elias E, Stahlberg A, Olofsson A, Andersson C, Aman P: Myxoid liposarcoma FUS-DDIT3 fusion oncogene induces C/EBP beta-mediated interleukin 6 expression. Int J Cancer 2005, 115:556-560.
18. Barretina J, Taylor BS, Banerji S, Ramos AH, Lagos-Quintana M, Decarolis PL, Shah K, Socci ND, Weir BA, Ho A, Chiang DY, Reva B, Mermel CH, Getz G, Antipin Y, Beroukhim R, Major JE, Hatton C, Nicoletti R, Hanna M, Sharpe T, Fennell TJ, Cibulskis K, Onofrio RC, Saito T, Shukla N, Lau C, Nelander S, Silver SJ, Sougnez C, Viale A, Winckler W, Maki RG, Garraway LA, Lash A, Greulich H, Root DE, Sellers WR, Schwartz GK, Antonescu CR, Lander ES, Varmus HE, Ladanyi M, Sander C, Meyerson M, Singer S: Subtype-specific genomic alterations define new targets for soft-tissue sarcoma therapy. Nat Genet 2010. 42, 715 - 721 (2010)
19. Goransson M, Andersson MK, Forni C, Stahlberg A, Andersson C, Olofsson A, Mantovani R, Aman P: The myxoid liposarcoma FUS-DDIT3 fusion oncoprotein deregulates NF-kappaB target genes by interaction with NFKBIZ. Oncogene 2009, 28:270-278.
20. Karin M: Nuclear factor-kappaB in cancer development and progression. Nature 2006, 441:431-436.
21. Richmond A: Nf-kappa B, chemokine gene transcription and tumour growth. Nat Rev Immunol 2002, 2:664-674.
22. Panagopoulos I, Mertens F, Isaksson M, Mandahl N: A novel FUS/CHOP chimera in myxoid liposarcoma. Biochem Biophys Res Commun 2000, 279:838-845.
23. Sarno S, Reddy H, Meggio F, Ruzzene M, Davies SP, Donella-Deana A, Shugar D, Pinna LA: Selectivity of 4,5,6,7-tetrabromobenzotriazole, an ATP sitedirected inhibitor of protein kinase CK2 ('casein kinase-2'). FEBS Lett 2001, 496:44-48.
24. Trembley JH, Wang G, Unger G, Slaton J, Ahmed K: Protein kinase CK2 in health and disease: CK2: a key player in cancer biology. Cell Mol Life Sci 2009, 66:1858-1867.
25. Grant SK: Therapeutic protein kinase inhibitors. Cell Mol Life Sci 2009, 66:1163-1177.
26. Perez-Mancera PA, Bermejo-Rodriguez C, Sanchez-Martin M, Abollo-Jimenez F, Pintado B, Sanchez-Garcia I: FUS-DDIT3 prevents the development of adipocytic precursors in liposarcoma by repressing PPARgamma and C/EBPalpha and activating eIF4E. PLoS One 2008, 3:e2569.
27. Tontonoz P, Spiegelman BM: Fat and beyond: the diverse biology of PPARgamma. Annu Rev Biochem 2008, 77:289-312.
28. Willems SM, van RA, van ZR, Deelder AM, McDonnell LA, Hogendoorn PC: Imaging mass spectrometry of myxoid sarcomas identifies proteins and lipids specific to tumour type and grade, and reveals biochemical intratumour heterogeneity. J Pathol 2010, in press epub 2010, DOI:10.1002/path.2771.
29. Crozat A, Aman P, Mandahl P, Ron D: Fusion of CHOP a novel RNA-binding protein in human myxoid liposarcoma. Nature 1993, 363:640-644.
30. Kuroda M, Ishida T, Takanashi M, Satoh M, Machinami R, Watanabe T: Oncogenic transformation and inhibition of adipocytic conversion of preadipocytes by TLS/FUS-CHOP type II chimeric protein. Am J Pathol 1997, 151:735-744.
31. Riggi N, Cironi L, Provero P, Suva ML, Stehle JC, Baumer K, Guillou L, Stamenkovic I: Expression of the FUS-CHOP fusion protein in primary mesenchymal progenitor cells gives rise to a model of myxoid liposarcoma. Cancer Res 2006, 66:7016-7023.

32. Engstrom K, Willen H, Kabjorn-Gustafsson C, Andersson C, Olsson M, Goransson M, Jarnum S, Olofsson A, Warnhammar E, Aman P: The myxoid/round cell liposarcoma fusion oncogene FUS-DDIT3 and the normal DDIT3 induce a liposarcoma phenotype in transfected human fibrosarcoma cells. Am J Pathol 2006, 168:1642-1653.
33. Demetri GD, Fletcher CDM, Mueller E, Sarraf P, Naujoks R, Campbell N, Spiegelman BM, Singer S: Induction of solid tumor differentiation by the peroxisome proliferator-activated receptor-gamma ligand troglitazone in patients with liposarcoma. Proc Natl Acad Sci U S A 1999, 96:3951-3956.
34. Debrock G, Vanhentenrijk V, Sciot R, Debiec-Rychter M, Oyen R, Van Oosterom A: A phase II trial with rosiglitazone in liposarcoma patients. Br J Cancer 2003, 89:1409-1412.
35. Huang HY, Antonescu CR: Molecular variability of TLS-CHOP structure shows no significant impact on the level of adipogenesis: a comparative ultrastructural and RT-PCR analysis of 14 cases of myxoid/round cell liposarcomas. Ultrastruct Pathol 2003, 27:217-226.
36. Perkins ND: Integrating cell-signalling pathways with NF-kappaB and IKK function. Nat Rev Mol Cell Biol 2007, 8:49-62.
37. Romieu-Mourez R, Landesman-Bollag E, Seldin DC, Sonenshein GE: Protein kinase CK2 promotes aberrant activation of nuclear factor-kappaB, transformed phenotype, and survival of breast cancer cells. Cancer Res 2002, 62:6770-6778.
38. Schwarzbach MH, Koesters R, Germann A, Mechtersheimer G, Geisbill J, Winkler S, Niedergethmann M, Ridder R, Buechler MW, von Knebel DM, Willeke F: Comparable transforming capacities and differential gene expression patterns of variant FUS/CHOP fusion transcripts derived from soft tissue liposarcomas. Oncogene 2004, 23:6798-6805.
39. Uranishi H, Tetsuka T, Yamashita M, Asamitsu K, Shimizu M, Itoh M, Okamoto T: Involvement of the pro-oncoprotein TLS (translocated in liposarcoma) in nuclear factor-kappa B p65-mediated transcription as a coactivator. J Biol Chem 2001, 276:13395-13401.
40. Gerritsen ME, Williams AJ, Neish AS, Moore S, Shi Y, Collins T: CREB-binding protein/p300 are transcriptional coactivators of p65. Proc Natl Acad Sci US A 1997, 94:2927-2932.
41. Perkins ND, Felzien LK, Betts JC, Leung K, Beach DH, Nabel GJ: Regulation of NF-kappaB by cyclin-dependent kinases associated with the p300 coactivator. Science 1997, 275:523-527.
42. Reuther JY, Reuther GW, Cortez D, Pendergast AM, Baldwin AS, Jr.: A requirement for NF-kappaB activation in Bcr-Abl-mediated transformation. Genes Dev 1998, 12:968-981.
43. Duncan JS, Litchfield DW: Too much of a good thing: the role of protein kinase CK2 in tumorigenesis and prospects for therapeutic inhibition of CK2. Biochim Biophys Acta 2008, 1784:33-47.
44. Riedl SJ, Shi Y: Molecular mechanisms of caspase regulation during apoptosis. Nat Rev Mol Cell Biol 2004, 5:897-907.
45. Hengartner MO: The biochemistry of apoptosis. Nature 2000, 407:770-776.
46. Solares AM, Santana A, Baladron I, Valenzuela C, Gonzalez CA, Diaz A, Castillo D, Ramos T, Gomez R, Alonso DF, Herrera L, Sigman H, Perea SE, Acevedo BE, Lopez-Saura P: Safety and preliminary efficacy data of a novel casein kinase 2 (CK2) peptide inhibitor administered intralesionally at four dose levels in patients with cervical malignancies. BMC Cancer 2009, 9:146.
47. Rudd CE, Trevillyan JM, Dasgupta JD, Wong LL, Schlossman SF: The CD4 receptor is complexed in detergent lysates to a protein-tyrosine kinase (pp58) from human T lymphocytes. Proc Natl Acad Sci U S A 1988, 85:5190-5194.
48. Irby RB, Mao W, Coppola D, Kang J, Loubeau JM, Trudeau W, Karl R, Fujita DJ, Jove R, Yeatman TJ: Activating SRC mutation in a subset of advanced human colon cancers. Nat Genet 1999, 21:187-190.
49. Cheng H, Dodge J, Mehl E, Liu S, Poulin N, van de RM, Nielsen TO: Validation of immature adipogenic status and identification of prognostic biomarkers in myxoid liposarcoma using tissue microarrays. Hum Pathol 2009, 40:1244-1251.
50. Kopetz S, Lesslie DP, Dallas NA, Park SI, Johnson M, Parikh NU, Kim MP, Abbruzzese JL, Ellis LM, Chandra J, Gallick GE: Synergistic activity of the SRC family kinase inhibitor dasatinib and oxaliplatin in colon carcinoma cells is mediated by oxidative stress. Cancer Res 2009, 69:3842-3849.
51. Du J, Bernasconi P, Clauser KR, Mani DR, Finn SP, Beroukhim R, Burns M, Julian B, Peng XP, Hieronymus H, Maglathlin RL, Lewis TA, Liau LM, NghiemphuP, Mellinghoff IK, Louis DN, Loda M, Carr SA, Kung AL, Golub TR: Beadbased profiling of tyrosine kinase phosphorylation identifies SRC as a potential target for glioblastoma therapy. Nat Biotechnol 2009, 27:77-83.
52. Chou TC: Theoretical basis, experimental design, and computerized simulation of synergism and antagonism in drug combination studies. Pharmacol Rev 2006, 58:621-681.

53. Thelin-Jarnum S, Lassen C, Panagopoulos I, Mandahl N, Aman P: Identification of genes differentially expressed in TLS-CHOP carrying myxoid liposarcomas. Int J Cancer 1999, 83:30-33.
54. Aman P, Ron D, Mandahl N, Fioretos T, Heim S, Arheden K, Willen H, Rydholm A, Mitelman F: Rearrangement of the transcription factor gene CHOP in myxoid liposarcomas with t(12;16)(q13;p11). Genes Chromosomes Cancer 1992, 5:278-285.
55. Willems SM, Debiec-Rychter M, Szuhai K, Hogendoorn PCW, Sciot R: Local recurrence of myxofibrosarcoma is associated with increase in tumour grade and cytogenetic aberrations, suggesting a multistep tumour progression model. Mod Pathol 2006, 19:407-416.
56. Willems SM, Mohseny AB, Balog C, Sewrajsing R, Briaire-de Bruijn IH, Knijnenburg J, Cleton-Jansen AM, Sciot R, Fletcher CDM, Deelder AM, Szuhai K, Hensbergen PJ, Hogendoorn PCW: Cellular/intramuscular myxoma and grade I myxofibrosarcoma are characterized by distinct genetic alterations and specific composition of their extracellular matrix. J Cell Mol Med 2009, 13:1291-1301.
57. Szuhai K, Tanke HJ: COBRA: combined binary ratio labeling of nucleic-acid probes for multi-color fluorescence in situ hybridization karyotyping. Nat Protoc 2006, 1:264-275.
58. Willems SM, Schrage YM, Baelde JJ, Briaire-de Bruijn I, Mohseny A, Sciot R, Bovee JVMG, Hogendoorn PCW: Myxoid tumours of soft tissue: the socalled myxoid extracellular matrix is heterogeneous in composition. Histopathology 2008, 52:465-474.
59. Tuynman JB, Vermeulen L, Boon EM, Kemper K, Zwinderman AH, Peppelenbosch MP, Richel DJ: Cyclooxygenase-2 inhibition inhibits c-Met kinase activity and Wnt activity in colon cancer. Cancer Res 2008, 68:1213-1220.

# Chapter 8

## Summary and future perspectives

## Summary and future perspectives

### *8.1 Molecular genetics and cytogenetics to classify myxoid tumours of soft tissue*

An increasing number of (cyto-) genetic aberrations have been identified in (myxoid) soft tissue tumours during the last decade. This gives a. insight in their underlying biology, b. often provides tools for differential diagnosis, prediction of clinical outcome and potential clues for more targeted therapy (1-3). Chapter 2 gives an overview of the myxoid tumours of soft tissue recognized and their characteristic molecular/cytogenetic aberrations. Roughly, sarcomas can be divided in two major groups: (a) sarcomas with relatively "simple" karyotypes showing specific genetic alterations, such as balanced translocations in about 15% in general, and reaching up till 95% of myxoid liposarcoma with t(12;16) leading to the formation of the FUS/DDIT3 fusion gene or point mutations in a single gene like KIT/PDGFR in GIST (4) and (b) sarcomas with non-specific gene alterations and very complex karyotypes with structural and numerical aberrations, e.g. myxofibrosarcoma (5). Cytogenetic data on myxofibrosarcoma were scarce until now with only isolated cases described in the literature. In chapter 3 we describe a large serie of karyotyped myxofibrosarcoma showing that upon recurrence, there is an increase in tumour-grade (5); as well as, upon increase in grade, myxofibrosarcomas show an increase in non-tumourtype-specific cytogenetic aberrations. Our data suggests that myxofibrosarcoma arises and progresses by genetic instability via a multistep tumour progression model, which is estimated to be the case in about 50% of soft tissue sarcomas (6). The differential diagnosis of myxoid tumours of soft tissue can be difficult especially in biopsies and when presenting as an intramuscular tumour. An example of this is the differential diagnosis between low-grade myxofibrosarcoma and intramuscular myxoma (especially its cellular variant, a.k.a. cellular myxoma) (7, 8). In chapter 5 we show that karyotyping can be helpful to distinguish both entities as intramuscular myxoma (including cellular myxoma) often show no cytogenetic aberrations, whereas low-grade myxofibrosarcoma does (9). However, (molecular) karyotyping is a technique which is not routinely available in most pathology labs, is laborious and has a limited success rate. Therefore, we investigated the potential role of direct mutational analysis of GNAS1 activating mutations which is a more accessible technique and more easily to incorporate in pathology laboratory practice. GNAS1 activating mutations (codon 201 and 227) have previously been described in fibrous dysplasia, a benign bone tumour that can be associated with intramuscular myxoma in the Mazabraud-, and McCune-Albright syndromes (10). Scarse cases of intramuscular myxoma in both syndromatic as well as non-syndromatic context showed activating mutations in GNAS1 (11). We confirmed the presence of these mutations in 50% of intramuscular myxoma cases, in a larger series including its cellular variant, which has been confirmed in a similar study (12). We could not detect these mutations in low-

grade myxofibrosarcoma. GNAS1 codon 201/227 mutation analysis is thus a helpful and specific (though not very sensitive) method to distinguish intramuscular myxoma from low-grade myxofibrosarcoma. Activating mutations in GNAS1 lead to consecutive activation of cAMP, increased expression of c-Fos and subsequent transcription of genes involved in cell cycle regulation (13). We confirmed high expression of c-Fos on both the protein and the mRNA level in intramuscular myxoma as well as in low-grade myxofibrosarcoma. Thus immunohistochemistry for c-Fos is not a discriminatory diagnostical adjunct to differentiate between both entities. KRAS codon 12/13 and TP53 mutations were previously shown to be involved in sarcomatogenesis (14). We could not detect mutations in these genes in low-grade myxofibrosarcoma, nor in intramuscular myxoma.

Interestingly, previous immunohistochemical studies showed p53 overexpression in myxofibrosarcoma upon increase in grade, suggesting that TP53 mutations are a relatively late event in the tumourigenesis of myxofibrosarcoma (15). Because of its role in guarding cell cycle regulation, TP53 mutations probably contribute to genomic instability in myxofibrosarcoma, reflected in the increase in non-specific cytogenetic aberrations in higher grades (grade 2 and 3) whereas low-grade (grade 1) myxofibrosarcoma usually has a normal karyotype or only slight cytogenetic aberrations (5).

*8.2 Constitution of myxoid extracellular matrix depends on type and grade of tumours*

Myxoid tumours of soft tissue are, per definition, characterized by their myxoid ("jelly") extracellular matrix. In chapter 2, we describe how the concept of "myxoid" evolved over the years and still its exact constitution has not been elucidated, 150 years after Virchow introduced the term "myxoid" (16). In this chapter we give an overview of the literature of the high- and low-abundant constituents which have been reported to be present in the myxoid extracellular matrix in both reactive lesions and in tumours (17). We discuss their potential role and conclude that myxoid changes are not tumour specific at all since they can be found in tumours of both mesenchymal and epithelial origin (both benign as well as malignant). In chapter 4 we showed that next to glycosaminoglycans, serum proteins (IgGs and albumin) are major components of the myxoid extracellular matrix. With classical Alcian Blue staining using the CEC (critical electrolyte concentration) method, we demonstrated that the relative amount of these glycosaminoglycans in the myxoid extracellular matrix depends on histological type and grade of the tumour and how this might relate to their different clinical behavior (18). In chapter 5 we studied the myxoid extracellular matrix by liquid chromatography mass spectrometry, a more sophisticated technique not applied before in these tumours. We confirmed the abundant presence of serum proteins and collagens in the myxoid

extracellular matrix. Above that, we showed that low-grade myxofibrosarcoma contains certain small leucine rich proteins, such as biglycan, decorin, lumican, which we could not detect in intramuscular myxoma (9). We confirmed that decorin, collagen I, VI, XII and XIV were significantly overexpressed in low-grade myxofibrosarcoma (both on the protein and at the mRNA level) compared to intramuscular myxoma. Based on these results we argue that immunohistochemistry for decorin might be a helpful tool in the differential diagnosis between these two entities. Our findings are also interesting from a conceptional point of view, on one hand showing that the myxoid extracellular matrix is characterized by the presence of certain molecules and peptides (such as serum proteins, glycosaminoglycans, collagens etc.). On the other hand, the myxoid extracellular matrix (such as in intramuscular myxoma) is characterized by low expression of decorin and collagens which are important for the well-structured formation of the extracellular matrix (19). This paucity of structural proteins/molecules suggests that a myxoid histology reflects a merely improper organization of the extracellular matrix. In chapter 6 we show that direct profiling of tissue slides by imaging mass spectrometry, is an elegant and robust method to classify myxoid tumours of soft tissue (myxofibrosarcoma and myxoid liposarcoma) according to tumour-type and tumour-grade. Low-grade myxofibrosarcoma is characterized by a multinodular growth pattern on both the macroscopical and microscopical level. Using imaging mass spectrometry, we demonstrate that these histologically identical nodules express different peptides/proteins and thus display intratumour heterogeneity on the biochemical level. We hypothesize that this might be the reflection of clonal selection upon tumour progression in myxofibrosarcoma. With the same technique, we demonstrate that myxoid liposarcoma shows a transition in lipid profiles with decreased fatty acid content upon increase in grade, whereas phosphocholines were predominantly detected in the higher grades. Interestingly, these findings were reported in a different independent group of myxoid liposarcoma by ex vivo NMR spectroscopy (20-22). We speculate that these differences reflect the genetic changes occurring upon tumour progression especially in relation to the role of peroxisome proliferator-activated receptor γ (PPARγ), a key player in adipocytic differentiation. Hereby we illustrate how imaging mass spectrometry can form a bridge between the molecular genetics and the morphological features characteristic of myxoid liposarcoma.

*8.3 New therapeutic strategies for myxoid liposarcoma patients with advanced disease*

In chapter 5 we describe that activating mutations in exon 201 and 227 of the GNAS1 gene were present in intramuscular myxoma but not in low-grade myxofibrosarcoma. These mutations subsequently lead to consecutive activation of c-AMP and downstream transcription of c-Fos. From a theoretical point of view, targeting this pathway would be an option for targeted therapy, as these upstream activating mutations are highly

specific (despite its low sensitivity of 50%). However, intramuscular myxoma is a benign tumour and curative surgery suffices with no need for (neo) adjuvant therapy (23). In contrast to intramuscular myxoma, myxoid liposarcoma is a malignant soft tissue tumour metastasizing in about 30-80% of cases (24). In this respect, identification of new targets in treatment of liposarcomas makes especially sense because therapeutic options for patients with advanced/inoperable disease are rather limited. Chemotherapeutical options are restricted to ifosfamide and anthracyclins, which have only response rates of 20-40% although trabectidin (ET-743, Yondelis®) has recently shown activity in phase I and II trials and retrospective series (25-28). In chapter 6 we illustrate by imaging mass spectrometry that upon increase in grade, myxoid liposarcomas shows a decrease in the content of fatty acids, which is probably the effect of deceased signaling of PPARγ. Active signaling of the transcriptional activator PPARγ does not only play a key role in adipogenesis but also leads to cell cycle arrest (29, 30). In this perspective, PPARγ signaling might offer a promising target in the treatment of (myxoid) liposarcoma although activation of this pathway by PPARγ agonists (rosiglitazone) in patients with advanced disease was not conclusive (31, 32).

During the last decade, with the unraveling of (aberrant) cell signaling pathways in many cancers, small molecule targeting has been shown to be a promising therapeutic approach (33). This more "rationale" based targeting of cancer cells by (more or less) specifically inhibiting pathways involved in tumourigenesis has been shown to be effective, such as in translocation driven sarcomas and hematological malignancies as well tumours driven by activating mutations, such as in lung cancer and GIST (34). In chapter 7, we showed by in vitro kinome profiling and pathway analysis that Src and NF-kB pathway are active in myxoid liposarcoma cells. We were able to block these pathways by their respective inhibitors dasatinib® and 4,5,6,7-tetrabromobenzotriazole. This led in the case of 4,5,6,7-tetrabromobenzotriazole to a significant decrease in cell growth probably by induction of apoptosis. Interestingly, administration of both drugs had an addidative effect. Our results open perspectives to the development of new therapeutic strategies in the treatment of metastatic, or irresectable myxoid liposarcomas. For myxofibrosarcoma, no direct clues for targeted therapy were obtained, mainly hampered by the lack of myxofibrosarcoma cell lines for performing functional experiments.

*8.4 Future view*

The results as described in this thesis have provided a more profound understanding of the biology of myxoid tumours of soft tissue. With a wide array of techniques ranging from classical Alcian Blue to kinome analysis and imaging and liquid chromatography mass spectrometry of tissue samples, we analyzed myxoid tumours of soft tissue in

more depth. We showed that the myxoid extracellular matrix differs in composition according to tumour-type and tumour-grade, and how these differences might affect the biology/development of various myxoid tumours of soft tissue. We showed that for the study of the proteome of these tumours, mass spectrometry contributes to a more profound knowledge of high-and low abundant constituents of the myxoid extracellular matrix. An advantage of mass spectrometry is the simultaneous analysis of numerous proteins at the same time without a priori knowledge of these proteins (35). Imaging mass spectrometry adds spatial information of the identified molecules, which is especially interesting as the importance of spatial (next to temporal) protein expression is essential in many (inter) cellular processes both in physiological and pathological conditions (such as cancer) (35). Imaging mass spectrometry allows direct mass spectrometric analysis of tissue sections, which makes trypsinization -essential for subsequent tandem MS/MS experiments- rather challenging and hampers direct identification of m/z values of interest. Future challenge is to overcome this problem, as well as increasing the spatial resolution (yet up to 50 micrometer) to the level of the individual cell, without losing the quality of the spectra. The possibility to use not only frozen tissue samples but also (molecular cross-linked) formalin fixed paraffin embedded tissue would substantially expand its application and possibility. Another future challenge will be the analysis and integration of the huge amounts of datasets generated by (imaging) mass spectrometry. Especially in this respect, the field of mass spectrometry can learn a lot from the hurdles which had to be (and have been taken) in the field of genomics. Reserving substantial time, money and effort for data analysis in any mass spectrometry experiment is crucial and should be well considered beforehand.

Aberrant cell signaling has been shown to play a pivotal role in many cancers (33, 36). As cell signaling is predominantly regulated at the posttranslational level (thus at the level of the protein), proteomic analysis is not only complementary but even crucial for proper understanding the biology of cancer (37). Understanding the exact molecular pathways activated in intramuscular myxoma offer specific targets for molecular diagnostics. This has resulted in the incorporation of direct GNAS1 mutation analysis in the molecular diagnostic amendatory section of the department of pathology. So albeit without implications for targeted therapy with small inhibitory molecules, correct (molecular) classification by GNAS1 mutation analysis has a direct clinical application as it is helpful in differentiating intramuscular myxoma from low-grade myxofibrosarcoma (and thus whether free resection margins are required). In myxofibrosarcoma we could not detect any tumour specific karyotypic aberrations which might however be unrevealed by more detailed genomic screens in the future. Functional studies to validate potential molecular targets in myxofibrosarcoma are hampered by the lack of myxofibrosarcoma cell lines which are available for many other sarcomas. By such experiments, such as in vitro kinome analysis, we were able

to identify new treatment options for myxoid liposarcoma patients with advanced disease. This is especially relevant as conventional chemotherapeutic options in these patients are rather limited. Pathway analysis uncovers the mechanisms behind tumour biology and may offer potential treatment targets. In vitro blocking of kinases can also be achieved excellently, and sometimes more specifically with RNA interference. Given the way that kinase-inhibitors and RNAi have transformed basic research and the unprecedented speed with which they have reached the clinic, the near future promises to be exciting (38).

**References**


1. Osuna D, de Alava E: Molecular pathology of sarcomas. Rev Recent Clin Trials 4:12-26, 2009
2. de Alava E: Molecular pathology in sarcomas. Clin Transl Oncol 9:130-144, 2007
3. Chibon F, Lagarde P, Salas S, et al.: Validated prediction of clinical outcome in sarcomas and multiple types of cancer on the basis of a gene expression signature related to genome complexity. Nat Med 16:781-787, 2010
4. Aman P, Ron D, Mandahl N, et al.: Rearrangement of the transcription factor gene CHOP in myxoid liposarcomas with t(12;16)(q13;p11). Genes Chromosomes Cancer 5:278-285, 1992
5. Willems SM, Debiec-Rychter M, Szuhai K, et al.: Local recurrence of myxofibrosarcoma is associated with increase in tumour grade and cytogenetic aberrations, suggesting a multistep tumour progression model. Mod Pathol 19:407-416, 2006
6. Bovee JVMG, Hogendoorn PCW: Molecular pathology of sarcomas: concepts and clinical implications. Virchows Arch 456:193-199, 2010
7. Graadt van Roggen JF, Hogendoorn PCW, Fletcher CDM: Myxoid tumours of soft tissue. Histopathology 35:291-312, 1999
8. Graadt van Roggen JF, McMenamin ME, Fletcher CDM: Cellular myxoma of soft tissue: a clinicopathological study of 38 cases confirming indolent clinical behaviour. Histopathology 39:287-297, 2001
9. Willems SM, Mohseny AB, Balog C, et al.: Cellular/intramuscular myxoma and grade I myxofibrosarcoma are characterized by distinct genetic alterations and specific composition of their extracellular matrix. J Cell Mol Med 13:1291-1301, 2009
10. Weinstein LS, Liu J, Sakamoto A, et al.: Minireview: GNAS: normal and abnormal functions. Endocrinology 145:5459-5464, 2004
11. Okamoto S, Hisaoka M, Ushijima M, et al.: Activating Gs(alpha) mutation in intramuscular myxomas with and without fibrous dysplasia of bone. Virchows Arch 437:133-137, 2000
12. Delaney D, Diss TC, Presneau N, et al.: GNAS1 mutations occur more commonly than previously thought in intramuscular myxoma. Mod Pathol 22:718-724, 2009
13. Candeliere GA, Glorieux FH, Prud'homme J, et al.: Increased expression of the c-fos proto-oncogene in bone from patients with fibrous dysplasia. N Engl J Med 332:1546-1551, 1995
14. Kirsch DG, Dinulescu DM, Miller JB, et al.: A spatially and temporally restricted mouse model of soft tissue sarcoma. Nat Med 13:992-997, 2007
15. Oda Y, Takahira T, Kawaguchi K, et al.: Altered expression of cell cycle regulators in myxofibrosarcoma, with special emphasis on their prognostic implications. Hum Pathol 34:1035-1042, 2003
16. Virchow RLK: in Hirschwald (ed): Die cellularpathologie in ihrer Begrundung auf physiologische und patholo gische Gewebelehre. Berlin, 1858, pp 625-626
17. Willems SM, Wiweger M, Graadt van Roggen JF, et al.: Running GAGs: myxoid matrix in tumor pathology revisited : What's in it for the pathologist? Virchows Arch 456:181-192, 2010
18. Willems SM, Schrage YM, Baelde JJ, et al.: Myxoid tumours of soft tissue: the so-called myxoid extracellular matrix is heterogeneous in composition. Histopathology 52:465-474, 2008
19. Orgel JP, Eid A, Antipova O, et al.: Decorin core protein (decoron) shape complements collagen fibril surface structure and mediates its binding. PLoS One 4:e7028, 2009
20. Singer S, Millis K, Souza K, et al.: Correlation of lipid content and composition with liposarcoma histology and grade. Ann Surg Oncol 4:557-563, 1997
21. Millis K, Weybright P, Campbell N, et al.: Classification of human liposarcoma and lipoma using ex vivo proton NMR spectroscopy. Magn Reson Med 41:257-267, 1999

22. Chen JH, Enloe BM, Weybright P, et al.: Biochemical correlates of thiazolidinedione-induced adipocyte differentiation by high-resolution magic angle spinning NMR spectroscopy. Magn Reson Med 48:602-610, 2002
23. Hogendoorn PCW, Collin F, Daugaard S, et al.: Changing concepts in the pathological basis of soft tissue and bone sarcoma treatment. Eur J Cancer 40:1644-1654, 2004
24. Antonescu C, Ladanyi M: Myxoid liposarcoma, in Fletcher C.D.M., Unni KK, Mertens F (eds): World Health Organization classification of tumours. pathology and genetics. Tumours of soft tissue and bone. Lyon, IARC press, 2004, pp 40-43
25. Demetri GD, Chawla SP, von Mehren M, et al.: Efficacy and safety of trabectedin in patients with advanced or metastatic liposarcoma or leiomyosarcoma after failure of prior anthracyclines and ifosfamide: results of a randomized phase II study of two different schedules. J Clin Oncol 27:4188-4196, 2009
26. Grosso F, Jones RL, Demetri GD, et al.: Efficacy of trabectedin (ecteinascidin-743) in advanced pretreated myxoid liposarcomas: a retrospective study. Lancet Oncol 8:595-602, 2007
27. Grosso F, Sanfilippo R, Virdis E, et al.: Trabectedin in myxoid liposarcomas (MLS): a long-term analysis of a single-institution series. Ann Oncol 20:1439-1444, 2009
28. Dalal KM, Antonescu CR, Singer S: Diagnosis and management of lipomatous tumors. J Surg Oncol 97:298-313, 2008
29. Grommes C, Landreth GE, Heneka MT: Antineoplastic effects of peroxisome proliferator-activated receptor gamma agonists. Lancet Oncol 5:419-429, 2004
30. Tontonoz P, Spiegelman BM: Fat and beyond: the diverse biology of PPARgamma. Annu Rev Biochem 77:289-312, 2008
31. Debrock G, Vanhentenrijk V, Sciot R, et al.: A phase II trial with rosiglitazone in liposarcoma patients. Br J Cancer 89:1409-1412, 2003
32. Demetri GD, Fletcher CDM, Mueller E, et al.: Induction of solid tumor differentiation by the peroxisome proliferator-activated receptor-gamma ligand troglitazone in patients with liposarcoma. Proc Natl Acad Sci U S A 96:3951-3956, 1999
33. Tuveson DA, Fletcher JA: Signal transduction pathways in sarcoma as targets for therapeutic intervention. Curr Opin Oncol 13:249-255, 2001
34. Mitelman F, Johansson B, Mertens F: The impact of translocations and gene fusions on cancer causation. Nat Rev Cancer 7:233-245, 2007
35. McDonnell LA, Corthals GL, Willems SM, et al.: Peptide and protein imaging mass spectrometry in cancer research. J Proteomics, 222(4):400-9, 2010
36. Krause DS, Van Etten RA: Tyrosine kinases as targets for cancer therapy. N Engl J Med 353:172-187, 2005
37. Sebolt-Leopold JS, English JM: Mechanisms of drug inhibition of signalling molecules. Nature 441:457-462, 2006
38. Castanotto D, Rossi JJ: The promises and pitfalls of RNA-interference-based therapeutics. Nature 457:426-433, 2009

# Chapter 9

## Nederlandse Samenvatting

## Nederlandse samenvatting

### 9.1 Moleculaire genetica en cytogenetica ter classificatie van myxoide wekedelen tumoren

De laatste jaren is een toenemend aantal (cyto-) genetische afwijkingen geïdentificeerd in (myxoide) wekedelen tumoren. Deze geven a. inzicht in hun onderliggende biologie, en b. bieden handvatten voor differentiaaldiagnostiek, voorspelling van klinische prognose en mogelijke aanknopingspunten voor gerichtere ("targeted") therapie (1-3). Hoofdstuk 2 geeft een overzicht van de tot nu toe bekende myxoide wekedelen tumoren met hun karakteristieke moleculaire/cytogenetische afwijkingen. Ruwweg kunnen sarcomen worden in twee grote groepen ingedeeld: (a) sarcomen met relatief "eenvoudige" karyotypes met veelal specifieke genetische afwijkingen zoals gebalanceerde translocaties in 15 % van de gevallen in het algemeen, en oplopend tot 95% (zoals t(12;16) in het myxoid liposarcoom, resulterend in de vorming van het FUS/DDIT3 fusie gen, of punt mutaties in één enkel gen zoals KIT/PDGFR in GIST (4) en (b) sarcomen met niet specifieke genetische veranderingen en erg ingewikkelde karyotypes met structurele en numerieke afwijkingen, zoals bijvoorbeeld in het myxofibrosarcoom (5). Cytogenetische gegevens over het myxofibrosarcoom zijn tot op heden zeldzaam met slechts enkele geïsoleerde gevallen beschreven in de litteratuur. In hoofdstuk 3 beschrijven we een grote serie gekaryotypeerde myxofibrosarcomen en laten zien dat er bij het lokaal recidief van deze tumor een toename is van graad van de tumor (5). Tevens toont het myxofibrosarcoom bij toename in graad een toename van cytogenetische afwijkingen die overigens niet specifiek zijn voor de tumor. Onze gegevens suggereren dus dat het myxofibrosarcoom ontstaat en zich verder ontwikkelt via genetische instabiliteit volgens een meerstaps-tumorprogresssiemodel, wat het geval is in ongeveer 50% van de wekedelen tumoren (6). De differentiaaldiagnostiek van myxoide wekedelen tumoren kan moeilijk zijn, m.n. op biopsien en als de tumor zich intramusculair presenteert. Een voorbeeld hiervan is de differentaaldiagnose tussen het laaggradig myxofibrosarcoom en het intramusculair myxoom (m.n. de celrijke variant, ookwel celrijk myxoom genaamd) (7, 8). In hoofdstuk 5 laten we zien dat karyotypering behulpzaam kan zijn in het onderscheiden van beide entiteiten gezien het intramusculair myxoom (inclusief het celrijk myxoom) vaak geen cytogenetische afwijkingen heeft, in tegenstelling tot het laaggradig myxofibrosarcoom (9). Echter, (moleculaire) karyotypering is een techniek die niet routinematig beschikbaar is in de meeste pathologielaboratoria, arbeidsintensief is en slechts een beperkte mate van succes kent. Daarom onderzochten we de mogelijke rol van directe mutatie-analyse van GNAS1 activerende mutaties, wat een veel toegankelijker methode is en bovendien makkelijker te incorporeren binnen de dagelijkse pathologiepraktijk. GNAS1 activerende mutaties (codon 201 and 227) zijn reeds eerder beschreven in fibreuze dysplasie, een goedaardige bottumor die geassocieerd kan zijn met het intramusculair myxoom in

het kader van het syndroom van Mazabraud of McCune-Albright (10). GNAS1 activerende mutaties werden eerder beschreven in een kleine serie gevallen van intramusculair myxoom zowel syndromatisch als niet-syndromatisch (11). Wij hebben in 50% van gevallen van intramusculair myxoom de aanwezigheid van deze mutaties bevestigd, in een grotere serie en inclusief de celrijke variant, wat ook bevestigd werd door een andere studie (12). We konden deze mutaties niet detecteren in het laaggradig myxofibrosarcoom. Mutatieanalyse van GNAS1 codon 201/227 is dus een behulpzame en specifieke (hoewel niet erg sensitieve) methode om het intramusculair myxoom van het laaggradig myxofibrosarcoom te onderscheiden.

Activerende mutaties in GNAS1 leiden tot activatie van cAMP, toegenomen expressie van c-Fos en zetten vervolgens aan tot transcriptie van genen die betrokken zijn in de regulatie van de celcyclus (13). We toonden de verhoogde expressie van c-Fos aan zowel op eiwit als mRNA niveau in het intramusculair myxoom alsook in het laaggradig myxofibrosarcoom. Immuunhistochemische kleuring voor c-Fos bleek dus niet een diagnostisch hulpmiddel om deze beide entiteiten beter te onderscheiden. Van KRAS codon 12/13 en TP53 mutaties is aangetoond dat ze een rol spelen in sarcomatogenese (14). Wij konden zowel in het laaggradig myxofibrosarcoom als in het intramusculair myxoom geen mutaties in deze genen aantonen Interessant genoeg hebben eerdere immuunhistcohemische studies aangetoond dat het myxofibrosaroom overexpressie toont van p53 en wel in toenemende mate in hogere graad van de tumor, wat suggereert dat mutaties in TP53 een relatieve late stap zijn in de tumorgenese van het myxofibrosarcoom (15). Gezien de rol van p53 in het bewaken van de regulatie van de celcyclus, dragen deze mutaties waarschijnlijk bij aan de genomische instabiliteit in het myxofibrosarcoom, wat tot uiting komt in de toename van aspecifieke cytogenetische afwijkingen in de hogere tumorgraden (graad 2 en 3) terwijl het laaggradig myxofibrosarcoom (graad 1) meestal een normaal karyotype heeft of slechts geringe afwijkingen hierin toont (5).

### 9.2 Samenstelling van de myxoide extracellulaire matrix is afhankelijk van het type en de graad van de tumor

Myxoïde wekedelen tumoren worden, per definitie, gekenmerkt door hun myxoide ("slijmerige") extracellulaire matrix. In hoofdstuk 2 beschrijven we hoe het concept "myxoid" vorm gekregen heeft door de jaren heen, en dat de precieze samenstelling van de myxoide extracellulaire matrix nog steeds niet is opgehelderd, zelfs niet 150 jaar nadat Virchow de term "myxoid" introduceerde (16). In dit hoofdstuk geven we een overzicht van de litteratuur van de veel- en weinigvoorkomende bestanddelen waarvan gerapporteerd is dat ze aanwezig zijn in de myxoide extracellulaire matrix van zowel reactieve laesies als tumoren(17). We bediscussiëren hun mogelijke rol en concluderen dat myxoide veranderdingen helemaal niet tumorspecifiek zijn en kunnen voorkomen in tumoren

van zowel epitheliale als mesenchymale oorsprong (goedaardig en kwaadaardig). In hoofdstuk 4 laten we zien dat naast glycosaminoglycanen, serum eiwitten (IgGs en albumine) de belangrijkste componenten zijn in de myxoide extracellulaire matrix. Met behulp van klassieke Alcian Blue kleuringen volgens de CEC methode (CEC = "critical electrolyte concentration"), hebben we aangetoond dat de relatieve hoeveelheid van deze glycosaminoglycanene in de myxoide extracellulaire matrix afhangt van het histoloische type en de graad van de tumor en hoe dit gerelateerd zou kunnen worden aan het verschillend klinisch gedrag van deze tumoren (18). In hoofdstuk 5 hebben we de myxoide extracellulaire matrix met behulp van LC-MS (LC-MS = "liquid chromatography mass spectrometry") bestudeerd, wat een meer gesofisticeerde techniek is en die nog niet eerder in deze tumoren werd toegepast. We bevestigden de veel voorkomendheid van serumeiwitten en collagenen in de myxoide extracellulaire matrix. Daarenboven toonden we aan dat de extracellulaire matrix van het laaggradig myxofibrosarcoom bepaalde SLRPs (SLRP = "small leucine rich proteins") bevat zoals biglycan, decorine, lumican, die we niet konden aantonen in het intramuscular myxoom (9). We verifieerden dat decorine en collageen I, VI, XII en XIV significant tot overexpressie kwamen in het laaggradig myxofibrosarcoom (zowel op eiwit niveau als op RNA niveau) in vergelijking met het intramusculair myxoom. Op basis van deze resultaten stellen wij dat immuunhistochemie voor decorine behulpzaam kan zijn in de differentaaldiganotiek van deze twee entiteiten. Onze bevindingen zijn daarnaast ook interessant vanuit conceptioneel oogpunt, waarbij we aan de ene kant laten zien dat de myxoide extracellulaire matrix gekenmerkt wordt door de aanwezigheid van bepaalde moleculen (zoals serumeiwitten, glycosaminoglycanen, collagenen, etc.). Aan de andere kant, wordt de myxoide extracellulaire matrix (zoals in het intramusculair myxoom) gekenmerkt door een lage expressie van decorine en collagenen die belangrijk zijn voor een goede structurele opbouw van de extracellulaire matrix (19). Deze spaarzaamheid van structurele eiwitten/moleculen doet vermoeden dat de myxoide extracellulaire matrix in essentie de afspiegeling is van een onvoldoende en slecht georganiseerde extracellulaire matrix. In hoofdstuk 6 laten we zien direct profilen van weefselcoupes met behulp van imaging massa spectrometrie een elegante en robuuste methode is om myxoide wekedelen tumoren (zoals het myxofibrosaroom en het myxoid liposarcoom) te classificeren naar type en graad van de tumor. Het laaggradig myxofibrosarcoom wordt zowel macroscopisch als microscopisch gekenmerkt door een multinodulair groeipatroon. Met behulp van imaging massa spectrometrie hebben we aangetoond dat deze histologisch identieke nodulen verschillende eiwitten tot expressie brengen en dus intratumoraal heterogeniteit tonen op biochemisch niveau. Onze hypothese is dat dit de weerspiegeling is van klonale selectie gedurende tumorprogressie in het myxofibrosarcoom. Met dezelfde techniek hebben we laten zien dat het myxoid liposarcooom een verandering in lipideprofiel met minder vetzuren naarmate de graad van de tumor toeneemt, terwijl phosphocholines domineren in de hogere graden. Interessant is daarbij dat dezelfde bevindingen gerapporteerd werden in een andere, onaf-

hankelijke groep myxoid liposarcomen met behulp van ex vivo NMR spectroscopie (20-22). We speculeren dat deze verschillen een weerspiegeling zijn van de genetische veranderingen die optreden tijdens tumorprogressie, met name in relatie tot de rol van PPARγ (PPARγ = " peroxisome proliferator-activated receptor γ''), dat een belangrijke rol speelt in de vetceldifferentiatie. Hiermee hebben we laten zien hoe imaging mass spectrometrie een brug kan slaan tussen moleculaire genetica en de morfologische eigenschappen van het myxoid liposarcoom.

### 9.3 Niewe therapeutische strategieën voor de behandeling van patiënten met myxoid liposarcoom in een gevorderd stadium

In hoofdstuk 5 beschrijven we dat actieverende mutaties in exon 201 and 227 van het GNAS1 gen aanwezig zijn in het intramusculaire myxoom, maar niet in het laaggradig myxofibrosarcoom. Deze mutaties leiden vervolgens tot de activatie van cAMP en hierna tot transcriptie van c-Fos. Vanuit theoretisch oogpunt zou het ingrijpen op deze signaleringsroute een behandelingsoptie kunnen zijn, omdat deze activerende mutatie zeer specifiek zijn (ondanks de lage sensitiviteit van 50%). Het intramusculair myxoom is echter een goedaardige tumor waarbij curatieve chirurgie volstaat, en er geen noodzaak bestaat voor (neo) adjuvante therapie (23). In tegenstelling tot het intramusculaire myxoom, is het myxoid liposarcoom wel een kwaadaardige tumor die metastaseert in ongeveer 30-80% van de gevallen (24). In dit opzicht is het vinden van nieuwe moleculaire aangrijpingspunten voor behandeling voor het myxoid liposarcoom wel relevant, zeker gezien de behandelingsmogelijkheden voor patiënten met vergevorderde/ gemetastaseerde ziekte beperkt zijn. Chemotherapeutische mogelijkheden zijn hierbij beperkt tot ifosfamide and anthracyclines, met respectievelijke "response rates" van 20-40% hoewel er hoop gloort aan de horizon sinds de introductie van trabectidin (ET-743, Yondelis®) dat veelbelovend bleek in fase I en fase II studies en retrospectieve series en vooral bij het myxoid liposarcoom (25-28). In hoofdstuk 6 laten we door middel van imaging massa spectrometrie zien dat er in het myxoid liposarcoom, bij toename in graad, een afname is van de inhoud van vetzuren, wat meest waarschijnlijk het effect is van verminderde celsignalering van PPARγ. Actieve celsignalering van de transcriptie-activator PPARγ speelt niet alleen een belangrijke rol in de vetceldifferentiatie, maar leidt ook tot stilzetting van de celcyclus (29, 30). In dit opzicht zou de celsignaleringsroute van PPARγ een veelbelovend aangrijpingspunt kunnen zijn in de behandeling van het (myxoid) liposarcoom hoewel activering van deze signaleringsroute door middel van PPARγ agonisten (rosiglitazone) in patiënten met vergevorderde ziekte niet conclusief bleek (31, 32).

Bij het ontrafelen van de (afwijkende) celsignaleringsroutes in talrijke kankers gedurende de laatste jaren, is gebleken dat doelgerichte behandeling met kleinmoleuclaire kinase remmers ("small molecule targeting") een veelbelovende behandelings-

mogelijkheid is (33). Deze rationelere wijze om kanker cellen aan te pakken door het (min of meer) specifiek remmen van celsignaleringsroutes betrokken in tumorgenese, is een erg effectieve methode gebleken bij de behandeling van bv. sarcomen en hematologische maligniteiten die gedreven worden door translocaties, alsook in de behandeling van longkanker en GIST (34). In hoofdstuk 7 hebben we laten zien dat met behulp van het in vitro profilen van het kinoom en analyseren van celsignaleringsroutes, de Src en NF-kB signaleringsroutes geactiveerd zijn het myxoid liposarcoom. We waren in staat deze celsignaleringsroutes te blokkeren met hun respectievelijke inhibitoren dasatinib® and 4,5,6,7-tetrabromobenzotriazole. Dit leidde in het geval van 4,5,6,7-tetrabromobenzotriazole tot een significante daling van celgroei waarschijnlijk door de inductie van apoptose. Interessant was dat toevoeging van beide inhibitoren een additief effect had. Onze resultaten bieden een veelbelovende mogelijkheid op de ontwikkeling van nieuwe behandelingsopties voor gemetastaseerd of irresectabel myxoid liposarcoom. Voor het myxofibrosarcoom werden geen directe aanwijzingen voor dergelijke behandelingsopties gevonden, wat vooral bemoeilijkt werd door het ontbreken van cellijnen van het myxofibrosarcoom voor het uitvoeren van functionele experimenten.

## 9.4 Toekomstperspectief

De resultaten beschreven in dit proefschrift hebben tot een dieper inzicht geleid in de onderliggende biologie van myxoide wekedelen tumoren. Met behulp van een breed pallet aan technieken, variërend van ouderwetse Alcian Blue kleuringen tot kinoom analyse en "imaging" en "liquid chromatography" massa spectrometrie, hebben we de myxoide wekedelen tumoren in detail geanalyseerd. Wij hebben laten zien dat samenstelling van de myxoide extracellulaire matrix verschilt naar het type en de graad van de tumor, en hoe deze verschillende biologie/genese van de verscheidene myxoide wekedelen tumoren zouden kunnen beïnvloeden. We hebben laten zien dat bestudering van het proteoom van deze tumoren met massa spectrometrie leidt tot een dieper inzicht van de veelvoorkomende maar ook weinig abundante componenten van de myxoide extracellulaire matrix. Een voordeel van massa spectrometrie is de gelijktijdige analyse van talrijke eiwitten zonder a priori kennis hiervan (35). Imaging massa spectrometrie voegt daarenboven spatiële informatie toe aan de geïdentificeerde moleculen, wat bijzonder interessant is omdat spatieel (naast temporele) gereguleerde eiwitexpressie wezenlijk is voor veel (inter) cellulaire processen zowel in fysiologische als pathologische omstandigheden (zoals in kanker) (35). Imaging massa spectrometrie maakt het mogelijk om direct massa spectrometrie te verrichten op weefselcoupes, wat trypsinisering - essentieel voor de hieraan gekoppelde MS/MS experimenten- tot een uitdaging maakt en de directe identificatie van interessante m/z waarden bemoeilijkt. Het wordt een uitdaging om dit probleem in de toekomst te overwinnen, alsook om de spatiële resolutie (nu tot circa 50 micrometer) terug te brengen tot het niveau van de

individuele cel, zonder dat de kwaliteit van de gemeten spectra minder wordt. De mogelijkheid om naast vers ingevroren weefsel, ook (moleculair gecross-linked) in formaline gefixeerd materiaal te gebruiken, zal haar toepassingsbereik en mogelijkheden aanzienlijk vergroten. Een andere uitdaging voor de toekomst is de analyse en integratie van de enorme datasets verkregen met (imaging) massa spectrometrie. Met name zou de massa spectrometrie hierbij kunnen leren van de hordes die genomen moe(s)ten worden in het genomicsveld. Het reserveren van voldoende tijd, geld en energie voor de data-analyse is cruciaal en moet op voorhand goed overwogen worden.

Afwijkingen in celsignalering spelen een voorname rol in vele soorten kankers (33, 36). Gezien celsignalering voornamelijk op posttranslationeel (dus op eiwit-niveau) wordt gereguleerd, is analyse van het proteoom niet alleen complementair maar zelfs cruciaal om de biologie van kanker goed te begrijpen (37). Begrip van de precieze onderliggende moleculaire signaleringsroutes in het intramusculaire myxoom biedt specifieke aanknopingspunten voor moleculaire diagnostiek. Dit heeft reeds geresulteerd in de incorporatie van directe GNAS1 mutatieanalyse in het moleculair diagnostische repertoire op de pathologie-afdeling. Hoewel er dus geen implicaties zijn voor gerichte therapie, heeft (correcte) moleculaire classificatie met behulp van GNAS1 mutatieanalyse wel een directe klinische toepasbaarheid omdat deze techniek behulpzaam is in het differentiëren van het intramusculair myxoom van het laaggradig myxofibrosarcoom op biopsies (en dus of vrije resectiemarges noodzakelijk zijn). In het myxofibrosarcoom konden we geen tumorspecifieke karyotypische afwijkingen ontdekken, die echter misschien in de toekomst wel zouden kunnen worden aangetoond met meer gedetailleerde genomische screening. Functionele studies om mogelijke moleculaire aangrijpingspunten in het myxofibrosarcoom te valideren, worden bemoeilijkt door het gebrek aan cellijnen. Met behulp van dergelijke experimenten, zoals bijvoorbeeld in vitro kinoomanalyse, bleken we in staat om aanknopingspunten voor gerichtere therapie te identificeren voor patiënten met het myxoid liposarcoom in een vergevorderd stadium. Dit is juist interessant omdat de conventionele chemotherapeutische mogelijkheden in deze patiëntengroep beperkt zijn. Analyse van celsignaleringsroutes legt de mechanismen bloot achter de onderliggende biologie van tumoren en biedt mogelijke aangrijpingspunten voor behandeling. Het in vitro blokkeren van kinasen kan ook uitstekend worden bereikt met RNA interference. Gelet de wijze waarop kinase-inhibitoren en RNAi het basaal-wetenschappelijke onderzoek beïnvloed hebben, alsook de ongekende snelheid waarmee dit de kliniek heeft bereikt, beloven de komende jaren opwindend te worden (38).

**References**


1. Osuna D, de Alava E: Molecular pathology of sarcomas. Rev Recent Clin Trials 4:12-26, 2009
2. de Alava E: Molecular pathology in sarcomas. Clin Transl Oncol 9:130-144, 2007
3. Chibon F, Lagarde P, Salas S, et al.: Validated prediction of clinical outcome in sarcomas and multiple types of cancer on the basis of a gene expression signature related to genome complexity. Nat Med 16:781-787, 2010
4. Aman P, Ron D, Mandahl N, et al.: Rearrangement of the transcription factor gene CHOP in myxoid liposarcomas with t(12;16)(q13;p11). Genes Chromosomes Cancer 5:278-285, 1992
5. Willems SM, Debiec-Rychter M, Szuhai K, et al.: Local recurrence of myxofibrosarcoma is associated with increase in tumour grade and cytogenetic aberrations, suggesting a multistep tumour progression model. Mod Pathol 19:407-416, 2006
6. Bovee JVMG, Hogendoorn PCW: Molecular pathology of sarcomas: concepts and clinical implications. Virchows Arch 456:193-199, 2010
7. Graadt van Roggen JF, Hogendoorn PCW, Fletcher CDM: Myxoid tumours of soft tissue. Histopathology 35:291-312, 1999
8. Graadt van Roggen JF, McMenamin ME, Fletcher CDM: Cellular myxoma of soft tissue: a clinicopathological study of 38 cases confirming indolent clinical behaviour. Histopathology 39:287-297, 2001
9. Willems SM, Mohseny AB, Balog C, et al.: Cellular/intramuscular myxoma and grade I myxofibrosarcoma are characterized by distinct genetic alterations and specific composition of their extracellular matrix. J Cell Mol Med 13:1291-1301, 2009
10. Weinstein LS, Liu J, Sakamoto A, et al.: Minireview: GNAS: normal and abnormal functions. Endocrinology 145:5459-5464, 2004
11. Okamoto S, Hisaoka M, Ushijima M, et al.: Activating Gs(alpha) mutation in intramuscular myxomas with and without fibrous dysplasia of bone. Virchows Arch 437:133-137, 2000
12. Delaney D, Diss TC, Presneau N, et al.: GNAS1 mutations occur more commonly than previously thought in intramuscular myxoma. Mod Pathol 22:718-724, 2009
13. Candeliere GA, Glorieux FH, Prud'homme J, et al.: Increased expression of the c-fos proto-oncogene in bone from patients with fibrous dysplasia. N Engl J Med 332:1546-1551, 1995
14. Kirsch DG, Dinulescu DM, Miller JB, et al.: A spatially and temporally restricted mouse model of soft tissue sarcoma. Nat Med 13:992-997, 2007
15. Oda Y, Takahira T, Kawaguchi K, et al.: Altered expression of cell cycle regulators in myxofibrosarcoma, with special emphasis on their prognostic implications. Hum Pathol 34:1035-1042, 2003
16. Virchow RLK: in Hirschwald (ed): Die cellularpathologie in ihrer Begrundung auf physiologische und patholo gische Gewebelehre. Berlin, 1858, pp 625-626
17. Willems SM, Wiweger M, Graadt van Roggen JF, et al.: Running GAGs: myxoid matrix in tumor pathology revisited : What's in it for the pathologist? Virchows Arch 456:181-192, 2010
18. Willems SM, Schrage YM, Baelde JJ, et al.: Myxoid tumours of soft tissue: the so-called myxoid extracellular matrix is heterogeneous in composition. Histopathology 52:465-474, 2008
19. Orgel JP, Eid A, Antipova O, et al.: Decorin core protein (decoron) shape complements collagen fibril surface structure and mediates its binding. PLoS One 4:e7028, 2009
20. Singer S, Millis K, Souza K, et al.: Correlation of lipid content and composition with liposarcoma histology and grade. Ann Surg Oncol 4:557-563, 1997
21. Millis K, Weybright P, Campbell N, et al.: Classification of human liposarcoma and lipoma using ex vivo proton NMR spectroscopy. Magn Reson Med 41:257-267, 1999
22. Chen JH, Enloe BM, Weybright P, et al.: Biochemical correlates of thiazolidinedione-induced adipocyte differentiation by high-resolution magic angle spinning NMR spectroscopy. Magn Reson Med 48:602-610, 2002
23. Hogendoorn PCW, Collin F, Daugaard S, et al.: Changing concepts in the pathological basis of soft tissue and bone sarcoma treatment. Eur J Cancer 40:1644-1654, 2004
24. Antonescu C, Ladanyi M: Myxoid liposarcoma, in Fletcher C.D.M., Unni KK, Mertens F (eds): World Health Organization classification of tumours. pathology and genetics. Tumours of soft tissue and bone. Lyon, IARC press, 2004, pp 40-43
25. Demetri GD, Chawla SP, von Mehren M, et al.: Efficacy and safety of trabectedin in patients with advanced or metastatic liposarcoma or leiomyosarcoma after failure of prior anthracyclines and ifosfamide: results of a randomized phase II study of two different schedules. J Clin Oncol 27:4188-4196, 2009

26. Grosso F, Jones RL, Demetri GD, et al.: Efficacy of trabectedin (ecteinascidin-743) in advanced pretreated myxoid liposarcomas: a retrospective study. Lancet Oncol 8:595-602, 2007
27. Grosso F, Sanfilippo R, Virdis E, et al.: Trabectedin in myxoid liposarcomas (MLS): a long-term analysis of a single-institution series. Ann Oncol 20:1439-1444, 2009
28. Dalal KM, Antonescu CR, Singer S: Diagnosis and management of lipomatous tumors. J Surg Oncol 97:298-313, 2008
29. Grommes C, Landreth GE, Heneka MT: Antineoplastic effects of peroxisome proliferator-activated receptor gamma agonists. Lancet Oncol 5:419-429, 2004
30. Tontonoz P, Spiegelman BM: Fat and beyond: the diverse biology of PPARgamma. Annu Rev Biochem 77:289-312, 2008
31. Debrock G, Vanhentenrijk V, Sciot R, et al.: A phase II trial with rosiglitazone in liposarcoma patients. Br J Cancer 89:1409-1412, 2003
32. Demetri GD, Fletcher CDM, Mueller E, et al.: Induction of solid tumor differentiation by the peroxisome proliferator-activated receptor-gamma ligand troglitazone in patients with liposarcoma. Proc Natl Acad Sci U S A 96:3951-3956, 1999
33. Tuveson DA, Fletcher JA: Signal transduction pathways in sarcoma as targets for therapeutic intervention. Curr Opin Oncol 13:249-255, 2001
34. Mitelman F, Johansson B, Mertens F: The impact of translocations and gene fusions on cancer causation. Nat Rev Cancer 7:233-245, 2007
35. McDonnell LA, Corthals GL, Willems SM, et al.: Peptide and protein imaging mass spectrometry in cancer research. J Proteomics 2010; 10; 73 (10) :1921-44.
36. Krause DS, Van Etten RA: Tyrosine kinases as targets for cancer therapy. N Engl J Med 353:172-187, 2005
37. Sebolt-Leopold JS, English JM: Mechanisms of drug inhibition of signalling molecules. Nature 441:457-462, 2006
38. Castanotto D, Rossi JJ: The promises and pitfalls of RNA-interference-based therapeutics. Nature 457:426-433, 2009

**Curriculum Vitae**

Stefan Martin Willems werd op 8 maart 1979 geboren te Brunssum. Na het behalen van het gymnasiumdiploma aan het Bernardinuscollege te Heerlen werd in 1996 begonnen aan de studie Geneeskunde (kandidatuursjaren) aan de universiteit van Hasselt te België. Tijdens zijn studie werkte hij als student onderzoeker onder leiding van Prof. Dr. Piet Stinissen aan het Biomedisch Onderzoeksinstituut te Hasselt (directeur: Prof. Dr. Jef Raus). Na het behalen van de kandidatuur (summa cum laude), werd de studie (doctoraatsjaren) voortgezet aan de Katholieke Universiteit Leuven. Tijdens zijn studie werkte hij als student onderzoeker onder leiding van Prof. Dr. Anton Roebroek op de afdeling Experimentele Genetica (hoofd: Prof. Dr. Fred van Leuven) van het Centrum voor Menselijke Erfelijkheid van de Katholieke Universiteit Leuven. Coschappen werden onder andere gelopen in Bristol en Newcastle upon Tyne in het Verenigd Koninkrijk. Tijdens het 4de docteraatsjaar volgde hij de prespecialisatie pathologie (afdelingshoofd: Prof. Dr. Raf Sciot). Na het behalen van het diploma Geneeskunde (cum laude) begon hij in oktober 2003 als assistent in opleiding tot medisch specialist en klinisch onderzoeker (AIOSKO) bij de afdeling Pathologie aan het Leids Universitair Medisch Centrum (afdelingshoofd: Prof. Dr. Gert-Jan Fleuren). In 2006 werd een AIOSKO Stipendium van NWO behaald waarmee gedurende 2 jaar fulltime promotie-onderzoek werd verricht onder leiding van Prof. Dr. Pancras Hogendoorn, waarvan de resultaten zijn beschreven in dit proefschrift. Delen hieruit werden gepresenteerd op (inter)nationale congressen van onder andere de Europen Society for Pathology (2005 en 2007), de United States and Canadian Academy of Pathology (2009) en de American Society of Mass Spectrometry (2010). Tijdens zijn AIOSKO periode was hij lid van de landelijke werkgroep leverpathologie (WELP). Van 2007 t/m 2009 was hij voorzitter van de Landelijke Pathologie Assistenten Vereniging (LPAV). Verder werd vanaf 2008 begonnen met de studie filosofie ter voorbereiding van de master wetenschapsfilosofie (MA) aan de Universiteit van Amsterdam. Vanaf oktober 2010 is hij als staflid patholoog werkzaam op de afdeling pathologie van het Universitair Medisch Centrum in Utrecht (afdelingshoofd: Prof. Dr. Paul van Diest). In december 2010 werd een Rubiconsubsidie van NWO behaald waarmee hij vanaf maart 2011 gedurende een jaar onderzoek zal verrichten op de afdeling Celbiologie (hoofd: Prof. Dr. Steven Gygi) van Harvard Medical School, te Boston.

**List of publications**

1. **S.M. Willems**, C.H. van Deurzen, P.J. van Diest Breast cancer diagnosis: fine needle aspiration cytology or core needle biopsy? Submitted

2. S.R. Ramautar, A.M. Pereira, **S.M. Willems**, J.A. Romijn, J.W.A. Smit Localizing Occult Insulinomas, A Diagnostic Challenge: Case Report and Review of the Literature. Submitted.

3. T. Gautier, W. de Haan, D. Ye, M.J. Bahr, T. Claudel, N. Nijstad, T.J.C. Van Berkel, L.M. Havekes, M.P. Manns, J. Grober, **S.M. Willems**, P.C.W. Hogen doorn, L. Lagrost, F. Kuipers, M. Van Eck, P.C.N. Rensen, U.J.F. Tietge Farnesoid X receptor activation induces cholesteryl ester transfer protein expression in humans and transgenic mice. Submitted

4. M. Verseveld, J.H. de Jong-Odding, M.G. Weisglass, **S.M. Willems**, H. Putter, R.C.M. Pelger, S. Osanto Foxp3 T-regs but not CAIX is associated with Survival in Clear Cell Renal Cell Carcinoma. Submitted

5. R.J.L. Stuyt, **S.M. Willems**, M.J. Wagtmans, B. van Hoek Chewing khat and chronic liver disease, Liver International, in press

6. **S.M. Willems**, A. van Remoortere, R. van Zeijl, A.M. Deelder, L.A. McDonnell, P.C.W. Hogendoorn Imaging mass spectrometry of myxoid sarcomas identifies proteins and lipids specific to tumour type and grade, and reveals biochemical intratumour heterogeneity. J Pathol 2010; 222(4): 400-9.

7. **S.M. Willems**, Y.M Schrage, I.H. Briaire-de Bruijn, K. Szuhai, P.C.W. Hogen doorn, J.V.M.G. Kinome profiling of myxoid liposarcoma reveals atypical NF-kB-pathway activity and CK2 inhibitor TBB as a potential treatment target. Bovée; Mol Cancer 2010; 23; 9; 257.

8. L..A. McDonnell, G.L. Corthals, **S.M. Willems**, A van Remoortere, A.M. Deel der. Peptide and protein imaging mass spectrometry in cancer research. J Proteomics, 2010; 10: 73 (10): 1921-44.

9. **S.M. Willem**s, M. Wiweger, F.J. Graadt van Roggen, P.C.W. Hogendoorn Running gags: myxoid matrix revisited. What is in it for the pathologist? Virchow Arch, 456, 2010:181-92.

10. **S.M. Willems**, Knellend keurslijf, Medisch Contact, 16; 2009, 702-704.

11. **S.M. Willems**, A.B. Mohseny, C. Balog, R. Sewrajsing, I.H. Briaire-de Bruijn, A.M. Cleton-Jansen, R. Sciot, C.D.M. Fletcher, A.M. Deelder, K. Szuhai, P.J. Hensbergen, P.C.W. Hogendoorn, Cellular/intramuscular myxoma and grade I myxofibrosarcoma are characterized by distinct genetic alterations and specific composition of their extracellular matrix J Cell Mol Med 7, 2009, 1291-1301.

12. D. Ye, A.O. Kraaijeveld, R.W. Grauss, **S.M. Willems**, L.C. van Vark-van der Zee, S.C. de Jager, M. Jauhiainen, J.A. Kuivenhoven, G.M. Dallinga-Thie, D.E. Atsma, P.C.W. Hogendoorn, E.A. Biessen, T.J. Van Berkel, J.W. Jukema, M. van Eck, Reduced leucocyte choleteryl ester transfer protein expression in acute coronary syndromes. J Intern Med. 264; 571-85.

13. **S.M. Willems**, J. Beck J, J. von der Thüsen. Macroscopic hematuria in patient with myelofibrosis caused by extramedullary hematopoiesis of bladder; Urology 72, 2008, e13-4.

14. W.H. De Vos Tot Nederveen Cappel, J. Dubbeld, **S.M. Willems**, J. Ringers J, B. van Hoek. Liver transplantation in a patient with encapsulating peritoneal sclerosis. Neth J Med. 2008;280-2.

15. **S.M. Willems**, K. Szuhai, H. Hartgrink, J.M.M.G. Bovée, A. De Schepper, P.C.W. Hogendoorn.CT-guided, COBRA-FISH-assisted diagnosis of well-differentiated liposarcoma (inflammatory subtype) of the retroperitoneum. Histopathology, 51 2007, 422-6.

16. **S.M. Willems**, Y.M. Schrage, J.J. Baelde, I.H. Briaire-de Bruijn, A. Mohseny, R. Sciot, J.V.M.G. Bovée, P.C.W. Hogendoorn. Myxoid tumours of soft tissue: the so-called myxoid extracellular matrix is heterogeneous in composition. Histopathology, 52, 2008:465-74.

17. J.M. Van de Kamp, D.J. Lefeber, G.J. Ruijter, S.J. Steggerda, N.S. den Hollan der, **S.M. Willems**, G. Matthijs, B.J. Poorthuis, R.A. Wevers. Congenital dis order of gycosylation type Ia presenting with hydrops fetalis. J Med Genet. 44, 2007:227-80.

18. Q.D. Pieterse, G.G. Kenter, K.N. Gaarenstroom, A.A. Peters, **S.M. Willems**, G.J. Fleuren, J.B. Trimbos. The number of pelvic lymph nodes in the quality control and prognosis of radical hysterectomy for the treatment of cervical cancer. Eur J Surg Oncol, 33, 2007: 216-21.

19. **S.M. Willems**, M. Debiec-Rychter, K. Szuhai, P.C.W. Hogendoorn, R. Sciot; Local recurrence of myxofibrosarcoma is associated with increase in tumour grade and cytogenetic aberrations, suggesting a multistep tumour progression model. Modern Pathol. 19, 2006: 407-16.

20. R.D. Thijs, M.G. Hazekamp, M.E. Rijlaarsdam, **S.M. Willems**, P.J. Schutte, L.A. Laan. An unexpected cause of a recurrent cerebral hemorrhage. Neuropediatrics 36, 2005, 324-7.

21. **S. Willems**, F. Carneiro, K. Geboes Gastric carcinoma with osteoclast-like giant cells and lymphoepithelioma - like carcinoma of the stomach: two of a kind? Histopathology. 47, 2005, 331-3.

22. G. van der Mieren, **S. Willems**, R. Sciot, H. Dumez, A. van Oosterom, W. Flameng, P. Herijgers; Pericardial Synovial Sarcoma: 14 Year Survival with Multimodality Therapy. Ann Thorac Surg. 78, 2004, 41-42.

23. L. Smeijers, **S. Willems**, A. Lauwers, E. Thiry, F. van Leuven, A. Roebroek. Functional expression of murine LRP1 requires correction of Lrp1 cDNA sequences. Biochim Biophys Acta. 1577, 2002, 155-8.

**Dankwoord**

Ik wil ieder danken, die op enigerlei wijze heeft bijgedragen tot de totstandkoming van dit proefschrift.

Gert-Jan Fleuren wil ik als afdelingshoofd van de pathologie, hartelijk bedanken voor het faciliteren van het welslagen van het "sandwich model" van onderzoek en diagnostiek. Als geen ander wist je de boel altijd weer vlot te trekken.

Pancras dank ik voor de motivatie en mogelijkheid van het doen van translationeel onderzoek binnen zijn onderzoeksgroep. De analisten, promovendi, postdoc's en stafleden uit de onderzoeksgroep "bot- en weke delen tumoren" dank ik voor al hun wijze en praktische input alsook de prettige samenwerking.

Mijn collega-onderzoekers van de pathologie, m.n. van P1-39 en P3-35, dank ik voor hun steun en gezelligheid; mijn mede arts-assistenten in opleiding tot patholoog dank ik voor hun collegialiteit en gezelligheid, ook naast het werk.

Een bijzonder woord gaat uit naar André Deelder en de analisten en postdoc's/UD’s van zijn Biomolecular Mass Spectrometry Unit (afdeling parasitologie) met wie ik heb mogen samenwerken. Zonder jullie was het niet gelukt!

Graag wil ik al mijn familie, vrienden en kennissen bedanken die zorgden voor de nodige afleiding, vertier en mind-(re)setting.

Veel dank ben ik verschuldigd aan mijn ouders die altijd geïnteresseerd waren en, me een gezonde portie relativerings- en doorzettingsvermogen hebben bijgebracht en aan wie ik dit proefschrift opdraag.

Lieve Debbie, dank voor alle steun, geduld, vertrouwen en interesse tijdens deze AIOSKO-periode en voor de geweldig mooie kinderen die je ons geschonken hebt.